Institute of Organic Chemistry
Polish Academy of Sciences

DISSERTATION

in the form of a coherent thematic series of articles published in scientific journals

The synthesis and photophysical properties of novel indolizine-based fluorophores

Jaqueline Stella Araujo Badarò M.Sc.

Supervisor: prof. dr hab. Daniel T. Gryko

Warsaw 2025

Doctoral thesis completed as part of the project:

"New generation of fluorescent probes for stimulated emission depletion microscopy"

Realizowanego w ramach programu TEAM

Fundacji na rzecz Nauki Polskiej

Numer grantu: POIR.04.04.00-00-3CF4/16-00-TEAM/2016-3/22

Acknowledgements

The four years I spent in Poland were not only an academic chapter of my life but also a complete experience of growth that allowed me to develop both as a chemist and as a person. For these years and this opportunity, I am immensely grateful to Prof. Daniel T. Gryko, who was for me not only a supervisor but also a mentor, and without whom the life I live today would be very different. He gave me a chance at a time when I had completely lost faith in the future. He always encouraged and supported me when I set ambitious goals, but he also showed understanding when I was too hard on myself and failed to meet my own expectations. I truly looked up to him as a supervisor because he always brought to the table not only his undoubtedly profound scientific knowledge but also his personality, irony, humanity, and compassion—qualities too often overlooked in academia. Working with him was, for me, a truly joyful and inspiring experience.

I am equally grateful to the pillars of Group X—Zenia, Mariusz, Olena, and Beata—for the time and patience they dedicated to teaching me everything I know today about lab experiments, purification and characterization methods, photophysical experiments and calculations, and much more. I also wish to acknowledge everyone else in the group who lent me a hand whenever I struggled with basic, or less basic, chemistry problems.

My heartfelt gratitude goes to Beata once again, as well as to Paula, Łukasz K., Kamil Sz., and Bartek, for sharing with me lab 37 (the best one, if I may say). We talked, laughed, shared; sometimes I even danced and sang, and in that cheerful and sometimes chaotic environment we performed excellent chemistry. This atmosphere led me to an *Angewandte* publication—the best way to close this chapter and proof that productivity has nothing to do with working in a rigid and overly serious environment.

I also wish to express my sincere appreciation to all the collaborators of my published papers: Dr. B. Koszarna and M. Perkowska for their help in the synthesis of the compounds; Dr. M. H. E. Bousquet, Prof. D. Jacquemin, and Dr. I. Deperasińska for the theoretical calculations; Dr. E. T. Ouellette for the single-crystal X-ray diffraction (SCXRD) measurements; Dr. O. Morawski for the fluorescence decay experiments; Dr. A. Wrzosek, Prof. A. Szewczyk, D. V. Kolygina, J. Park, K. Kandere-Grzybowska, and Prof. B. Grzybowski for confocal imaging of the fluorescent compounds in living cells; and finally, B. Godlewski for joining me in writing the review and, once again, Prof. D. T. Gryko for supervising all my work.

I gratefully acknowledge FNP-TEAM for funding my PhD, the MSCA for allowing me to spend some time in Malaysia, and NAWA for supporting me during a research visit in France. Most importantly, I also thank all IChO members—especially the administration and analysis teams—for their daily commitment and assistance, which allow research to run smoothly.

To all of you mentioned above: this thesis and my publications exist only because of your support.

I am deeply grateful also to the friends and colleagues who shared even a small part of this journey with me: Gana and Katia for being my PhD buddies; Ahmad and Yasemin for being among the first friends I made; Meme, Grace, and Franco for becoming good friends in such a short time; my friends

in Warsaw: Arturo, Vishali, Deepshikha, Shantanu, Souvik, and Mohad for the joyful moments together; Paola, Emiliano, Monica, and Debora for allowing me to always have a bit of Italy with me in Poland; and last, but most importantly, Kitti, for being the first person I met at IChO and, since day one, my best friend.

Finally, I am grateful to those who, even from afar, never felt distant: my friends in Italy—Miriam, Elisabetta, Ludovica, Silvia, Vanessa, Fabrizio and Gabriele; my family in the USA and Brazil, especially my parents, for always supporting me; and Federico, for being my person and feeling so close no matter how far.

Abstract in English

In the quest to develop small fluorescent molecules for bioimaging applications, this work focused on a deeper understanding of π-expanded indolizines; the improvement of existing pathways for the synthesis of known cores; the development of novel strategies for new ones; the rationalization of the relationship between substituents and photophysical properties; and, finally, the investigation of promising candidates for bioimaging applications.

Around this topic, three articles and a review were published, all of which are included in this dissertation.

The first project I worked on led to the publication *"The Kröhnke synthesis of benzo[a]indolizines revisited: towards small, red light emitters"*, in which I described the improvement of the synthetic methodology and the broadening of the scope for obtaining **benzo[*a*]indolizines**, a class of π-expanded indolizines first described by Kröhnke in the 70s, and the rationalization of their photophysical properties in relation to the different substituents introduced.
Kröhnke described the synthesis of benzo[*a*]indolizines starting from pyridinium salts and 1-chloro-2,4,6-trinitrobenzene in two steps, using first an inorganic base, K_2CO_3 in $CHCl_3$, followed by an organic base, piperidine, in DMSO. This methodology led to a limited number of products in relatively low yield.
The first change I implemented over the proposed path was the substitution of the highly explosive 1-chloro-2,4,6-trinitrobenzene with the less hazardous 4-chloro-3,5-dinitrobenzene derivatives, yielding three products in 20–30% yield. The second was the identification of a more suitable combination of base and solvent to avoid the isolation step of the intermediate. After a series of attempts using different bases and solvents to enhance the yields, I was able to reduce the number of synthetic operations, increase the yields, and accelerate the reactivity of the pyridinium salt and the 4-chloro-3,5-dinitrobenzene derivatives by employing Cs_2CO_3 and sulfolane. This led to the isolation of eleven different products in yields ranging from 5 to 80%. Further functionalization afforded two additional derivatives.
Once a more efficient synthetic pathway was established, attention was turned to the photophysical investigation. The analysis of the photophysical properties based on the different substituents and their positions allowed for a rationalization of the structure-photophysics relationship of this class of fluorophores (fig 1).

In the second project I followed the same general approach and worked on optimizing the methodology for the synthesis of **2-oxo-2H-pyrano[2,3-*b*]indolizine-3-carboxylates**, first proposed by Kakehi in the 90s, and on investigating their photophysical properties. This work led to the following publication: *"Strongly fluorescent indolizine-based coumarin analogs".*
Starting from pyridinium salts and diethyl 2-(ethoxymethylene)malonate Kakehi obtained products in one-pot reaction after one week using K_2CO_3 as base in EtOH. I instead switched the base to Cs_2CO_3 and used a diverse array of pyridinium salts, preparing 8 products in 5-50% yield. Further functionalization was performed, and five additional structures were obtained.
With a plethora of 2-oxo-2H-pyrano[2,3-*b*]indolizine-3-carboxylates available, the photophysical investigation and rationalization of the fluorescent properties was carried out (representatives displayed in fig. 1). Among those, the styryl dye was selected for H9c2 cell line staining and demonstrated, after permeabilization with digitonin, selective localization in the nuclei.

The last project extended beyond the improvement and expansion of previous works and resulted in the discovery a completely new class of fluorophores which culminated with recently published article: *The Hybrid of Indolizine and Merocyanine – A New Class of Organelle-specific Dyes.*

In this work, starting from indolizin-ol intermediates and 2,3,5,6-tetrafluoro-4-hydroxybenzaldehyde in xylene, I obtained six hybrids polymethine dyes which I called **indolizine-merocyanines (IndMers)**, in a one-pot procedure with yields ranging from 26-90%. The developed methodology was also tested with different aldehydes of similar characteristics, generating two additional heretofore structures: a V-shaped xanthene dye and a cyanine type dye.

A comprehensive photophysical investigation was carried out on the obtained structures (representatives are shown in fig. 1) providing a broad understanding of their structure-photophysics relationship. In addition, for some selected structures, photostability and solubility in aqueous media were investigated.

Among those compounds one showed emission in the NIR region, solubility in aqueous media, high cell permeability in HT1080 fibrosarcoma and MRC5 normal human lung fibroblast cells, and context dependent accumulation in mitochondria and RNA rich nucleoli when compared to MitoTracker™ Green FM and SYTO RNASelect™ respectively suggesting our success in developing a new dye for bioimaging.

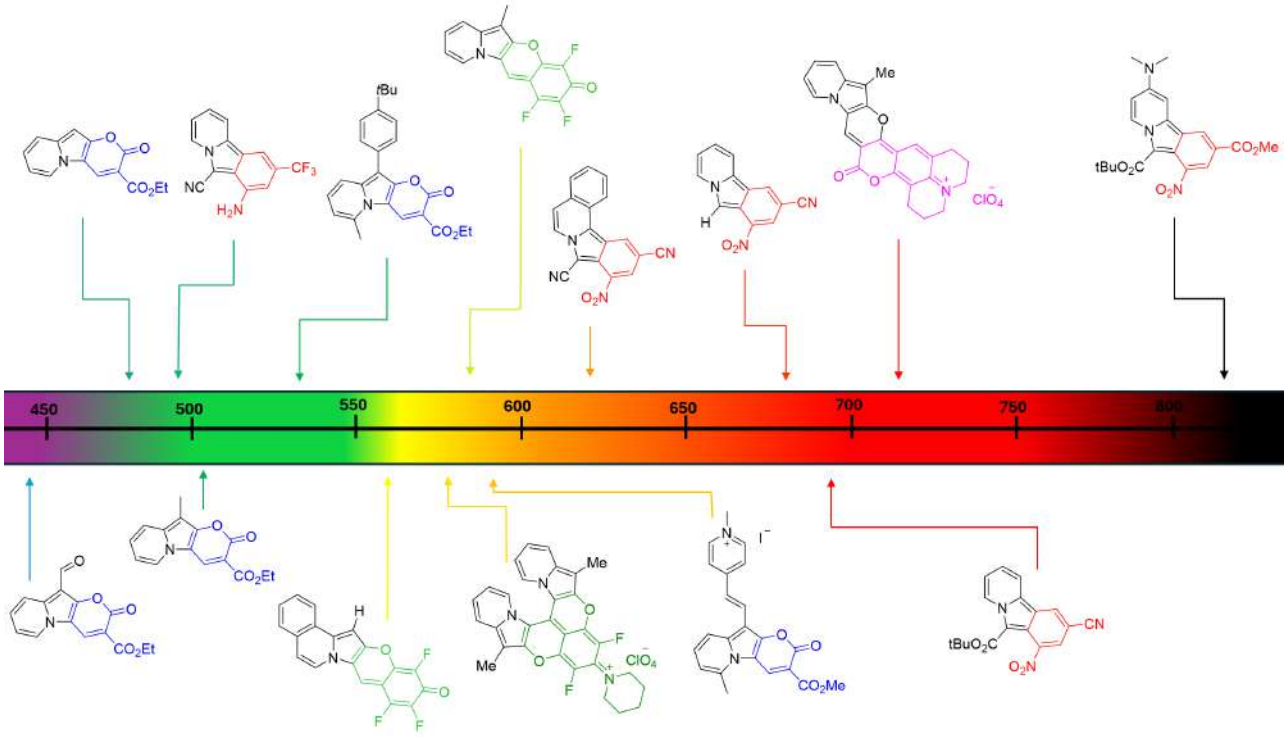

Figure 1: *Structure and visual comparison of the fluorescence emission of some representatives of benzo[a]indolizines, pyrano[b]indolizines and IndMers in DCM.*

Streszczenie w języku polskim

Celem niniejszej rozprawy doktorskiej jest pogłębienie wiedzy dotyczącej indolizyn o rozszerzonym układzie sprzężonym π, traktowanych jako potencjalni kandydaci do zastosowań w bioobrazowaniu. Zakres badań obejmował zarówno udoskonalanie istniejących ścieżek syntezy znanych rdzeni indolizynowych, jak i opracowanie nowych strategii syntetycznych prowadzących do wcześniej nieopisanych struktur. Szczególny nacisk położono na racjonalizację wpływu podstawników na właściwości fotofizyczne otrzymywanych związków, co umożliwiło identyfikację struktur o szczególnie obiecujących właściwościach do dalszych zastosowań biologicznych. Przedstawione wyniki stanowią istotny wkład w rozwój chemii indolizyn oraz w projektowanie nowych sond fluorescencyjnych dla celów bioobrazowania.

W ramach tego tematu opublikowano trzy artykuły oraz jedną pracę przeglądową, które zostały w całości włączone do niniejszej dysertacji.

Pierwszy projekt, którym się zajmowałam, zaowocował publikacją: „The Kröhnke synthesis of benzo[*a*]indolizines revisited: towards small, red light emitters", w której opisałam zoptymalizowaną metodologię syntezy oraz rozszerzyłam bibliotekę **benzo[*a*]indolizyn**. Przedstawiłam również racjonalizację ich właściwości fotofizycznych w zależności od wprowadzonych podstawników. Synteza benzo[*a*]indolizyn – klasy indolizyn o rozszerzonym układzie sprzężonym π – została po raz pierwszy opisana przez Kröhnkego w latach 70. Opierała się ona na dwuetapowej reakcji soli pirydyniowych z 1-chloro-2,4,6-trinitrobenzenem, w której pierwszy etap prowadzono w $CHCl_3$ z użyciem nieorganicznej zasady K_2CO_3, a drugi w DMSO z piperydyną pełniącą rolę zasady. Metodologia ta ograniczała się do otrzymania kilku produktów ze stosunkowo niskimi wydajnościami. Pierwszą modyfikacją, którą wprowadziłam w syntezie, było zastąpienie silnie wybuchowego 1-chloro-2,4,6-trinitrobenzenu mniej niebezpiecznymi pochodnymi 4-chloro-3,5-dinitrobenzenu, co pozwoliło mi uzyskać trzy produkty z wydajnościami na poziomie 20–30%. Drugą istotną zmianą było opracowanie bardziej odpowiedniego układu zasada–rozpuszczalnik, eliminującego konieczność izolowania związku pośredniego. Po przeprowadzeniu szeregu prób z różnymi zasadami i rozpuszczalnikami, dzięki zastosowaniu Cs_2CO_3 w sulfolanie, udało mi się zmniejszyć liczbę etapów syntetycznych, zwiększyć wydajności oraz skrócić czas reakcji soli pirydyniowej z pochodnymi 4-chloro-3,5-dinitrobenzenu. Pozwoliło mi to wyizolować jedenaście różnych produktów w wydajnościach od 5% do 80%, a dalsza funkcjonalizacja umożliwiła otrzymanie dwóch dodatkowych pochodnych. Po opracowaniu bardziej efektywnej ścieżki syntetycznej skupiłam się na badaniach właściwości fotofizycznych otrzymanych związków. Analiza wpływu różnych podstawników oraz ich położenia na właściwości fotofizyczne pozwoliła mi zracjonalizować zależności pomiędzy strukturą a fotofizyką tej klasy fluoroforów (rys. 1).

W drugim projekcie skupiłam się na optymalizacji metodologii syntezy estrów **2-okso-2H-pirano[2,3-*b*]indolizyno-3-karboksylowych**, zaproponowanej po raz pierwszy przez Kakehiego w latach 90., oraz na zbadaniu właściwości fotofizycznych otrzymanych pochodnych. Prace te doprowadziły do publikacji pt. „Strongly fluorescent indolizine-based coumarin analogs". Kakehi przeprowadził reakcję wybranych soli pirydyniowych z dietylo-2-(etoksymetyleno)malonianem w EtOH, stosując K_2CO_3 jako zasadę. Zastępując węglan potasu Cs_2CO_3, udało mi się skrócić czas reakcji, a stosując zróżnicowany zestaw soli pirydyniowych, uzyskałam osiem produktów o wydajnościach 5–50%. Następnie przeprowadziłam dalszą funkcjonalizację, otrzymując pięć dodatkowych struktur. Dysponując szeroką gamą estrów 2-okso-2H-pirano[2,3-*b*]indolizyno-3-karboksylowych, przeprowadziłam badania fotofizyczne oraz racjonalizację ich właściwości fluorescencyjnych (przykłady pokazano na rys. 1). Wśród

nich barwnik styrylowy został wybrany do barwienia linii komórkowej H9c2 i wykazał, po permeabilizacji digitoniną, selektywną lokalizację w jądrach komórkowych.

Ostatni projekt wykraczał poza udoskonalanie i rozwijanie wcześniejszych prac, prowadząc do odkrycia zupełnie nowej klasy fluoroforów. Wyniki tej pracy zostały opisane w publikacji pt. „The Hybrid of Indolizine and Merocyanine – A New Class of Organelle-specific Dyes". W ramach tego projektu przeprowadziłam reakcję „one pot" indolizynoli, otrzymanych z soli pirydyniowych, z 2,3,5,6-tetrafluoro-4-hydroksybenzaldehydem w ksylenie, uzyskując sześć hybrydowych barwników polimetinowych (z wydajnościami 26–90%), które **nazwałam indolizyno-merocyjaninami (IndMers)**. Opracowaną metodologię rozszerzyłam również na reakcję z innymi aldehydami o podobnych właściwościach, uzyskując dwie nowe, dotychczas nieopisane struktury: barwnik ksantenowy w kształcie litery V oraz barwnik typu cyjanina. Dla otrzymanych struktur przeprowadziłam kompleksowe badania fotofizyczne (przykłady przedstawiono na rys. 1), które pozwoliły ustalić zależności między strukturą a właściwościami fotofizycznymi tych związków. Ponadto, dla wybranych struktur zbadałam fotostabilność i rozpuszczalność w środowisku wodnym. Co ważne jeden z otrzymanych związków charakteryzował się szczególnie korzystnymi właściwościami, w tym emisją w zakresie NIR, rozpuszczalnością w wodzie, wysoką przenikalnością do komórek HT1080 (fibrosarcoma) oraz MRC5 (normalne ludzkie fibroblasty płucne), a także zależną od kontekstu akumulacją w mitochondriach i jąderkach bogatych w RNA (w porównaniu odpowiednio z MitoTracker™ Green FM i SYTO RNASelect™). Świadczy to o tym, że udało mi się opracować nowy barwnik do bioobrazowania.

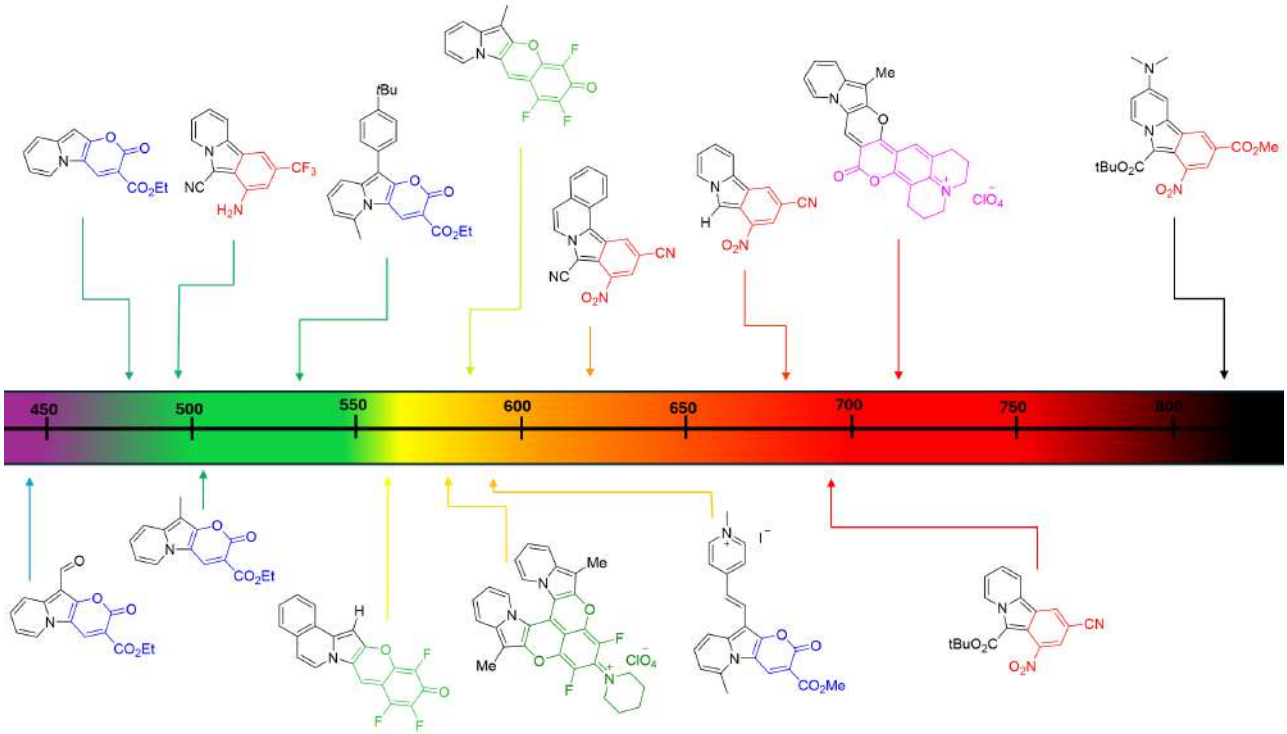

Rysunek 1. *Struktura i wizualne porównanie emisji fluorescencyjnej wybranych przedstawicieli benzo[a]indolizyn, pirano[b]indolizyn oraz IndMerów w DCM.*

Table of Contents:

List of Publications for the Doctoral Dissertation

1. **Badaro, J. S. A.**; Koszarna, B.; Bousquet, M. H. E.; Ouellette, E. T.; Jacquemin, D.; Gryko, D. T. 'The Kröhnke synthesis of benzo[a]indolizines revisited: towards small, red light emitters', Org. Chem. Front. 2022, 9, 1861-1874. https://doi.org/10.1039/D2QO00097K

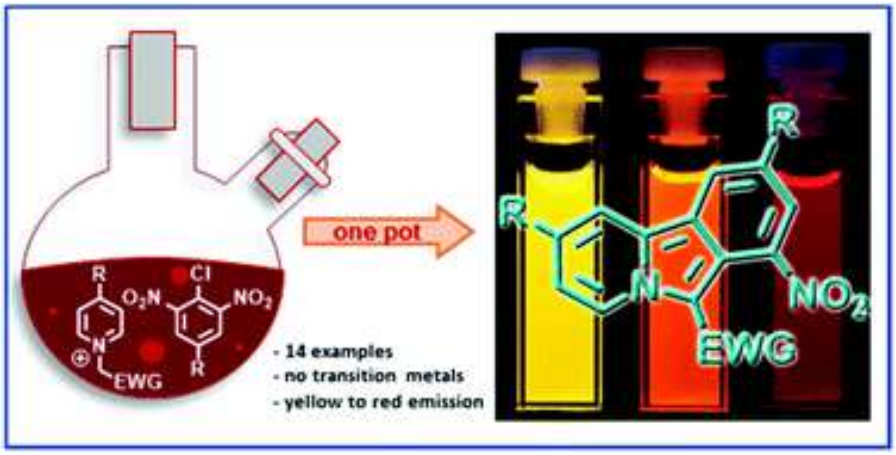

2. **Badaro, J. S. A.**; Wrzosek, A; Morawski, O.; Szewczyk, A; Deperasinska, I; Gryko, D. T. 'Strongly fluorescent indolizine-based coumarin analogs' Org. Chem. Front., 2024, 11, 6627-6641. https://doi.org/10.1039/D4QO01216J

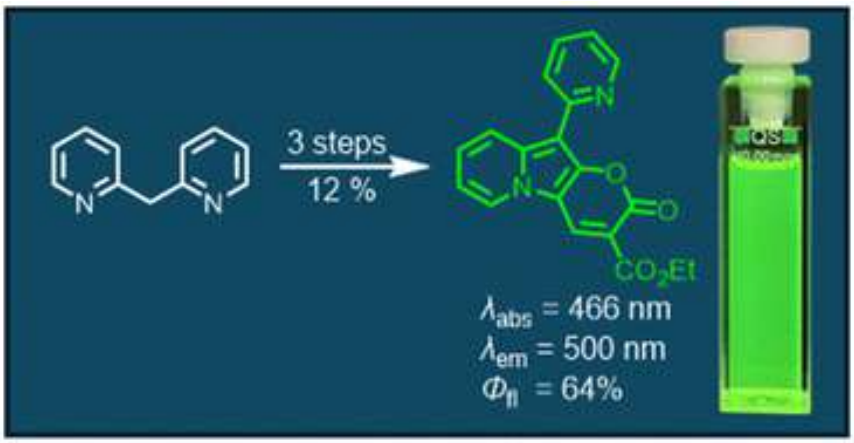

3. **Badaro, J. S. A**.; Godlewski, B.; Gryko, D. T., 'Advances in the synthesis of indolizines and their π-expanded analogues: update 2016-2024', Org. Chem. Front., 2025, 12, 2860-2907. https://doi.org/10.1039/D4QO02082K

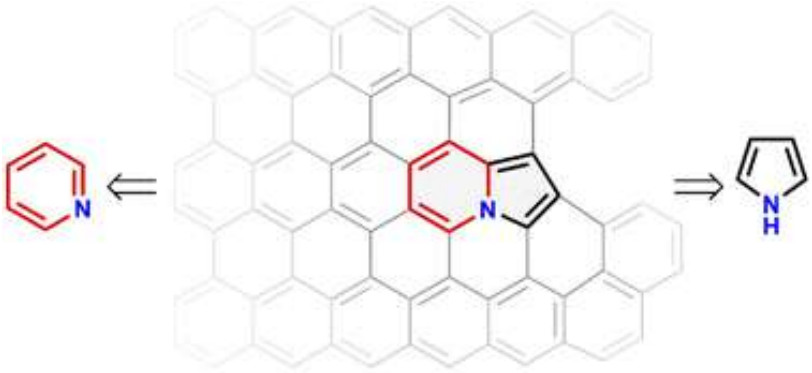

4. **Badaro, J. S. A**; Koszarna, B.; Perkowska, M.; Kandere-Grzybowska, K.; Kolygina, D. V.; Morawski, O.; Park, J.; Grzybowski, B.; Deperasinska, I.; Gryko, D. T., 'The Hybrid of Indolizine and Merocyanine - A New Class of Organelle-specific Dyes', Angew. Chem. Int. Ed.. 2025, e202508044. https://doi.org/10.1002/ange.202508044

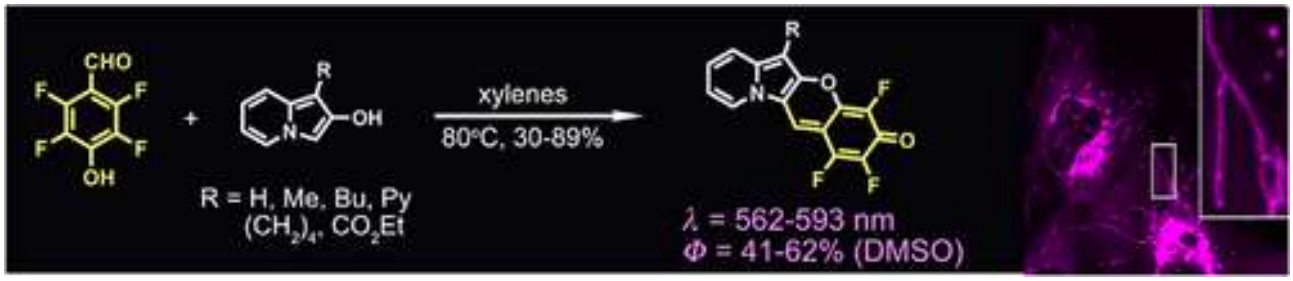

Participation in Conferences

The 19th international symposium on novel aromatic compounds (ISNA 2019)
Warsaw, 3rd-8th July 2022.
'The Kröhnke synthesis of benzo[*a*]indolizines revisited: towards small, red light emitters'

Aims and Objectives

A cell is a key functional unit of life. All forms of life rely on cellular processes to maintain normal functions, and changes in cell function induced by metabolic disturbances, physicochemical damage or infection may cause disease. Along with advances in fluorescence microscopy and *in-vitro* cell culture, live-cell imaging has become an essential tool in modern biology for the study of molecular and cellular events by means of specifically targeted fluorescent labels and sensors. Fluorescence imaging has a wide range of benefits not offered by other imaging modalities, derived from its combination of high specificity, high sensitivity, and high spatio-temporal resolution. Fluorescent dyes are widely used as indispensable markers and sensors in biology-related optical microscopy. At the same time, current dyes do not perfectly fulfill many requirements for use in fluorescence microscopy. They lack one or more of the following properties: (1) photostability; (2) large Stokes shift; (3) large fluorescence quantum yield (particularly in the near-infrared [NIR] region) and (4) cell permeability.

As far as fluorescence microscopy is concerned, cell biologists are entirely focused on rhodamines, coumarins, fluoresceins, cyanines and BODIPYs mostly because of reasonable combination of favorable photophysical properties.[1] My central hypothesis was that small electron-rich aromatic heterocycle, indolizine, can be a suitable platform to prepare alternative dyes with suitable combination of photophysical properties. In the quest for developing small fluorescent molecules for bioimaging applications, indolizines, despite being discovered more than 100 years ago,[2] were set aside. According to PubMed, the peak in the number of publications on indolizines was reached in 2012 (around 1500 articles). In contrast, in the same year, publications on fluoresceins nearly doubled those on indolizines and has continued to grow to date.[3] This discrepancy has created a vicious cycle: the limited development of indolizine scaffolds and the insufficient fine-tuning of their properties have restricted their adoption in bioimaging, which in turn has further discouraged efforts to optimize them.

Several factors contributed to this stagnation[4]

1) Photophysical limitations

Many indolizines absorb and emit in the blue region of the UV spectra, which is not ideal for bioimaging due to strong background autofluorescence, limited tissue penetration and potential photodamage. Additionally, their quantum yield and photostability tend to be inferior compared to those of established fluorophores.

2) Chemical stability

The large electron density of indolizines makes them highly chemically reactive, allowing them to undergo multiple reactivity pathways as described in §1.2 and shown in Scheme 4. This reactivity undermines their stability in biological environments compared to more robust dye families.

3) Synthetic accessibility and tunability

Although indolizines have been known for more than a century, their synthetic chemistry remains underdeveloped. Routes to expanded indolizines are especially scarce, as they typically rely on pre-formed expanded pyridines or pyrroles, which restricts structural diversity and limits opportunities for systematic fine-tuning.

4) Limited commercial development and biological applications assessment

Because the field has long been dominated by BODIPYs, cyanines, rhodamines, and fluoresceins, indolizines and their expanded analogues received little attention. This lack of investment left key practical issues, such as aqueous solubility and stability under physiological conditions, largely unresolved, further discouraging their adoption in bioimaging.

The general aim of my PhD research was to address these limitations and expand the understanding of indolizine as fluorescent scaffold, with the ultimate goal of improving their 'photophysical performance' and bioimaging applicability. Along these lines my work focused on π-expanded indolizines which intrinsically exhibit bathochromically shifted absorption/emission and enhanced stability due to greater electron delocalization. At the same time they maintain the appealing features of the parent indolizine: small size, rigidity, electron density and the ability to form push-pull systems through fine-tuned substituents.

Specific objectives of my thesis were:

1) To expand the knowledge and understanding of π-expanded indolizines by improving existing synthetic methodologies and developing new synthetic paths for the synthesis of two classes: benzo[*a*]indolizines and pyrano[2,3-*b*]indolizines, both reported in the last century as promising fluorophores, but obtained in low yield and with limited scope and characterization.

2) To conduct a comprehensive study of the absorption, emission and stability profiles, therefore building a foundation for their rational design, guided structural modification and optimization through tailored substituents.

3) To develop a new class of polymethine dyes possessing indolizine as an electron donor i.e. replacing classical dialkylamino group in merocyanine type of structures with indolizine. Consequently, I aimed at entirely new type of π-expanded indolizine dyes, leveraging on the insights acquired during the realization of the first two objectives. Simultaneously my goal were functional dyes with properties compatible with fluorescence bioimaging requirements.

1. Introduction

1.1. Indolizines

The first indolizine derivative was synthesized by A. Angeli in 1890, *via* the intramolecular cyclization of the ethyl pyrroyl pyruvate under basic condition, and he suggested that the fully unsaturated system, later isolated by Scholtz[5], should be named "pyrindole" as it is an isomer of the already known indole.[2] However, it was only with the methodology proposed by Chichibabin in the early 20th century that indolizines, also known as "pyrrolo[1,2-*a*]pyridine", started to become more popular.[6] He developed a base-mediated, straightforward, versatile and efficient method starting from α-picoline and α-halogenated ketones that became the go-to strategy for indolizines synthesis for decades and is up to now the most known and used (Scheme 1).

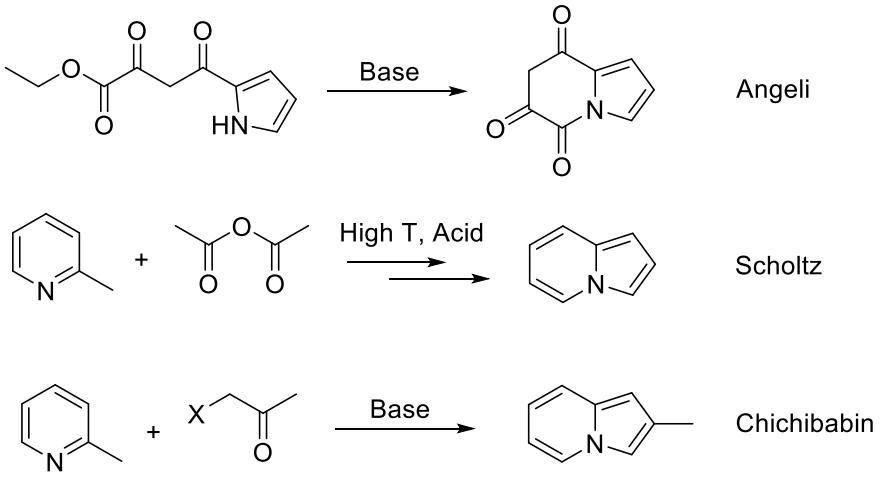

Scheme 2: *First synthesis of indolizines*

Structurally, indolizines have a 10π delocalized electron system composed of an electron-rich pyrrole-type five-membered ring and an electron-deficient six-membered ring. Different naming and numbering systems were used since their discovery, but for this Thesis the name "indolizine" will be used and the numbering system adopted by the American Chemical Society will be the standard. Unsubstituted indolizine have a resonance energy of 0.29 kcal/mol and is best represented by a resonance hybrid of three structures (I), (II), and (III) (Scheme 2).[7]

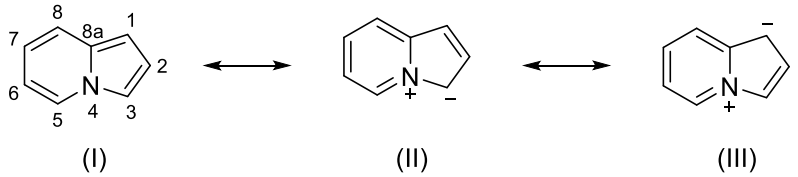

Scheme 3: *Numbering and resonance structures of indolizine*

Although not naturally occurring in their aromatic form, these compounds have been encountered in a few cases as π-expanded derivatives. More commonly, however, they are found as saturated alkaloids isolated from plants, animals, and microbes, where they exhibit potent biological activity (Figure 1).[7–12]

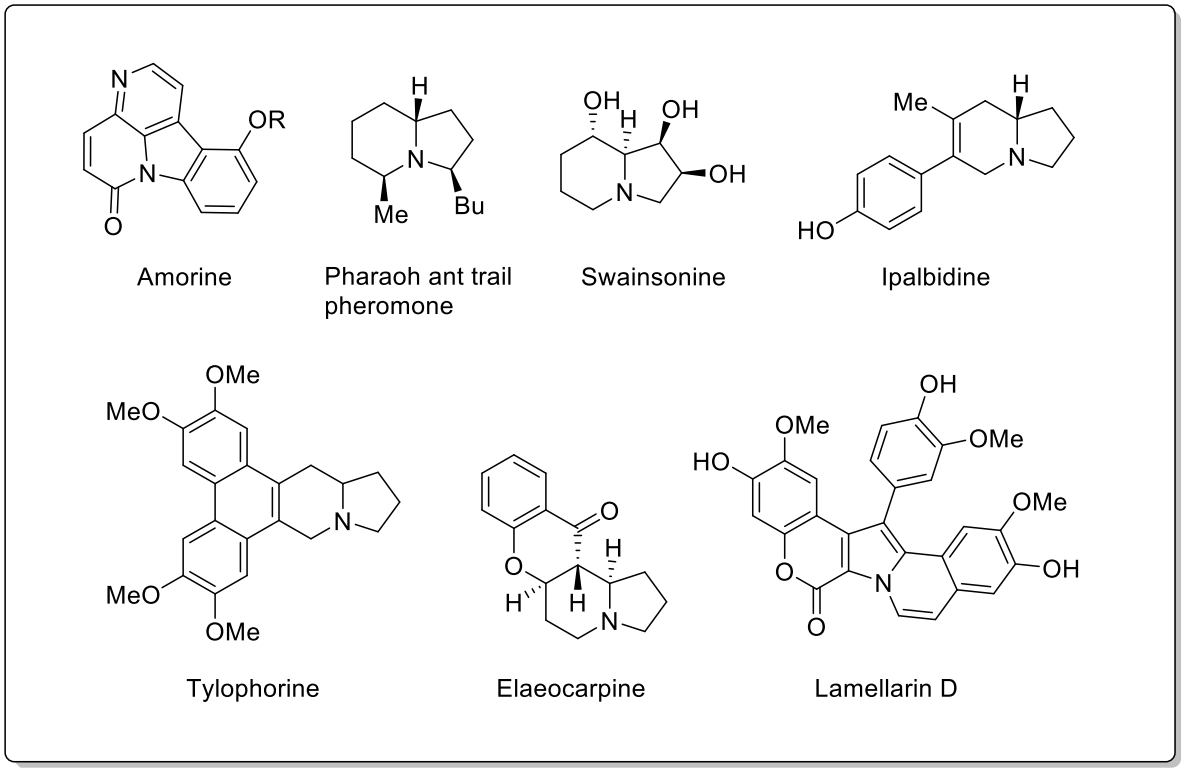

Figure 1: *Naturally available partially or fully saturated indolizines*

Typical methodologies for their synthesis can be classified into methods starting from Pyridine, and methods starting from pyrroles (Scheme 3), the latter being the least explored and only recently more popular. This is because pyrrole-based building blocks face significant challenges due to their higher cost, lower availability, and reduced stability. Despite these limitations, their unique reactivity and potential provide promising opportunities for indolizine synthesis in a fashion complementary to the classic pyridine-based methods.[13–25]

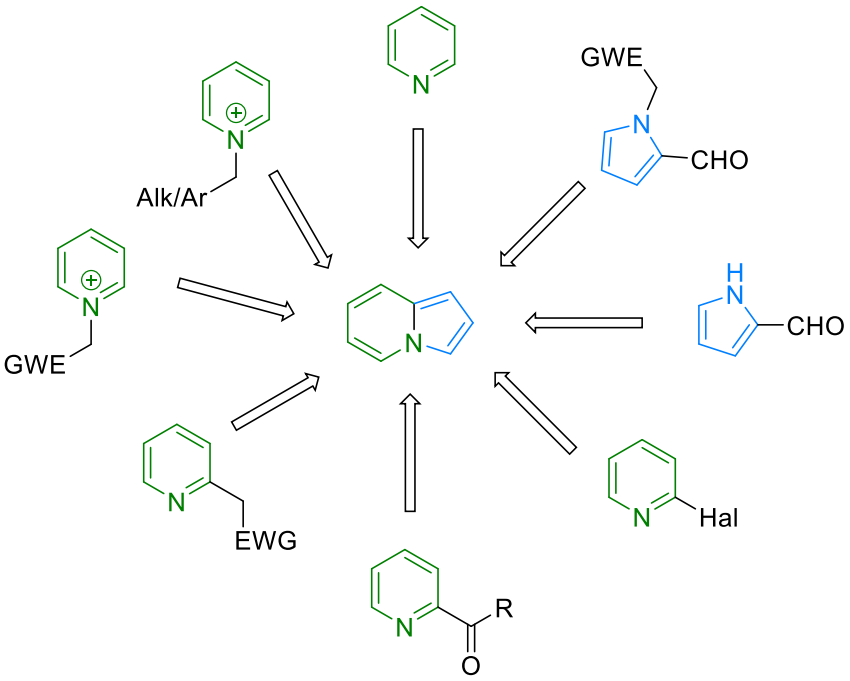

Scheme 3: *Indolizine synthesis from different pyridines and pyrroles*

1.2. Reactivity of indolizines

Indolizines exhibit sensitivity to air and light. They demonstrate high reactivity *via* electrophilic substitution and infrequently could also undergo nucleophilic attack. They produce a colorful reaction with Ehrlich's reagent and are highly fluorescent.[26] Density Functional Theory (DFT) calculations indicate that the highest occupied molecular orbital (HOMO) is situated on the pyrrole-type ring, with the highest electron density located at C-3, making it the preferred site for electrophilic attack, followed by C-1.[27] Resonance structures corroborate these findings, with structure **II** (Scheme 2) being the more stable configuration due to lower energy charge separation. Conversely, the lowest unoccupied molecular orbital (LUMO) is positioned on the pyridine-type ring.

Classical reactions occurring at C-1 and/or C-3 were well documented in the last century and have been further developed recently. These include protonation,[28–30] nitration,[31,32] nitrosation,[32,33] and diazo coupling,[32] as well as alkylation,[34–36] acylation,[37–39] and halogenation.[40–42] Oxidation[43,44] and reduction[5,45,37,46] reactions are also feasible. However, oxidation typically results in ring opening and "decomposition," while reduction leads to a saturated system crucial for alkaloid synthesis. Coupling reactions at position C-3 are possible via usually palladium-catalyzed coupling.[27] Metalation of indolizines[47,48] serves as a viable functionalization approach, permitting the introduction of various substituents at C-5, including halogens and providing access to less common substituted indolizines.[48] Additionally, reactivity at C-5 can involve a nucleophilic attack if an electron-withdrawing group is present and functions as a leaving group.[49]

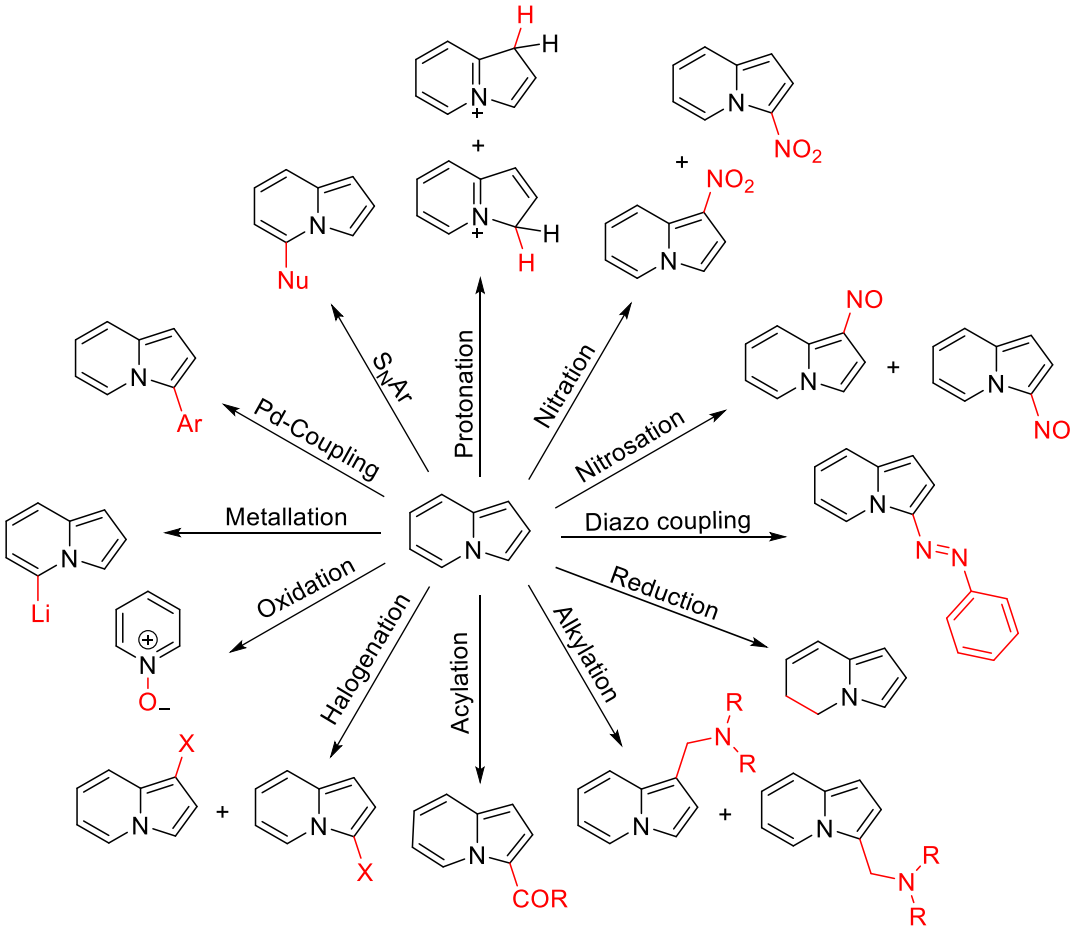

Scheme 4: *Reactivity of indolizines*

1.3. π-Expanded indolizines

As previously mentioned, expanded indolizines have been discovered in nature and have demonstrated promising antibiotic and cytotoxic activities, both in their natural environment and in medical applications.[50] In addition to their biological relevance, these compounds exhibit intriguing photophysical properties, making them excellent candidates for development in photoluminescent materials[51,52], solar cells[53], and fluorescent dyes for bioimaging.[54,55] From a synthetic point of view, in many cases the π-expansion is achieved simply by using quinolines[56–58] or isoquinolines[59–62] as starting materials. However, in the context of this introductory chapter, attention will be focused on more structurally complex and less conventional systems, those more closely related to the scaffolds studied in my own research. Particular emphasis will be placed on their photophysical behavior, which will later be critically compared with the properties of the indolizines developed in this work. The extensive overview of the recent developments in the synthesis of π-expanded indolizines can be found in the review of which I am co-author and which is part of this PhD-Thesis.

1.3.1. Benzo-indolizines

In 2016, Outlaw *et al.* developed a new method to synthesize 6-amino-8-cyanobenzo[1,2-*b*]indolizines from substituted indoles and fumaronitrile *via* a Wittig mechanism followed by deprotonation of the indole N-H (Scheme 5).[63] This strategy promotes cyclization towards the formation of indolizines rather than carbazoles and works well with both electron-donating and electron-withdrawing groups at the 4-position of the indole. A comparison of the optical properties of these newly synthesized 6-amino-8-cyanobenzo[1,2-*b*]indolizines (**1**) with those of 6,9,10-trimethyl-pyrido[1,2-*a*]indole, previously synthesized by Saxton *et al.* in the 1950s,[64] reveals a bathochromic shift in absorption. This red-shift is attributed to the presence of amino and cyano substituents in the benzoindolizine system. Compounds absorb light at 270, 340, and 440 nm, and emit fluorescence between 490 and 520 nm, with an average fluorescence quantum yield of 10%, while trimethyl-pyrido[1,2-*a*]indole displays peaks at 210 and 320 nm. Furthermore, the 6-amino-8-cyanobenzo indolizines demonstrate pH-sensitive fluorescence: protonation breaks aromaticity and causes a hypsochromic (blue) shift in emission. Upon the addition of trifluoroacetic acid (TFA), a new equilibrium leads to increased emission at 440 nm and a higher quantum yield of 20%, corresponding to a non-aromatic protonated form.

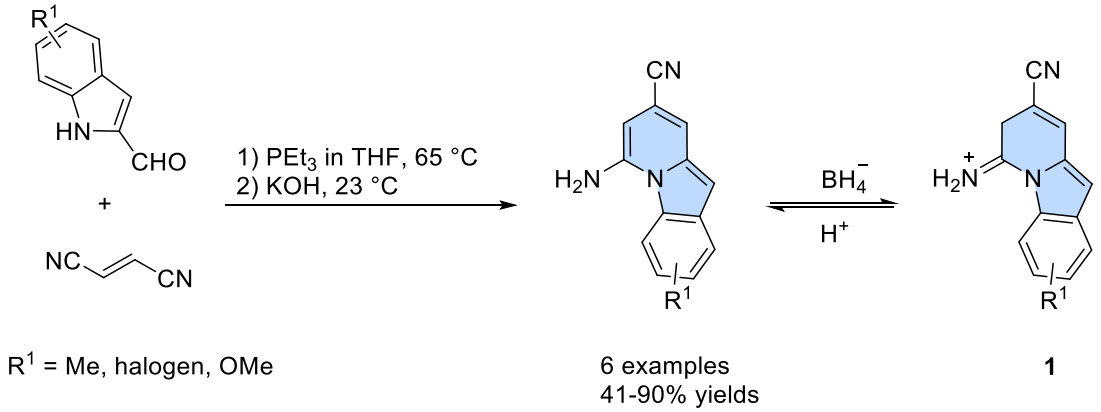

Scheme 5: *Synthesis of pH-sensitive benzo[1,2-b]indolizines*

Even more expanded and red shifted benzo[1,2-*b*]indolizine derivatives (**2**) were recently reported by Gaweł and co-workers, who proposed an improved method for synthesizing indolizinequinones[51] from methylquinones, iodine, and pyridine derivatives in DMSO, building upon Delcanale's earlier protocol.[65,66] The resulting indolizinequinones were further derivatized in a one-pot process to produce substituted π-expanded indolizines. The synthetic route involves the initial addition of acetylene derivatives to quinone *via* a *n*-butyllithium-mediated reaction, forming an intermediate that then undergoes reductive elimination using $SnCl_2$ in 10% aqueous HCl (Scheme 6). The final compounds display notable photophysical properties, with absorption and emission maxima in the visible region. The most pronounced bathochromic shift was observed for a π-extended system with six fused aromatic rings (λ_{abs} = 594 nm, λ_{em} = 621 nm, Φ_{fl} = 17%).

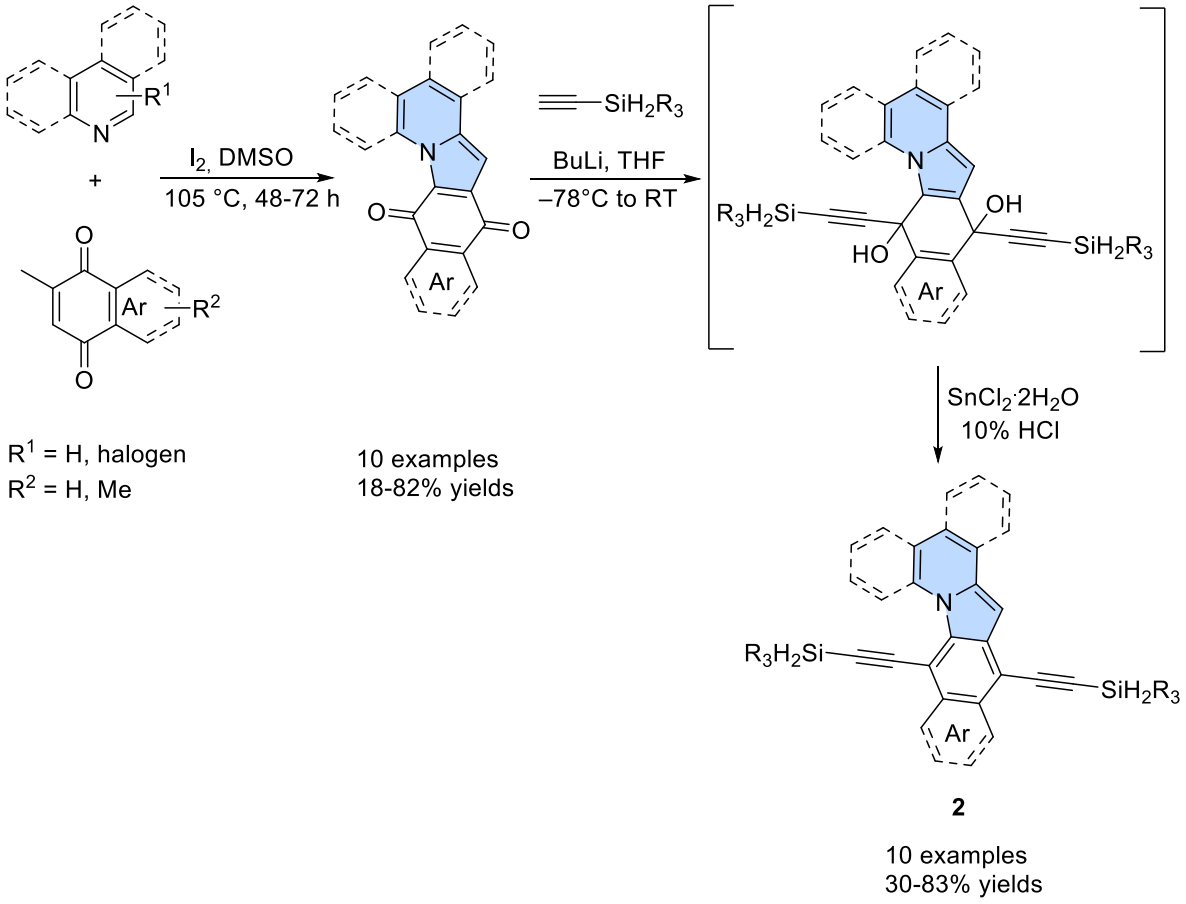

Scheme 6: *Synthesis of π-expanded indolizines from quinones.*

Long before the recent developments in benzo[1,2-*b*]indolizines, a different structural isomer, benzo[*a*]indolizine (**3**), had already been explored. In 1966, Kröhnke *et al.,* described the synthesis of these red fluorescent derivatives using a three-step methodology (Scheme 7).[67] The sequence begins with the quaternization of pyridine using (Hal)CH_2(EWG) reagents, followed by a nucleophilic aromatic substitution (SNAr) of the resulting pyridinium salts with 1-chloro-2,4,6-trinitrobenzene, and concludes with a 1,5-electrocyclization, which forms the five-membered central ring. The mechanism of the last key step relies on the formation of vinylpyridinium ylides which are prone toward 1,5-electrocyclization. Notably, despite the structural similarity to benzo[*b*]indolizines,

benzo[*a*]indolizines have remained relatively unexplored and were only recently brought back into focus.

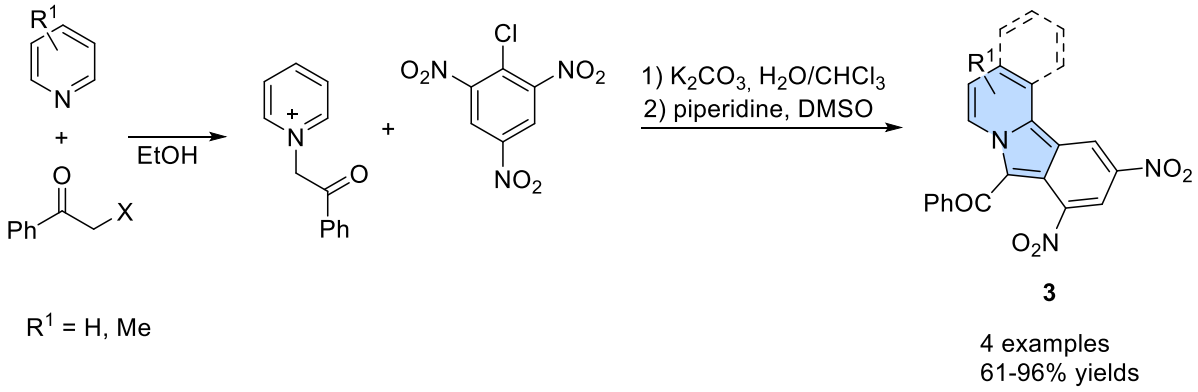

Scheme 7: *Synthesis of benzo[a]indolizines from picryl chloride*

1.3.2. Pyrano-indolizinones and coumarin-indolizines

In the 80s, Kakehi *et al*. synthesized a new class of molecules, pyrano[2,3-*b*]indolizin-2-ones (**4**), which can be considered as analogues of coumarins and benzocoumarins (Scheme 8).[68] Their synthetic route comprised four steps: (1) quaternization of pyridines with ethyl 2-bromoacetate; (2) Dieckmann condensation to form the indolizin-2-ol intermediate; (3) Friedel-Crafts reaction of the intermediate with diethyl 2-(ethoxymethylene)malonate; (4) final intramolecular cyclization *via* transesterification with the formation of the lactone ring. It should be noted that the last three steps occur in one pot. Interestingly, the authors reported strong fluorescence for these compounds, although this property was not investigated further.

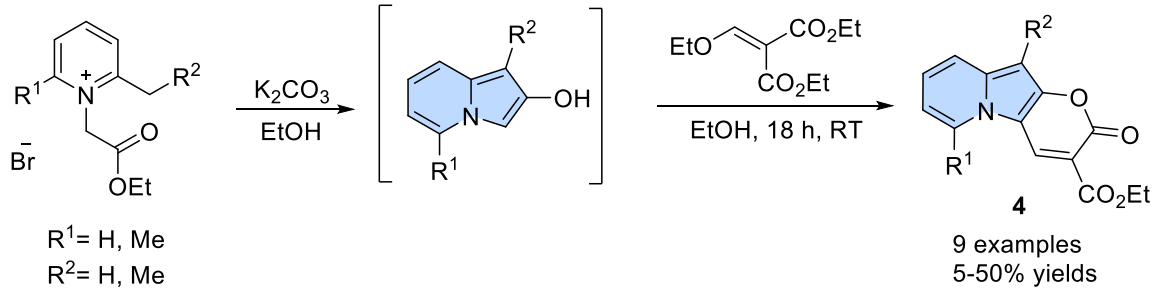

Scheme 8*: Synthesis of pyrano-indolizinones from pyridinium salts*

A coumarin-fused indolizine was recently reported by Rusanov *et al*., who developed a novel synthetic methodology for the construction of pentacyclic lamellarin analogues (**5**) lacking the typical E-ring (Scheme 9).[69] The key step involved generating an indolizine intermediate *via* a [3 + 2] cycloaddition reaction. This reaction used pyridinium ylides, α-nitrostilbenes, and benzoyl peroxide as an oxidant. Subsequent transformations included O-demethylation of the ortho-methoxy group and a final lactonization step, leading to the formation of a coumarin-fused indolizine product. The authors also reported a preliminary biological evaluation of these new lamellarin analogues; however, no data on their emissive properties were provided.

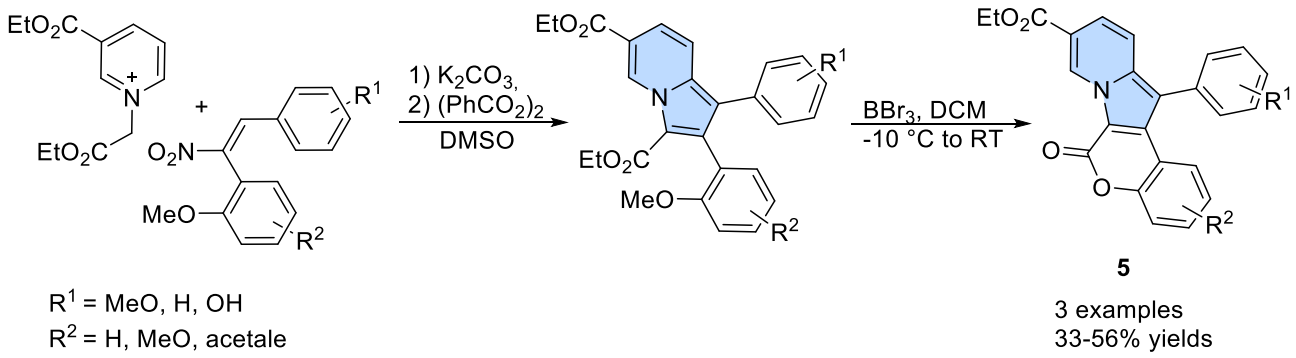

Scheme 9: *Synthesis of coumarin-indolizines*

1.4. π-Extended indolizines

Another creative use of indolizines is their incorporation into extended π-systems through π-conjugation. Over the past decade, significant advancements were made by Delcamp's group in the development of extended-indolizine dyes capable of operating in the short-wave infrared (SWIR) region (Scheme 10).[70] A key breakthrough was the development of xanthene-indolizine dyes with NIR-II (1000–1700 nm) emission that was achieved via a successful C-H bond functionalization strategy. This approach enabled the coupling of an electron-rich indolizine donor with an electron-deficient xanthene core, yielding the dye **RhIndz** (**6**). The optimal conditions for this transformation involved $PdCl_2(PPh_3)_2$ as the catalyst, KOAc as the base, and NMP as the solvent at 110 °C. The fluorescent properties of RhIndz were recorded as follows: (λ_{abs} = 920 nm, λ_{em} = 1092 nm, Φ_{fl} = 0.03%).

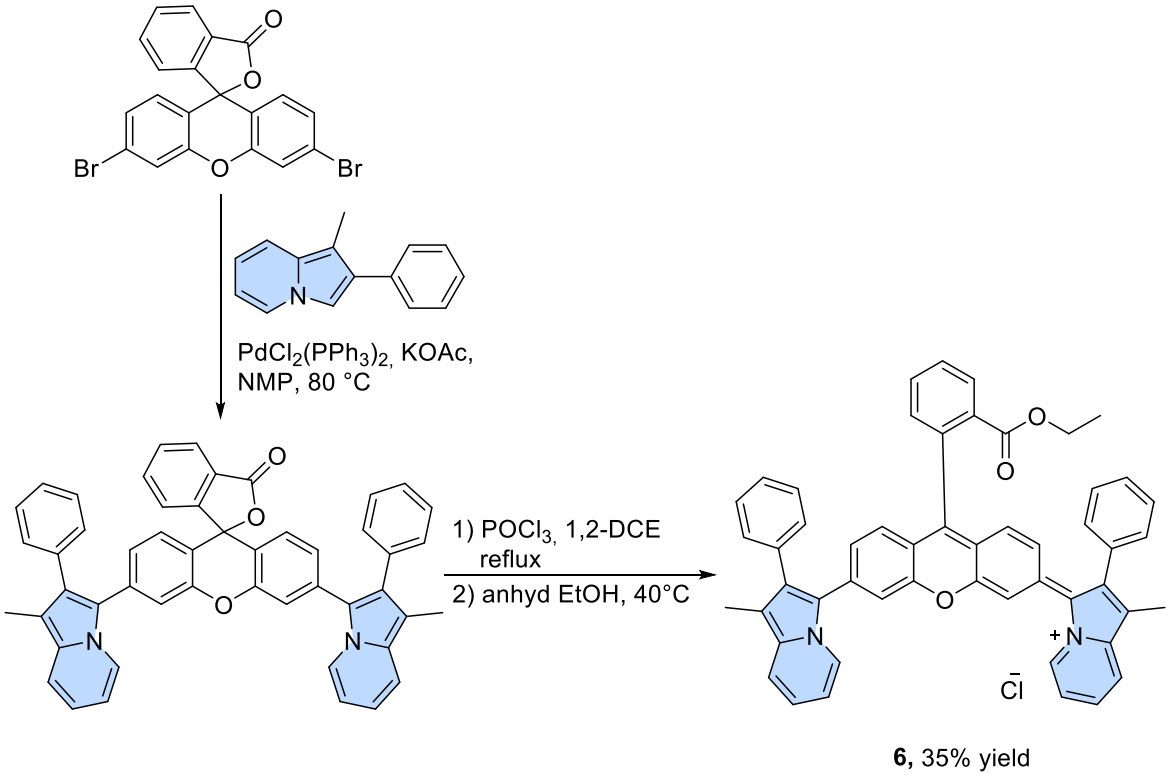

Scheme 10: *Synthesis of xanthene dyes possessing indolizines as donors (RhIndz)*

Building on this platform, in 2024 the same research group achieved a bathochromic shift of absorption and emission by substituting the xanthene oxygen atom with silicon and introducing a

dimethylaminoaryl substituent on the indolizine core (Scheme 11). This led to the synthesis of three fluorophores **SiRos** (**7**) through a sequence involving deoxygenation, silylation-cyclization, oxidation, and palladium-catalyzed C–H activation to install the indolizine donors.[71] Final conversion to the desired perchlorate salts was completed via a Grignard reaction followed by acidic work-up. These dyes (**SiRos1300**, **SiRos1550** and **SiRos1700**) exhibit λ_{em} of 1,300 nm, 1,557 nm, and 1,700 nm in DCM, with quantum yields of 0.0056%, 0.0025%, and 0.0011%, respectively.

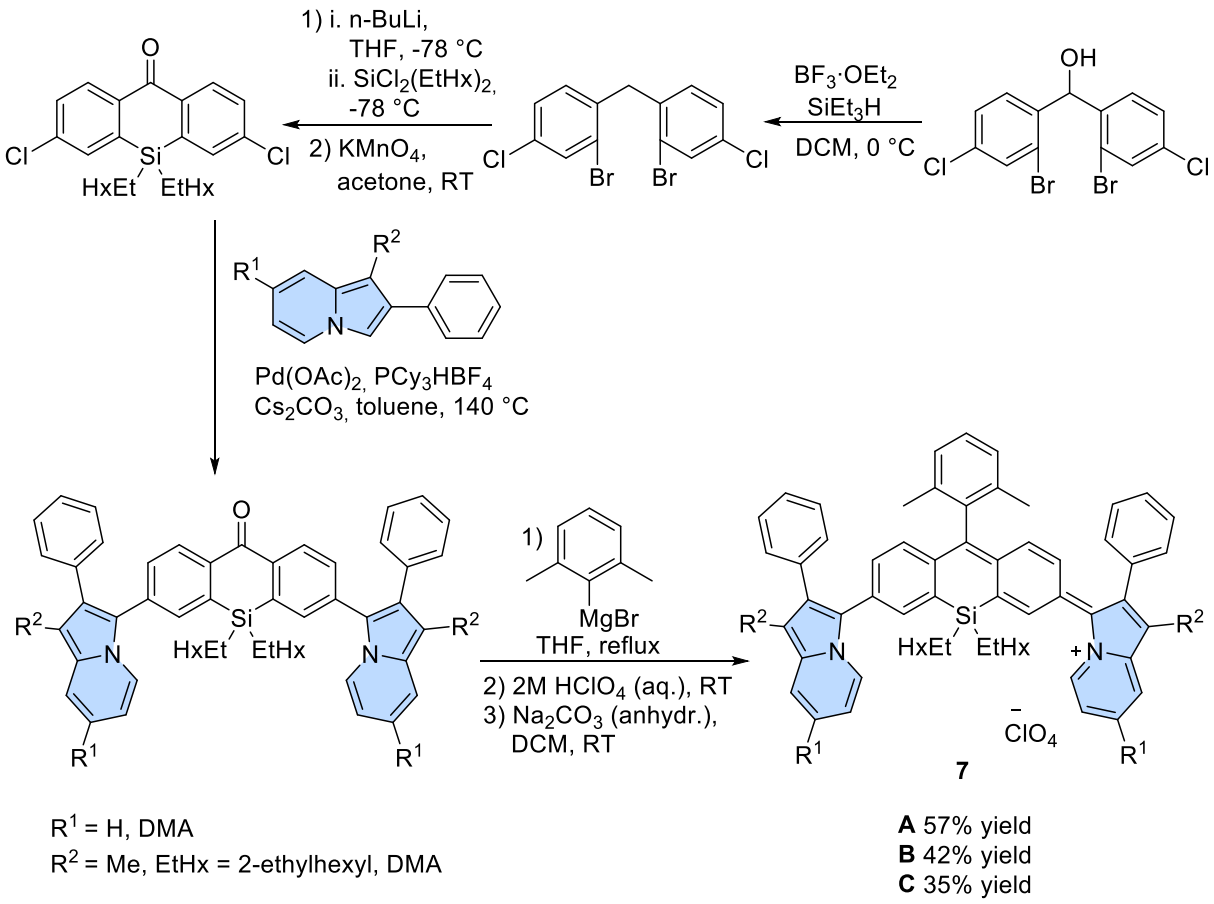

Scheme 11: *Synthesis of SiRos1300, SiRos1550 and SiRos1700*

To further explore the effect of heteroatom substitution, Delcamp *et al.* later replaced the bridging oxygen with a phosphoryl group (P=O), yielding **PRos1450** (**8**), which emits at 1,450 nm red-shifted relative to **SiRos1300**.[72] The synthetic route mirrored that used for the previous analogues, except that in this case, $PhPCl_2$ was used as the phosphorus source in the synthesis of the xanthene ring.

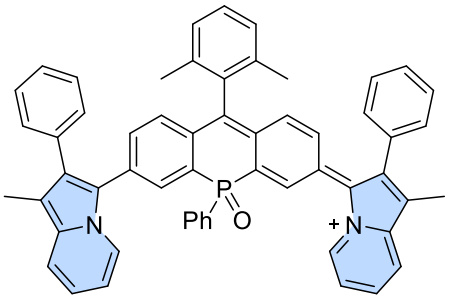

8, 31% yield

Scheme 12: *Synthesis of PRos1450*

2. Results and Discussion

2.1. Synthesis and Photophysical Properties of Substituted Benzo[a]indolizines

My first project focused on revisiting Kröhnke's synthesis of benzo[*a*]indolizines and investigating their photophysical properties.[73] I chose to focus on this specific isomer of benzo-indolizines due to its promising fluorescent properties, briefly mentioned by the authors, and because it is significantly less explored compared to other isomers. In Kröhnke's work the synthesis (Scheme 13) involved the use of pyridinium salts and 1-chloro-2,4,6-trinitrobenzene, a compound known for its explosive nature in a two-step methodology. The first step was carried out with K_2CO_3 in $CHCl_3$, followed by a second step using piperidine in DMSO.[67] The obtained structure was decorated with two nitro groups on the benzene ring and one ketone on the pyrrole moiety. From a photophysical perspective, such electron-withdrawing groups are generally responsible for hypsochromic shifts in both absorption and emission, as well as a quench in fluorescence emission due to enhanced intersystem crossing (ISC). Nevertheless, authors observed in structure **9aNO** a red fluorescence which was worth investigating further.

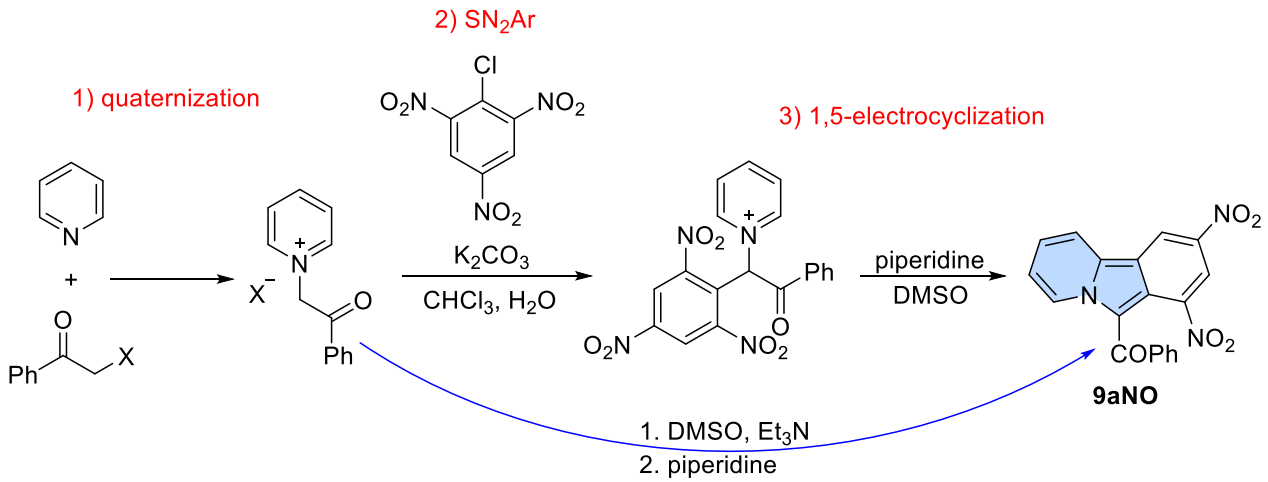

Scheme 13: *Kröhnke's synthesis of Benzo[a]indolizines*

Taking it into account, my whole research focus was devoted to obtaining benzo[*a*]indolizines bearing different substituents, using tailored building blocks to investigate how structural modifications influence their optical properties.

Initially, three derivatives (**9aCF**, **9aCN**, **9aCO**) incorporating CO_2Me, CN and CF_3 in position Y were obtained in 20-30% yield (Scheme 14). This was possible by following Kröhnke's first methodology and substituting the 1-chloro-2,4,6-trinitrobenzene with the less dangerous 4-chloro-3,5-dinitrobenzene derivatives. These structures, however, exhibited weak fluorescence indicating a limited ability to modulate the photophysical properties through variations at position Y alone and suggesting a significant influence of the substituent at position R^1, which in all three cases was a carbonyl group (COPh). Thus, I decided to try modulating the properties by replacing the COPh group at position R^1 with a cyano group (CN) (Scheme 15). Indeed, this change resulted in a novel compound obtained in 30% yield (**9cCF**) and showing a visibly higher fluorescence emission, thereby confirming the critical role of the substituent at position R^1 in tuning the photophysical behavior of the benzo[*a*]indolizine scaffold.

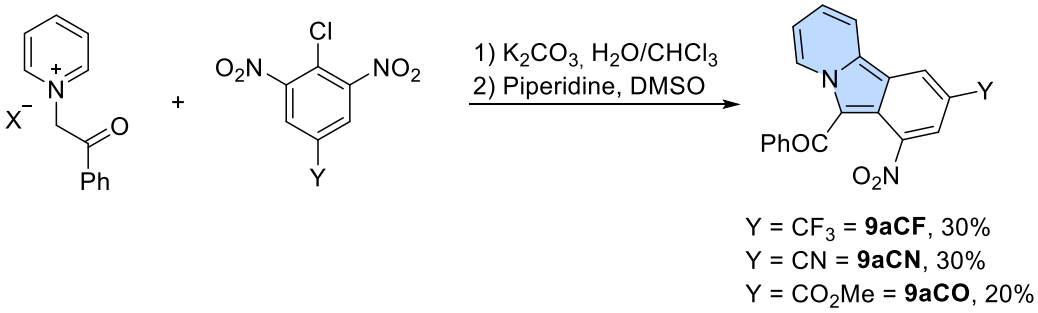

Scheme 14: *Kröhnke's method for the synthesis of benzo[a]indolizines*

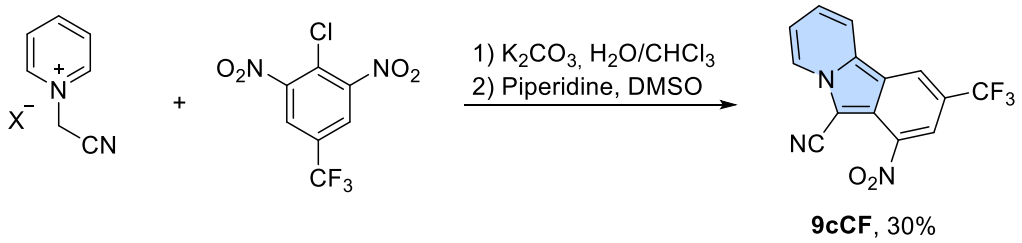

Scheme 15: *Kröhnke's method for the synthesis of* ***9cCF***

From this point onwards, I focused on improving the synthetic methodology with the aim of increasing products' yields and reducing the number of synthetic steps. Compound **9cCF** was selected as a model for optimization studies. A few years after the initial publication on this topic, an improved protocol was proposed, which employed a one-pot strategy using Et_3N and piperidine added sequentially in DMSO (Scheme 13, blue arrow).[74] Building upon this approach, I tested various organic bases such as DBU and piperidine, as well as inorganic bases including K_2CO_3, KOtBu, CsOPiv, and Cs_2CO_3, the latter proving to be the most effective. In addition, several polar aprotic solvents were screened, including DMSO, DMPU, NMP, and sulfolane. Sulfolane was ultimately selected due to its superior performance under the chosen reaction conditions. Interestingly, increasing the reaction temperature and duration did not lead to further improvements in yield. Nevertheless, with the optimized conditions, I was able to improve the yield of **9cCF** from the previously reported 30% to 68%.

Compounds **9cCN** and **9cCO** were synthesized, followed by the derivatives **9dCF**, **9dCN**, and **9dCO** obtained by introducing a different electron-withdrawing group (CO2*t*Bu) at position R^1. Each substituent at position Y influenced the reaction outcome, highlighting not only their effect on the photophysical properties but also on the chemical reactivity (Scheme 16).

Next, an additional substituent was introduced into the system at position R^2, employing 4-substituted pyridines. Although this modification proved detrimental to reactivity, it still allowed the isolation of compounds **9eCF**, **9eCN**, **9eCO**, with yields around 20% and **9fCO** in 13% yield. Pyridine with EWG in position R^2 were less reactive, but what turned out to be even more interesting is that also pyridine with EDG showed the same behavior.

To improve the reactivity of the 4-substituted pyridines a new reaction condition was investigated using **9eCN** as the model. The use of *tert*-butylimino-tri(pyrrolidino)phosphorane (BTPP) DMSO proved to be optimal for this dye but not so efficient for **9eCF** and **9eCO** (Scheme 16). These results reaffirmed the criticality of the system to substituent effects in the *para* position of the pyridine ring.

Alternative approaches were explored to check the reactivity on the benzene ring. However, neither 1-chloro-2,4-dinitro-6-trifluoromethylbenzene nor 2-chloro-3,5-dinitropyridine led to the formation of the desired products. Similarly, less activated C-Hal bond like those in 2,4-dinitrofluorobenzene or 2,4-dichloro-1,5-dinitrobenzene, also proved ineffective, suggesting that the presence of two NO_2 in ortho position relative to Cl is crucial for reactivity, limiting the number of suitable starting materials.

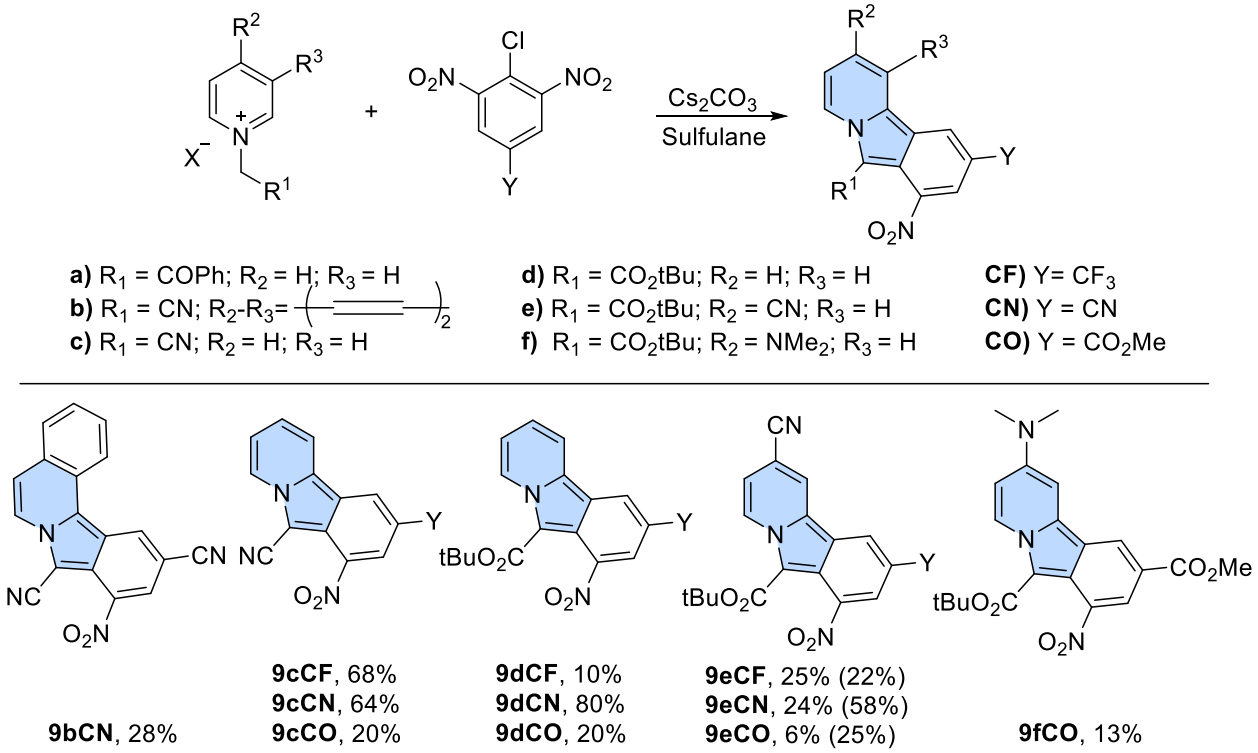

Scheme 16: *Scope of benzo[a]indolizines*

Additional modifications to the available products were possible due to the presence of reactive functional groups such as NO_2 and CO_2t-Bu. A classic reduction of the nitro group to amino group in **9cCF** led to structure **10**. While in a different transformation, a reverse Friedel-Crafts reaction TFA mediated was used to cut out the ester group in compound **9dCN,** affording structure **11** with a free R^1 position (Schemes 17 and 18)

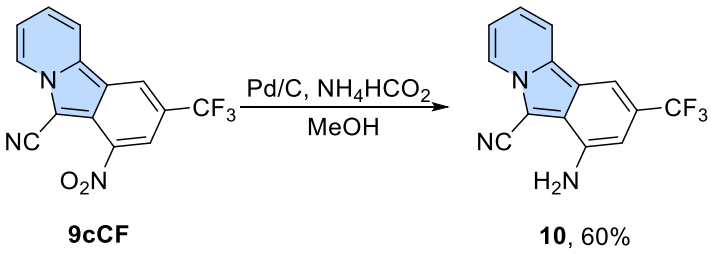

Scheme 17*: Post-functionalization of* ***9cCF***

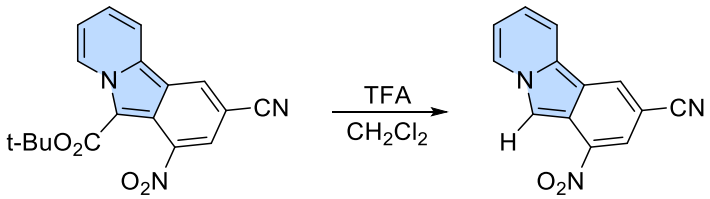

9dCN **11**, 35%

Scheme 18: *Post-functionalization of* ***9dCN***

To unravel the photophysical properties of the synthesized benzo[*a*]indolizine derivatives, I recorded absorption and emission spectra for all the obtained structures in DCM and toluene and compared them to the parent benzo[*a*]indolizines exhibiting fluorescence quantum yield of 14% in DCM with λ_{abs} = 368 nm and λ_{em} = 498 nm.[75] Most of the new compounds displayed λ_{abs} between 400-500 nm and emission localized in the orange-red region of the visible spectrum with Φ_{fl} ranging from negligible to 60%. These results demonstrate a significant bathochromic shift relative to the unsubstituted benzo[*a*]indolizine core and its isomer, benzo[1,2-*b*]indolizine (**2**-**3**), indicating a strong influence of both substituents and the position of the nitrogen atom within the core on their photophysical behavior. A marked solvatochromism was observed when moving from toluene to DCM consistent with an intramolecular charge transfer (ICT) process that was later confirmed by computational studies.

A comparative analysis of molar absorptivity (solid lines) and normalized emission spectra (dashed lines) for **9aCO**, **9cCO**, **9dCO**, **9eCO**, and **9fCO** (represented in pink, orange, green, blue, and black, respectively) in toluene revealed the impact of substituents on the pyridine and pyrrole rings, while maintaining fixed CO_2Me and NO_2 groups on the benzene moiety. Notably, the introduction of an electron-donating group (EDG) such as NMe_2 on the six-membered ring resulted in the largest Stokes shift and the lowest fluorescence quantum yield (<0.1%). Conversely, replacing the COPh group at position R^1 with a cyano group **9cCO** led to the smallest Stokes shift and the highest Φ_{fl} (0.58%) (Fig. 2a).

A similar comparison was conducted for compounds **9cCF**, **9cCN**, and **9cCO** (blue, red, and orange), all bearing a CO_2tBu group at position R^1 and varying substituents at position Y, in DCM. The results showed minimal variation in their photophysical properties, confirming that the substituent at position R^1 plays a critical role, while the effect of substituents at position Y is negligible (Fig. 2b). This was further supported by the comparison of **9dCN** (orange) and its deprotected analog **11** (purple), where a significant bathochromic shift in λ_{abs} was observed, whereas the emission wavelength remained largely unchanged (Fig. 2c). For both compounds, photostability measurements were performed in comparison to Rhodamine 6G. The results showed that both compounds are less stable than Rhodamine 6G but notably lower stability of **11** supported the already known behavior of indolizine-based dyes, confirming that position R^1 is a hotspot for electron density and highly reactive. (Fig 3)

An another particularly interesting observation emerged from this photophysical analysis: contrary to expectations, the NO_2 group, typically associated with fluorescence quenching, contributed to a bathochromic shift in both absorption and emission spectra, along with relatively large fluorescence quantum yields. When comparing compound **9cCF** with its reduced analog **10** (bearing an NH_2 group instead of NO_2), a drop in emission intensity (38% vs 26%) and a hypsochromic shift of both λ_{abs} (488 vs 377 nm) and λ_{em} (603 vs 495 nm) were observed.

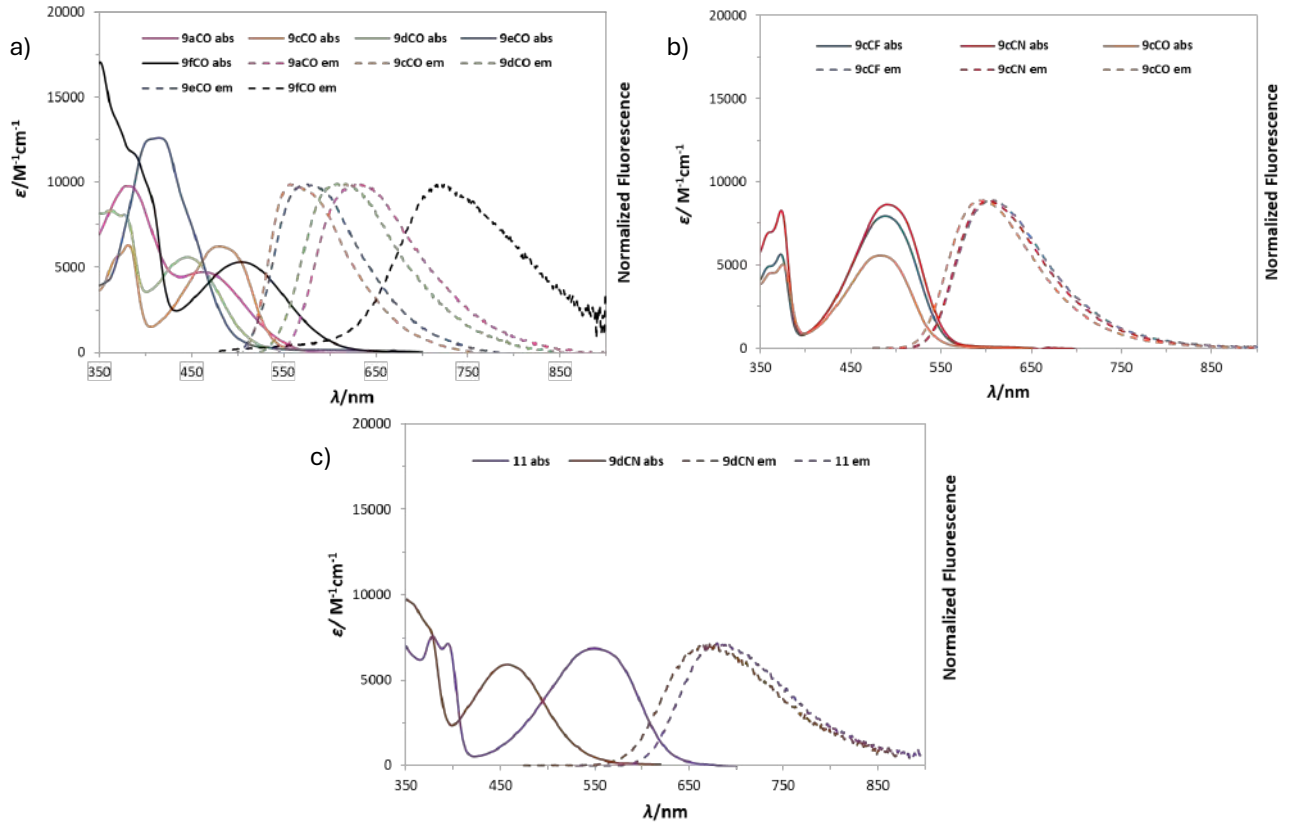

Figure 2: *a) Absorption and emission spectra of dyes **9aCO**, **9cCO**, **9dCO**, **9eCO**, and **9fCO** (pink, orange, green, blue, and black) in toluene, b) Absorption and emission spectra of **9cCF**, **9cCN**, and **9cCO** in DCM (blue, red, and orange) c) Absorption and emission spectra of **11** and **9dCN** in DCM (purple and brown)*

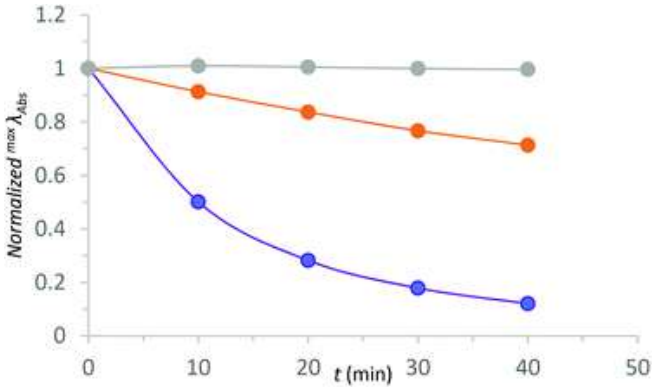

Figure 3: *Photostability of compound **11** compared to **9dCN** and Rhodamine 6G*

Theoretical calculations carried out by collaborators corroborated my experimental findings and confirmed the limited influence of substituents at position Y. Moreover, the calculations highlighted the key role of the NO_2, which acts as a strong electron-withdrawing group (EWG) and facilitates intramolecular charge transfer (ICT) with the electron-rich pyrrole ring, functioning as an electron-donating group (EDG). As expected, the donor strength of the pyrrole was modulated by the substituent at position R^1. Surprisingly, however, substituents typically classified as EWGs, such as CN, COPh, and CO_2tBu, exhibited donor-like behavior in this molecular framework, acting as secondary donors and participating in ICT.

In addition, simulated fluorescence quantum yields Φ_{fl} aligned well with the experimental data and provided further insight into structure-property relationships. The calculations explained the

dramatic drop in fluorescence efficiency observed for compounds bearing bulky groups at position R^1. These substituents induce significant distortion from planarity, which enhances intersystem crossing (ISC) due to a reduced singlet–triplet (S-T) energy gap and increased spin–orbit coupling (SOC), particularly evident in compound **9fCO**.

Conversely, derivatives from series ***9b*** and ***9c***, bearing smaller EWGs, exhibited relatively large S-T gaps (> 0.3 eV) and negligible SOC, supporting their higher fluorescence efficiency. The remaining compounds displayed intermediate photophysical behavior, consistent with moderate structural distortion and partial SOC contribution.

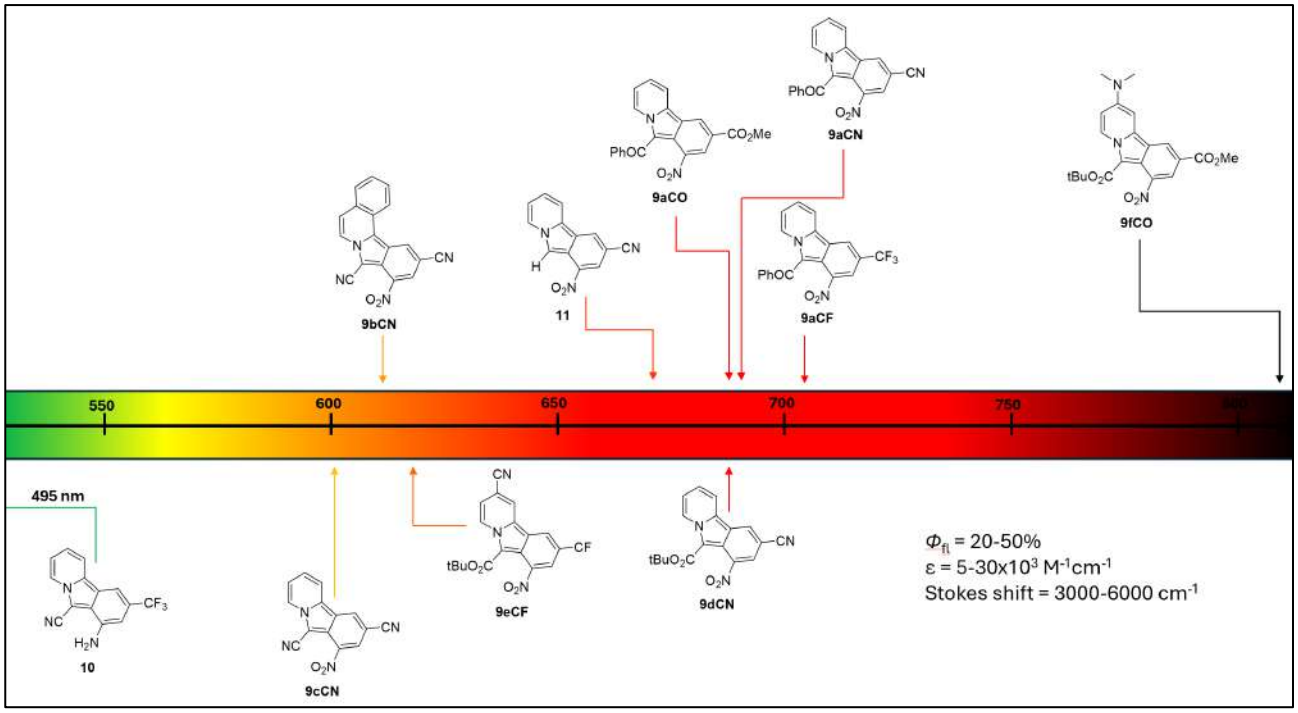

Figure 4: *Visual comparison of benzo[a]indolizine derivatives' emission in DCM.*

2.2. Synthesis and Photophysical Properties of Substituted Pyrano[2,3-b]indolizin-2-ones

The second project I worked on followed the same vision; I wanted to further investigate another type of nearly forgotten, but extremely promising class of π-expanded indolizines. Between the 80s and the 90s Kakehi and co-workers developed different methodologies to synthesize derivatives of 2-oxo-2H-pyrano[2,3-*b*]indolizine-3-carboxylates, structures that can be considered analogs of coumarins exhibiting interesting fluorescent properties and potential applicability in bioimaging. Although authors proposed different paths, all involved long time reaction (7 days) and afforded relatively low product yields (38%), thus opening the doors to methodology improvement and photophysical investigations.

The proposed reaction mechanism involved the synthesis of pyridinium salts, a Dieckman condensation to obtain the indolizin-ol intermediate followed by a Friedel-Crafts reaction, and a last step being an intramolecular transesterification to obtain the lactone ring. The last three steps occur in one pot (Scheme 19).

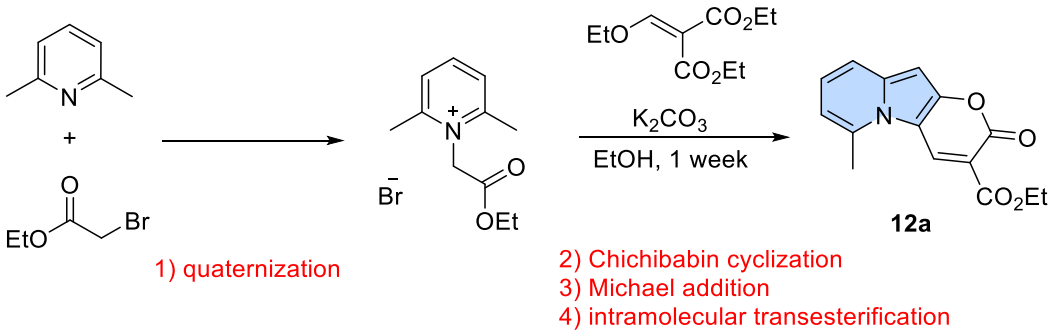

Scheme 19: *Kakehi's synthesis of pyrano[2,3-b]indolizin-2-ones*

For the development of an improved reaction condition compound **12a** was used as a model. Initial changes of the solvent, (DMF instead of EtOH) and on the base (NaOEt instead of K_2CO_3) did not lead to the expected outcome and caused me to rethink my plan. Considering that the mechanism involved the formation of a critical intermediate I thought that the best would be to allow sufficient time for the first reaction to happen before the addition of the malonate. Consequently, in this 2-steps approach different bases were studied in the classical solvent used (EtOH), and I found the best to be Cs_2CO_3 affording the product **12a** in 50% yield.

Using this optimal condition, I evaluated the substrate scope and a total of eight new structures were synthesized starting from different pyridinium salts. 'Formal' picolinium salts reacted as expected and yielded pyrano-indolizines (**12a**, **12b**, **12c**) possessing a hydrogen or an alkyl substituent in position R^5 (Scheme 20). Similar but cyclic pyridinium salts such as 2,3-cyclopentenopyridinium and 5,6,7,8-tetrahydroquinolinium were also tested, but giving two different outcomes. The first one failed to give the product while the latter generated the expected product **12d** in 30% yield. Reactivity was also good for expanded pyridinium salts like 2-methylquinolinium and 1-methylisoquinolinium and two expanded products with free R^5 position (**12e**, **12f**) were achieved in 30 and 28% yield. Lastly, with the aim of having EWG in position C-5 α-picolines with EWG (2-Py and CO_2Et) in the methylene group were used and products **12g** and **12h** were obtained in 44% and 5% yield respectively. Differently from the previous cases the first reaction step, the formation of the indolizin-ol happened, without the need of a base, right after

the quaternization. Interestingly, both EWG and EDG in para position to the pyridine prevented the synthesis of the final product.

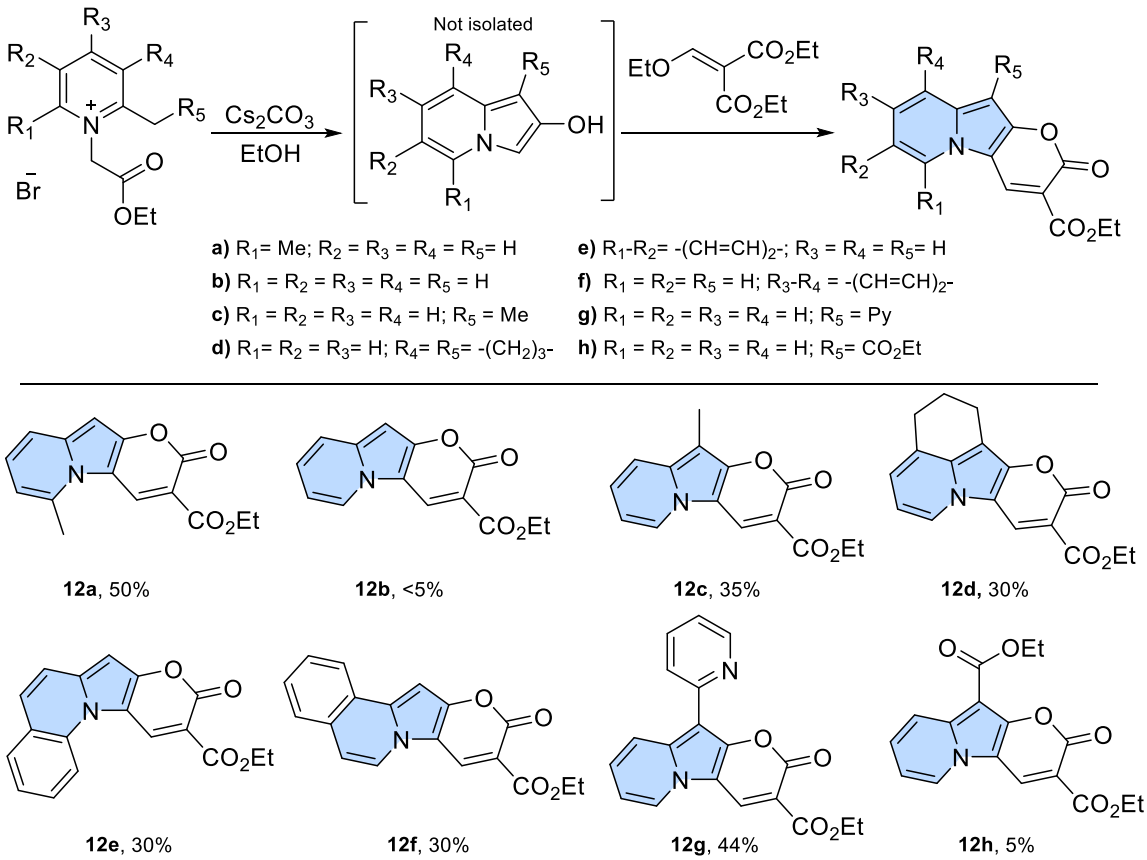

Scheme 20: *Scope of pyrano[2,3-b]indolizin-2-ones*

In order to achieve a broader variety of substituents in C-5, I used structure **12a** for further functionalization. The highly electron-rich carbon was a good candidate for direct arylation and products **13aa**, **13ab**, **13ac** were obtained in 17-60% yield (Scheme 21).

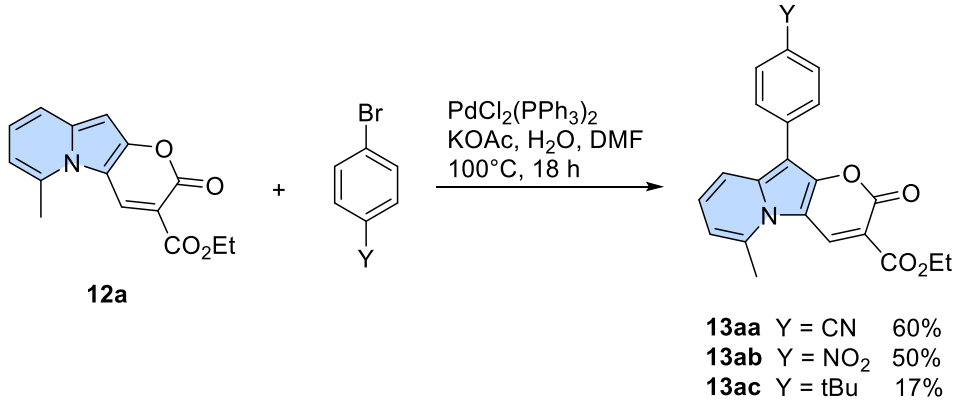

Scheme 21: *Post-functionalization of dye* ***12a***

Then, I also envisioned in the Vilsmeier-Haack formylation the opportunity not only to get a different EWG, but mostly the chance to obtain a new styryl dye through a sequent Knoevenagel condensation (Scheme 22), with potential for cell staining. In these last steps compounds **14a** and **15a** were isolated in 83 and 37% yields respectively.

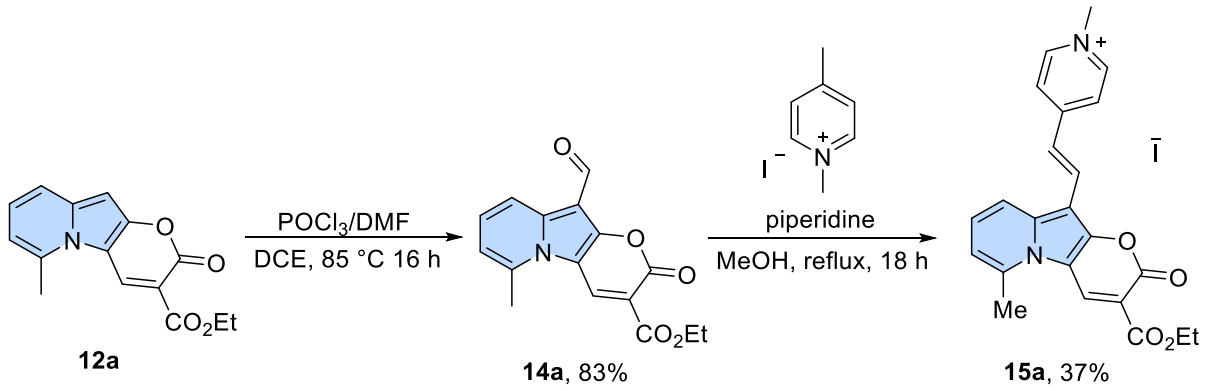

Scheme 22: *Post-functionalization of dye* ***12a***

For this class of compounds Uv-Vis absorption and emission were measured in toluene, DCM and DMSO and compared with indolo-coumarins like 11-benzyl-7-hydroxyisochromeno[4,3-*b*]indol-5-one (Φ_{fl} = 42% in DCM, with λ_{abs} = 382 and λ_{em} 496) and methyl 2-oxo-4-(pyrrolidin-1-yl)-2,4a,5,9b-tetrahydropyrano[3,2-*b*]indole-3-carboxylate (λ_{abs} = 335 in EtOH). Results showed a significant bathochromic shift for absorption (420-470 nm) while emission remained in the same range (440-520 nm), and a solvatochromism emerged when moving from apolar to polar solvents.

The distinctly different fluorescence emissions of compounds **12a**, **12b**, and **12c**, clearly discernible to the naked eye and supported by the recorded data, prompted me to begin analyze the impact of substituent positions on this core structure, even for simple groups such as methyl. In fact, having Me in R^5 (**12c**) caused a bathochromic shift compared to **12b** while the same group in R^1 (**12a**) caused a hypsochromic shift of bands. These findings were later rationalized by my colleague as a consequence of the largest change in HOMO energy for **12c** with methyl in R^5 (Fig. 5a).

Interestingly, the expansion of the π-system which usually is responsible for shifts towards the red region, in these structures was dependent on the actual direction of the expansion. Dye **12f** has hypsochromically shifted emission compared to dye **12b**, and *vice versa* **12e** displayed a slight shift of the signals towards lower energies (Fig. 5b), computational calculations computed energies for these two systems as such: E_{LUMO}(**12e**) < E_{LUMO}(**12f**).

Further investigations into the effect of different substituents in R^5 on the photophysics clarified the role of EWG in **14a** (CHO λ_{abs} = 426 nm and λ_{em} = 448 nm), EDG in **12c** (Me λ_{abs} = 468 nm and λ_{em} = 494 nm), and the π-extension of **13aa** (4-CN λ_{abs} = 453 nm and λ_{em} = 490 nm), and **13ac** (4-*t*Bu λ_{abs} = 457 nm and λ_{em} = 514 nm). (Fig. 5c) The presence of the expanded system shifts the absorption and emission to the blue region and an even stronger effect on the same direction is given by the presence of the aldehyde. All the small changes on the spectra caused by the different substituents in R^5 were explained with computational investigation by a slight modification of the HOMO and LUMO of the substituted molecules compared to the parent dye **12b**.

When recording the data for **13ab** (4-NO_2 λ_{abs} = 452 nm and λ_{em} = 491/642 nm), I noticed an increase in the Φ_{fl} in apolar solvents (toluene) compared to the other structure, and the presence of a second peak in the emission in both DCM and DMSO, showing two emission bands overlapping, one at the 'expected' wavelength (491 nm) and another one around 642 nm. To rule out the possibility of the second signal being caused by impurities I recorded excitation spectra and confirmed that both peaks were coming from the investigated molecule. I then hypothesized that this structure, composed of a strong electron donor (2-oxo-pyrano[2,3-*b*]indolizine) and a strong electron acceptor (nitrophenyl), could undergo intramolecular charge transfer (ICT) in polar solvents. This process may

lead to the formation of two distinct excited states, depending on the molecular geometry, thereby enabling two possible emission pathways. This hypothesis was then confirmed by experiments on fluorescence decay (τ_F) and computational simulations which confirmed the presence of both a low emissive and a TICT emissive states.

Finally, I investigated the optical properties of the dye **15a** (λ_{abs} = 509 nm and λ_{em} = 575 nm), a potential cell probe, compared to its precursor **14a** (Fig. 5d). By adding a conjugated pyridinium system, a large red shift on the emission was observed which was later rationalized by my colleague as a consequence of a qualitative change of LUMO from localized on the main indolizine core to localized on the substituent, the same situation was envisioned for **13ab**.

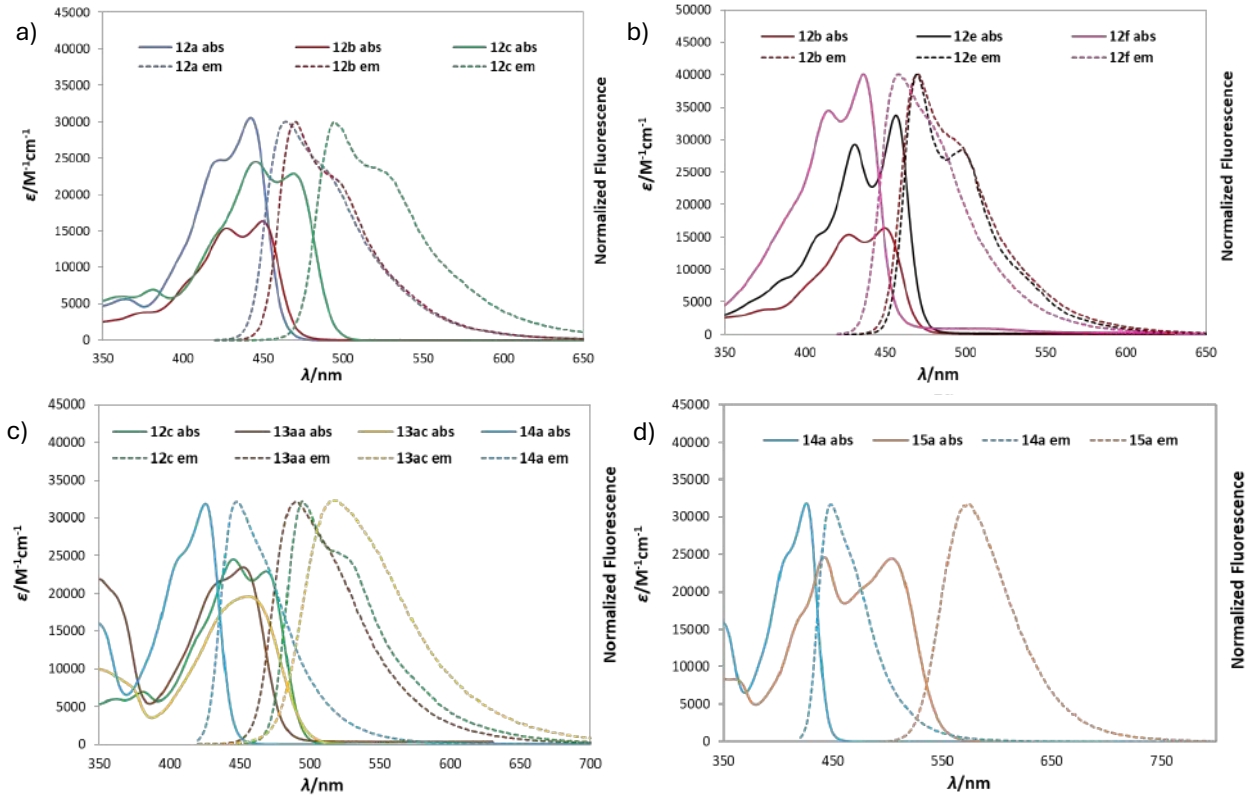

Figure 5: *a) Absorption (solid line) and normalized emission (dashed line) of **12a**, **12b**, **12c** (blue, red, green) b) Absorption (solid line) and normalized emission (dashed line) of **12b**, **12e** and **12f** (red, black, pink) c) Absorption (solid line) and normalized emission (dashed line) of **12c**, **13aa**, **13ac** and **14a** (green, brown, yellow and light blue) d) Absorption (solid line) and normalized emission (dashed line) of **14a** and **15a** (light blue, orange).*

Preliminary cell staining experiments were carried out by collaborators on rat embryonic cardiomyoblast-derived cells H9c2 for dye **15a**, but the styryl dye alone was unable to permeate the cell membrane. Therefore, digitonin was required to facilitate its entry. Once inside the cell, however, compound **15a** exhibited remarkable behavior: it accumulated in the nucleus and along the nuclear membrane, as confirmed by co-localization with the standard nuclear stain Hoechst 33342. Interestingly, unlike the standard dye, **15a** appeared to selectively stain specific subnuclear structures, suggesting potential for more refined nuclear imaging.

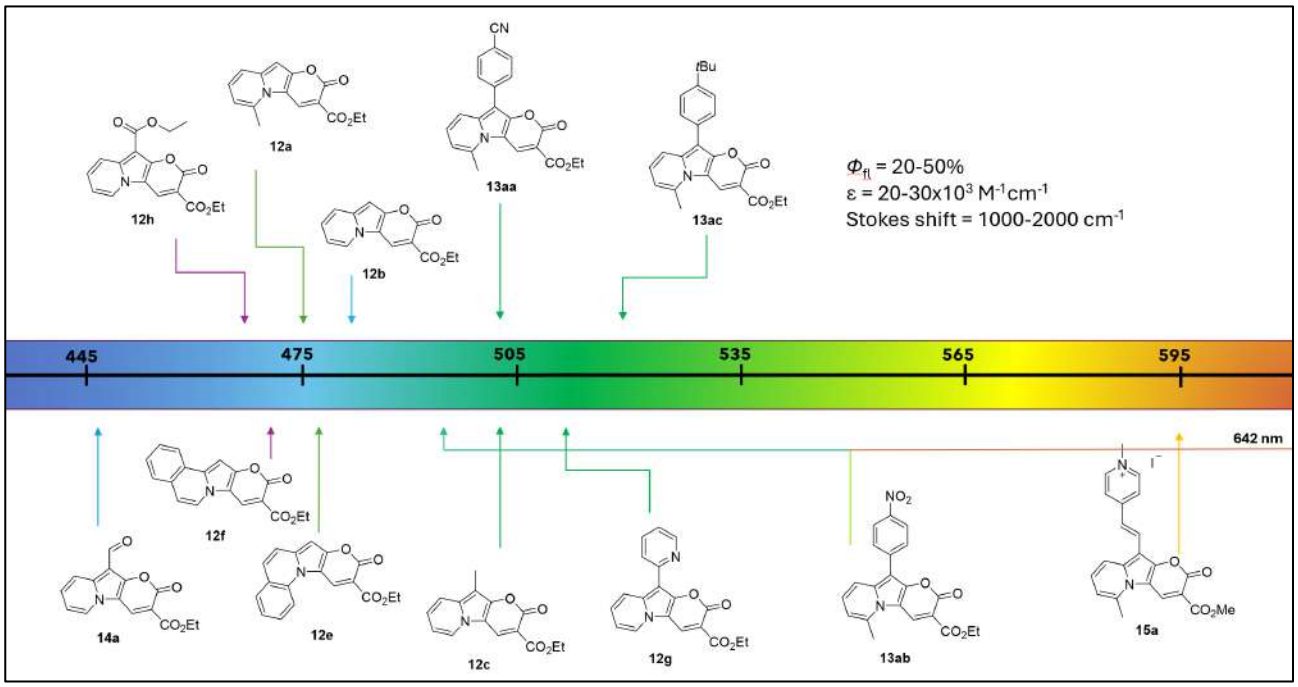

Figure 6: *Visual comparison of pyrano[b]indolizines' emission in DCM*

2.3. Synthesis and Photophysical Properties of Substituted Indolizine-merocyanines (IndMer)

While working on the second project, the idea that the indolizin-ol intermediate could serve as an electron-donating building block for the synthesis of xanthene-like systems emerged. Additionally, the recent work of Delcamp on π-extended rhodol-indolizines **8** emitting in the near-infrared (NIR) region further inspired the conceptual development of this project. In this context hydroxyindolizines should behave in a similar manner to the electron-rich phenols typically used for the synthesis of systems like rhodols but thanks to its stronger electron-donating character, push the optical properties of these new fused systems towards the red region of the UV-vis spectrum compared to classical rhodols.

I employed a Friedel-Crafts alkylation/nucleophilic aromatic substitution, which was previously discovered in our group for the reaction of 2,3,5,6-tetrafluoro-4-hydroxybenzaldehyde with aminophenols.[76] Instead, I used substituted indolizin-ols with the above mentioned aldehyde in xylenes at 80 °C and compound **16a (IndMer)** was obtained in 72% yield.

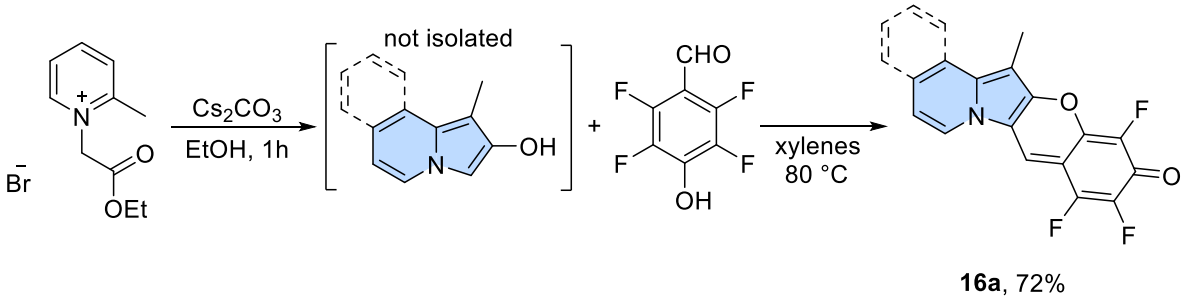

Scheme 23: *Synthesis of* ***IndMer 16a***

The scope of the reaction was assessed by changing the substituents on the indolizine core and 5 additional derivatives were obtained with both electron-withdrawing and slightly electron-donating group in R in yields from 26 to 90% and isolated *via* precipitation thanks to their poor solubility (Scheme 24). The only exception was compound **16d** which was designed to improve the solubility and was purified *via* chromatography. Additionally, a post functionalization on **16e** was performed, quaternization of the pyridyl group led to product **16eMe.**

Using the same methodology other products (**ImpMer** in 24-62 % yields) were achieved through the reaction of 2-hydroxyimidazo[1,2-*a*]pyridine and 2,3,5,6-tetrafluoro-4-hydroxybenzaldehyde in similar conditions (xylenes, 100-150 °C). However, since the focus of this thesis are indolizines, those structures will not be discussed further but were worth mentioning to validate the success and versatility of the presented methodology.

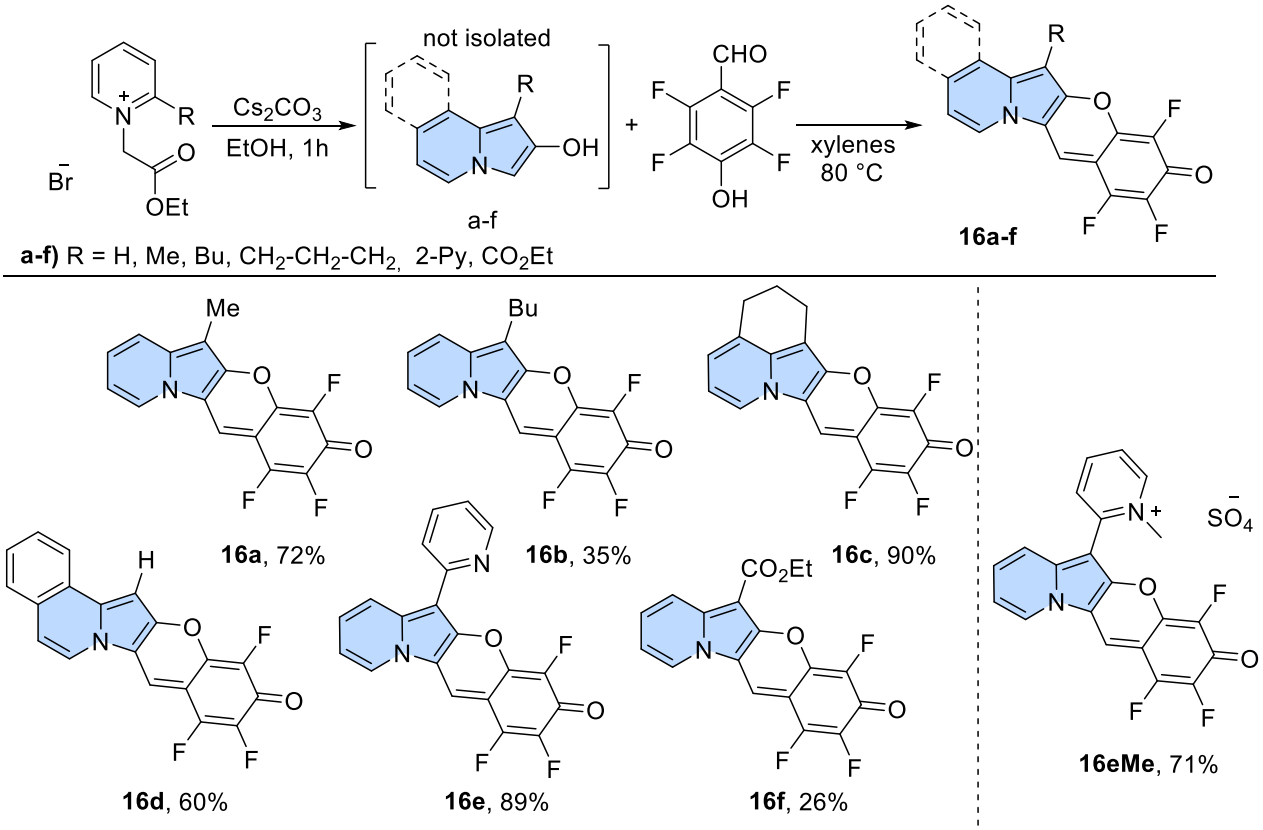

Scheme 24: *Synthesis and scope of indolizine-merocyanines (**IndMer**)*

In order to verify the compatibility of this methodology with different aldehydes having similar characteristics (a halogen atom in vicinal position to CHO, and an electron-deficient character of the aromatic ring) I used 2,3,5,6-tetrafluoro-4-(piperidin-1-yl)benzaldehyde and a coumarin-based aldehyde (Scheme 25). Both aldehydes reacted with 2-hydroxyindolizines affording however completely different products, the first one led to a V-shaped bis-xanthene dye **17** in 10% yield with the incorporation of two indolizines and one aldehyde, while the latter afforded a cyanine-type dye **18** in 27% yield.

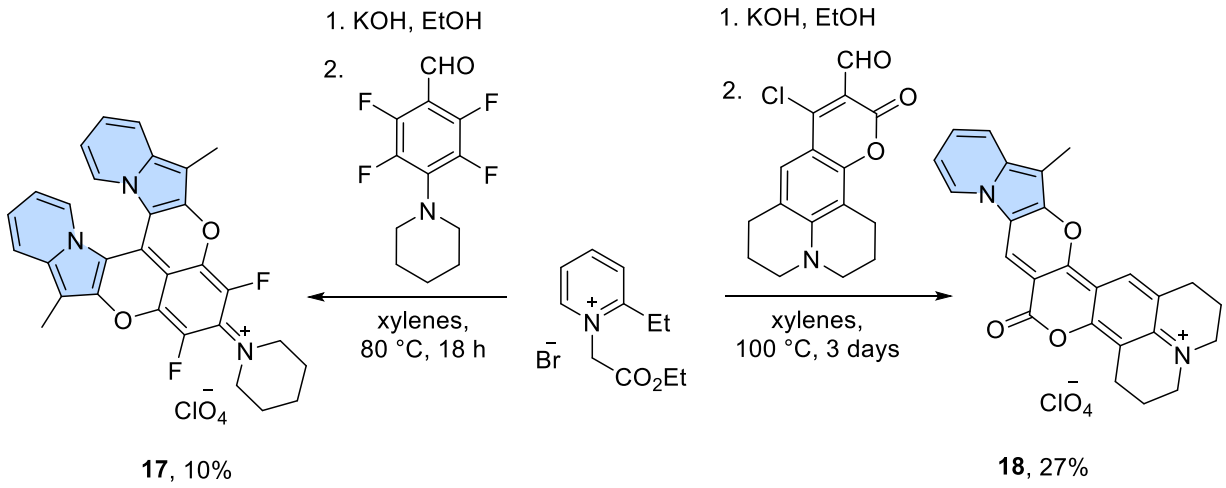

Scheme 25: *Synthesis of two alternative indolizine-cyanine hybrids **17** and **18** from aldehydes **N** and **C**.*

I then performed photophysical characterization with UV-Vis absorption and emission spectra recorded in DCM, THF, DMSO, and for some selected representatives, in aqueous media

(H_2O+DMSO). A comparison was made with classical rhodols and merocyanine dyes and a slight bathochromic shift was observed, but no solvatochromism. This feature was later explained by collaborators who computed a large dipole moment in the ground S_0 state which changes little in the excited S_1. Consequently, no difference in the solute-solvent interaction energies was observed. Moreover, a comparison between the dyes showed no significant influence of the group in position R suggesting that the main properties come from the core structure (Fig. 7a). Stokes shifts are rather small, compatible with the rigidity of the structure and the negligible solvent influence. Surprisingly, for almost all the dyes Φ_{fl} was above 50% even in polar solvent such as DMSO. Structures **17** and **18** have a larger Stokes Shift 50-80 nm DCM, but a decrease in Φ_{fl} (32 and 2%) compared to the previous systems.

More interesting properties were encountered for dye **18** (λ_{abs}^{max} = 624 nm and λ_{em}^{max} = 705 nm) (Fig. 7b) which could be compared to the rhodol-fused coumarin **19** (λ_{abs}^{max} = 586 nm λ_{em}^{max} =625 nm) obtained by Bardi *et al*.[76], and showing intriguing possible applicability for cell imaging (Fig. 8).

This compound showed good solubility and photostability in aqueous media, comparable to Rhodamine 6G, which guided further experiments in cells to assess its potential for organelle visualization.

Confocal microscopy studies performed on compound **18**, by our collaborators in Korea, in HT1080 fibrosarcoma and MRC5 normal human lung fibroblast cells showed high cell permeability and context dependent accumulation in mitochondria and RNA-rich nucleoli when compared to MitoTracker™ Green FM and SYTO RNASelect™ respectively, in both MRC5 and HT1080 cells.

These findings align with the recent reports of single probes exhibiting dual localization, which allows for studying mitochondrial damage and monitoring mitochondrial state in live cells under both physiological and stress conditions.

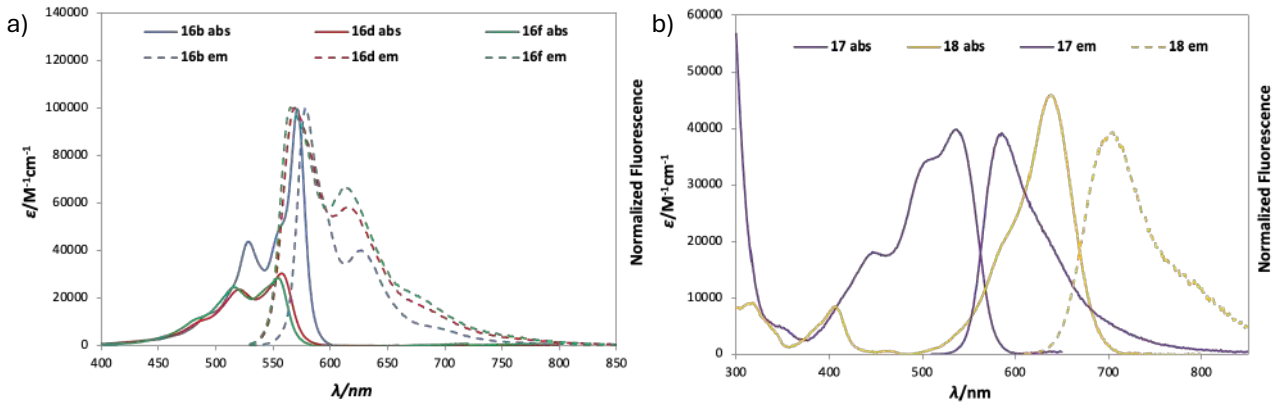

Figure 7: *a) UV-vis absorption spectra (solid lines) and fluorescence spectra (dashed lines) of compounds* ***16b***, ***16d***, *and* ***16f*** *measured in DCM. b) UV-vis absorption spectra (solid lines) and fluorescence spectra (dashed lines) of compounds* ***17*** *and* ***18*** *measured in DCM.*

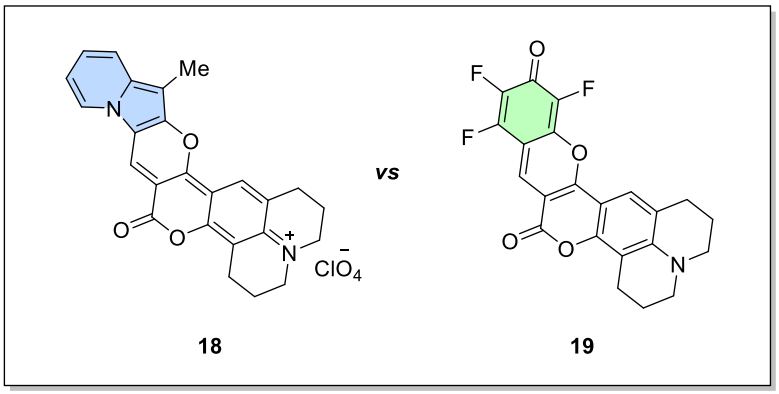

Figure 8: *Structural comparison between an indolizine fused coumarin and a rhodol fused coumarin*

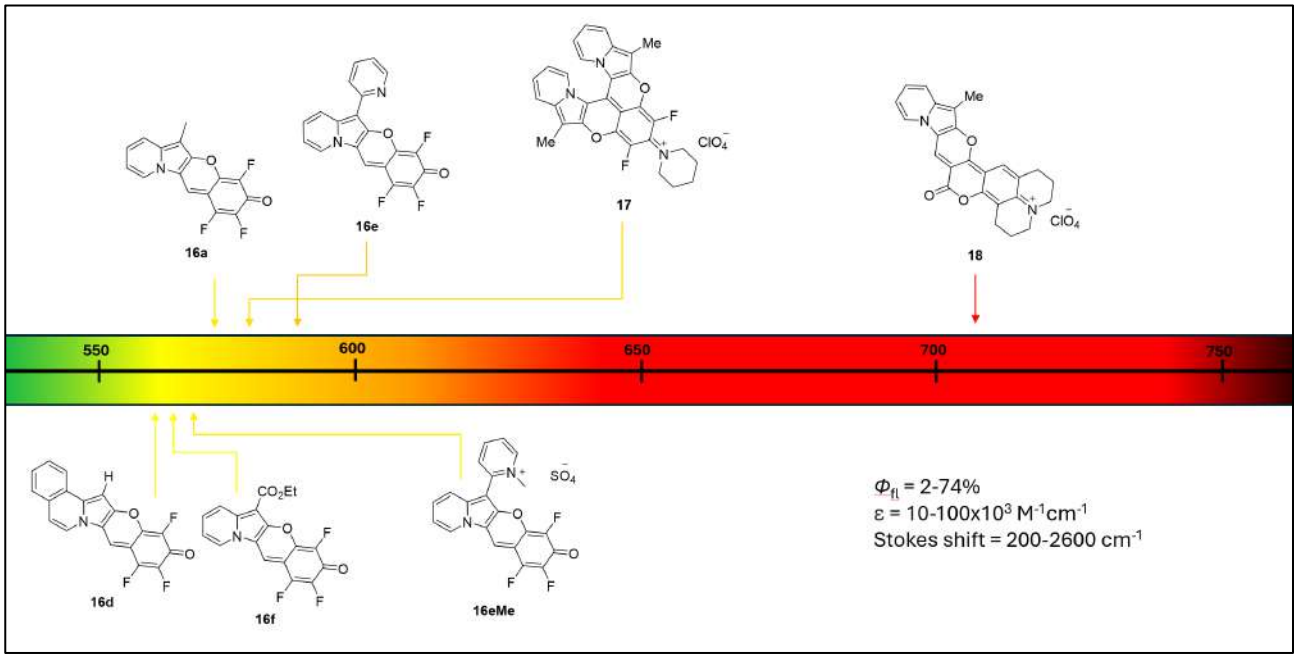

Figure 9: *Visual comparison of emission of the* ***IndMer*** *derivatives in DCM.*

3. Summary and Conclusions

In conclusion, over the past years, I have improved two existing methodologies for the synthesis of pyrano- and benzo-indolizines, discovered a novel approach for constructing an entirely new indolizine-fused xanthene system, and explored their photophysical properties.

In the first two cases, I succeeded in shortening the reaction time and eliminating a purification step by implementing a one-pot procedure, thereby saving both time and laboratory resources. These optimizations led to higher yields and allowed for significantly broader substrate (and product) scope. My equally important contribution to the field was the comprehensive photophysical characterization of the resulting structures, along with a rational analysis of how different substituents, positioned around the indolizine core, moderate these properties.

The final project, in contrast, involved not only a comprehensive photophysical investigations but also the discovery of a completely novel type of polymethine dyes which are at the same time π-expanded indolizines. This work was made possible by a deeper understanding of the reactivity and handling of highly reactive indolizin-ol intermediates gained during the second project. It also stemmed from the successful adaptation of a straightforward methodology, originally developed by our group in recent years for the synthesis of rhodols, by employing 2,3,5,6-tetrafluoro-4-hydroxybenzaldehyde as key component.

All the methodologies proposed in my projects for the synthesis of the indolizine core start from pyridines and rely on classical organic chemistry approaches, demonstrating their continued relevance even after decades from their development. The last two projects followed a Chichibabin-type mechanism, involving the formation of a pyridinium ylide that facilitates closure of the pyrrole ring, followed by π-system expansion. In contrast, the first project featured a final step of 1,5-electrocyclization, which was responsible for the formation of the indolizine core. This pericyclic reaction was enabled by prior extension of the conjugated system, made possible through a nucleophilic aromatic substitution (SN_2Ar) involving electron-deficient benzene derivatives and pyridinium salts via formation of a vinylpyridinium ylides. Yields were generally good across all reactions, averaging between 50% and 70%, with variations largely depending on the specific starting pyridine and its intrinsic reactivity.

Considering the photophysical properties of the synthesized products, their λ_{abs}^{max} and λ_{em}^{max} span the entire visible spectrum, from the blue to the red region. Pyrano-indolizines are the most blue-shifted, benzo-indolizines are the most red-shifted, and IndMer structures exhibit intermediate properties (Fig. 10). From a general point of view, any of the considered structural expansion led to a red shift in the photophysical properties and an increase in the fluorescence compared to the parent indolizine which has λ_{abs} = 368 nm and λ_{em} = 498 nm with Φ_{fl} of 14% in DCM.

When considering the impact of the substituents on the optical properties, substituents at position R^6 of the benzo-indolizines have a greater impact than those at position R^1 of the pyrano-indolizines and IndMer. In the latter cases, changes in the electronic nature of the substituent moderately influenced the photophysics. This observation is supported by computational studies, which showed that variations in the HOMO and LUMO energies of the pyrano-indolizine and IndMer derivatives are small, indicating limited electronic delocalization through those positions. While in the case of benzo-indolizines, the different size and character of substituents in R^6 change the geometry of the molecule thus changing their orbital energies.

This work also highlights the influence of isomerism, as expanded [*a*]indolizines having λ_{abs} around 500 nm and λ_{em} in the red region exhibit a greater red shift than the expanded [*b*]indolizine counterparts presented in the introduction, such as structure **1** (λ_{abs} = 440 nm, λ_{em} = 490 and 520 nm) and structure **2** (λ_{abs} = 594 nm, λ_{em} = 621 nm, Φ_{fl} = 17%).

Lastly, the solvatochromism observed for IndMer is less pronounced compared to the other discussed cores, due to the minimal increase in dipole moment upon excitation to the S_1 state relative to the S_o state. As a result, the differential stabilization by solvents is limited, leading to a smaller solvent-dependent shift in the absorption and emission spectra.

To sum up, with my PhD research, I contributed to advancing the knowledge and understanding of the photophysical properties of two largely overlooked classes of compounds: **benzo[*a*]indolizines** and **pyrano[*b*]indolizines**. These scaffolds can be synthesized efficiently through short, one-pot procedures. In addition, I developed a straightforward methodology for the synthesis of a completely novel structure (**IndMer**) and provided a comprehensive analysis of its optical properties.

Out of the plethora of synthesized and characterized molecules few interesting structures stood out for their photophysical properties and ability to enable organelle visualization. Among them, compounds 15a and 18 exhibited the most promising features.

Altogether, these findings highlight the significant potential of this class of fluorophores for bioimaging applications, as demonstrated by cell studies performed by our collaborators.

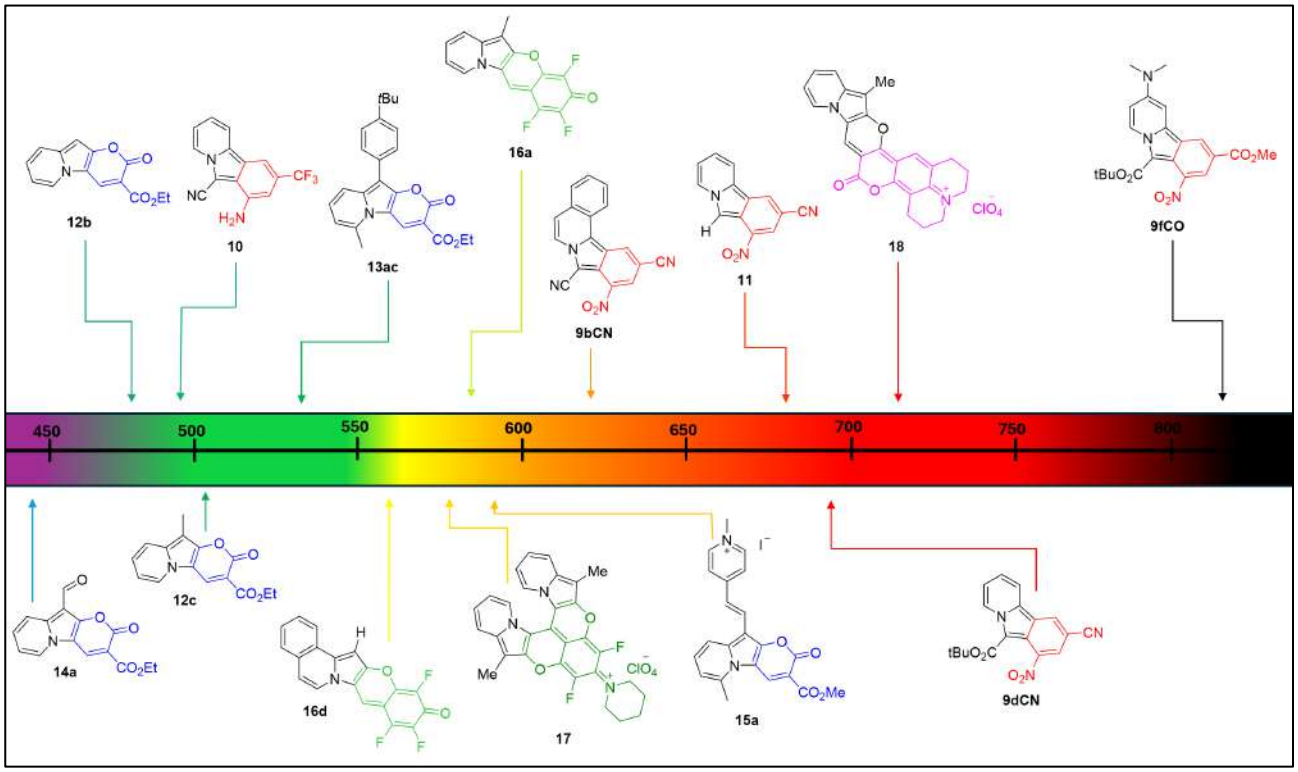

Figure 10: *Visual comparison of the fluorescence emission of some representatives of* ***benzo[a]indolizines****,* ***pyrano[b]indolizines*** *and* ***IndMers*** *in DCM*

References

[1] E. Kim, Y. Lee, S. Lee, S. B. Park, "Discovery, Understanding, and Bioapplication of Organic Fluorophore: A Case Study with an Indolizine-Based Novel Fluorophore, Seoul-Fluor" *Acc. Chem. Res.* **2015**, *48*, 538–547.

[2] A. Angeli, "Ueber die Einwirkung des Oxaldiäthylesters auf das Pyrrylmethylketon" *Berichte Dtsch. Chem. Ges.* **1890**, *23*, 1793–1797.

[3], "PubMed," can be found under https://pubmed.ncbi.nlm.nih.gov/(accessed 23 September 2025), **n.d.**

[4] Y. Lee, *Systematic Exploration of Indolizine-Based Small Fluorescent Molecules: Synthesis, Analysis and Application*, Springer, Singapore, **2018**.

[5] M. Scholtz, "Die Einwirkung von Essigsäureanhydrid auf α-Picolin" *Berichte Dtsch. Chem. Ges.* **1912**, *45*, 734–746.

[6] A. E. Tschitschibabin, "Tautomerie in der Pyridin-Reihe" *Berichte Dtsch. Chem. Ges. B Ser.* **1927**, *60*, 1607–1617.

[7] W. Flitsch in *Compr. Heterocycl. Chem.*, Elsevier, **1984**, pp. 443–495.

[8] J. W. Daly, "Thirty Years of Discovering Arthropod Alkaloids in Amphibian Skin" *J. Nat. Prod.* **1998**, *61*, 162–172.

[9] J. P. Michael, "Indolizidine and quinolizidine alkaloids" *Nat. Prod. Rep.* **2008**, *25*, 139–165.

[10] G. S. Singh, "Recent progress in synthesis and bioactivity studies of indolizines" *Eur. J. Med. Chem.* **2011**.

[11] C. Sandeep, K. N. Venugopala, M. A. Khedr, M. Attimarad, B. Padmashali, R. S. Kulkarni, R. Venugopala, B. Odhav, "Review on Chemistry of Natural and Synthetic Indolizines with their Chemical and Pharmacological Properties" *J. Basic Clin. Pharm.* **2017**, *8*.

[12] C. Bailly, "Anticancer Properties of Lamellarins" *Mar. Drugs* **2015**, *13*, 1105–1123.

[13] E. T. Borrows, D. O. Holland, "The chemistry of the pyrrocolines and the octahydropyrrocolines" *Chem. Rev.* **1948**, *42*, 611–643.

[14] H. R. Ing, R. C. Elderfield (Ed.), *Heterocyclic Compounds*, WILEY, **1952**.

[15] T. Uchida, K. Matsumoto, "Methods for the Construction of the Indolizine Nucleus*" *Synthesis* **1976**, *1976*, 209–236.

[16] H. L. Blewitt, *Special Topics in Heterocyclic Chemistry*, Wiley, **n.d.**

[17] F. J. Swinbourne, J. H. Hunt, G. Klinkert in *Adv. Heterocycl. Chem.*, Elsevier, **1979**, pp. 103–170.

[18] B. Sadowski, J. Klajn, D. T. Gryko, "Recent advances in the synthesis of indolizines and their π-expanded analogues" *Org. Biomol. Chem.* **2016**, *14*, 7804–7828.

[19] J. Hui, Y. Ma, J. Zhao, H. Cao, "Recent advances in the synthesis of indolizine and its derivatives by radical cyclization/cross-coupling" *Org. Biomol. Chem.* **2021**, *19*, 10245–10258.

[20] S. Ghosh, K. Biswas, "Microwave-assisted synthesis of indolizine derivatives: Recent developments: A review (2003-present)" *Synth. Commun.* **2024**, *54*, 505–525.

[21] A. A. Nevskaya, A. D. Zinoveva, E. V. Van der Eycken, L. G. Voskressensky, "Synthetic Strategies for the Construction of Indolizines and Indolizine-fused Compounds: Thienoindolizines and Indolizinoindoles" *Asian J. Org. Chem.* **2023**, *12*, e202300359.

[22] Priyanka, P. Rani, Kiran, J. Sindhu, "Indolizine: A Promising Framework for Developing a Diverse Array of C−H Functionalized Hybrids" *ChemistrySelect* **2023**, *8*, e202203531.

[23] X. Liu, H. Fu, Q. Hu, H. Cao, "Recent Advances on the Construction of Functionalized Indolizine and Imidazo[1,2-a]pyridine Derivatives" *Chem. Rec.* **2024**, *24*, e202400135.

[24] J. Huang, C. Li, X. Li, G. Li, Z. Yang, Y. Yu, Y. Xie, H. Huang, F. Yu, Z. He, "Recent Advances in the Development of Indolizine Scaffolds: Synthetic Methodology and Mechanistic Insights" *Chin. J. Chem.* **2025**, *43*, 315–348.
[25] J. S. A. Badaro, B. Godlewski, D. T. Gryko, "Advances in the synthesis of indolizines and their π-expanded analogues: update 2016–2024" *Org. Chem. Front.* **2025**, *12*, 2860–2907.
[26] C. R. de Souza, A. C. Gonçalves, M. F. Z. J. Amaral, "RECENT SYNTHETIC DEVELOPMENTS AND REACTIVITY OF AROMATIC INDOLIZINES" *Targets Heterocycl. Syst. Vol 20* **2016**, 365.
[27] C.-H. Park, V. Ryabova, I. V. Seregin, A. W. Sromek, V. Gevorgyan, "Palladium-Catalyzed Arylation and Heteroarylation of Indolizines" *Org. Lett.* **2004**, *6*, 1159–1162.
[28] M. Fraser, S. McKenzie, D. H. Reid, "Nuclear magnetic resonance. Part IV. The protonation of indolizines" *J. Chem. Soc. B Phys. Org.* **1966**, 44–48.
[29] M. Fraser, A. Melera, B. B. Molloy, D. H. Reid, "651. Nuclear magnetic resonance. Part I. The structure of indolizinium salts" *J. Chem. Soc. Resumed* **1962**, 3288–3294.
[30] W. L. F. Armarego, "C-1 and C-3 protonation of indolizines" *J. Chem. Soc. B Phys. Org.* **1966**, 191–194.
[31] E. T. Borrows, D. O. Holland, J. Kenyon, "238. The chemistry of the pyrrocolines. Part III. Nitration" *J. Chem. Soc. Resumed* **1946**, 1077–1083.
[32] J. A. Hickman, D. G. Wibberley, "Indolizines. Part V. The synthesis of 3-amino- and 3-acetamido-indolizines and their precursors, the 3-azo-, -nitroso-, -nitro-, and -acetyl-indolizines" *J. Chem. Soc. Perkin 1* **1972**, 2954–2958.
[33] E. T. Borrows, D. O. Holland, J. Kenyon, "237. The chemistry of the pyrrocolines. Part II. Nitroso-derivatives of some substituted pyrrocolines" *J. Chem. Soc. Resumed* **1946**, 1075–1077.
[34] W. B. Harrell, "Mannich bases from 1,2-diphenylindolizine: Ephedrine and methamphetamine as amine components" *J. Pharm. Sci.* **1970**, *59*, 275–275.
[35] Y.-Z. Zhang, F.-T. Sheng, Z. Zhu, Z.-M. Li, S. Zhang, W. Tan, F. Shi, "Organocatalytic C3-functionalization of indolizines: synthesis of biologically important indolizine derivatives" *Org. Biomol. Chem.* **2020**, *18*, 5688–5696.
[36] A. F. Kassir, N. Rad, P. Klochowicz, J. M. Granda, "Diversity-oriented chiral phosphoric acid catalyzed alkylation of indolizines with aminals" *Org. Chem. Front.* **2024**, *11*, 7186–7198.
[37] M. L. Bode, P. T. Kaye, R. George, "Indolizine studies. Part 3. Synthesis and dynamic NMR analysis of indolizine-2-carboxamides" *J. Chem. Soc. Perkin 1* **1994**, 3023–3027.
[38] H. Liu, S. Ren, C. Ma, G. Shi, Y. Li, G. Duan, Y. Ge, "Copper-Promoted Direct Decarboxylative C3-Acylation of Electron-Rich Indolizines Using α-Keto Acids" *ChemistrySelect* **2022**, *7*, e202104426.
[39] K. Watanabe, N. Terao, T. Niwa, T. Hosoya, "Direct 3-Acylation of Indolizines by Carboxylic Acids for the Practical Synthesis of Red Light-Releasable Caged Carboxylic Acids" *J. Org. Chem.* **2021**, *86*, 11822–11834.
[40] E. T. Borrows, D. O. Holland, "127. The chemistry of the pyrrocolines. Part V. The action of Grignard reagents and of iodine on 3-acetyl-2-phenylpyrrocoline" *J. Chem. Soc. Resumed* **1947**, 670–672.
[41] L. Sun, X. Zhang, Z. Li, J. Ma, Z. Zeng, H. Jiang, "A Versatile C–H Halogenation Strategy for Indole Derivatives under Electrochemical Catalyst- and Oxidant-Free Conditions" *Eur. J. Org. Chem.* **2018**, *2018*, 4949–4952.
[42] J.-B. Xia, S.-L. You, "Synthesis of 3-Haloindolizines by Copper(II) Halide Mediated Direct Functionalization of Indolizines" *Org. Lett.* **2009**, *11*, 1187–1190.

[43] O. Diels, K. Alder, “Synthesen in der hydroaromatischen Reihe. XVII. Mitteilung. („Dien-Synthesen” stickstoffhaltiger Heteroringe. 5. Dien-Synthesen des Pyridins, Chinolins, Chinaldins und Isochinolins.)” *Justus Liebigs Ann. Chem.* **1932**, *498*, 16–49.
[44] H. Zheng, H. Xiong, C. Su, H. Cao, H. Yao, X. Liu, “Photoinduced successive oxidative ring-opening and borylation of indolizines with NHC–boranes” *RSC Adv.* **2022**, *12*, 470–474.
[45] O. Diels, R. Meyer, “Synthesen in der hydroaromatischen Reihe. XXI. „Dien-Synthesen” stickstoffhaltiger Heteroringe. 8. Über den Verlauf der Dien-Synthese des Pyridins in methylalkoholischer Lösung” *Justus Liebigs Ann. Chem.* **1934**, *513*, 129–145.
[46] J. T. Kim, V. Gevorgyan, “Selective Partial Reduction of Various Heteroaromatic Compounds with Bridgehead Nitrogen via Birch Reduction Protocol” *J. Org. Chem.* **2005**, *70*, 2054–2059.
[47] M. Renard, J. Gubin, “Metallation of 2-phenylindolizine” *Tetrahedron Lett.* **1992**, *33*, 4433–4434.
[48] A. G. Kuznetsov, A. A. Bush, V. B. Rybakov, E. V. Babaev, “An Improved Synthesis of Some 5-Substituted Indolizines Using Regiospecific Lithiation” *Mol. J. Synth. Chem. Nat. Prod. Chem.* **2005**, *10*, 1074–1083.
[49] E. V. Babaev, N. I. Vasilevich, A. S. Ivushkina, “Efficient synthesis of 5-substituted 2-aryl-6-cyanoindolizines via nucleophilic substitution reactions” *Beilstein J. Org. Chem.* **2005**, *1*, 9.
[50] M. V. R. Reddy, M. R. Rao, D. Rhodes, M. S. T. Hansen, K. Rubins, F. D. Bushman, Y. Venkateswarlu, D. J. Faulkner, “Lamellarin α 20-Sulfate, an Inhibitor of HIV-1 Integrase Active against HIV-1 Virus in Cell Culture” *J. Med. Chem.* **1999**, *42*, 1901–1907.
[51] A. Pareek, M. Y. Mehboob, M. Cieplak, M. Majdecki, H. Szabat, K. Noworyta, P. Połczyński, M. Morawiak, P. S. Sharma, C. Foroutan-Nejad, P. Gaweł, “Indoloindolizines: The Complete Story of a Polycyclic Aromatic Scaffold from Theoretical Design to Organic Field-Effect Transistor Applications” *J. Am. Chem. Soc.* **2025**, DOI 10.1021/jacs.4c16189.
[52] D. B. Granger, Y. Mei, K. J. Thorley, S. R. Parkin, O. D. Jurchescu, J. E. Anthony, “Synthesis and Electrical Properties of Derivatives of 1,4-bis(trialkylsilylethynyl)benzo[2,3-b:5,6-b']diindolizines” *Org. Lett.* **2016**, *18*, 6050–6053.
[53] D. Miao, C. Aumaitre, J.-F. Morin, “Photochemical synthesis of π-extended ullazine derivatives as new electron donors for efficient conjugated D–A polymers” *J. Mater. Chem. C* **2019**, *7*, 3015–3024.
[54] S. Yi, D. Kim, W. Cho, J. H. Lee, J. H. Kwon, J. Kim, S. B. Park, “Rational Design of Pyrido[3,2-b]indolizine as a Tunable Fluorescent Scaffold for Fluorogenic Bioimaging” *JACS Au* **2024**, *4*, 2896–2906.
[55] B. Zhou, M. Guo, Q. Pan, M. Zhou, L. Xu, Y. Rao, K. Wang, B. Yin, J. Zhou, J. Song, “Rhodium-catalyzed annulation of pyrrole substituted BODIPYs with alkynes to access π-extended polycyclic heteroaromatic molecules and NIR absorption” *Org. Chem. Front.* **2021**, *8*, 868–875.
[56] M. He, N. Chen, J. Wang, S. Peng, “Rhodium-Catalyzed Regiodivergent [3 + 2] and [5 + 2] Cycloadditions of Quinolinium Ylides with Alkynes” *Org. Lett.* **2019**, *21*, 5167–5171.
[57] Y. Zhang, W. Wang, J. Sun, Y. Liu, “TEMPO-catalyzed decarboxylation reactions for the synthesis of 1,2-unsubstituted indolizines” *J. Heterocycl. Chem.* **2020**, *57*, 210–217.
[58] S. Tiwari, D. S. Rawat, “Regiodivergent Synthesis of Densely Functionalized Indolizines via (2 + 2 + 1) Cycloaddition” *J. Org. Chem.* **2023**, *88*, 6805–6815.
[59] B. Shen, B. Li, B. Wang, “Rh(III)-Catalyzed Oxidative Annulation Leading to Substituted Indolizines by Cleavage of C(sp2)–H/C(sp3)–H Bonds” *Org. Lett.* **2016**, *18*, 2816–2819.

[60] J.-Q. Zhang, D. Hu, J. Song, H. Ren, "[3 + 2]-Annulation of gem-Difluoroalkenes and Pyridinium Ylides: Access to Functionalized 2-Fluoroindolizines" *J. Org. Chem.* **2021**, DOI 10.1021/acs.joc.0c03041.
[61] J. Zheng, X. He, H. Xu, H. Liu, W. Yang, "A formal [3 + 2] annulation reaction of propargyl sulfonium compounds and N-ylides: access to pyrrolo[2,1-a]quinolines, pyrrolo[2,1-a]phthalazines and indolizines" *Org. Biomol. Chem.* **2020**, *18*, 8867–8875.
[62] S. Dong, J. Huang, H. Sha, L. Qiu, W. Hu, X. Xu, "Copper-catalyzed formal [1 + 2 + 2]-annulation of alkyne-tethered diazoacetates and pyridines: access to polycyclic indolizines" *Org. Biomol. Chem.* **2020**, *18*, 1926–1932.
[63] V. K. Outlaw, J. Zhou, A. E. Bragg, C. A. Townsend, "Unusual blue-shifted acid-responsive photoluminescence behavior in 6-amino-8-cyanobenzo[1,2-b]indolizines" *RSC Adv.* **2016**, *6*, 61249–61253.
[64] R. Robinson, J. E. Saxton, "611. A synthesis of substituted 2 : 3-benzpyrrocolines" *J. Chem. Soc. Resumed* **1950**, 3136–3140.
[65] A. Citterio, M. Fochi, A. Marion, A. Mele, R. Sebastiano, M. Delcanale, "ChemInform Abstract: Synthesis of Naphtho[2,3-b]indolizine-6,11-dione Derivatives by Iodine Oxidation of 2-Alkyl-1,4-naphthoquinones in the Presence of Substituted Pyridines." *ChemInform* **1999**, *30*, DOI 10.1002/chin.199907163.
[66] E. F. Pratt, R. G. Rice, R. W. Luckenbaugh, "Reactions of Naphthoquinones with Malonic Ester and its Analogs. III. 1-Substituted Phthaloyl- and Phthaloylbenzopyrrocolines1" *J. Am. Chem. Soc.* **1957**, *79*, 1212–1217.
[67] W. Augstein, F. Kröhnke, "Synthesen des Benzo[a]- und des Naphtho[2.3-b]indolizin-Ringsystems" *Justus Liebigs Ann. Chem.* **1966**, *697*, 158–170.
[68] A. Kakehi, S. Ito, K. Nakanishi, K. Watanabe, M. Kitagawa, "Preparation of New Nitrogen-bridged Heterocycles. A Facile Synthetic Method of Pyrano[2,3-b]indolizinone Derivatives" *Bull Chem Soc Jpn* **1980**, *53*, 1115–1120.
[69] D. A. Rusanov, S. Mutasim Alfadul, E. Yu. Portnyagina, E. A. Silyanova, N. A. Kuznetsov, K. E. Podpovetny, A. V. Samet, V. V. Semenov, M. V. Babak, "Toward 'E-Ring-Free' Lamellarin Analogues: Synthesis and Preliminary Biological Evaluation" *ChemBioChem* **2023**, *24*, e202300161.
[70] C. S. L. Rathnamalala, J. N. Gayton, A. L. Dorris, S. A. Autry, W. Meador, N. I. Hammer, J. H. Delcamp, C. N. Scott, "Donor–Acceptor–Donor NIR II Emissive Rhodindolizine Dye Synthesized by C–H Bond Functionalization" *J. Org. Chem.* **2019**, *84*, 13186–13193.
[71] W. E. Meador, E. Y. Lin, I. Lim, H. C. Friedman, D. Ndaleh, A. K. Shaik, N. I. Hammer, B. Yang, J. R. Caram, E. M. Sletten, J. H. Delcamp, "Silicon-RosIndolizine fluorophores with shortwave infrared absorption and emission profiles enable in vivo fluorescence imaging" *Nat. Chem.* **2024**, *16*, 970–978.
[72] M. A. Saucier, N. A. Kruse, B. E. Seidel, N. I. Hammer, G. S. Tschumper, J. H. Delcamp, "Phospha-RosIndolizine Dye with Shortwave Infrared (SWIR) Absorption and Emission" *J. Org. Chem.* **2024**, *89*, 9092–9097.
[73] J. S. A. Badaro, B. Koszarna, M. H. E. Bousquet, E. T. Ouellette, D. Jacquemin, D. T. Gryko, "The Kröhnke synthesis of benzo[a]indolizines revisited: towards small, red light emitters" *Org. Chem. Front.* **2022**, *9*, 1861–1874.
[74] D. Reuschling, F. Kröhnke, "Ringschlüsse unter HNO_2-Abspaltung und C-C-Verknüpfung, II. Synthese neuer Ringsysteme" *Chem. Ber.* **1971**, *104*, 2103–2109.
[75] S. M. McDonald, S. K. Mellerup, C. Barran, X. Wang, S. Wang, "Binding Modes and Reactivity of Pyrido[2,1-*a*]isoindole as a Neutral Carbon Donor with Main-Group and Transition-Metal Elements" *Organometallics* **2017**, *36*, 4054–4060.

[76] B. Bardi, K. V. Vygranenko, B. Koszarna, O. Vakuliuk, Ł. Dobrzycki, D. T. Gryko, F. Terenziani, A. Painelli, “Novel Method for the Synthesis of Merocyanines: New Photophysical Possibilities for a Known Class of Fluorophores” *Chem Eur J* **2023**, *29*, e202300979.

Original Publications and Authors' Contribution Declarations

ORGANIC CHEMISTRY FRONTIERS

RESEARCH ARTICLE

View Article Online
View Journal | View Issue

Cite this: *Org. Chem. Front.*, 2022, **9**, 1861

The Kröhnke synthesis of benzo[*a*]indolizines revisited: towards small, red light emitters†

Jaqueline S. A. Badaro, [a] Beata Koszarna,[a] Manon H. E. Bousquet, [b] Erik T. Ouellette, [c,d] Denis Jacquemin *[b] and Daniel T. Gryko *[a]

Received 20th January 2022,
Accepted 9th February 2022

DOI: 10.1039/d2qo00097k

rsc.li/frontiers-organic

Benzo[*a*]indolizines with an ordered arrangement of various electron-withdrawing substituents (NO_2, CF_3, CN, CO_2R and COPh) were prepared directly from pyridinium salts and chloronitroarenes, allowing for refined control of the photophysical properties. Facile entry into almost unknown isoindolo[1,2-*a*]isoquinolines is disclosed to demonstrate the potential of this method. The rational manipulation of the substituents makes it possible to obtain electron-deficient dyes (HOMO ≈ −5.6 eV) with yellow, orange to red emission, large Stokes shifts (up to 9000 cm^{-1}) and fluorescence quantum yields reaching 0.58. Strong emission in spite of the presence of an NO_2 group has been rationalized by a large singlet–triplet energy gap combined with small spin–orbit couplings, hence small intersystem crossing. The ability to substitute various electron-withdrawing groups at multiple positions on this heterocyclic skeleton offers an unprecedented opportunity to study their effect on the fate of the molecules in the excited state.

Introduction

Indolizines, although known since the 19th century,[1–4] have always been overshadowed by regioisomeric indoles. Only during the last two decades was their chemistry rejuvenated, likely because of their potential as fluorophores,[5–11] which is especially strong for π-expanded indolizines. In recent years, multiple new methods for indolizine synthesis have been revealed,[12–19] nicely complementing older approaches.[20–24]

There are a few basic classes of benzoindolizines: pyrrolo[1,2-*a*]quinolines,[25–36] pyrrolo[2,1-*a*]isoquinoline,[37–40] benzo[*b*]indolizine[41–48] and benzo[*a*]indolizines (pyrido[2,1-*a*]isoindoles)[49–61] (Fig. 1). The latter ones attracted our particular attention since they are considered as π-expanded isoindoles, which are rarely encountered. However, benzo[*a*]indolizines are reported to be very unstable under ambient conditions.[49] To overcome this instability issue, adding several electron-withdrawing groups (EWGs) could be an advantageous strategy. At the same time, the presence of electron-withdrawing groups would polarize the π-system and induce bathochromic shifts in both the absorption and emission spectra.[62] Taking this into account, we reasoned that a one-pot reaction with the potential to assemble a π-expanded indolizine core decorated with several EWGs would be an appreciated addition to the existing repertoire of benzo[*a*]indolizines synthetic methodologies. Inspired by a lego™-type philosophy, our target strategy was to build a final scaffold from easily available building blocks.

In light of all these requirements, we identified the Kröhnke method for the synthesis of benzo[*a*]indolizines from pyridines, ω-bromoacetophenones, and picryl chloride (Scheme 1)[52,63,64] as the most promising starting point. This methodology consists of three steps: (1) quaternization of pyridine with (Hal)CH_2(EWG) reagents; (2) *C*-arylation of the

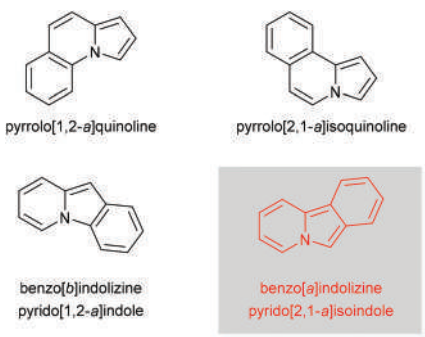

Fig. 1 Structures of various benzoindolizines.

[a]*Institute of Organic Chemistry, Polish Academy of Sciences, Kasprzaka 44/52, 01-224 Warsaw, Poland. E-mail: dtgryko@icho.edu.pl*
[b]*CEISAM Lab—UMR 6230, CNRS, University of Nantes, Nantes, France. E-mail: Denis.Jacquemin@univ-nantes.fr*
[c]*Department of Chemistry, University of California, Berkeley, 420 Latimer Hall, Berkeley, CA, USA*
[d]*Chemical Sciences Division, Lawrence Berkeley National Laboratory, 1 Cyclotron Road, Berkeley, CA, USA*

†Electronic supplementary information (ESI) available: Synthetic optimization studies, crystallographic data, electrochemical and computational details, copies of NMR spectra. CCDC 2132628. For ESI and crystallographic data in CIF or other electronic format see DOI: 10.1039/d2qo00097k

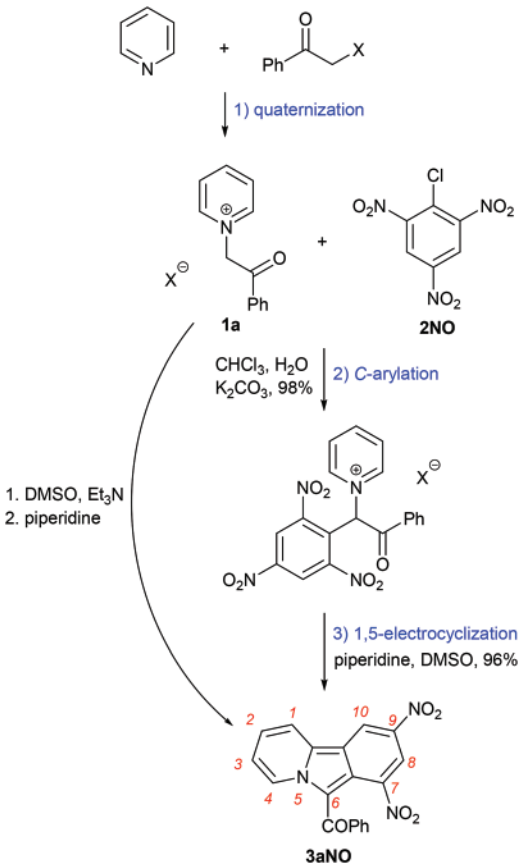

Scheme 1 The Kröhnke method for the benzo[*a*]indolizine synthesis.

resulting pyridinium salts with 1-chloro-2,4,6-trinitrobenzene; and (3) final 1,5-electrocyclization forming a five-membered central ring. The mechanism of the last key step relies on the formation of vinylpyridinium ylides which are prone toward 1,5-electrocyclization.[65,66] The initially formed dihydroindolizine eliminates NO_2^- and furnishes the final aromatic product. The trouble with Kröhnke's approach is that it is mostly limited to explosive 1-chloro-2,4,6-trinitrobenzene. The intriguing feature, however, is that authors consistently reported strong red fluorescence for the resulting nitro-derivatives, which is both rare[67,68] and worth exploring. In addition, given that almost all published derivatives possess a PhCO at position 6, which typically leads to fluorescence quenching due to enhanced intersystem crossing, the observed emission is even more perplexing. Having all these aspects in mind we conceived a journey aiming at exploring this methodology, expanding the scope, and revisiting the emissive properties of benzo[*a*]indolizine.

Results and discussion

Synthesis

Our investigation started from the synthesis of benzoindolizines **3aCF**, **3aCN** and **3aCO** (Scheme 2) following the method developed by Augstein and Kröhnke in 1966 (conditions A).[52] We found that these three heterocycles could be prepared under the conditions originally published for **3aNO** (*i.e. C*-arylation in $CHCl_3/H_2O/K_2CO_3$ system followed by 1,5-electrocyclization mediated by piperidine, Scheme 1) in yields ranging from 20% to 30%. Lower yields may originate from the decreased reactivity of chloroarenes **2CN** and **2CF** relative to **2NO** However, these benzo[*a*]indolizines featuring a PhCO group at position 6 possessed rather weak fluorescence, most plausibly due to the presence of the carbonyl group (*vide infra*).

Thus, we decided to replace the C═O with the CN group at position 6 and we synthesized dye **3cCF**, aiming at stronger emission intensity. Novel benzo[*a*]indolizine **3cCF** indeed possessed a visibly stronger fluorescence and was used as a model for synthetic optimization studies (see ESI† for details).

Having established the optimal reaction conditions (Cs_2CO_3, sulfolane, RT, 16 h), the substrate scope of benzo[*a*]indolizine synthesis was evaluated. As shown in Scheme 2, various pyridinium salts, as well as an isoquinolinium salt reacted with different 4-chloro-3,5-dinitrobenzenes, successfully giving the products that exhibited different combinations of groups at positions 6 (R^1), 9 (Y), and 2 (R^2). The presence of CO_2Me as Y led to lower yields of the final products (**3aCO**, **3cCO**, and **3dCO**), but what dramatically compromised the success of the reaction was the presence of a substituent R^2. The tested building blocks possessing only one NO_2 at position *ortho* to Cl, such as 1-chloro-2,4-dinitro-6-trifluoromethylbenzene or 2-chloro-3,5-dinitropyridine, were found to be inefficient. A similar outcome was observed for chloroarenes possessing less activated C–Hal bond such as 2,4-dinitrofluorobenzene or 2,4-dichloro-1,5-dinitrobenzene. This evidence suggests that it is mandatory to have two NO_2 in *ortho* positions to the halogen atom for the reaction to proceed to completion.

In the course of this scope investigation, it was noted that quaternary salts derived from pyridines substituted at position 4 with an electron-withdrawing group, such as CN (**3eCF**, **3eCN**, and **3eCO**), were less reactive than the salts **3a**, **3c** and **3d** derived from unsubstituted pyridine. In fact, a four-fold decrease in the yield was observed, with the exception of **3eCF**. Similarly, the presence of an electron-donating group such as NMe_2 (**3fCO**) decreased the product yield from 20% to 13%. Furthermore, further expanding the scope, *i.e.*, starting from 4-methoxypyridine and 4-trifluoromethylpyridine, was unsuccessful. Consequently, another optimization study (see ESI† for details), was conducted using **3eCN** as a model which enabled to identify *tert*-butylimino-tri(pyrrolidino) phosphorane (BTPP) as the suitable base (the yield of **3eCN** was increased to 58%).

The novel reaction conditions (BTPP, DMSO, RT, 16 h) were then tested for the synthesis of other benzo[*a*]indolizines from salt **1e**. It turned out, however, that yields of dyes **3eCF** and **3eCO** were considerably lower, and the efficiency of the reactions starting from quaternary salts derived from unsubstituted pyridine were below 5% (Scheme 2).

The obtained benzo[*a*]indolizines offer significant synthetic possibilities due to the presence of several functional groups.

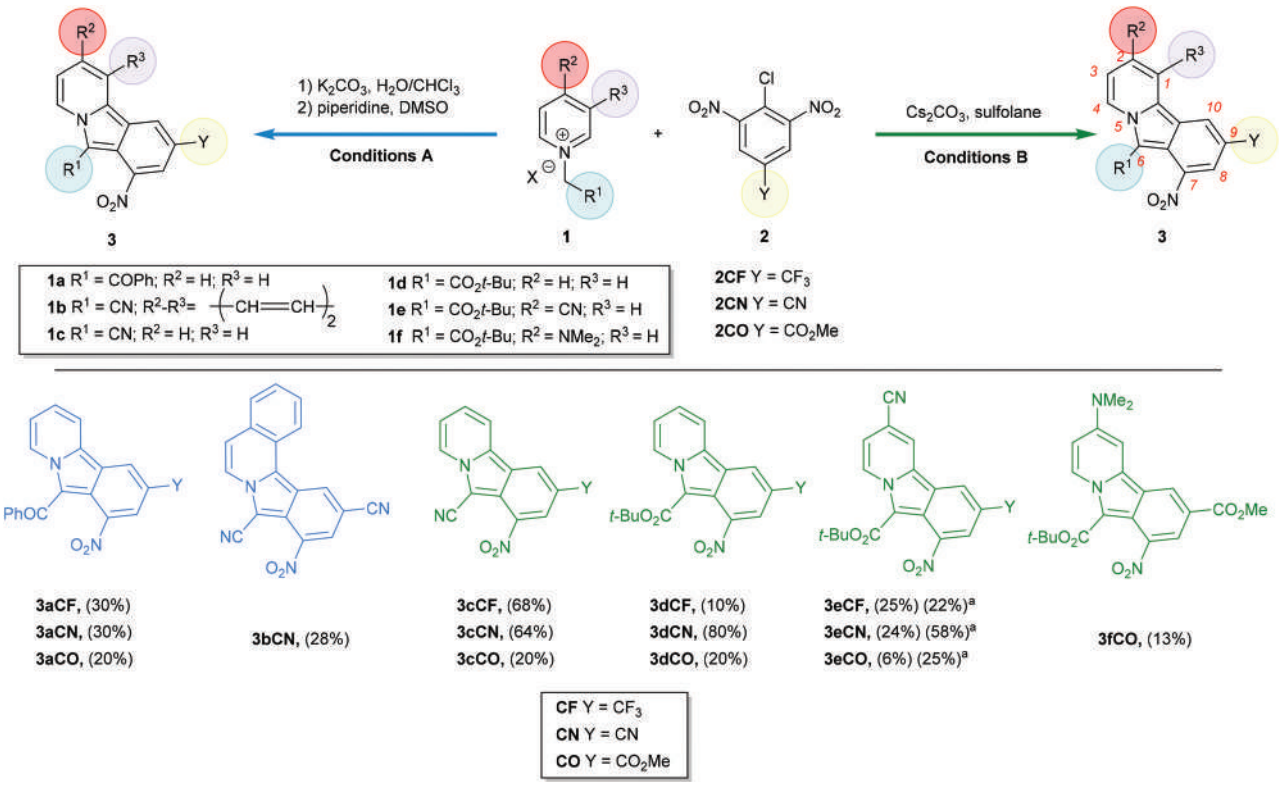

Scheme 2 Scope of benzo[*a*]indolizines. Structures of products obtained according to conditions A (blue) or B (green). [a] Yields obtained according to the best condition of the second optimization study (BTPP as base and DMSO as solvent).

In order to explore these possibilities two additional derivatives (**4** and **5**) were obtained *via* transformations of **3cCF** and **3dCN**, respectively (Scheme 3). The former was obtained thanks to the reduction of the nitro group to an amine, catalyzed by Pd/C with ammonium formate as the proton source.[69] The latter resulted from the removal of CO_2t-Bu in a reverse Friedel-Crafts[70] reaction with TFA as a source of proton and acidic species.

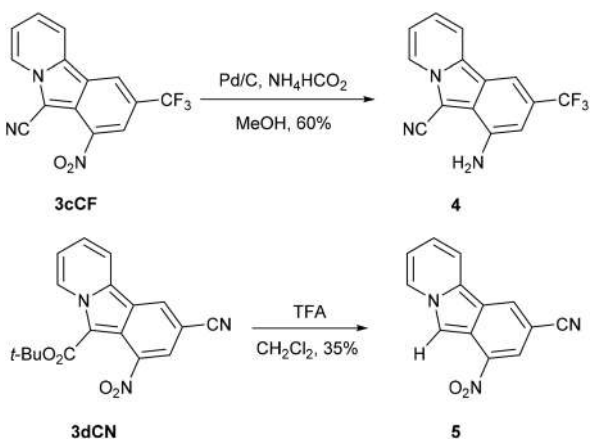

Scheme 3 Synthesis of **4** and **5** from **3cCF** and **3dCN**.

Single-crystal X-ray diffraction study

To date, only a handful of synthetic procedures were developed affording an isoindolo[1,2-*a*]isoquinoline core[52,55,59,60,71] and to demonstrate that we have successfully obtained compound **3bCN** possessing the expected geometry, single-crystal X-ray diffraction studies were performed (Fig. 2). The crystal for analysis was obtained from the slow diffusion of diethylether into a DMF solution and data obtained show us that the structure is planar and belongs to the *P*2(1)/*n* space group within the monoclinic crystal system (*for further information* see ESI†). Note that the CN at position 6 is slightly deformed from linearity to accommodate for the vicinal nitro group.

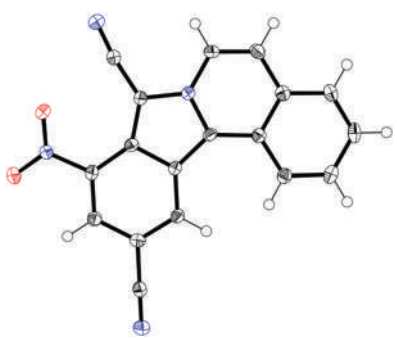

Fig. 2 Crystallographic structure of dye **3bCN**.

Photophysical properties

The UV-VIS absorption and emission spectra were recorded in DCM and toluene for all dyes, and the related data are collected in Table 1. A comparison between the photophysical parameters and those available for parent benzo[*a*]indolizine (fluorescence quantum yield = 14% in DCM, with λ_{abs} = 368 nm and λ_{em} = 498 nm)[72] reveals a significant bathochromic shift of both absorption and emission spectra for the novel highly polarized benzo[*a*]indolizines. The λ_{abs} of the vast majority of the obtained dyes are located within 400–500 nm range. Emission is typically in the yellow-orange-red region of the visible spectral range and the related fluorescence quantum yield (Φ_{fl}) varies from 0.6 to hardly detectable level. The presence of an electron-donating NMe_2 group (**3fCO**) led to the strongest bathochromic shift, especially in the case of emission (λ_{em} = 832 nm in DCM). Significant solvatochromism of both absorption and emission, as well as a clear trend of decreasing Φ_{fl} while moving from toluene to DCM for all compounds, clearly point to marked intramolecular charge transfer character (ICT). Comparisons between some representative benzo[*a*]indolizines are displayed in Fig. 3a–c.

There are a few clear trends. According to expectations the fluorescence strength is weak (≈0.1) in the *3a series* where all dyes possess a PhCO group. The strongest emission ($\Phi_{fl} \approx 0.5$) has been observed for dyes bearing a CN group at position 6 (*i.e. 3c series*, **3bCN** and **4**). Fluorescence is weaker in the *3d series* and *3e series*, although they do not have a keto group at position 6 ($\Phi_{fl} \approx 0.1$–0.2). The presence of an additional CN

Table 1 Photophysical data of synthesized benzo[*a*]indolizines

Cmpd	Solv	λ_{abs} [nm]	λ_{em} [nm]	$\Delta\mu\nu$ [cm^{-1}]	ε [M^{-1} cm^{-1}]	Φ_{fl}
3aCF[a]	DCM	475	704	6800	5000	0.02
	Tol	468	644	5800	5600	0.09
3aCN[a]	DCM	480	687	6300	4600	0.03
	Tol	471	641	5600	4500	0.10
3aCO[a]	DCM	461	681	7000	4500	0.03
	Tol	415	630	4600	4600	0.24
3bCN[a]	DCM	494	616	4000	11 000	0.40
	Tol	490	574	3000	7200	0.58
3cCF[a]	DCM	488	603	3900	8000	0.38
	Tol	483	569	3100	5900	0.58
3cCN[a]	DCM	490	601	3800	8800	0.38
	Tol	486	569	3000	7600	0.53
3cCO[a]	DCM	482	597	4000	5600	0.45
	Tol	481	557	2800	6300	0.58
3dCF[b]	DCM	452	685	7500	11 800	0.02
	Tol	449	618	6100	10 500	0.09
3dCN[b]	DCM	457	674	7000	6000	0.03
	Tol	451	622	6100	5700	0.10
3dCO[b]	DCM	449	664	7200	5800	0.03
	Tol	446	616	6200	5400	0.13
3eCF[b]	DCM	447	629	6500	31 000	0.17
	Tol	448	596	5500	25 000	0.20
3eCN[b]	DCM	400	628	9100	16 000	0.16
	Tol	402	585	7800	14 000	0.20
3eCO[b]	DCM	404	617	8500	14 000	0.22
	Tol	415	575	6700	12 000	0.24
3fCO[a]	DCM	510	832	7600	5000	<0.001
	Tol	504	721	6000	5300	0.01
4[c]	DCM	377	495	6300	13 000	0.26
	Tol	378	495	6300	13 000	0.20
5[d]	DCM	549	677	3400	6900	0.04
	Tol	529	635	3200	5000	0.11

[a] Fluorescence quantum yield measured with Fluorescein in 0.1 M aqueous solution of NaOH (Φ_{fl} = 0.79) as reference. [b] Fluorescence quantum yield measured with Coumarin 153 in ethanol (Φ_{fl} = 0.38) as reference. [c] Fluorescence quantum yield measured with 9,10-diphenylanthracene in cyclohexane (Φ_{fl} = 1) as reference. [d] Fluorescence quantum yield measured with Sulforhodamine 101 in ethanol (Φ_{fl} = 0.9) as reference.

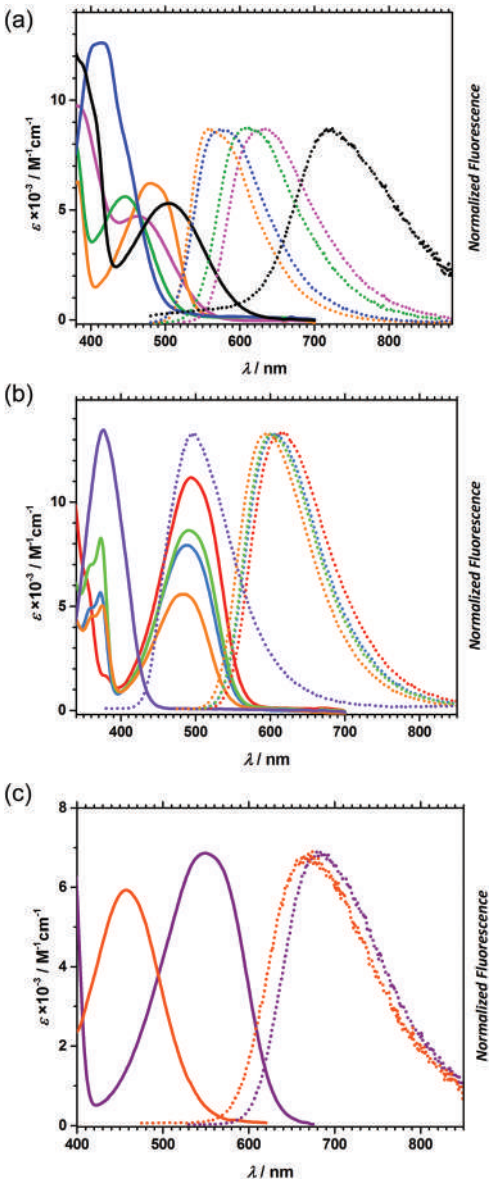

Fig. 3 Absorption and emission spectra of the representative benzo[*a*]indolizines in DCM and toluene. (a) Molar absorptivity (solid line) and normalized emission (round dot) spectra of **3aCO**, **3cCO**, **3dCO**, **3eCO**, and **3fCO** (pink, orange, green, blue, black) in toluene. (b) Molar absorptivity (solid line) and normalized emission (round dot) spectra of **3dCN**, **3cCF**, **3cCN**, **3cCO**, **4** (red, blue, green, orange, purple) in DCM. (c) Molar absorptivity (solid line) and normalized emission (round dot) spectra of **3dCN** (orange) and **5** (purple) in DCM.

group at position 2 improves emission intensity (*3d series versus 3e series*). The reasons for these complex behaviours were rationalized by first principles calculations (*vide infra*).

The broad comparison of photophysical properties reveals that that the substituent at position 6 and not the one in position 9 has a major influence. Indeed, the difference in the electronic character of the groups in position 6 influences the λ_{abs}. If a CN group is there (**3cCO**), λ_{abs} = 481 nm *i.e.* it is red-shifted compared to the other benzo[*a*]indolizines possessing a CO_2Me group at position 9 (λ_{abs} = 404–446 nm) (Fig. 3a). Still, in the *3a series*, the strength of an electron-withdrawing group at position 9 also contributes to a moderate bathochromic shift. The presence of an additional benzene ring (**3bCN** *vs.* **3cCN**) has a limited effect on photophysical properties. Adding a CN group at position 2 causes hypsochromic shift of both absorption and emission (**3dCN** *vs.* **3eCN**).

Interestingly truncating an electron-withdrawing ester group at position 6 (**3dCN** *vs.* dye **5**) causes a bathochromic shift of absorption (≈100 nm in DCM) but not of emission (Fig. 3c). The presence of a CO_2t-Bu group also increases the Stokes shift ($\Delta\bar{\nu}$) from 5000 cm^{-1} to 5700 cm^{-1}. For both dyes, Φ_{fl} is small (only 0.10 and 0.11 in toluene), but **5** is also unstable, decomposing only a few seconds after irradiation.

It is clear that the presence of NO_2 at position 7 controls the photophysics of these dyes. Its replacement with electron-donating NH_2 (compound **4**) causes marked hypsochromic shift of both absorption and fluorescence (Fig. 3b, purple curve). Furthermore, in contrast to what was expected, the absence of NO_2 did not increase the fluorescence yield, instead it decreased by almost a third (0.38 and 0.26, respectively).

Theoretical analysis

We have performed theoretical calculations (see Computational details) to understand the unusual photophysical properties of the synthesized compounds. All calculations were made using DCM as solvent. First, in Fig. 4, we show density difference plots for selected compounds. In all structures, it is clear that the nitro group at position 7, the strongest EWG group acts as an accepting group (mostly in red), whereas the five-membered ring acts as the main electron-rich moiety (main in blue). Equally interesting is that the substituent at position 9 plays a limited role in the excited state. This is consistent with the data listed in Table 1 that show similar values in a given series of compounds (*e.g.*, **3aCF**, **3aCN**, and **3aCO** have similar absorption spectra). What is even more valuable is that the substituents at position 6, either COPh, CO_2t-Bu, or even CN appear to play the role of a secondary donor (see **3bCN** in Fig. 4 for example). According to computational studies, replacement of CN with a bulkier group at position 6 induces significant twisting of the structure, including of the nitro group (see **3cCN** → **3eCN**, in Fig. S3 of the ESI†).

To allow for more quantitative comparisons between theory and experiment, we have computed the excited-state properties, which are summarized in Table 2. First, let us note that the trends in both vertical absorption and emission wavelengths nicely follow their experimental counterparts with R =

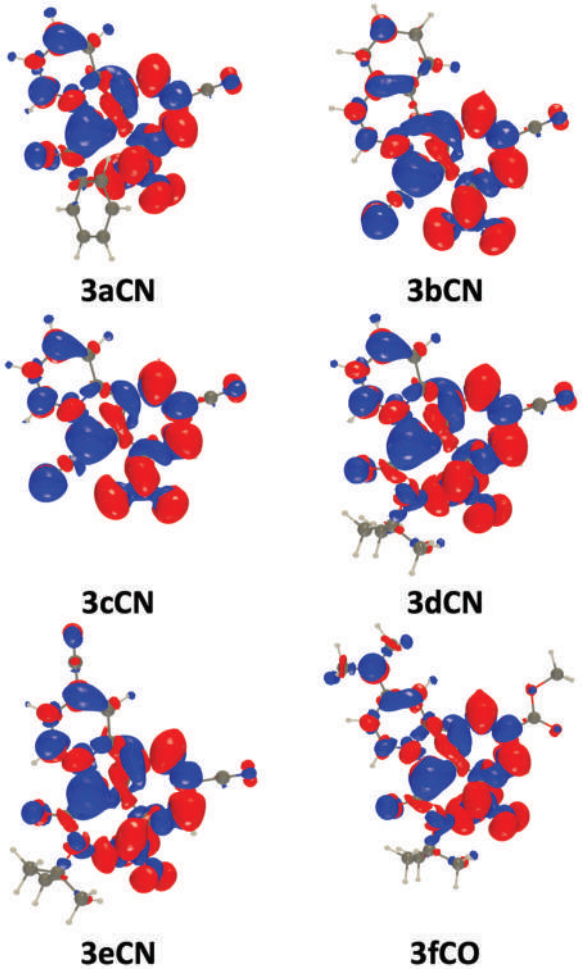

Fig. 4 Density difference plots for selected compounds. Blue and red lobes correspond to zones of decrease and increase of electron density upon absorption. Contour: 8×10^{-4}.

0.91 for both properties. Nevertheless, to allow more physically well-grounded comparisons, we have also determined 0–0 energies for all compounds. These values, which include the difference of zero-point vibrational energy (ZPVE) between the two states, can be compared directly to the absorption/emission crossing point. The mean absolute error (MAE) obtained by such comparison is 0.12 eV, a value typical of excited state calculations performed at the CC2 level.[73] The correlation coefficient is 0.92. These data indicate that the selected level of theory is well suited to investigate this specific class of compounds. In Table 2, we report the ICT parameters as obtained by Le Bahers' model.[74] As expected, and consistent with the experimental solvatochromic effects, we note significant ICT (except in **4**), the largest effect being the displacement of 0.73 e over 2.05 Å (**3fCO**), large values for rather compact dyes.[74] In a given series, it is the CF_3 that induces the strongest ICT and not the CN, consistent with the topology of the excited states in Fig. 4 indicating that the accepting groups at position 9 do not strongly impact the topology of the excited states.

Table 2 Computed photophysical data in DCM for all benzo[*a*]indolizines: vertical absorption and emission (in nm), 0–0 energies (in eV), ICT distance and charge (in Å and e, respectively). Fluorescence quantum yields computed on the basis of radiative rates and internal conversion rates only. Singlet–triplet gaps (at the S_1 geometry, eV) and spin–orbit coupling between the S and T states (cm^{-1}) at that same geometry

Cmpd	λ_{abs} [nm]	λ_{em} [nm]	ΔE_{00} [eV]	d^{CT} [Å]	q^{CT} [e]	Φ_{fl}	ΔE_{ST} [eV]	SOC [cm^{-1}]
3aCF	440	639	2.07	2.04	0.75	0.21	0.26	0.14
3aCN	447	634	2.08	1.88	0.71	0.22	0.23	0.10
3aCO	439	619	2.11	1.97	0.72	0.24	0.25	0.16
3bCN	448	551	2.22	1.89	0.66	0.45	0.44	0.02
3cCF	447	547	2.26	2.11	0.70	0.43	0.33	0.04
3cCN	452	546	2.25	1.91	0.67	0.45	0.31	0.01
3cCO	443	531	2.31	1.98	0.67	0.49	0.34	0.01
3dCF	426	621	2.14	1.92	0.72	0.25	0.28	0.20
3dCN	434	617	2.13	1.76	0.69	0.24	0.27	0.16
3dCO	425	599	2.19	1.82	0.69	0.29	0.29	0.19
3eCF	406	564	2.30	1.97	0.65	0.43	0.44	0.13
3eCN	414	559	2.30	1.81	0.61	0.45	0.43	0.09
3eCO	406	541	2.36	1.79	0.60	0.51	0.47	0.11
3fCO	504	768	1.79	2.05	0.73	0.12	0.16	0.13
4[a]	353	425	2.96	0.91	0.42	0.66	0.21	0.04
5	492	608	2.04	2.00	0.65	0.26	0.35	0.01

[a] S–T gaps with the second and not first triplet state.

Certainly, more intriguing are the rather good emissive properties of some of the dyes. We have therefore put efforts into the simulations of the quantum yield of emission of all compounds. Within the formalism (see Computational details),[75] it is possible to have a uniform description of the radiative (k_r) and internal conversion rates (k_{ic}) from first-principle calculations of the vibronic couplings, and hence to deduce a theoretical Φ_{fl}, but such a computed yield neglects all other non-radiative pathways. Considering the nitro-bearing dyes have a quite rigid core, the likely competitive non-radiative pathway is intersystem crossing (ISC) to the triplet state, a phenomenon typically invoked to explain the quenching of emission in nitro derivatives.[59,62] The theoretical values of Φ_{fl} determined neglecting ISC should therefore be equal (if ISC is negligible) or larger (if ISC is significant) than their experimental counterparts. This is exactly what is found when comparing Tables 1 and 2. For **3bCN**, **3cCF**, **3cCN**, and **3cCO**, the computed and measured values are very nicely matching (*ca.* 40%), the trends in the series being equivalent in both theory and experiment.

Consistently, for these four compounds, the singlet–triplet gaps determined at the excited-state geometry are large (>0.3 eV), and the spin–orbit coupling elements are totally negligible (<0.05 cm^{-1}), indicating trifling ISC. In other words, theory indicates that the $\Phi_{fl} \approx 40\%$ measured in DCM is related to the vibrational and electronic structure of the dyes and is not perturbed by other factors (electron transfer, TICT, ISC, *etc.*). Let us now turn towards the *3e series*, for which the computed Φ_{fl} remains similar to the one of *3c series*, but the experimental values have dropped by a factor of 2 (to *ca.* 20%). In this case, while the computed S–T gap remains large, the SOC are notably increased (≈0.10 cm^{-1}), indicating that ISC might start playing a role in decreasing the yields. For the compounds in both *3a series* and *3d series*, as well as **3fCO**, the Φ_{fl} computed on the basis of vibronic couplings are *ca.* 20%, whereas the emission measured in DCM are very weak (3% at most). However, for all those compounds, one notices rather small S–T gaps (<0.3 eV, even 0.16 eV in **3fCO**) together with SOCs exceeding 0.10 cm^{-1}, indicative of stronger ISC than in the other series. For derivatives of the *3a series* and *3d series*, not only is the ratio between the radiative and internal conversion rates less favourable than in *3c series*, but ISC is also playing a role. This illustrates the challenge of optimizing the fluorescence quantum yield. Finally, **4** is more difficult to analyse because the presence of the NH_2 group makes non-harmonic vibrational effects larger. Additionally, in strong contrast with the other systems, two triplet states are accessible from the lowest singlet in **4**.

Photostability

To examine the photostability of compounds **3dCN** and **4**, their solutions in DCM were exposed to a Xe lamp monitoring the absorption maximum at the appropriate wavelength with respect

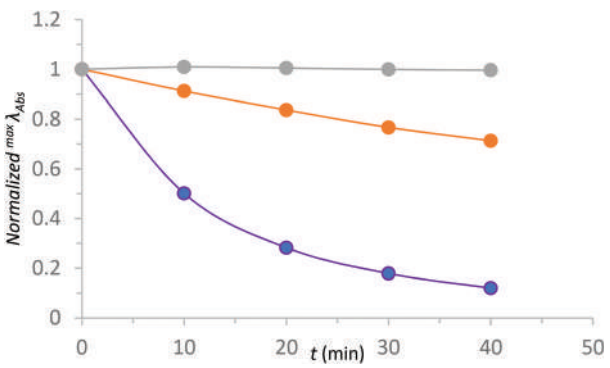

Fig. 5 Photostability of benzo[*a*]indolizines. Photostability of **3dCN** (orange) and **4** (purple) in DCM compared to Rhodamine 6G (grey), in EtOH using a collimated light source from a 300 W Xe lamp.

Table 3 Redox potentials measured in dichloromethane[a]

Compound	E^{pa}_{ox1} [V]	E^{onset}_{ox1} [V]	E^{pa}_{ox2} [V]	IP [eV]	E^{pa}_{red1} [V]	E^{pc}_{red1} [V]	E^{onset}_{red1} [V]	$E^{1/2}_{red1}$ [V]	E^{pc}_{red2} [V]	EA [eV]
3dCN	1.41	1.30	—	−5.6	−1.1	−0.97	−0.94	—	−1.70	−3.4
3fCO	0.69	0.60	1.22	−4.9	—	−0.94	−0.72	−1.28	—	−3.6
3aCF	1.38	1.24	1.45	−5.6	−0.89	−0.70	−0.85	—	—	−3.5
3eCN	1.67	1.52	—	−5.9	—	−0.92	−0.74	—	−1.63	−3.6
3cCN	1.53	1.43	—	−5.8	−0.8	−0.72	−0.72	—	−1.44	−3.6

[a] Measurement conditions: electrolyte (NBu_4ClO_4, c = 0.1 M), dry CH_2Cl_2, potential sweep rate: 100 mV s^{-1}, working electrode: glassy carbon (GC), auxiliary electrode: Pt wire, reference electrode: Ag/AgCl; all measurements were conducted at room temperature.

to the irradiation time (Fig. 4). Comparing both structures with Rhodamine 6G we can see that **4** is much less stable than **3dCN**, but both are visibly less stable than the reference compound (see Fig. 5). During all experiments, the concentration of the former was stable, while after only 10 min of irradiation, the content of **4** decreased by 50%, while the **3dCN** was decreased by 10%. At half of the experiment time, the **3dCN** concentration was around 80% while for **4** it dropped to *ca.* 30%. After 40 min irradiation, the absorption intensity at the λ_{max} decreased one order of magnitude for **4** but a factor of 3 only for **3dCN**. All of this information is consistent with the expected reactivity of indolizines.[76] Structures without substituents at position 6 are very reactive, and the electron density is located in this region, making it a good substrate for electrophilic aromatic substitution.

Electrochemical properties

To investigate the electrochemical properties of exemplary benzo[*a*]indolizines, cyclic voltammetry was conducted in DCM. As shown in Table 3, oxidation events are irreversible for all compounds measured (**3dCN**, **3fCO**, **3aCF**, **3eCN**, **3cCN**). In contrast, the reduction is quasi-reversible for compounds **3dCN**, **3eCN**, and **3cCN**, irreversible for **3aCF**, and reversible for compound **3fCO**. The ionization potentials are similar for all compounds bearing an electron-withdrawing group (CN) in position 2 as well as no substituents.

For compound **3fCO**, possessing an electron-donating group (NMe_2), the ionization potential is lower. The electron affinity is similar for all investigated compounds, hinting that the different substitution patterns have no direct effect on the LUMO energy.

Conclusions

We reported that the synthesis of benzo[*a*]indolizines from pyridinium salts and derivatives or analogues of 1-chloro-2-nitrobenzene has a reasonable scope and could be used under one-pot protocol to achieve the final dyes in 20–80% overall yields. The presence of up to four different electron-withdrawing groups allowed for studying their impact on desired photophysical properties. The combination of a highly-polarized core and the presence of a nitro group is responsible for yellow to red emission. The nitro group, which often quenches fluorescence to undetectable levels, still gives fluorescence yield of *ca.* 20–60% for the present dyes, despite its clear participation in the electronic transition. Moderate intramolecular charge transfer which has been introduced to these molecules is strong enough to supress ISC and weak enough to prevent formation of dark TICT states. The replacement of small electron-withdrawing groups with larger ones at position 6 causes distortion from planarity, which in turn decreases the singlet–triplet energy gap and causes partial fluorescence quenching.

Experimental section

General synthetic information

All reagents and solvents were purchased from commercial sources and used as received. Reactions with moisture and oxygen sensitive compounds were performed under an argon atm. Reaction progress was monitored by means of thin-layer chromatography (TLC), performed on aluminum foil plates, covered with Silica gel 60 F_{254} (Merck). Pure products were achieved by means of column chromatography with silica gel 60 (230–400 mesh). The identity and purity of final products were established by ^{1}H and ^{13}C NMR spectrometry as well as by MS-spectrometry (EI-MS, ESI-MS or APCI-MS). All reported ^{1}H NMR and ^{13}C NMR spectra were recorded on Bruker AM 500 MHz, Varian AM 500 MHz or Varian AM 600 MHz spectrometers. Chemical shifts (ppm) were determined with TMS as internal reference; J values are given in Hz. All melting points were measured with EZ-Melt apparatus.

Salts **1a**,[77] **1b**,[78] **1c**,[79] **1d**,[80] **1e**,[79] and methyl 4-chloro-3,5-dinitrobenzoate (**2O**[81]) were synthesized according to previously published procedure, and spectroscopic data are consistent.

1-(2-Oxo-2-phenylethyl)pyridin-1-ium bromide (1a). ^{1}H NMR (400 MHz, DMSO-d_6) δ 8.98 (d, J = 5.5 Hz, 2H), 8.73 (t, J = 7.8 Hz, 1H), 8.30–8.21 (m, 2H), 8.09–8.03 (m, 2H), 7.78 (d, J = 7.4 Hz, 1H), 7.69–7.61 (m, 2H), 6.47 (s, 2H).

2-(Cyanomethyl)isoquinolin-2-ium chloride (1b). ^{1}H NMR (500 MHz, DMSO-d_6) δ 10.31 (s, 1H), 8.91 (dd, J = 6.8, 1.3 Hz, 1H), 8.70 (d, J = 6.8 Hz, 1H), 8.60 (d, J = 8.3 Hz, 1H), 8.41 (d, J = 8.2 Hz, 1H), 8.37–8.32 (m, 1H), 8.16–8.11 (m, 1H), 6.22 (s, 2H).

1-(Cyanomethyl)pyridin-1-ium bromide (1c). ^{1}H NMR (600 MHz, DMSO-d_6) δ 9.25 (d, J = 5.6 Hz, 2H), 8.71 (t, J = 7.8, 1H), 8.26–8.20 (m, 2H), 6.11 (s, 2H).

1-(2-(*tert*-Butoxy)-2-oxoethyl)pyridin-1-ium bromide (1d). ^{1}H NMR (500 MHz, $CDCl_3$) δ 9.43 (d, J = 5.6 Hz, 2H), 8.59 (t, J = 7.8, 1H), 8.16–8.07 (m, 2H), 6.08 (s, 2H), 1.51 (s, 9H).

1-(2-(*tert*-Butoxy)-2-oxoethyl)-4-cyanopyridin-1-ium chloride (1e). ^{1}H NMR (500 MHz, DMSO-d$_6$) δ 9.36 (d, J = 6.5 Hz, 2H), 8.76 (d, J = 6.5 Hz, 2H), 5.68 (s, 2H), 1.45 (s, 9H).

Methyl 4-chloro-3,5-dinitrobenzoate (2CO). ^{1}H NMR (400 MHz, Chloroform-d) δ 8.59 (s, 2H), 4.02 (s, 3H).

Procedure for the synthesis of 1-(2-(*tert*-butoxy)-2-oxoethyl)-4-(dimethylamino)pyridin-1-ium chloride (1f). In a round bottom flask under inert atmosphere, 4-(dimethylamino)pyridine (2.44 g, 20 mmol) was mixed together with *tert*-butyl chloroacetate (2.86 mL, 20 mmol) in neat condition at room temperature. After 30 minutes a light pink fluffy power started to form. Reaction was stirred for an additional 2.5 hours than the precipitate was filtered off and washed with Et$_2$O. (3.26 g, 70%); R_f = 0.37 (MeOH/DCM, 1 : 4) M.p. 178–180 °C. ^{1}H NMR (500 MHz, DMSO-d$_6$) δ 8.24 (d, J = 7.8 Hz, 2H), 7.07 (d, J = 7.8 Hz, 2H), 5.10 (s, 2H), 3.19 (s, 6H), 1.43 (s, 9H). ^{13}C NMR (126 MHz, DMSO-d$_6$) δ 167.1, 156.5, 143.6, 107.8, 83.3, 57.4, 40.3, 28.2 ppm. HRMS (ESI): m/z calcd for $C_{13}H_{21}N_2O_2$, 237.1603 $[M]^+$; found, 237.1599.

General procedure for the synthesis of benzo[*a*]indolizines (condition A)

Salt **1** (2 mmol, 1 equiv.) was dissolved in 10 mL of water, 3,5-dinitrobenzoderivative **2** (2 mmol, 1 equiv.) was dissolved in 10 mL of chloroform, and K_2CO_3 (0.552 g, 4 mmol) was dissolved in 5 mL of water. All the solutions were cooled to 0 °C, added in order to a 50 mL round bottom flask and stirred at 0 °C for 30 min. A violet solid, when formed, was filtered. The organic phase containing betaine intermediate was extracted, evaporated, and combined with the solid for the next step. Betaine (2 mmol, 1 equiv.) was dissolved in 6 mL of DMSO at RT. Piperidine (395 mL, 4 mmol) was added and the mixture was stirred for 3 h. The reaction was quenched with a solution of CH_3COOH in H_2O (1 : 1) and the precipitate was filtered off. The crude product was purified by column chromatography (AcOEt/hexane, 3 : 7), unless differently stated.

General procedure for the synthesis of benzo[*a*]indolizines (condition B)

In a 50 mL round bottom flask, equipped with magnetic stirrer, pyridinium salt **1** (1 mmol, 1 equiv.) and dinitro-benzo derivative **2** (1 mmol, 1 equiv.) were dissolved in 3 mL of sulfolane. Cs_2CO_3 (1.302 g, 4 mmol) was added, and the reaction mixture was stirred overnight at room temperature. After completion, the reaction was quenched with 3 mL of a solution of CH_3COOH in water (1 : 1). A precipitate was formed, filtered, and washed with water, unless differently specified. Crude products, when needed, were purified by column chromatography.

7-Nitro-9-(trifluoromethyl)pyrido[2,1-*a*]isoindol-6-yl(phenyl) methanone (3aCF). According to the general procedure (condition A) 1-(2-oxo-2-phenylethyl)pyridin-1-ium bromide (0.198 g, 1 mmol) and 4-chloro-3,5-dinitrobenzotrifluoride (0.270 g, 1 mmol) were reacted affording **3aCF** (0.110 g, 30%) as orange crystals. R_f = 0.48 (AcOEt/hexane, 1 : 2); M. p. 204–206 °C. ^{1}H NMR (500 MHz, CDCl$_3$) δ 9.93 (d, J = 7.1, 1H), 8.73 (s, 1H), 8.40 (d, J = 8.7, 1H), 8.33 (s, 1H), 7.69–7.63 (m, 1H), 7.63–7.57 (m, 2H), 7.54–7.45 (m, 2H), 7.45–7.38 (m, 2H). ^{13}C NMR (126 MHz, CDCl$_3$) δ 186.7, 141.4, 140.6, 132.5, 132.4, 129.0, 128.0, 127.6, 125.6, 124.8, 123.5 (q, J = 3.5 Hz), 122.3 (q, J = 3.5 Hz), 121.7, 120.8 (q, J = 34 Hz), 120.3, 120.0, 118.0, 112.9 ppm. HRMS (ESI): m/z calcd for $C_{20}H_{11}N_2O_3F_3Na$, 407.0619 $[M + Na]^+$; found, 407.0625.

6-Benzoyl-7-nitropyrido[2,1-*a*]isoindole-9-carbonitrile (3aCN). According to the general procedure (condition A) 1-(2-oxo-2-phenylethyl)pyridin-1-ium bromide (0.198 g, 1 mmol) and 4-chloro-3,5-dinitrobenzonitrile (0.227 g, 1 mmol) were reacted affording **3aCN** (0.105 g, 30%) as orange crystals. R_f = 0.28 (AcOEt/hexane, 1 : 2); M.p. 243–245 °C. ^{1}H NMR (600 MHz, CDCl$_3$) δ 9.85 (d, J = 7.0 Hz 1H), 8.78 (s, 1H), 8.39 (d, J = 8.6 Hz, 1H), 8.30 (s, 1H), 7.71 (dd, J = 9.7, 7.8 Hz, 1H), 7.61 (d, J = 7.5 Hz, 2H), 7.53 (dd, J = 8.3, 7.3 Hz, 2H), 7.44–7.38 (m, 2H). ^{13}C NMR (126 MHz, CDCl$_3$) δ 186.8, 171.1, 141.0 (2), 140.3, 132.7, 132.3, 131.0, 129.1, 128.0, 127.8, 127.1, 126.3, 121.1, 120.5, 120.4, 118.2, 118.0, 101.0.

HRMS (EI): m/z calcd for $C_{20}H_{11}N_3O_3$, 341.0800 $[M^{\bullet+}]$; found 341.0797. (Additional solvent peaks are present in NMR spectra and was not possible to remove even after drying overnight.)

Methyl 6-benzoyl-7-nitropyrido[2,1-*a*]isoindole-9-carboxylate (3aCO). According to the general procedure (condition A) 1-(2-oxo-2-phenylethyl)pyridin-1-ium bromide (0.198 g, 1 mmol) and methyl 4-chloro-3,5-dinitrobenzoate (0.260 g, 1 mmol) were reacted affording **3aCO** (0.031 g, 8%) as orange crystals. R_f = 0.28 (AcOEt/hexane, 1 : 2); M.p. 249–251 °C. ^{1}H NMR (500 MHz, CDCl$_3$) δ 9.91 (d, J = 7.0 Hz, 1H), 9.18 (s, 1H), 8.74 (s, 1H), 8.41 (d, J = 8.5 Hz, 1H), 7.66 (dd, J = 9.0, 7.8 Hz, 1H), 7.61 (d, J = 7.4 Hz, 2H), 7.53–7.45 (m, 2H), 7.43–7.38 (m, 2H), 4.01 (s, 3H). ^{13}C NMR (126 MHz, CDCl$_3$) δ 186.8, 165.7, 141.4, 140.1, 133.3, 132.3, 129.0, 128.5, 128.0, 127.7, 126.2, 125.9, 122.4, 120.7, 120.6, 119.8, 118.1, 113.2, 52.6 ppm. HRMS (EI): m/z calcd for $C_{21}H_{14}N_2O_5$, 374.0903 $[M^{\bullet+}]$; found 374.0907.

9-Nitroisoindolo[1,2-*a*]isoquinoline-8,11-dicarbonitrile (3bCN). According to the general procedure (condition A) 1-(cyanomethyl)isoquinolinium chloride (0.338 g, 2 mmol) and 4-chloro-3,5-dinitrobenzonitrile (0.454 g, 2 mmol) were reacted affording **3bCN** (0.173 g, 28%) as red crystals after washing with water, MeOH, Et$_2$O and recrystallized from DMF/Et$_2$O. R_f = 0.45 (AcOEt/hexane, 1 : 1); M.p. 389–391 °C. ^{1}H NMR (500 MHz, DMF-d$_7$) δ 10.06 (s, 1H), 9.41 (d, J = 8.4 Hz, 1H), 8.96–8.92 (m, 2H), 8.33 (d, J = 7.9 Hz, 1H), 8.26 (d, J = 7.3 Hz, 1H); missing signal for 2H is probably hided under DMF peak at around 7.9 ppm; crystals were hardly soluble and it was not possible to dissolved them in any standard deuterated solvents. ^{13}C NMR was not possible to record. (APCI): m/z calcd for $C_{18}H_8N_4O_2$, 312.0647 $[M^-]$; found 312.0649.

7-Nitro-9-(trifluoromethyl)pyrido[2,1-*a*]isoindole-6-carbonitrile (3cCF). According to the general procedure (condition B) *N*-(cyanomethyl)pyridinium bromide (0.119 g, 1 mmol) and 4-chloro-3,5-dinitrobenzotrifluoride (0.270 g, 1 mmol) were reacted, affording **3cCF** (0.192 g, 63%) as orange/red crystals. R_f = 0.35 (AcOEt/hexane, 1 : 1); M.p. 309–311 °C. ^{1}H NMR (500 MHz, DMSO-d$_6$) δ 9.42 (s, 1H), 8.97 (d, J = 6.6 Hz, 1H),

8.94 (d, J = 8.5 Hz, 1H), 8.65 (s, 1H), 7.92–7.86 (m, 1H), 7.81–7.75 (m, 1H). ^{13}C NMR (126 MHz, DMSO-d_6) δ 136.7, 133.6, 128.3, 127.8, 127.6, 123.1, 122.3, 122.1, 121.2, 120.4, 120.4, 119.6 (q, J = 36 Hz), 114.1, 89.1 ppm. HRMS (ESI): m/z calcd for $C_{14}H_6F_3N_3O_2Na$, 328.0310 $[M + Na]^+$; found, 328.0315.

7-Nitropyrido[2,1-*a*]isoindole-6,9-dicarbonitrile (3cCN). According to the general procedure (condition B) *N*-(cyanomethyl)pyridinium bromide (0.119 g, 1 mmol) and 4-chloro-3,5-dinitrobenzonitrile (0.227 g, 1 mmol) were reacted, affording **3cCN** (0.167 g, 64%) as red crystals. R_f = 0.25 (AcOEt/hexane, 1 : 1); M.p. 329–331 °C. ^{1}H NMR (500 MHz, acetone-d_6) δ 9.38 (d, J = 1.1 Hz, 1H), 9.09 (d, J = 6.7 Hz, 1H), 8.90 (d, J = 8.4 Hz, 1H), 8.85 (d, J = 1.1 Hz, 1H), 8.05–7.97 (m, 1H), 7.96–7.91 (m, 1H). ^{13}C NMR (126 MHz, acetone-d_6) δ 205.2, 133.6, 133.2, 132.4, 128.3, 128.0, 127.1, 121.8, 121.5, 121.0, 119.6, 117.7, 112.8, 101.4 ppm. HRMS (APCI): m/z calcd for $C_{14}H_6N_4O_2$, 262.0491 $[M^+]$; found, 262.0498.

Methyl 6-cyano-7-nitropyrido[2,1-*a*]isoindole-9-carboxylate (3cCO). According to the general procedure (condition B) *N*-(cyanomethyl)pyridinium bromide (0.119 g, 1 mmol) and methyl 4-chloro-3,5-dinitrobenzoate (0.260 g, 1 mmol) were reacted, affording **3cCO** (0.062 g, 20%) as orange crystals. R_f = 0.45 (AcOEt/hexane, 2 : 1); M.p. 312–314 °C. ^{1}H NMR (500 MHz, $CDCl_3$) δ 9.25–9.19 (m, 2H), 8.97–8.92 (m, 1H), 8.41 (d, J = 8.5 Hz, 1H), 7.74–7.67 (m, 1H), 7.62–7.58 (m, 1H), 4.05 (s, 3H). ^{13}C NMR (126 MHz, $CDCl_3$) δ 165.4, 129.8, 127.3, 126.6, 126.3, 121.6, 120.6, 120.2, 118.8, 113.6, 52.7, 51.1, 22.8 ppm. HRMS (EI): m/z calcd for $C_{15}H_9N_3O_4$, 295.0593 $[M^{\bullet+}]$; found 295.0594.

***tert*-Butyl 7-nitro-9-(trifluoromethyl)pyrido[2,1-*a*]isoindole-6-carboxylate (3dCF).** According to the general procedure *N*-(*tert*-butyloxycarbonylmethyl)pyridinium bromide (0.194 g, 1 mmol) and 4-chloro-3,5-dinitrobenzotrifluoride (0.270 g, 1 mmol) were reacted affording **3dCF** (0.030 g, 8%), as orange crystals. R_f = 0.46 (AcOEt/hexane, 1 : 5); M.p. 225–227 °C. ^{1}H NMR (500 MHz, $CDCl_3$) δ 10.04 (d, J = 7.1 Hz, 1H), 8.63 (s, 1H), 8.30 (d, J = 1.6 Hz, 1H), 8.23 (d, J = 1.5 Hz, 1H), 7.60–7.53 (m, 1H), 7.45 (td, J = 7.0, 1.4 Hz, 1H), 1.64 (s, 9H). ^{13}C NMR (126 MHz, $CDCl_3$) δ 161.0, 141.7, 132.2, 128.0, 124.9, 124.2, 122.3, 121.3, 120.7, 120.5, 119.9, 119.4, 117.8, 106.4, 83.4, 28.4 ppm. HRMS (EI): m/z calcd for $C_{18}H_{15}N_2O_4F_3$, 380.0984 $[M^+]$; found 380.0988.

***tert*-Butyl 9-cyano-7-nitropyrido[2,1-*a*]isoindole-6-carboxylate (3dCN).** According to the general procedure (condition B) *N*-(*tert*-butyloxycarbonylmethyl)pyridinium bromide (0.194 g, 1 mmol) and 4-chloro-3,5-dinitrobenzonitrile (0.227 g, 1 mmol) were reacted affording **3dCN** (0.299 g, 85%), as dark red crystals. R_f = 0.65 (AcOEt/hexane, 1 : 1); M.p. 185–187 °C. ^{1}H NMR (500 MHz, $CDCl_3$) δ 10.02 (d, J = 7.0 Hz, 1H), 8.67 (d, J = 1.3 Hz, 1H), 8.30 (d, J = 8.5, 1H), 8.17 (d, J = 1.3 Hz, 1H), 7.62 (ddd, J = 8.5, 7.0, 1.0 Hz, 1H), 7.50 (ddd, J = 7.0, 7.0, 1.3 Hz, 1H), 1.63 (s, 9H). ^{13}C NMR (126 MHz, $CDCl_3$) δ 160.8, 141.5, 141.0, 132.0, 129.9, 128.2, 126.0, 125.2, 120.2, 120.1, 119.9, 118.2, 117.9, 100.8, 83.8, 28.4 ppm. HRMS (EI): m/z calcd for $C_{18}H_{15}N_3O_4$, 337.1063 $[M^{\bullet+}]$; found 337.1067.

6-(*tert*-Butyl) 9-methyl 7-nitropyrido[2,1-*a*]isoindole-6,9-dicarboxylate (3dCO). According to the general procedure (condition B) *N*-(*tert*-butyloxycarbonylmethyl)pyridinium bromide (0.194 g, 1 mmol) and methyl 4-chloro-3,5-dinitrobenzoate (0.260 g, 1 mmol) were reacted affording **3dCO** (0.074 g, 20%) as orange crystals. R_f = 0.64 (AcOEt/hexane, 1 : 1); M. p. 216–218 °C. ^{1}H NMR (500 MHz, $CDCl_3$) δ 10.01 (d, J = 7.0 Hz, 1H), 9.09 (d, J = 1.3 Hz, 1H), 8.63 (d, J = 1.4 Hz, 1H), 8.33 (d, J = 8.5 Hz, 1H), 7.59–7.53 (m, 1H), 7.46–7.41 (m, 1H), 4.01 (s, 3H), 1.64 (s, 9H). ^{13}C NMR (126 MHz, $CDCl_3$) δ 165.9, 161.1, 141.2, 132.9, 128.1, 127.4, 125.1, 124.5, 121.2, 120.4, 120.3, 119.3, 117.9, 106.7, 83.3, 52.5, 28.4 ppm. HRMS (EI): m/z calcd for $C_{19}H_{18}N_2O_6$, 370.1165 $[M^{\bullet+}]$; found 370.1164.

***tert*-Butyl 2-cyano-7-nitro-9-(trifluoromethyl)pyrido[2,1-*a*]isoindole-6-carboxylate (3eCF).** According to the general procedure (condition B) 1-(2-(*tert*-butoxy)-2-oxoethyl)-4-cyanopyridin-1-ium chloride (0.219 g, 1 mmol) and 4-chloro-3,5-dinitrobenzonitrile (0.227 g, 1 mmol) 4-chloro-3,5-dinitrobenzotrifluoride (0.270 g, 1 mmol) were reacted affording **3eCF** (0.100 g, 25%), as orange crystals. R_f = 0.60 (AcOEt/hexane, 1 : 1); M.p. 205–207 °C. ^{1}H NMR (500 MHz, $CDCl_3$) δ 9.96 (dd, J = 7.4, 1.0 Hz, 1H), 8.70 (s, 1H), 8.65–8.63 (m, 1H), 8.29 (s, 1H), 7.52 (dd, J = 7.4, 1.9 Hz, 1H), 1.63 (s, 9H). ^{13}C NMR (126 MHz, $CDCl_3$) δ 160.2, 142.4, 129.3, 127.4, 124.4, 123.4 (q, J = 34.4 Hz), 122.9, 122.01 (q, J = 4.1 Hz), 121.6 (q, J = 3.1 Hz), 120.9, 120.5, 119.2, 117.0, 110.0, 105.2, 84.9, 28.2 ppm. HRMS (EI): m/z calcd for $C_{19}H_{14}F_3N_3O_4$, 405.0936 $[M^{\bullet+}]$; found 405.0950.

***tert*-Butyl 2,9-dicyano-7-nitropyrido[2,1-*a*]isoindole-6-carboxylate (3eCN).** According to the general procedure (condition B) 1-(2-(*tert*-butoxy)-2-oxoethyl)-4-cyanopyridin-1-ium chloride (0.219 g, 1 mmol) and 4-chloro-3,5-dinitrobenzonitrile (0.227 g, 1 mmol) were reacted affording **3eCN** (0.089 g, 24%), as orange crystals. R_f = 0.65 (AcOEt/hexane, 1 : 1); M. p. 340–342 °C. ^{1}H NMR (600 MHz, $CDCl_3$) δ 9.97 (d, J = 7.4 Hz, 1H), 8.75 (s, 1H), 8.63 (s, 1H), 8.25 (s, 1H), 7.55 (dd, J = 7.4, 1.9 Hz, 1H), 1.62 (s, 9H). ^{13}C NMR (151 MHz, $CDCl_3$) δ 160.0, 142.3, 131.9, 129.7, 129.2, 127.6, 126.1, 122.9, 121.0, 120.2, 119.7, 117.3, 116.7, 106.1, 104.2, 85.3, 28.2 ppm. HRMS (APCI): m/z calcd for $C_{19}H_{14}N_4O_4$, 362.1015 $[M^+]$; found 362.1021.

6-(*tert*-Butyl) 9-methyl 2-cyano-7-nitropyrido[2,1-*a*]isoindole-6,9-dicarboxylate (3eCO). According to the general procedure (condition B) 1-(2-(*tert*-butoxy)-2-oxoethyl)-4-cyanopyridin-1-ium chloride (0.219 g, 1 mmol) and methyl 4-chloro-3,5-dinitrobenzoate (0.260 g, 1 mmol) were reacted affording **3eCO** (0.026 g, 6%) as orange crystals. R_f = 0.62 (AcOEt/hexane, 1 : 2); M.p. decomposed at 270 °C; ^{1}H NMR (600 MHz, $CDCl_3$) δ 9.93 (d, J = 7.3 Hz, 1H), 9.14 (s, 1H), 8.70 (s, 1H), 8.65 (s, 1H), 7.50 (dd, J = 6.8, 1.1 Hz, 1H), 4.04 (s, 3H), 1.64 (s, 9H). ^{13}C NMR (151 MHz, $CDCl_3$) δ 165.2, 160.3, 141.9, 129.9, 127.4, 126.9, 125.3, 123.2, 122.9, 121.3, 121.2, 119.1, 117.1, 110.2, 105.2, 84.8, 52.8, 28.2 ppm. HRMS (APCI): m/z calcd for $C_{20}H_{17}N_3O_6$, 395.1117 $[M^-]$; found 395.1119.

6-(*tert*-Butyl) 9-methyl 2-(dimethylamino)-7-nitropyrido[2,1-*a*]isoindole-6,9-dicarboxylate (3fCO). According to the general procedure 1-(2-(*tert*-butoxy)-2-oxoethyl)-4-(dimethylamino) pyridin-1-ium chloride (0.237 g, 1 mmol) and methyl 4-chloro-

3,5-dinitrobenzoate (0.260 g, 1 mmol) were reacted affording **3fCO** (0.053 g, 13%) as purple crystals. R_f = 0.55 (AcOEt/hexane, 2 : 1); M.p. decomposed at 220 °C. ^{1}H NMR (600 MHz, DMF-d$_7$) δ 9.71 (d, J = 7.8 Hz, 1H), 9.29 (d, J = 1.4 Hz, 1H), 8.41 (d, J = 1.4 Hz, 1H), 8.07 (d, J = 2.9 Hz, 1H), 7.33 (dd, J = 7.9, 2.9 Hz, 1H), 3.94 (s, 3H), 3.27 (s, 6H), 1.57 (s, 10H).^{13}C-NMR was not possible to record because of low solubility. HRMS (EI): m/z calcd for $C_{21}H_{23}N_3O_6$, 436.1485 $[M + Na]^+$; found 436.1481.

Procedure for the synthesis of 7-amino-9-(trifluoromethyl) pyrido[2,1-*a*]isoindole-6-carbonitrile (4). 3cCF (0.170 g, 0.5 mmol) was dissolved in 3 mL of MeOH in a Schlenk tube under Argon flow. Pd/C (0.020 g, 0.18 mmol, 10 wt%) and ammonium formate (0.250 g, 4 mmol) were added, and the resulting mixture was stirred for 24 h under inert atmosphere. When the reaction was complete (monitored by TLC), Pd/C was filtered off through a Celite pad using MeOH as eluent. The solvent was removed under reduced pressure and the crude product was purified by column chromatography (silica; AcOEt/hexane, 3 : 7). Pale yellow crystals were obtained in the yield of 0.165 g, 60%. R_f = 0.60 (AcOEt/hexane, 1 : 2); Mp. 205–206 °C. ^{1}H NMR (500 MHz, $CDCl_3$) δ 8.60 (d, J = 6.7 Hz, 1H), 8.13 (d, J = 8.5 Hz, 1H), 7.82 (s, 1H), 7.37–7.33 (m, 1H), 7.32–7.27 (m, 1H), 6.83 (s, 1H), 4.51 (s, 2H). ^{13}C NMR (126 MHz, $CDCl_3$) δ 137.4, 132.0, 125.8, 125.5, 125.1, 123.5, 122.5, 118.9, 118.1, 117.4, 115.9 (q, J = 177 Hz), 107.8 (q, J = 4.8 Hz), 105.3 (q, J = 2.5 Hz), 84.8 ppm. HRMS (ESI): m/z calcd for $C_{14}H_7F_3N_3$, 274.0592 $[M - H]^-$; found, 274.0583.

Procedure for the synthesis of 7-nitropyrido[2,1-*a*]isoindole-9-carbonitrile (5). 3dCN (0.240 g, 0.7 mmol) was dissolved in 3 mL of DCM in a round bottom flask. A pipette of TFA was added, the mixture changed color from red to yellow and was stirred overnight at RT. When the reaction was complete (monitored by TLC), $NaHCO_3$ (aqueous solution) was added, and extraction was performed with AcOEt. Organic phases (purple) were collected, washed, and dried under vacuum. The product was purified by column chromatography (silica; AcOEt/hexane, 3 : 7). A dark purple solid was obtained in the yield of 0.059 g 35%. R_f = 0.68 (AcOEt/hexane, 3 : 7); M. p. 291–293 °C. ^{1}H NMR (600 MHz, $CDCl_3$) δ 8.76 (br s, 1H), 8.65 (d, J = 1.2 Hz, 1H), 8.53 (d, J = 6.7 Hz, 1H), 8.52 (s, 1H), 8.26 (d, J = 8.6 Hz, 1H), 7.42–7.37 (m, 1H), 7.37–7.32 (m, 1H). ^{13}C NMR (126 MHz, $CDCl_3$) δ 137.0, 132.6, 129.6, 126.2, 125.9, 121.6, 120.0, 119.0, 118.9, 118.8, 106.7, 98.4 ppm. HRMS (EI): m/z calcd for $C_{13}H_7N_3O_2$, 237.0538 $[M^{\bullet+}]$; found, 237.0546. HRMS (EI): m/z calcd for $C_{13}H_7N_3O_2$, 237.0538 $[M^{\bullet+}]$; found, 237.0546.

Photophysical measurements

HPLC grade solvents were purchased from Sigma-Aldrich and used as obtained. For optical studies, solutions of molecules at low concentrations were used to avoid dimerization or reabsorption effects. All absorption and fluorescence spectra were taken at room temperature (21 °C). A Szimadzu UV/VIS-NIR spectrophotometer, model UV-3600i Plus, was used for absorption spectra measurement. Fluorescence spectra were recorded with an FS5 spectrofluorometer from Edinburgh Instruments. Fluorescence quantum yields (FQY) of molecules in solvents at 21 °C were determined using Cumarin 153, 9,10-diphenylanthracene, Fluorescein and Sulforhodamine 101 as FQY standards. Solutions of low absorbance (A < 0.1) were used to avoid reabsorption or concentration quenching. Refractive index correction for solvents have been performed in the calculations of quantum yields. Molar absorption coefficient, ε, was calculated from the absorbance, A, of a solution of the given molar concentration, c, in a cuvette of length, l, according to Lambert–Beer formula:

$$A = c \times \varepsilon \times l.$$

Crystallography

X-ray diffraction data was collected at the Advanced Light Source (ALS), Lawrence Berkeley National Lab, Berkeley, CA, endstation 12.2.1 using a silicon monochromated beam of 17 keV (λ = 0.7288 Å). A single crystal of **3bCN** was mounted on a MiTeGen 10 μm aperture Dual-Thickness MicroMount, and data collection was conducted at 100 K, with the crystal cooled by a stream of dry nitrogen. Bruker APEX3 software was used for data collection, Bruker SAINT V8.38A software was used to conduct the cell refinement and data reduction procedures, and absorption corrections were carried out utilizing the TWINABS program due to non-merohedral twinning.[82] Initial structure solutions were found using direct methods (SHELXT),[83] and refinements were carried out using SHELXL-2014,[83] as implemented by Olex2.[84] Thermal parameters for all non-hydrogen atoms were refined anisotropically. Hydrogen atoms were placed in calculated positions and refined isotropically. The structure has been deposited to the Cambridge Crystallographic Data Centre (CCDC) under deposition number 2132628.†

Computational details

We have started by performing DFT and TD-DFT calculations with the Gaussian 16 code[85] on all dyes. Default Gaussian16 thresholds and algorithms were used but for an improved optimization threshold (10^{-5} au on average residual forces), a stricter self-consistent field convergence criterion (10^{-10} a.u.) and the use of the *ultrafine* DFT integration grid. Firstly, the S_0 geometries have been optimized with DFT and the vibrational frequencies have been analytically determined, using the M06-2X *meta*-GGA hybrid exchange–correlation functional.[86] These calculations were performed with the 6-311G(d,p) atomic basis set and account for solvent effects through the Polarizable Continuum Model (PCM) approach considering DCM as solvent.[87] Secondly, starting from the optimal ground-state geometries, we have used TD-DFT with the same functional and basis set to optimize the S_1 geometry and compute the corresponding vibrational frequencies. All optimized structures are true minima of the potential energy surface (no imaginary frequency). Thirdly, the vertical transition energies were determined with TD-DFT and the same functional, but a larger basis set, namely 6-311+G(2d,p), in gas-phase as well as in solution using the recently-developed cLR[2] variant of the

PCM,[88] in its *non-equilibrium* limit. As the shortcomings of TD-DFT for CT derivatives as well as for are known, the transition energies were also computed using CC2[89] and SCS-CC2[90] with the Turbomole 7.3 code.[91] The (SCS-)CC2 energies were calculated in gas phase applying the resolution of identity scheme, and using the *aug*-cc-pVTZ atomic basis set and the corresponding auxillary basis. Combining the CC2 and TD-DFT data using a well-known protocol,[73] one can obtain accurate CC2-corrected estimates of the 0–0 energies that can be straightforwardly compared to experimental values. Vertical absorption and emission energies were corrected in the same way. The reported S–T gaps are gas-phase SCS-CC2 values computed in the S_1 geometry, as SCS-CC2 is known to be exceptionally efficient for these gaps.[92] The SOC matrix elements were determined at the M06-2X/*def2*-TZVP level using ORCA.5.0.1[93] with Dichloromethane as solvent was modelled with the SMD solvation model. The RIJCOSX method was used to accelerate the calculation and TightSCF settings were applied, whereas TDA was turned off. The SOC reported in the body of the text were determined as:

$$\sqrt{\frac{1}{3}S_x{}^2 + \frac{1}{3}S_y{}^2 + \frac{1}{3}S_z{}^2}.$$

The vibronic couplings were determined with the FCClasses 3 program, on the basis of TD-DFT data.[94,95] The radiative and internal conversion rates were obtained within the time-dependent formulation, the FC approach and the *Vertical Gradient* model,[96] thanks to the TVCF formalism of Peng and Shuai,[75] implemented in FCClasses by Cerezo and Santoro. For both the radiative and internal conversion rates, we used a 10 cm^{-1} broadening Gaussian, which is a typical value when modeling organic dyes.[97,98]

Author contributions

Conceptualization: D. T. G., J. S. A. B.; investigation: J. S. A. B., B. K., M. H. E. B., E. T. O., D. J.; supervision: D. T. G., D. J.; visualization: J. S. A. B., D. J.; writing – original draft: J. S. A. B., D. J.; D. T. G.; writing – review & editing: D. T. G., B. K., J. S. A. B., D. J., E. T. O.

Conflicts of interest

There are no conflicts to declare.

Acknowledgements

The work was financially supported by the Polish National Science Centre, Poland (HARMONIA 2018/30/M/ST5/00460), the Foundation for Polish Science (TEAM POIR.04.04.00-00-3CF4/16-00). This project received funding from European Union's Horizon 2020 research and innovation programme under Grant Agreement No 860762. M. H. E. B. and D. J. thank the CCIPL computational center installed in Nantes for generous allocation of computational time. We extend our gratitude to Dr Simon J. Teat for training and guidance through our crystallography studies at the Advanced Light Source (ALS), Lawrence Berkeley National Laboratory, supported by the Office of Science, Office of Basic Energy Sciences, of the U.S. Department of Energy under Contract No. DE-AC02-05CH11231. The authors thank J. Cerezo and F. Santoro for kindly making their code available.

Notes and references

1 A. E. Tschitschibabin, Tautomerie in der Pyridin–Reihe, *Ber. Dtsch. Chem. Ges. B*, 1927, **60**, 1607–1617.
2 A. Angeli, Ueber die Einwirkung des Oxaldiäthylesters auf das Pyrrylmethylketon, *Ber. Dtsch. Chem. Ges.*, 1890, **23**, 1793–1797.
3 A. Angeli, Ueber die Einwirkung des Oxaldiäthylesters auf das Pyrrylmethylketon, *Ber. Dtsch. Chem. Ges.*, 1890, **23**, 2154–2160.
4 A. Angeli, Sui prodotti di condensazione del pirrilmetilchetone con l'etere ossalico, *Gazz. Chim. Ital.*, 1890, **20**, 753–772.
5 E. Kim, Y. Lee, S. Lee and S. B. Park, Discovery, Understanding, and Bioapplication of Organic Fluorophore: A Case Study with an Indolizine-Based Novel Fluorophore, Seoul-Fluor, *Acc. Chem. Res.*, 2015, **48**, 538–547.
6 R. Ji, A. Liu, S. Shen, X. Cao, F. Li and Y. Ge, An indolizine–rhodamine based FRET fluorescence sensor for highly sensitive and selective detection of Hg2+ in living cells, *RSC Adv.*, 2017, **7**, 40829–40833.
7 H. Sonnenschein, G. Hennrich, U. Resch-Genger and B. Schulz, Fluorescence and UV/Vis spectroscopic behaviour of novel biindolizines, *Dyes Pigm.*, 2000, **46**, 23–27.
8 A. J. Huckaba, A. Yella, L. E. McNamara, A. E. Steen, J. S. Murphy, C. A. Carpenter, G. D. Puneky, N. I. Hammer, M. K. Nazeeruddin, M. Grätzel and J. H. Delcamp, Molecular Design Principles for Near-Infrared Absorbing and Emitting Indolizine Dyes, *Chem. – Eur. J.*, 2016, **22**, 15536–15542.
9 J. Wan, C.-J. Zheng, M.-K. Fung, X.-K. Liu, C.-S. Lee and X.-H. Zhang, Multifunctional electron-transporting indolizine derivatives for highly efficient blue fluorescence, orange phosphorescence host and two-color based white OLEDs, *J. Mater. Chem.*, 2012, **22**, 4502.
10 B. Koszarna, R. Matczak, M. Krzeszewski, O. Vakuliuk, J. Klajn, M. Tasior, J. T. Nowicki and D. T. Gryko, Direct arylation of electron-poor indolizines, *Tetrahedron*, 2014, **70**, 225–231.
11 G. Martinez-Ariza, B. T. Mehari, L. A. G. Pinho, C. Foley, K. Day, J. C. Jewett and C. Hulme, Synthesis of fluorescent heterocycles via a Knoevenagel/[4+1]-cycloaddition cascade using acetyl cyanide, *Org. Biomol. Chem.*, 2017, **15**, 6076–6079.
12 D. Chernyak, C. Skontos and V. Gevorgyan, Two-Component Approach Toward a Fully Substituted N-Fused Pyrrole Ring, *Org. Lett.*, 2010, **12**, 3242–3245.

13 R.-R. Liu, C.-J. Lu, M.-D. Zhang, J.-R. Gao and Y.-X. Jia, Palladium-Catalyzed Three-Component Cascade Reaction: Facial Access to Densely Functionalized Indolizines, *Chem. – Eur. J.*, 2015, **21**, 7057–7060.
14 M. Kucukdisli and T. Opatz, One-Pot Synthesis of Polysubstituted Indolizines by an Addition/Cycloaromatization Sequence, *J. Org. Chem.*, 2013, **78**, 6670–6676.
15 J. Barluenga, G. Lonzi, L. Riesgo, L. A. López and M. Tomás, Pyridine Activation via Copper(I)-Catalyzed Annulation toward Indolizines, *J. Am. Chem. Soc.*, 2010, **132**, 13200–13202.
16 H. Zhu, N. Shao, T. Chen and H. Zou, Functionalized heterocyclic scaffolds derived from Morita–Baylis–Hillman Acetates, *Chem. Commun.*, 2013, **49**, 7738.
17 D. Coffinier, L. El Kaim and L. Grimaud, Nef-Perkow Access to Indolizine Derivatives, *Synlett*, 2010, 2474–2476.
18 T. Xu and H. Alper, Synthesis of Indolizine Derivatives by Pd-Catalyzed Oxidative Carbonylation, *Org. Lett.*, 2015, **17**, 4526–4529.
19 S. Chuprakov, F. W. Hwang and V. Gevorgyan, Rh-Catalyzed Transannulation of Pyridotriazoles with Alkynes and Nitriles, *Angew. Chem., Int. Ed.*, 2007, **46**, 4757–4759.
20 B. Sadowski, J. Klajn and D. T. Gryko, Recent advances in the synthesis of indolizines and their π-expanded analogues, *Org. Biomol. Chem.*, 2016, **14**, 7804–7828.
21 T. Uchida and K. Matsumoto, Methods for the Construction of the Indolizine Nucleus, *Synthesis*, 1976, 209–236.
22 F. J. Swinbourne, J. H. Hunt and G. Klinkert, *Advances in Heterocyclic Chemistry*, Elsevier, 1979, vol. 23, pp. 103–170.
23 N. S. Prostakov and O. B. Baktibaev, Indolizines, *Russ. Chem. Rev.*, 1975, **44**, 748.
24 H. L. Blewitt, *Chemistry of Heterocyclic Compounds*, John Wiley & Sons, Ltd, 1977, pp. 117–178.
25 D. Basavaiah, B. Devendar, D. Lenin and T. Satyanarayana, The Baylis-Hillman Bromides as Versatile Synthons: A Facile One-Pot Synthesis of Indolizine and Benzofused Indolizine Frameworks, *Synlett*, 2009, 411–416.
26 B. Yan and Y. Liu, Gold-Catalyzed Multicomponent Synthesis of Aminoindolizines from Aldehydes, Amines, and Alkynes under Solvent-Free Conditions or in Water, *Org. Lett.*, 2007, **9**, 4323–4326.
27 S. S. Patil, S. V. Patil and V. D. Bobade, Synthesis of Aminoindolizine and Quinoline Derivatives via Fe(acac)3/TBA- OH-Catalyzed Sequential Cross-Coupling–Cycloisomerization Reactions, *Synlett*, 2011, **16**, 2379–2383.
28 Y. Yang, C. Xie, Y. Xie and Y. Zhang, Synthesis of Functionalized Indolizines via Copper-Catalyzed Annulation of 2-Alkylazaarenes with α,β-Unsaturated Carboxylic Acids, *Org. Lett.*, 2012, **14**, 957–959.
29 C. Feng, Y. Yan, Z. Zhang, K. Xu and Z. Wang, Cerium(III)-catalyzed cascade cyclization: an efficient approach to functionalized pyrrolo[1,2-a]quinolines, *Org. Biomol. Chem.*, 2014, **12**, 4837–4840.
30 Z. Li, D. Chernyak and V. Gevorgyan, Palladium-Catalyzed Carbonylative Cyclization/Arylation Cascade for 2-Aroylindolizine Synthesis, *Org. Lett.*, 2012, **14**, 6056–6059.
31 R.-R. Liu, Z.-Y. Cai, C.-J. Lu, S.-C. Ye, B. Xiang, J. Gao and Y.-X. Jia, Indolizine synthesis via Cu-catalyzed cyclization of 2-(2-enynyl)pyridines with nucleophiles, *Org. Chem. Front.*, 2015, **2**, 226–230.
32 K.-S. Lee, T.-K. Kim, J. H. Lee, H.-J. Kim and J.-I. Hong, Fluorescence turn-on probe for homocysteine and cysteine in water, *Chem. Commun.*, 2008, 6173.
33 X. Wang, S. Li, Y. Pan, H. Wang, H. Liang, Z. Chen and X. Qin, Samarium(III)-Catalyzed C(sp^3)–H Bond Activation: Synthesis of Indolizines *via* C–C and C–N Coupling between 2-Alkylazaarenes and Propargylic Alcohols, *Org. Lett.*, 2014, **16**, 580–583.
34 X. Meng, P. Liao, J. Liu and X. Bi, Silver-catalyzed cyclization of 2-pyridyl alkynyl carbinols with isocyanides: divergent synthesis of indolizines and pyrroles, *Chem. Commun.*, 2014, **50**, 11837–11839.
35 M. Nayak and I. Kim, Construction of benzo-fused indolizines, pyrrolo[1,2-a]quinolines via alkyne–carbonyl metathesis, *Org. Biomol. Chem.*, 2015, **13**, 9697–9708.
36 E. M. Roberts, M. Gates and V. Boekelheide, A Synthesis of 5,6-benzopyrrocoline [1], *J. Org. Chem.*, 1955, **20**, 1443–1447.
37 J. Liu, L. Zhou, W. Ye and C. Wang, Formal [3+2] cycloaddition of 1-cyanocyclopropane 1-ester with pyridine, quinoline or isoquinoline: a general and efficient strategy for construction of cyanoindolizine skeletons, *Chem. Commun.*, 2014, **50**, 9068–9071.
38 D. Basavaiah, G. Veeraraghavaiah and S. S. Badsara, Ketones as electrophiles in two component Baylis–Hillman reaction: a facile one-pot synthesis of substituted indolizines, *Org. Biomol. Chem.*, 2014, **12**, 1551.
39 J. Brioche, C. Meyer and J. Cossy, Synthesis of 2-Aminoindolizines by 1,3-Dipolar Cycloaddition of Pyridinium Ylides with Electron-Deficient Ynamides, *Org. Lett.*, 2015, **17**, 2800–2803.
40 I. V. Seregin and V. Gevorgyan, Gold-Catalyzed 1,2-Migration of Silicon, Tin, and Germanium en Route to C-2 Substituted Fused Pyrrole-Containing Heterocycles, *J. Am. Chem. Soc.*, 2006, **128**, 12050–12051.
41 B. Sahoo, M. N. Hopkinson and F. Glorius, External-Photocatalyst-Free Visible-Light-Mediated Synthesis of Indolizines, *Angew. Chem., Int. Ed.*, 2015, **54**, 15545–15549.
42 S. Park and I. Kim, Electron-withdrawing group effect in aryl group of allyl bromides for the successful synthesis of indolizines via a novel [3+3] annulation approach, *Tetrahedron*, 2015, **71**, 1982–1991.
43 W. Hao, H. Wang, Q. Ye, W.-X. Zhang and Z. Xi, Cyclopentadiene-Phosphine/Palladium-Catalyzed Synthesis of Indolizines from Pyrrole and 1,4-Dibromo-1,3-butadienes, *Org. Lett.*, 2015, **17**, 5674–5677.
44 S. G. Dawande, B. S. Lad, S. Prajapati and S. Katukojvala, Rhodium-catalyzed pyridannulation of indoles with diazoenals: a direct approach to pyrido[1,2-a]indoles, *Org. Biomol. Chem.*, 2016, **14**, 5569–5573.
45 Y. Jung and I. Kim, Deformylative Intramolecular Hydroarylation: Synthesis of Benzo[*e*]pyrido[1,2-*a*]indoles, *Org. Lett.*, 2015, **17**, 4600–4603.

46 Y. Jung and I. Kim, Synthesis of 6-Aryl-5-iodobenzo[e] pyrido[1,2-a]indoles by 6-endo-dig Iodocyclization, *Asian J. Org. Chem.*, 2016, **5**, 147–152.
47 L. Dalton and T. Teitei, Synthesis of Benz[b]indolizinies and related compounds, *Aust. J. Chem.*, 1969, **22**, 1525.
48 F. D. Saeva and H. R. Luss, Novel synthesis of the 2,3-benzindolizine ring system. Mechanism of formation, redox, electronic absorption, and fluorescence behavior, *J. Org. Chem.*, 1988, **53**, 1804–1806.
49 A. Fozard and C. K. Bradsher, Synthesis of the pyrido[2,1-a] isoindole system by an intramolecular photochemical cyclization, *J. Org. Chem.*, 1967, **32**, 2966–2969.
50 C. K. Bradsher and C. F. Voigt, Electrophilic substitution of the pyrido[2,1-a]isoindole system, *J. Org. Chem.*, 1971, **36**, 1603–1607.
51 S. Kajigaeshi, S. Mori, S. Fujisaki and S. Kanemasa, *exo* -Selective Peripheral Cycloaddition Reactions of Pyrido[2,1-*a*]isoindole, *Bull. Chem. Soc. Jpn.*, 1985, **58**, 3547–3551.
52 W. Augstein and F. Kröhnke, Synthesen des Benzo[a]- und des Naphtho[2.3-b]indolizin-Ringsystems, *Justus Liebigs Ann. Chem.*, 1966, **697**, 158–170.
53 C. C. Chintawar, M. V. Mane, A. G. Tathe, S. Biswas and N. T. Patil, Gold-Catalyzed Cycloisomerization of Pyridine-Bridged 1,8-Diynes: An Expedient Access to Luminescent Cycl[3.2.2]azines, *Org. Lett.*, 2019, **21**, 7109–7113.
54 B. Zhao, M. Yu, H. Liu, Y. Chen, Y. Yuan and X. Xie, Rhodium-Catalyzed Direct Oxidative C-H Acylation of 2-Arylpyridines with Terminal Alkynes: A Synthesis of Pyrido[2,1-*a*]isoindoles, *Adv. Synth. Catal.*, 2014, **356**, 3295–3301.
55 C. Xie, Y. Zhang and P. Xu, Novel Synthesis of Pyrido[2,1-*a*] isoindoles via a Three-ComponentAssembly Involving Benzynes, *Synlett*, 2008, 3115–3120.
56 T. Mitsumori, M. Bendikov, O. Dautel, F. Wudl, T. Shioya, H. Sato and Y. Sato, Synthesis and Properties of Highly Fluorescent Indolizino[3,4,5-*ab*]isoindoles, *J. Am. Chem. Soc.*, 2004, **126**, 16793–16803.
57 S. Asako, T. Kobashi and K. Takai, Use of Cyclopropane as C1 Synthetic Unit by Directed Retro-Cyclopropanation with Ethylene Release, *J. Am. Chem. Soc.*, 2018, **140**, 15425–15429.
58 X. Chen, X. Hu, Y. Deng, H. Jiang and W. Zeng, A [4+1] Cyclative Capture Access to Indolizines via Cobalt(III)-Catalyzed Csp ^{2} –H Bond Functionalization, *Org. Lett.*, 2016, **18**, 4742–4745.
59 X. Huang and T. Zhang, Multicomponent reactions of pyridines, α-bromo carbonyl compounds and silylaryl triflates as aryne precursors: a facile one-pot synthesis of pyrido [2,1-a]isoindoles, *Tetrahedron Lett.*, 2009, **50**, 208–211.
60 T.-J. Gong, M.-Y. Xu, S.-H. Yu, C.-G. Yu, W. Su, X. Lu, B. Xiao and Y. Fu, Rhodium(III)-Catalyzed Directed C–H Coupling with Methyl Trifluoroacrylate: Diverse Synthesis of Fluoroalkenes and Heterocycles, *Org. Lett.*, 2018, **20**, 570–573.
61 S. Liu, X. Li and J. Cheng, *Facile Synthesis of Pyrido[2,1-a] isoindoles via Iron-Mediated 2-Arylpyridine C–H Bond Cleavage*, *N. Y.*, 2013, p. 5.
62 B. Valeur, *Molecular Fluorescence: Principles and Applications*, Wiley, 1st edn, 2001.
63 D. Reuschling and F. Kröhnke, Ringschlüsse unter HNO_2 –Abspaltung und C-C–Verknüpfung, II. Synthese neuer Ringsysteme, *Chem. Ber.*, 1971, **104**, 2103–2109.
64 E. Stefănescu and M. Petrovanu, [(p. tolyl)-pyridaziniumylides. (VII). Action of picryl chlorides and chloranil on 3-(p. tolyl)-pyridazine-phenacylide], *Rev. Med.-Chir. Soc. Med. Nat. Iasi*, 1977, **81**, 475–478.
65 S.-W. Liu, Y.-J. Gao, Y. Shi, L. Zhou, X. Tang and H.-L. Cui, Synthesis of Benzoindolizines through 1,5-Electrocyclization/Oxidation Cascades, *J. Org. Chem.*, 2018, **83**, 13754–13764.
66 E. C. Taylor and I. J. Turchi, 1,5-Dipolar cyclizations, *Chem. Rev.*, 1979, **79**, 181–231.
67 M.-C. Chen, D.-G. Chen and P.-T. Chou, Fluorescent Chromophores Containing the Nitro Group: Relatively Unexplored Emissive Properties, *ChemPlusChem*, 2021, **86**, 11–27.
68 W. Rodríguez-Córdoba, L. Gutiérrez-Arzaluz, F. Cortés-Guzmán and J. Peon, Excited state dynamics and photochemistry of nitroaromatic compounds, *Chem. Commun.*, 2021, **57**, 12218–12235.
69 S. Ram and R. E. Ehrenkaufer, A general procedure for mild and rapid reduction of aliphatic and aromatic nitro compounds using ammonium formate as a catalytic hydrogen transfer agent, *Tetrahedron Lett.*, 1984, **25**, 3415–3418.
70 P. H. Gore, The Friedel-Crafts Acylation Reaction and its Application to Polycyclic Aromatic Hydrocarbons, *Chem. Rev.*, 1955, **55**, 229–281.
71 Y. Tominaga, Y. Shiroshita, Y. Matsuda and A. Hosomi, The Effect of Benzannelation Toward Cycl(3.2.2)azine. Synthesis and Physical Properties of Dibenzo(a,h)cycl(3.2.2)azine, *Heterocycles*, 1987, **8**, 2073–2075.
72 S. M. McDonald, S. K. Mellerup, C. Barran, X. Wang and S. Wang, Binding Modes and Reactivity of Pyrido[2,1-*a*]isoindole as a Neutral Carbon Donor with Main-Group and Transition-Metal Elements, *Organometallics*, 2017, **36**, 4054–4060.
73 D. Jacquemin, I. Duchemin and X. Blase, 0–0 Energies Using Hybrid Schemes: Benchmarks of TD-DFT, CIS(D), ADC(2), CC2, and BSE/*GW* formalisms for 80 Real-Life Compounds, *J. Chem. Theory Comput.*, 2015, **11**, 5340–5359.
74 T. Le Bahers, C. Adamo and I. Ciofini, A Qualitative Index of Spatial Extent in Charge-Transfer Excitations, *J. Chem. Theory Comput.*, 2011, **7**, 2498–2506.
75 Q. Peng, Y. Yi, Z. Shuai and J. Shao, Excited state radiationless decay process with Duschinsky rotation effect: Formalism and implementation, *J. Chem. Phys.*, 2007, **126**, 114302.
76 K. M. Elattar, I. Youssef and A. A. Fadda, Reactivity of indolizines in organic synthesis, *Synth. Commun.*, 2016, **46**, 719–744.
77 D. He, Y. Xu, J. Han, H. Deng, M. Shao, J. Chen, H. Zhang and W. Cao, Facile one-pot tandem synthesis of perfluoroalkylated indolizines under metal-free mild conditions, *Tetrahedron*, 2017, **73**, 938–944.

78 L. G. Voskressensky, A. A. Festa, E. A. Sokolova and A. V. Varlamov, Synthesis of chromeno[2′,3′:4,5]imidazo [2,1-a]isoquinolines via a novel domino reaction of isoquinoline-derived immonium salts. Scope and limitations, *Tetrahedron*, 2012, **68**, 5498–5504.
79 M. Costa, A. I. Rodrigues and F. Proença, Synthesis of 3-aminochromenes: the Zincke reaction revisited, *Tetrahedron*, 2014, **70**, 4869–4875.
80 P. N. Praveen Rao, M. Amini, H. Li, A. G. Habeeb and E. E. Knaus, Design, Synthesis, and Biological Evaluation of 6-Substituted-3-(4-methanesulfonylphenyl)-4-phenylpyran-2-ones: A Novel Class of Diarylheterocyclic Selective Cyclooxygenase-2 Inhibitors, *J. Med. Chem.*, 2003, **46**, 4872–4882.
81 A. T. Nielsen, W. P. Norris, R. L. Atkins and W. R. Vuono, Nitrocarbons. 3. Synthesis of decanitrobiphenyl, *J. Org. Chem.*, 1983, **48**, 1056–1059.
82 *APEX3, SAINT, and TWINABS*. Bruker AXS, Madison, WI, USA.
83 G. M. Sheldrick, *SHELXT* – Integrated space-group and crystal-structure determination, *Acta Crystallogr., Sect. A: Found. Adv.*, 2015, **71**, 3–8.
84 O. V. Dolomanov, L. J. Bourhis and R. J. Gildea, J. a. K. Howard and H. Puschmann, OLEX2: a complete structure solution, refinement and analysis program, *J. Appl. Crystallogr.*, 2009, **42**, 339–341.
85 M. J. Frisch, *et al.*, *Gaussian 16, revision A.03*, Gaussian Inc., Wallingford, CT, 2016.
86 Y. Zhao and D. G. Truhlar, The M06 suite of density functionals for main group thermochemistry, thermochemical kinetics, noncovalent interactions, excited states, and transition elements: two new functionals and systematic testing of four M06-class functionals and 12 other functionals, *Theor. Chem. Acc.*, 2008, **120**, 215–241.
87 J. Tomasi, B. Mennucci and R. Cammi, Quantum Mechanical Continuum Solvation Models, *Chem. Rev.*, 2005, **105**, 2999–3094.
88 C. A. Guido, A. Chrayteh, G. Scalmani, B. Mennucci and D. Jacquemin, Simple Protocol for Capturing Both Linear-Response and State-Specific Effects in Excited-State Calculations with Continuum Solvation Models, *J. Chem. Theory Comput.*, 2021, **17**, 5155–5164.
89 O. Christiansen, H. Koch and P. Jørgensen, The second-order approximate coupled cluster singles and doubles model CC2, *Chem. Phys. Lett.*, 1995, **243**, 409–418.
90 C. Hättig, A. Hellweg and A. Köhn, Distributed memory parallel implementation of energies and gradients for second-order Møller–Plesset perturbation theory with the resolution-of-the-identity approximation, *Phys. Chem. Chem. Phys.*, 2006, **8**, 1159.
91 TURBOMOLE V7.3, a development of University of Karlsruhe and Forschungszentrum Karlsruhe GmbH, 1989–2007; TURBOMOLE GmbH.
92 A. Pershin, D. Hall, V. Lemaur, J.-C. Sancho-Garcia, L. Muccioli, E. Zysman-Colman, D. Beljonne and Y. Olivier, Highly emissive excitons with reduced exchange energy in thermally activated delayed fluorescent molecules, *Nat. Commun.*, 2019, **10**, 597.
93 F. Neese, F. Wennmohs, U. Becker and C. Riplinger, The ORCA quantum chemistry program package, *J. Chem. Phys.*, 2020, **152**, 224108.
94 J. Cerezo and F. Santoro, FCClasses 3.0, http://www.pi.iccom.cnr.it/fcclasses.
95 F. Santoro, R. Improta, A. Lami, J. Bloino and V. Barone, Effective method to compute Franck-Condon integrals for optical spectra of large molecules in solution, *J. Chem. Phys.*, 2007, **126**, 084509.
96 F. Santoro and D. Jacquemin, Going beyond the vertical approximation with time-dependent density functional theory: Going beyond the vertical approximation with TD-DFT, *Wiley Interdiscip. Rev.: Comput. Mol. Sci.*, 2016, **6**, 460–486.
97 A. Humeniuk, M. Bužančić, J. Hoche, J. Cerezo, R. Mitrić, F. Santoro and V. Bonačić-Koutecký, Predicting fluorescence quantum yields for molecules in solution: A critical assessment of the harmonic approximation and the choice of the lineshape function, *J. Chem. Phys.*, 2020, **152**, 054107.
98 Q. Ou, Q. Peng and Z. Shuai, Toward Quantitative Prediction of Fluorescence Quantum Efficiency by Combining Direct Vibrational Conversion and Surface Crossing: BODIPYs as an Example, *J. Phys. Chem. Lett.*, 2020, **11**, 7790–7797.

ORGANIC CHEMISTRY FRONTIERS

RESEARCH ARTICLE

View Article Online
View Journal | View Issue

Cite this: *Org. Chem. Front.*, 2024, **11**, 6627

Strongly fluorescent indolizine-based coumarin analogs†

Jaqueline S. A. Badaro, [a] Antoni Wrzosek, [b] Olaf Morawski, [c] Adam Szewczyk, *[b] Irena Deperasińska *[c] and Daniel T. Gryko *[a]

It is now possible to prepare 2-oxo-2*H*-pyrano[2,3-*b*]indolizine-3-carboxylates with an ordered arrangement of various substituents directly from pyridinium salts and diethyl 2-(ethoxymethylene)malonate, allowing for refined control of their photophysical properties. Facile entry into some previously unknown derivatives is disclosed to demonstrate the potential of this method. The use of substituted picolinium salts, as well as further functionalization of the pyrrole ring, permitted easy introduction of new moieties upon the dye, which enabled fine-tuning of the photophysical properties. The obtained dyes possess absorption and emission spectrum in the blue–green region and fluorescence quantum yields reaching 92%. The parent 2-oxo-pyrano[2,3-*b*]indolizine-3-carboxylate turned out to be an electron-deficient system with a low-lying LUMO, an electronic transition energy of 2.7 eV and possessing a large oscillator strength. Almost complete overlap of the HOMO and LUMO in the 2-oxo-pyrano[2,3-*b*]indolizine core is responsible for the large fluorescence quantum yields for almost all prepared derivatives. The reason for maintaining the large emission intensity in polar solvents is that the increase in the dipole moment is accompanied with a significant change in its orientation in space. Fluorescence imaging studies have proven that 2-oxo-pyrano[2,3-*b*]indolizines penetrate the membrane of living cells. A positively charged analog was synthesized and used to stain intracellular organelles in the H9c2 cell line. This compound did not penetrate the cell membrane, however after permeabilization, it specifically stained the nucleus.

Received 3rd July 2024,
Accepted 10th September 2024

DOI: 10.1039/d4qo01216j

rsc.li/frontiers-organic

Introduction

Pyrano[2,3-*b*]indolizin-2-ones are a unique class of heterocycles that, contrary to their analogues pyrano[3,2-*b*]indol-2-ones[1–12] and pyrano[2,3-*b*]indol-2-ones,[13–22] have been greatly ignored after they were synthesized by Kakehi *et al.* in the 80s[23–25] (together with their isomers pyrano[3,2-*a*]indolizin-2-ones)[25,26] (Fig. 1). However, their distinct structure, composed of a fused tricyclic system, in which a pyran ring is fused to an indolizine moiety, offers a wide range of opportunities for the design and development of novel compounds, exhibiting immense potential for applications in various fields, ranging from medicinal chemistry to materials science. Structurally, pyrano[2,3-*b*]indolizin-2-ones can be considered analogues of coumarins[27–34] and benzocoumarins.[35–42]

The synthesis of pyrano[2,3-*b*]indolizines was investigated by Kakehi and co-workers mainly from 1980 to 1998, driven by the need to establish an efficient and reliable methodology. Numerous synthetic routes have been explored, involving the use of pyridinium salts as starting materials and the formation of various intermediates, *e.g.* 3-bis(methylthio)methylene-2,3-dihydroindolizin-2-ones,[23] 2,3-dihydroindolizin-2-ones,[24] 3-vinylindolizines[25] as well as the hydrolysis of pyrano[2,3-*b*]indolizine-2-imines.[43] These synthetic efforts have resulted in the successful preparation of a diverse array of pyrano[2,3-*b*]

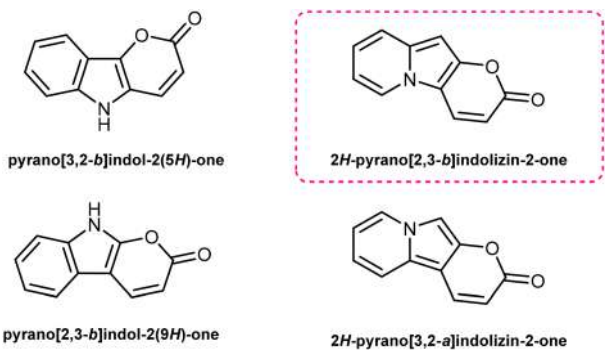

Fig. 1 Pyrano-indol-2-ones and pyrano-indolizin-2-ones.

[a]*Institute of Organic Chemistry, Polish Academy of Sciences, Kasprzaka 44/52, 01-224 Warsaw, Poland. E-mail: dtgryko@icho.edu.pl*
[b]*Nencki Institute of Experimental Biology, Polish Academy of Sciences, Pasteur 3, 02-093 Warsaw, Poland. E-mail: a.szewczyk@nencki.gov.pl*
[c]*Institute of Physics, Polish Academy of Sciences, Al. Lotników 32/46, 02-668 Warsaw, Poland. E-mail: deper@ifpan.edu.pl*

†Electronic supplementary information (ESI) available: NMR, UV/vis, fluorescence spectra and computational details. See DOI: https://doi.org/10.1039/d4qo01216j

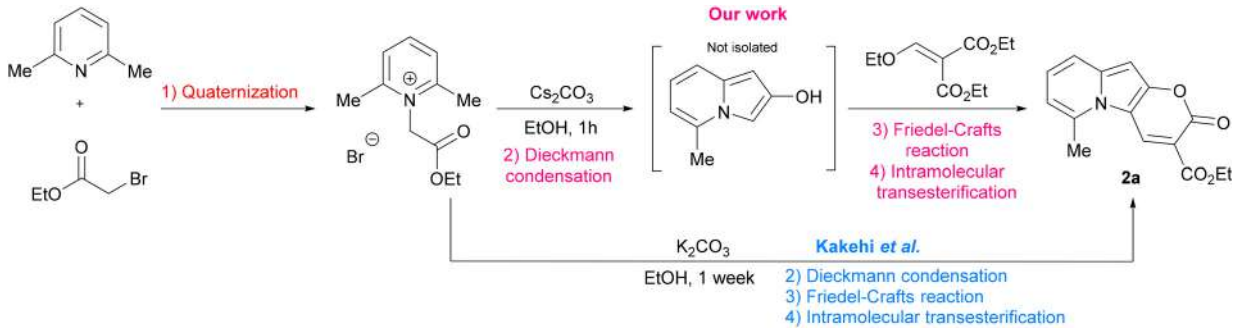

Scheme 1 Synthesis of ethyl 6-methyl-2-oxo-pyrano[2,3-*b*]indolizine-3-carboxylate.

indolizine derivatives, expanding the chemical space available for further exploration and application.

In the context of search for novel fluorescent platforms we resolved to explore 2-oxo-pyrano[2,3-*b*]indolizine-3-carboxylates because of the easily available starting materials and the strong fluorescence emission claimed by the authors in their paper, but not sufficiently explored.[24] The Kakehi's synthesis (Scheme 1) consisted of four steps: (1) quaternization of 2,6-dimethylpyridine with ethyl 2-bromoacetate; (2) Dieckmann condensation to form the 5-methylindolizin-2-ol intermediate; (3) Friedel–Crafts reaction of the intermediate with diethyl 2-(ethoxymethylene)malonate; (4) final intramolecular cyclization *via* transesterification with the formation of the lactone ring and additional ethanol elimination. It is noteworthy that the last three steps occur in one pot. However, the drawback of this methodology is that a long reaction time (7 days) is required, and the yield is relatively poor (38%). By solving the synthetic drawbacks and shedding light on the properties of this class of compounds, we aimed to provide a comprehensive understanding of this intriguing heterocyclic system, thus paving the way for further research and development of novel compounds with enhanced properties and biological application.

Results and discussion

Synthesis

Optimization. Our investigation started with the synthesis of the dye **2a** (Scheme 2), and we used this reaction as a model for the optimization studies, Table 1. First, we attempted to decrease the reaction time by changing the solvent to DMF (entry 2), but the expected product was not detected; instead, **2i** was obtained. Then we tried NaOEt as base (entry 3), but the product was observed only in trace amounts. At this point, before proceeding to test alternative bases, we hypothesized that sequential addition of reagents, allowing first the formation of the 5-methylindolizin-2-ol intermediate (Scheme 2) and then the following steps, could be the key to increasing the yield. Different bases were evaluated (entries 4–6) and we eventually found that the use of Cs_2CO_3 along with sequential addition of the reagents turned out to be pivotal to obtain a yield of 50% (entry 6). Interestingly, Cs_2CO_3 turned out to be the best base to promote the cyclization. This result can be partly attributed to the increased basicity strength *versus* that of K_2CO_3. And it is in line with some recently developed synthetic approaches.[44,45–47]

Scope. Having established the optimal reaction conditions (Cs_2CO_3, EtOH, RT, 18 h), the substrate scope was evaluated. As shown in Scheme 2, different 'formal' picolinium salts, prepared according to literature procedure (**1a–f**)[48–51] and used as such, reacted with Cs_2CO_3 to form the indolizin-2(3*H*)-one intermediate that, after addition of diethyl 2-(ethoxymethylene) malonate, successfully gave pyranoindolizines possessing a hydrogen or an alkyl substituent in position R^5 (**2a**, **2b**, **2c**) in 5–50% yield.

Consistent with what was observed by Kakehi and coworkers in 1986, the reaction with 2,3-cyclopentenopyridinium salts did not lead to the indolizine product,[52] while the reaction with a 5,6,7,8-tetrahydroquinolinium salt led to the expected product **2d** in 30% yield. 2-Methylquinolinium and 1-methylisoquinolinium salts also reacted nicely and gave π-expanded indolizine products with a free R^5 position (**2e**, **2f**) in 30 and 28% yield, respectively, while 3-methylisoquinolin-2-ium salt did not react as expected.

Additionally, α-picoline derivatives (**1g** and **1h**) bearing EWG groups (2-Py and CO_2Et) attached to the methylene group (R^5) furnished the target product (**2g**, **2h**) in 44% and 5% yield respectively. It is noteworthy that in those cases, due to the highly acidic character of the proton at the α-position, the quaternization of the pyridine with ethyl 2-bromoacetate led to a 3-substituted indolizin-2-ol directly, even in the absence of base. In such cases the base was added later, only to promote the last two steps: nucleophilic substitution and transesterification.

Meanwhile, the reaction from a 4-bromopyridinium salt and diethyl 2-(ethoxymethylene)malonate did not produce the expected product, probably due to a less reactive indolizin-2-ol intermediate. Similarly, the reaction with a 4-dimethylaminopyridinium salt did not give the target product, in this case probably due to the difficulty in the formation of the indolizine intermediate caused by the effect of the electron-donating group, which turned the proton in the α-position less acidic, thus the reagent is less prone to cyclization.

Functionalization. The structure of indolizine **2a** brings about exciting possibilities to create π-expanded, polarized

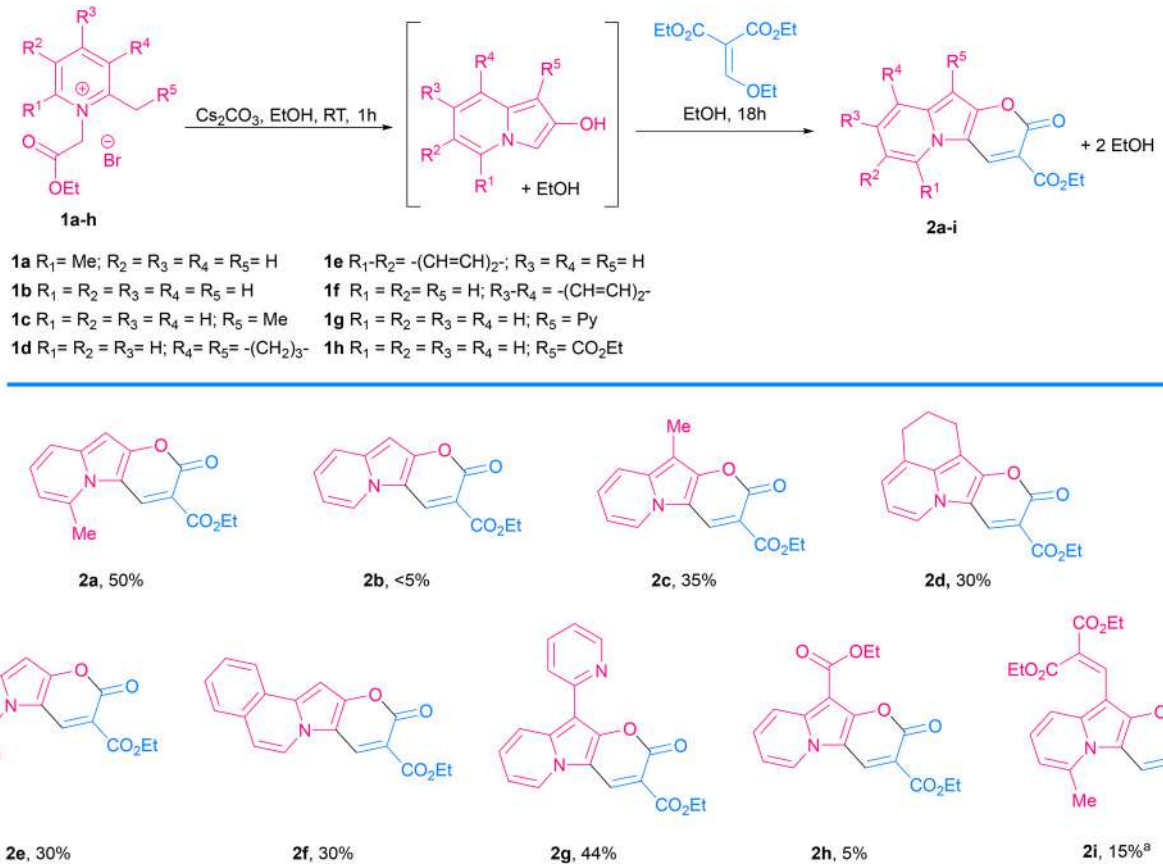

Scheme 2 Scope of 2-oxo-pyrano[2,3-*b*]indolizine-3-carboxylate. [a] Obtained by simultaneous addition of malonate.

Table 1 Conditions for the optimization of 6-methyl-2-oxo-pyrano[2,3-*b*]indolizine-3-carboxylate

Entry	Base	Solvent	*T*/°C	Time/h	Yield %
1[a]	K_2CO_3	EtOH	RT	7 days	38
2[b]	K_2CO_3	DMF	RT	18 h	15% of **2i**
3[b]	NaOEt	EtOH	RT	18 h	Traces
4[c]	KOH	EtOH	RT	18 h	30
5[c]	LiOH	EtOH	RT	18 h	15
6[c]	Cs_2CO_3	EtOH	RT	18 h	50

[a] Kakehi's methodology. [b] Simultaneous addition of malonate. [c] Postponed addition of malonate.

derivatives. Among a few possibilities, the presence of a highly electron-rich carbon β to the nitrogen was appealing to exploit (Scheme 3). To explore these possibilities, three additional derivatives (**3aa**, **3ab**, **3ac**) were obtained by direct arylation. As expected, bromoarenes with EWG in the *para* position, such as CN or NO_2, were more reactive in the direct arylation and the products were obtained in good yields (60% and 50%). In contrast, the bromoarene bearing an EDG, such as *t*Bu, gave the product **3ac** in poor yield (17%).

The Vilsmeier–Haack formylation also successfully occurred at the electron-rich position, resulting in the formation of **4a** in 83% yield.

To probe the potential of this class of dyes, Knoevenagel condensation was carried out between **4a** and 1,4-dimethylpyridin-1-ium iodide (**5**) (Scheme 3) forming a new styryl[53–55] dye **6a**, which was obtained in 37% yield and later evaluated for cell staining (*vide infra*).

Considering the principles of green chemistry,[56] the reactions leading to compounds **2a–2i** and **4a** are considered to have moderate atom economy (AE) efficiency, in the range of 40–60%. Meanwhile, direct arylation products (**3aa–3ac**) and Knoevenagel condensation were obtained with AE efficiency above 80%, which is considered optimal according to the above principles. For all reactions, the reaction mass efficiency is very low, less than 10%, mainly due to the significant impact of the solvent in the calculation.

Photophysical properties

UV-Vis absorption and emission spectra were recorded in non-polar toluene (dielectric constant ε = 2.38), moderately polar DCM (ε = 8.93), and polar DMSO (ε = 46.45) for all dyes, except **6a**, which was measured only in DCM and DMSO and will be discussed separately and correlated to its precursor **4a**.

A comparison between the photophysical parameters for 2-oxo-pyrano[2,3-*b*]indolizine-3-carboxylates and those available for similar structures (Fig. 2) such as 11-benzyl-7-hydroxyisochromeno[4,3-*b*]indol-5-one[9] (Φ_{fl} = 42% in DCM, with λ_{abs} =

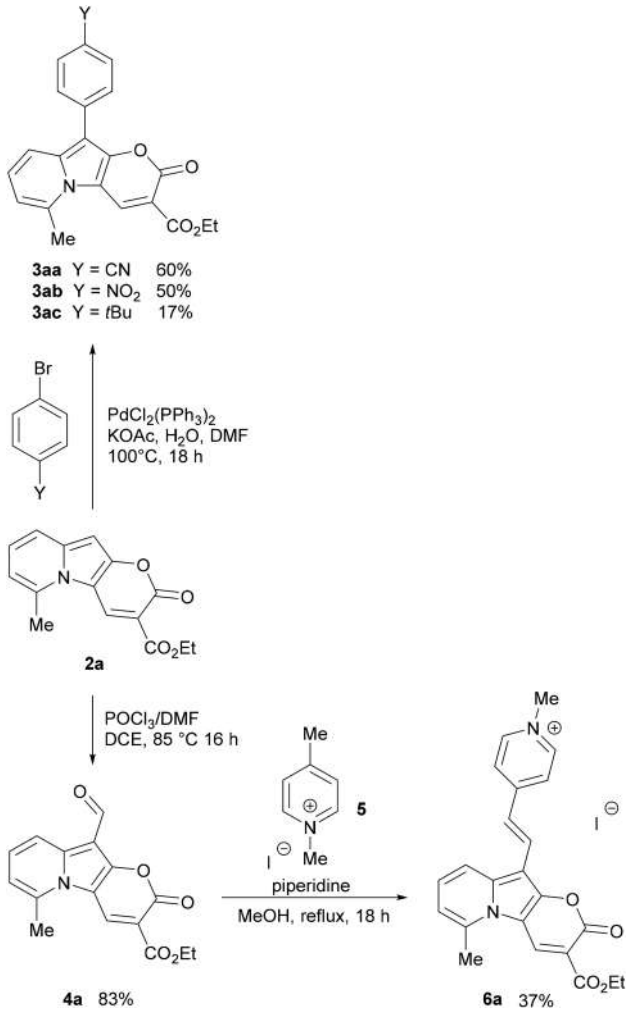

Scheme 3 Synthesis of **3aa**, **3ab**, **3ac** and **4a** from **2a**, and synthesis of **6a** from **4a**.

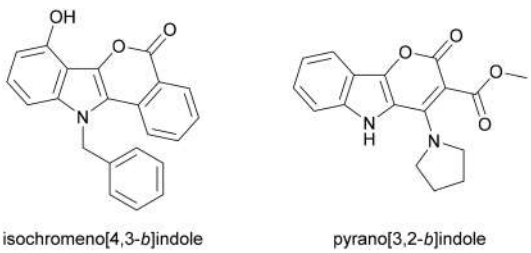

Fig. 2 Indoles structures used as reference to discuss photophysical properties of synthesized dyes.

382 and λ_{em} 496) or methyl 2-oxo-4-(pyrrolidin-1-yl)-2,5-dihydropyrano[3,2-*b*]indole-3-carboxylate[57] (λ_{abs} = 335 in EtOH) reveals a significant bathochromic shift for absorption, while emission and fluorescence quantum yield (Φ_{fl}) remain in the same range.

The collected data of compounds in DCM are presented in Table 2 and the spectra of selected dyes are compared in

Table 2 Photophysical data of synthesized 2-oxo-pyrano[2,3-*b*]indolizine derivatives in DCM

Cmp	Solv	λ_{abs} [nm]	λ_{em} [nm]	$\Delta\bar{\nu}$ [cm^{-1}]	ε [M^{-1} cm^{-1}]	Φ_{fl}
2a	DCM	446	464	900	30 500	0.71
2b	DCM	449	470	1000	16 300	0.77
2c	DCM	468	494	1100	22 900	0.61
2d	DCM	467	499	1400	24 600	0.64
2e	DCM	456	470	700	39 700	0.73
2f	DCM	436	458	1100	39 700	0.33
2g	DCM	466	500	1500	17 600	0.92
2h	DCM	433	452	1000	29 200	0.81
2i	DCM	446	485	1800	21 000	0.25
3aa	DCM	453	490	1700	22 928	0.64
3ab	DCM	452	491/642	6500	27 700	0.03
3ac	DCM	457	514	2400	19 600	0.65
4a	DCM	426	448	1200	31 800	0.77
6a[a]	DCM	509	575	2300	24 400	0.44

Fluorescence quantum yields measured with Coumarin 153 in EtOH as reference (Φ_{fl} = 0.55). [a] Fluorescence quantum yield measured with Rhodamine 6G in EtOH as reference (Φ_{fl} = 0.95).

Fig. 4, while the remaining data for the other solvents are available in Table S5 in ESI.† Absorption maxima (λ_{abs}) of the dyes obtained are located within 420–470 nm in all solvents, while the emission maxima (λ_{em}) falls between 440 and 520 nm for almost all of them and is more bathochromically shifted in polar solvents (solvatochromism). It is worth noting that compound **3ab** represents an exception to this trend in both DCM and DMSO, showing two emission bands overlapping, one at the 'expected' wavelength (491 nm) and another one around 642 nm. Excitation spectra were recorded to prove that both signals come from the same molecule and are not due to impurities in the sample. This property can be explained by hypothesizing that this structure, constituting of a strong donor, 2-oxo-pirano[2,3-*b*]indolizine, and a strong acceptor, nitrophenyl, can undergo internal charge transfer (ICT) in polar solvents and generate two possible excited states according to the geometry and consequently allow for two possible emitting paths.

The fluorescence quantum yields (Φ_{fl}) are in most cases on the same level regardless of the solvent and they vary among the studied 2-oxopyrano[3,2-*b*]indolizines from 0.92 for dye **2g** in DCM to being barely detectable for **3ab** in DCM and DMSO due to the preferred non-emissive decay (Fig. 3). Exceptions to this trend are **2c**, **2d**, **2g** that show lower fluorescence in toluene; and **3ab**, which shows a reverse trend by having the highest Φ_{fl} in the less polar solvent. The comparison of the photophysical properties of **2a**, **2b** and **2c** (Fig. 4A), which vary their position of a methyl group (or is absent), reveals that this alkyl group at position R^5 shifts both absorption and emission bathochromically (**2c** *vs.* **2b**) by about 20 nm, while the same group at position R^1 slightly shifts both signals hypsochromically (**2a** *vs.* **2b**).

Moreover, different electronic character of the substituent in R^5 (Fig. 4B) influences both λ_{abs} and λ_{em}. If CHO is present (**4a**), λ_{abs} = 426 nm and λ_{em} = 448 nm, while if Me is present (**2c**), λ_{abs} = 468 nm and λ_{em} = 494. The presence of a

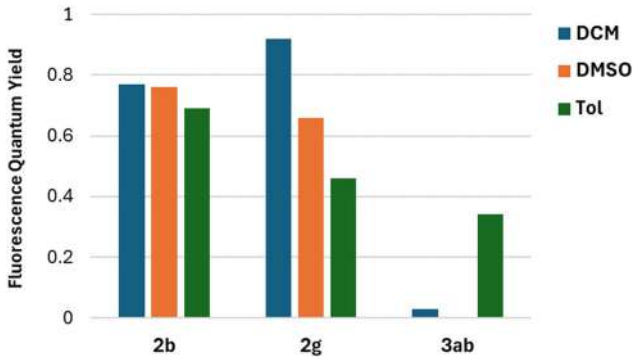

Fig. 3 Comparison of Fluorescence quantum yield in different solvents for representative compounds **2b**, **2g** and **3ab**.

π-extended system, as in **3aa** and **3ac**, slightly blue shifts the absorption. Additionally, having a *t*Bu group in the *para* position (**3ac**) red shifts the emission, consequently increasing the Stokes shift (2400 cm^{-1}). Interestingly, the effect of the π-expansion of the heterocyclic core strongly depends on the position of the fused benzene ring. In the case of dye **2f** a blue shift is observed accompanied with a decrease of the Φ_{fl} (0.33 *vs.* 0.77) compared to **2b** (Fig. 4C).

The addition of a methylpyridinium conjugated through an alkene to the 2-oxo-pirano[2,3-*b*]indolizine system (**6a**) allowed for an increased dipole moment that translates to a bathochromic shift of 83 nm for λ_{abs} and almost 130 nm for λ_{em} when compared to **4a** (Fig. 4D). Even though a decrease in the fluorescence quantum yield (0.44 *vs.* 0.77) was observed comparing **6a** and **4a**, the emission is still high suggesting that, in comparison to **3ab**, the decay through a radiative channel is favoured.

Fluorescence kinetic studies were performed for selected compounds: **2a** representing "typical" 2-oxo-pyrano[2,3-*b*]indolizine, **3ab** exhibiting dual fluorescence and salt **6a**. In all solvents fluorescence of dyes **2a** and **6a** decays exponentially (Fig. S11†) with decay times, τ_F, about 3.5 and 2.0 ns respectively (Table S6†). For both compounds τ_F changes slightly with solvent's polarity (represented by dielectric constant, ε) and the change is parallel to that of Φ_{fl}, – for **2a** both τ_F and Φ_{fl} grow with increasing ε whereas for **6a** they decrease (Table S6†). Consequently, the radiative rate constant $k_r = \Phi_{fl}/\tau_F$ of the $S_1 \rightarrow S_0$ transition remains constant and amounts to 1.3×10^8 s^{-1} and 2.1×10^8 s^{-1} respectively (Table S6†). Such high value is typical for the fully allowed ππ* transitions. For dye **3ab** kinetic traces are complex. In non-polar toluene fluorescence decays exponentially (Fig. S12a†) with characteristic time 2.62 ns (Table S7†). Radiative rate is 8.8×10^7 s^{-1}, much less than values obtained for dyes **2a** and **6a**. For polar solvents where dual fluorescence from LE and CT states is observed emission decays are non-exponential and depend on wavelength of observation. For DCM the high energy band of the LE state with maximum at 487 nm two components are clearly visible in the decay trace (Fig. S12b†), and deconvolution yields 20 and 356 ps decay times. Intensity of emission orig-

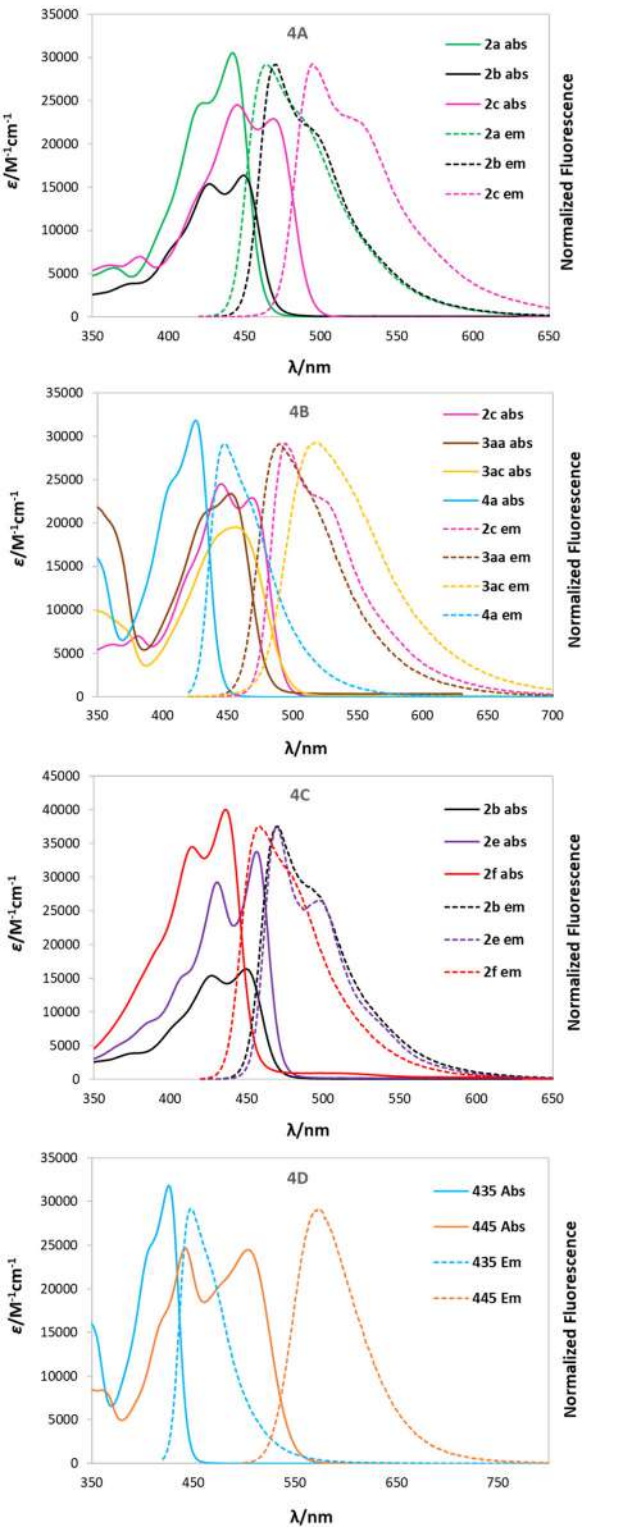

Fig. 4 Absorption and emission spectra of some representative 2-oxo-pyrano[2,3-*b*]indolizine-3-carboxylate derivatives in DCM. (A) Normalized absorption (solid line) and normalized emission (dashed line) of **2a**, **2b**, **2c** (green, black, pink) (B) normalized absorption (solid line) and normalized emission (dashed line) of **2c**, **3aa**, **3ac** and **4a** (pink, brown, yellow and light blue) (C) normalized absorption (solid line) and normalized emission (dashed line) of **2b**, **2e** and **2f** (black, purple, red) (D) normalized absorption (solid line) and normalized emission (dashed line) of **4a** and **6a** (light blue, orange).

inating from low energy CT band with maximum at 700 nm grows at early times and reaches maximum much later than the LE profile (Fig. S12b†). This points to precursor (LE) – successor (CT) scheme and suggests that that initial population of the CT state is null. Indeed, deconvolution reveals grow time of 55 ps and decay time of 356 ps (Table S7†). Negative amplitude of the grow time is comparable to the (positive) amplitude of the decay time what confirms that CT state is not directly excited and is populated from the LE state. This provides experimental proof for the TICT concept hypothesised below. Long component of the LE profile has same decay time as decay time of CT trace, pointing to thermalization of both states. However, grow time of CT is a bit longer than the short decay time of LE so one may expect presence of a transition state or a slow relaxation to emissive CT structure, so the simple two states model used commonly for TICT can be not adequate. In more polar DMSO kinetic profiles are faster (Fig. S12c†) and the LE decay time decreases down to 15 ps (Table S7†) pointing to the increase of the intramolecular CT rate constant. Formation of TICT enhances also non-radiative relaxation, hence the Φ_{fl} decreases by two orders of magnitude.

Theoretical analysis

The DFT and TDDFT O3LYP/6-31G(d,p) calculations were performed to corroborate the experimental data. The choice of the O3LYP functional allows for the best reconstruction of the spectral data in comparison to our attempts using other functionals (Table S1†). Calculations included the optimization of molecular structures in their ground (S_0) and lowest electronic excited (S_1) states along with the determination of the corresponding absorption and fluorescence energies. Corresponding data for the molecules in the three solvents, toluene, DCM and DMSO, are collected in Table S2.† The calculated dipole moments for the S_0 and S_1 states are summarized in Table S3.† The two highest occupied (HOMO's) and two lowest unoccupied molecular orbital (LUMO's) energy levels are shown in the diagram in Fig. S1,† while the values of HOMO and LUMO energies are given and compared in Table S4.† More detailed results of calculations are in the ESI.†

Dye **2b** lacking any substituents can be considered a model chromophore for this family of heterocycles (Scheme 2). This is a molecule with planar geometry in both S_0, and S_1, states. The electronic transition between them has a π–π^* character and essentially it is described by a single HOMO/LUMO electronic configuration. A diagram of the calculated electronic states of heterocycle **2b** with a short analysis is presented in ESI, Fig. S2.†

According to the computational results, the geometry of **2b** in the excited state undergoes relatively small changes. This result is consistent with the small Stokes shift observed experimentally. Small changes in geometry are manifested by small Franck–Condon factors (Fig. S3†) which well reproduce the experimental spectrum (Fig. 1). The small values of the calculated spin–orbit coupling elements (H_{so}) between the excited S_1 state and the energetically close triplet states (Fig. S2†) together with the small Franck–Condon factors are indicative of relatively small rate constants of non-radiative processes,[58,59] which in the experiment (Table 2) is visible as significant values of Φ_{fl} achieved for dye **2b**.

The calculation results show also, that **2b** is a molecule with a large dipole moment, increasing in the excited state (9.6 D for S_0 state and 12 D in S_1 – Table S3†). In this light, slight red-shifts of its electronic spectra (both observed, Table 2 and Table S5† and calculated, Table S2†) as the solvent polarity increases may seem surprisingly small. This phenomenon, has also been observed in the case of various other molecules,[60,61] and can be explained with the use of classical theory of the solvent effect,[60,61] and is related to the fact that dipole moments are vector quantities (and not scalars). When the increase in the dipole moment in the S_1 state (relative to the S_0 state) is accompanied by a change of orientation in space, the solvent effect is smaller than expected based on values alone (see Fig. S4†).

Fig. S2† shows the shapes of the HOMO and LUMO of molecule **2b**, providing high oscillator strength for the transition between the S_0 and S_1 states. They will constitute a reference orbital in the presentation of results for other 2-oxopyrano[3,2-*b*]indolizines.

The substitution of molecule **2b** causes changes in the energy of the molecular orbitals (Fig. S1†), including changes in the spacing between them (Table S4†). This is reflected by the shifts of the electronic spectra, since the electronic transition has an initial and final state, the magnitude of this shift depends on the energy changes in both states.

In Fig. 5, correlation between the absorption $S_0 \rightarrow S_1$ energy and the energy difference of the HOMO and LUMO for the studied 2-oxopyrano[2,3-*b*]indolizines is presented. This correlation demonstrates that transitions between the S_0 and S_1 states for all molecules, as in parent dye **2b**, are described by a single HOMO/LUMO electronic configuration. At the same

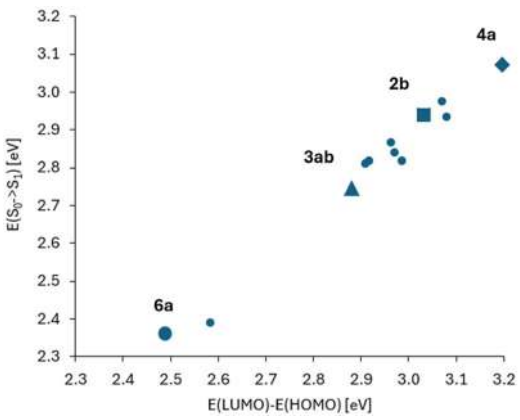

Fig. 5 Correlation between the absorption energy and the energy difference of HOMO and LUMO orbitals (numerical data in Tables S2 and S4†). The point corresponding to molecule **2b** is marked with a square. Two distant points (for lower energies, *i.e.* with red shift in comparison to **2b**) correspond to molecules **3ab** and **6a**. These two molecules also differ from the others in large values and changes of the dipole moment between S_0 and S_1 states (Table S3†).

time, two groups of molecules can be distinguished, the first with moderate changes in the HOMO/LUMO energy gaps and excitation energies (in relation to **2b**), and the other group of two molecules with large changes in these quantities.

Fig. 6 (part of the diagram in Fig. S1†) illustrates the variation of the *E*(HOMO)–*E*(LUMO) gap and shows the shapes of these orbitals for four representatives of the studied family of 2-oxopyrano[2,3-*b*]indolizines: **2b** – as a model chromophore, **3ac** – a dye with observed red-shift in the absorption and fluorescence spectra (relative to the spectra of **2b**), **4a** – with a blue-shift of the spectra and dye **6a** – as a molecule with large red-shift of electronic spectra (see also Fig. 4).

Based on Fig. 6, it can be concluded that the effect of substitution of molecule **2b** produces two qualitatively different effects depending on the electron affinity of the substituent. In the case of compounds **3ac** and **4a**, this is a modification effect, *i.e.* their HOMO and LUMO are the modified (to a larger or smaller extent) HOMO and LUMO of molecule **2b**, but this is no longer the case of the LUMO of molecule **6a**. Although the HOMO of **6a** is still a modified HOMO of molecule **2b**, the LUMO is the orbital located on the substituent (while the orbital located on core **2b** lies above it, as shown in Fig. 6).

In addition to the diagram shown on Fig. 6, two other diagrams are shown in the ESI (Fig. S5 and S6†): HOMO/LUMO energy changes from methylation of the dye **2b** in different positions (**2a** *vs.* **2c**) and with π-extension (**2e** *vs.* **2f**) of **2b**. Methylation of **2b** at the R^5 position causes the largest change in HOMO energy leading to a red shift of the **2c** spectra.

In contrast to the substitution with a single bond, the π-expansion of **2b** becomes a problem not only at the level of the HOMOs, but also at the level of the (so far untouched) LUMO of molecule **2b**.

Therefore, the reason for the large red shift of the **6a** (and **3ab**) spectra is a qualitative change of LUMO from localized on **2b** to localized on the substituent. The $S_0 \rightarrow S_1$ transition becomes, instead of the modified **2b** excitation, intramolecular charge-transfer between the core and the substituent.

Both orbitals are extended into the attached ring. The energy effect depends on the geometry in which the expansion is carried out (E_{LUMO}(**2e**) < E_{LUMO}(**2f**)).

The calculation results for excited states indicate that most of the considered molecules retain features characteristic of parent dye **2b**. The fluorescence energies of the molecules optimized in the excited state are not very far from the absorption energies, and these transitions are described by high oscillator strengths (Table S1†). Although these results are in agreement with the experiments, (small Stokes shift, large emission efficiencies) these facts may seem surprising at first. This is because in these dyes there is a convenient relaxation path, which is a rotation around a single bond connecting the substituents with the heterocyclic core **2b**. We can expect two effects to play a role: a difference between the dihedral angles corresponding to the energy minimum in the ground and excited states, as well as the formation of rotational conformers. Differences between geometries optimized in the ground and excited states do indeed exist. For example, in systems containing a phenyl substituent at position R^5, such as **3aa**, in the ground state, the aromatic ring makes an angle of 41.3° with the **2b** plane, while in the optimized excited state it makes an angle of 30.7°; a similar rotation occurs in **3ac**, from 35.9° to 29.5°. However, they do not have a major impact on the spectroscopic properties because the LUMO is not extended to the substituent (Fig. 6). The exceptions are two molecules: **3ab** and **6a**, because their LUMOs are located on the substituent (Fig. 6, S7 and S8†). In both cases, the dark rotational conformers were optimised in the excited state (Table S1†). These conformers are characterised by zero oscillator strength for $S_1 \rightarrow S_0$ transition at the perpendicular arrangement of the planes of the heterocyclic core and the substituent ring. The difference between **6a** and **3ab** is that the dark form of **3ab** is the only form optimized in the excited state in polar DMSO. This result is consistent with experimental: while **6a** in this solvent emits with significant efficiency, the emission yield of **3ab** is extremely low. This means that the relaxation of **6a** to the dark state is slower than the decay *via* the radiative channel or inhibited by a barrier due to a more complex link between substituent and the heterocyclic core.

In turn, the bright form of **3ab** is experimentally observed and optimised in calculations for the S_1 state, in a non-polar medium only. Fig. S8† shows a diagram of electronic states of isolated molecule **3ab** with both optimised forms of the excited state. This is a diagram typical of TICT systems.[62]

Overall, it is worth to acknowledge the consistency between experimental and theoretical results. The ratio of radiative rate constant of **2a** and **6a**, 1.3/2.1 = 0.62 is very similar to the ratio

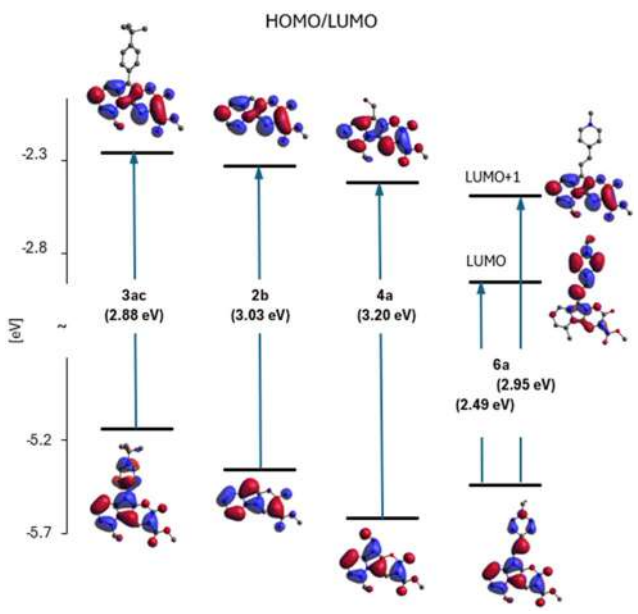

Fig. 6 Diagram of orbital energies: **2b** as the model heterocycle and its three derivatives, **3ac**, **4a** and **6a** in DMSO. The numbers in brackets indicate the size of the HOMO/LUMO energy gaps. In the case of **6a** two LUMOs are present in the considered energy region and in contrary to previous cases lowest of them is localised on substituent.

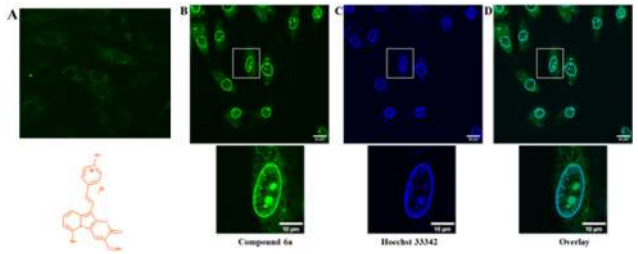

Fig. 7 Intracellular localization of compound **6a** in H9c2 cells detected using confocal fluorescence microscopy. (A) Image of the cells incubated with dye **6a** in a non-permeabilized cell membrane. Lower diagram structure of the dye. (B) Fluorescence of cells with digitonin (100 μg ml^{-1}) permeabilized membrane. (C) Fluorescence of permeabilized cell co-incubated with 0.5 μM Hoechst 33342 recorded with a 405 nm excitation wavelength and emission ranges from 420–520 nm. (D) Overlay of B and C. Lower pictures represents zoom upper square marked cells for B, C and D. The fluorescence of **6a** was recorded with a 473 nm excitation wavelength and emission ranges from 510–610 nm.

oscillator strength calculated for them, 0.64 : 1.06 (Tables S1 and S7†). Also, the radiative rate obtained experimentally for **3ab** is two/three times lower than for **2a**/**6a**, exactly like the oscillator strength calculated for **3ab** and **2a**/**6a** (Tables S1 and S7†). For **3ab** the theoretically predicted TICT mechanism is fully confirmed by fluorescence kinetic study. These as well as other correspondence between theory and experiment supports confidence for the HOMO and LUMO overlap statements.

Imaging studies

To prove the potential applicability of 2-oxo-pyrano[2,3-*b*]indolizines as a fluorescent probes, incubation of rat embryonic cardiomyoblast-derived cells H9c2 with selected dyes **2g**, **2c**, **4a** and **6a** was performed. The results showed that, neutral dyes from this family (*i.e.* **2g**, **2c** and **4a**) penetrate the living cell membrane and, as they are uncharged, accumulate nonspecifically in a wide range of cellular structures (Fig. S13†). In the case of dye **6a** which is a quaternary pyridinium salt, imaging experiments did not lead to accumulation of the dye intracellularly (Fig. 7A). To promote the access to the cytosol, H9c2 were permeabilized with digitonin (100 μg ml^{-1}). Addition of digitonin to the incubation medium resulted in permeabilization of the cell membrane and the successful penetration of the dye into the cytosol and cell organelles (Fig. 7B). It turned out that under these conditions, compound **6a**, as seen in the presented image (Fig. 7B), the dye was accumulated in the structure of the nucleus and the nuclear membrane. In order to compare the dye **6a** with the classical cell nuclear stain, co-staining with Hoechst 33342 was performed (Fig. 7C). It appears that the fluorescence of these two dyes overlaps except for some intranuclear structures, which are more strongly stained by pyranoindolizine **6a** (Fig. 7C and D). Additional intranuclear structures more strongly stained by the dye **6a** may prove useful in distinguishing specific cell nuclear structures.

Conclusions

In conclusion, the synthesis of pyrano[2,3-*b*]indolizin-2-ones from picolinium salts and diethyl 2-(ethoxymethylene) malonate under basic conditions could be optimized to reach 50% yields for the one-pot procedure. The presence of an electron-rich pyrrolic position can be harnessed to open the avenue towards various novel derivatives. The presence of different substituents on the starting picoline as well as post-functionalization allowed for detailed studies on their impact on the photophysical properties in polar and non-polar solvents. It was found that the fluorescence intensity is large for all studied pyrano[2,3-*b*]indolizin-2-ones regardless of the substitution pattern which originates from the almost complete overlap of the HOMO and LUMO. Combined experimental and computational study enabled to conclude that pyrano[2,3-*b*]indolizin-2-one core can be considered as an electron-acceptor and in most of the derivatives examined in this work, the consequence of π-expansion was the extension of the HOMO and the modification of the electronic transition energy in the range of 0.2 eV. We discovered that a simultaneous increase in the dipole moment and change of its orientation in space is the reason for maintaining the large emission intensity as well as the small Stokes shift and solvatochromism, in polar solvents. Studies on the staining of the H9c2 cell line with exemplary 2-oxo-pyrano[2,3-*b*]indolizines has proven that uncharged dyes easily penetrate the living cells' membrane. On the other hand styryl derivative **6a** does not, it specifically stains structures associated with the cell nucleus of permeabilized cells. All reported findings may serve as the guide enabling modulation of this class of molecules towards the design of improved dyes for cell imaging applications.

Experimental section

General synthetic information

All reagents and solvents were purchased from commercial sources and used as received. Reactions with moisture and oxygen sensitive compounds were performed under an argon atmosphere. The progress of reactions was monitored by thin-layer chromatography (TLC), performed on aluminum foil plates, covered with silica gel 60 F_{254} (Merck). Pure products were achieved by means of column chromatography with silica gel 60 (230–400 mesh). The identity and purity of final products were established by ^{1}H and ^{13}C NMR spectrometry as well as by MS-spectrometry (APCI-MS or ESI-MS). All reported ^{1}H NMR and ^{13}C NMR spectra were recorded on Varian AM 500 MHz, or Varian AM 600 MHz spectrometers. Chemical shifts (ppm) were determined with TMS as internal reference; *J* values are given in Hz. All melting points were measured with EZ-Melt apparatus.

Synthesis of precursors for pyrano[2,3-*b*]indolizin-2-ones

Pyridinium salts **1a**,[48] **1b**,[49] **1c**,[50] **1d**,[48] **1e**,[51] **1f**,[50] and bis(2-pyridyl)methane **0g**[63] were synthesized according to previously published procedures, and spectroscopic data are consistent.

1-(2-Ethoxy-2-oxoethyl)-2,6-dimethylpyridin-1-ium bromide (1a). ^{1}H NMR (600 MHz, DMSO-d_6) δ 8.46 (t, J = 7.9 Hz, 1H), 7.99 (d, J = 7.9 Hz, 2H), 5.62 (s, 2H), 4.26 (q, J = 7.1 Hz, 2H), 2.78 (s, 6H), 1.25 (t, J = 7.1 Hz, 3H).

1-(2-Ethoxy-2-oxoethyl)-2-methylpyridin-1-ium bromide (1b). ^{1}H NMR (600 MHz, DMSO-d_6) δ 9.01 (dd, J = 6.2, 1.3 Hz, 1H), 8.61 (td, J = 7.8, 1.5 Hz, 1H), 8.15 (d, J = 7.9 Hz, 1H), 8.08 (ddd, J = 7.7, 6.0, 1.5 Hz, 1H), 5.73 (s, 2H), 4.26 (q, J = 7.1 Hz, 2H), 2.77 (s, 3H), 1.26 (t, J = 7.1 Hz, 3H).

1-(2-Ethoxy-2-oxoethyl)-2-ethylpyridin-1-ium bromide (1c). ^{1}H NMR (600 MHz, DMSO-d_6) δ 9.07 (d, J = 5.4, Hz, 1H), 8.65 (td, J = 7.9, 1.5 Hz, 1H), 8.15 (d, J = 7.9 Hz, 1H), 8.11–8.07 (m, 1H), 5.78 (s, 2H), 4.23 (q, J = 7.1 Hz, 2H), 3.05 (q, J = 7.4 Hz, 2H), 1.28 (t, J = 7.4 Hz, 3H), 1.24 (t, J = 7.1 Hz, 3H).

1-(2-Ethoxy-2-oxoethyl)-5,6,7,8-tetrahydroquinolin-1-ium bromide (1d). ^{1}H NMR (500 MHz, DMSO-d_6) δ 8.90 (d, J = 6.1 Hz, 1H), 8.42 (d, J = 7.9 Hz, 1H), 7.97 (dd, J = 7.9, 6.2 Hz, 1H), 5.70 (s, 2H), 4.23 (q, J = 7.1 Hz, 2H), 3.00–2.97 (m, 4H), 1.90–1.84 (m, 2H), 1.76–1.70 (m, 2H), 1.23 (t, J = 7.1 Hz, 3H).

1-(2-Ethoxy-2-oxoethyl)-2-methylquinolin-1-ium bromide (1e). ^{1}H NMR (600 MHz, DMSO-d_6) δ 9.31 (d, J = 8.5 Hz, 1H), 8.48–8.50 (m, 2H), 8.30–8.23 (m, 2H), 8.03 (t, J = 7.5 Hz, 1H), 6.12 (s, 2H), 4.28 (q, J = 7.1 Hz, 2H), 3.12 (s, 3H), 1.27 (t, J = 7.1 Hz, 3H).

2-(2-Ethoxy-2-oxoethyl)-1-methylisoquinolin-2-ium bromide (1f). ^{1}H NMR (500 MHz, DMSO-d_6) δ 8.80 (d, J = 8.8, 1H), 8.70 (d, J = 6.9 Hz, 1H), 8.49 (d, J = 6.9 Hz, 1H), 8.33 (d, J = 8.1 Hz, 1H), 8.27 (dd, J = 7.5, 7.5 Hz, 1H), 8.08 (ddd, J = 8.4, 6.8, 1.3 Hz, 1H), 5.91 (s, 2H), 4.25 (q, J = 7.1 Hz, 2H), 3.21 (s, 3H), 1.25 (t, J = 7.1 Hz, 3H).

1-(Pyridin-2-yl)indolizin-2-ol (1g). In a round bottom flask, bis(2-pyridyl)methane (1.70 g, 10 mmol) was mixed with ethyl 2-bromoacetate (1.11 mL, 10 mmol) in ethanol and heated at 60 °C overnight. The pyridinium salt was not possible to isolate since the reaction spontaneously proceeded to the cyclization. After confirming the formation of the indolizine on TLC with Ehrlich's reagent, the solvent was evaporated, and the crude was used for the next reaction.

Ethyl 2-oxo-2,3-dihydroindolizine-1-carboxylate (1h). In a round bottom flask, ethyl 2-(pyridyn-2-yl)acetate (1.61 mL, 10 mmol) was mixed with ethyl 2-bromoacetate (1.11 mL, 10 mmol) in ethanol and heated at 60 °C overnight. The pyridinium salt was not possible to isolate since the reaction spontaneously proceeded to the cyclization. After confirming the formation of the indolizine on TLC with Ehrlich's reagent, solvent was evaporated, and the crude was used for the next reaction.

Di(pyridin-2-yl)methane (0g). ^{1}H NMR (600 MHz, DMSO-d_6) δ 8.45 (ddd, J = 4.9, 1.9, 0.9 Hz, 2H), 7.64 (td, J = 7.6, 1.9 Hz, 2H), 7.26 (dt, J = 7.9, 1.2 Hz, 2H), 7.16 (ddd, J = 7.7, 4.9, 1.2 Hz, 2H), 4.23 (s, 2H).

General procedure for the synthesis of 2-oxo-2*H*-pyrano[2,3-*b*]indolizine-3-carboxylates (condition A)

In a 20 mL Schlenk flask, pyridinium salt (6 mmol, 1 equiv.) and Cs_2CO_3 (6 mmol, 1 equiv.) were added and dissolved in 5 mL of ethanol. After 1–2 hours a color change in the mixture was observed and fluorescence, typical for indoles, was visible when irradiated with UV lamp. Diethyl 2-(ethoxymethylene) malonate (6 mmol, 1 equiv.) was added, and the reaction mixture was stirred overnight at room temperature. After completion, the mixture was extracted with DCM, and the combined organic layers were dried over Na_2SO_4 and concentrated under reduced pressure. The crude product was purified by column chromatography (silica, AcOEt/hexane 1 : 1).

Ethyl 6-methyl-2-oxo-2*H*-pyrano[2,3-*b*]indolizine-3-carboxylate (2a). According to the general procedure **(condition A)**, 1-(2-ethoxy-2-oxoethyl)-2,6-dimethylpyridin-1-ium bromide (500 mg, 1.82 mmol), Cs_2CO_3 (594 mg, 1.82 mmol) and diethyl 2-(ethoxymethylene)malonate (0.369 mL, 1.82 mmol) were reacted affording **2a** (250 mg, 50%) as yellow/orange crystals. R_f = 0.48 (SiO_2, AcOEt/hexane, 3 : 1); m.p. 189.0 °C. ^{1}H NMR (500 MHz, $CDCl_3$) δ 8.97 (s, 1H), 7.46 (d, J = 8.8 Hz, 1H), 7.25 (dd, J = 8.8, 7.0 Hz, 1H), 6.77 (d, J = 7.0 Hz, 1H), 6.43 (s, 1H), 4.41 (q, J = 7.1 Hz, 2H), 2.89 (s, 3H), 1.41 (t, J = 7.1 Hz, 3H). ^{13}C NMR (126 MHz, $CDCl_3$) δ 165.8, 158.3, 153.7, 142.1, 138.4, 138.1, 126.9, 117.0, 114.5, 112.7, 100.8, 89.0, 61.2, 22.0, 14.5 ppm. HRMS (ESI): m/z calcd for $C_{15}H_{13}NO_4Na$, 294.0742 $[M + Na]^+$; found, 294.0741.

Ethyl 2-oxo-2*H*-pyrano[2,3-*b*]indolizine-3-carboxylate (2b). According to the general procedure **(condition A)**, 1-(2-ethoxy-2-oxoethyl)-2-methylpyridin-1-ium bromide (0.500 mg, 2.77 mmol), Cs_2CO_3 (904 mg, 2.77 mmol) and diethyl 2-(ethoxymethylene)malonate (0.561 mL, 2.77 mmol) were reacted affording **2b** (20 mg, 5%) as yellow crystals. R_f = 0.32 (SiO_2, AcOEt/hexane, 3 : 1); m.p. 199.5 °C. ^{1}H NMR (500 MHz, $CDCl_3$) δ 8.81 (s, 1H), 8.27 (d, J = 6.9 Hz, 1H), 7.50 (d, J = 9.0 Hz, 1H), 7.26–7.20 (m, 1H), 6.90 (t, J = 6.9 Hz, 1H), 6.33 (s, 1H), 4.41 (q, J = 7.1 Hz, 2H), 1.41 (t, J = 7.1 Hz, 3H). ^{13}C NMR (126 MHz, $CDCl_3$) δ 165.1, 158.8, 152.9, 140.5, 133.7, 126.3, 124.6, 119.4, 113.0, 111.2, 101.9, 88.2, 61.3, 14.5. HRMS (ESI): m/z calcd for $C_{14}H_{11}NO_4Na$, 280.0586 $[M + Na]^+$; found, 280.0583.

Ethyl 10-methyl-2-oxo-2*H*-pyrano[2,3-*b*]indolizine-3-carboxylate (2c). According to the general procedure **(condition A)**, 1-(2-ethoxy-2-oxoethyl)-2-ethylpyridin-1-ium bromide (0.200 mg, 1.03 mmol), Cs_2CO_3 (335 mg, 1.03 mmol) and diethyl 2-(ethoxymethylene)malonate (0.208 mL, 1.03 mmol) were reacted affording **2c** (100 mg, 35%) as orange crystals. R_f = 0.54 (SiO_2, AcOEt/hexane, 3 : 1); m.p. 215.8 °C. ^{1}H NMR (500 MHz, $CDCl_3$) δ 8.76 (s, 1H), 8.23 (dt, J = 6.9, 1.1 Hz, 1H), 7.45 (dt, J = 9.0, 1.2 Hz, 1H), 7.21 (ddd, J = 9.0, 6.8, 1.1 Hz, 1H), 6.86 (td, J = 6.9, 1.2 Hz, 1H), 4.40 (q, J = 7.1 Hz, 2H), 2.30 (s, 3H), 1.41 (t, J = 7.1 Hz, 3H). ^{13}C NMR (126 MHz, $CDCl_3$) δ 165.3, 159.2, 150.7, 139.7, 133.1, 125.6, 124.5, 117.5, 112.6, 110.8, 100.8, 96.6, 61.1, 14.5, 6.2 ppm. HRMS (ESI): m/z calcd for $C_{15}H_{13}NO_4Na$, 294.0742 $[M + Na]^+$; found, 294.0739.

Ethyl 8-oxo-5,6-dihydro-4*H*,8*H*-pyrano[2′,3′:4,5]pyrrolo[3,2,1-*ij*]quinoline-9-carboxylate (2d). According to the general procedure **(condition A)**, 1-(2-ethoxy-2-oxoethyl)-5,6,7,8-tetrahydroquinolin-1-ium bromide (250 mg, 1.13 mmol), Cs_2CO_3 (370 mg, 1.13 mmol) and diethyl 2 (ethoxymethylene)malonate (0.229 mL, 1.13 mmol) were reacted affording **2d** (110 mg, 30%) as orange/red crystals. R_f = 0.48 (SiO_2, AcOEt/hexane, 3 : 1); m.p. 244.1 °C. ^{1}H NMR (600 MHz, $CDCl_3$) δ 8.76 (s, 1H), 8.05 (dd, J = 6.9, 0.8 Hz, 1H), 6.90 (dd, J = 6.9, 0.8 Hz, 1H), 6.79 (t, J = 6.8 Hz, 1H), 4.40 (q, J = 7.1 Hz, 2H), 2.93–2.86 (m, 4H), 2.03 (p, J = 6.1 Hz, 2H), 1.41 (t, J = 7.1 Hz, 3H). ^{13}C NMR (151 MHz, $CDCl_3$) δ 165.4, 159.3, 148.0, 139.5, 133.6, 130.8, 121.8, 121.5, 113.4, 111.5, 99.9, 98.3, 61.1, 27.4, 22.0, 19.8, 14.5 ppm. HRMS (ESI): m/z calcd for $C_{17}H_{15}NO_4Na$, 320.0899 $[M + Na]^+$; found, 320.0902.

Ethyl 9-oxo-9*H*-pyrano[2′,3′:4,5]pyrrolo[1,2-*a*]quinoline-10-carboxylate (2e). According to the general procedure **(condition A)**, 1-(2-ethoxy-2-oxoethyl)-2-methylquinolin-1-ium bromide (200 mg, 0.645 mmol), Cs_2CO_3 (210 mg, 0.645 mmol) and diethyl 2-(ethoxymethylene)malonate (0.130 mL, 0.645 mmol) were reacted affording **2e** (60 mg, 30%) as yellow crystals. R_f = 0.56 (SiO_2, AcOEt/hexane, 2 : 1); m.p. not measured, decomposed around 280 °C. ^{1}H NMR (500 MHz, $CDCl_3$) δ 9.36 (s, 1H), 8.32 (d, J = 8.5 Hz, 1H), 7.82 (dd, J = 7.9, 1.3 Hz, 1H), 7.77–7.72 (m, 1H), 7.54–7.48 (m, 2H), 7.41 (d, J = 9.2 Hz, 1H), 6.48 (s, 1H), 4.46 (q, J = 7.1 Hz, 2H), 1.45 (t, J = 7.1 Hz, 3H). ^{13}C NMR (126 MHz, $CDCl_3$) δ 165.5, 157.9, 154.3, 140.0, 138.0, 134.6, 130.6, 130.1, 127.8, 125.1, 124.3, 117.8, 115.6, 114.2, 103.5, 91.7, 61.6, 14.5 ppm. HRMS (APCI): m/z calcd for $C_{18}H_{13}NO_4$, 307.0845 [M−]; found, 307.0847.

Ethyl 10-oxo-10*H*-pyrano[2′,3′:4,5]pyrrolo[2,1-*a*]isoquinoline-9-carboxylate (2f). According to the general procedure **(condition A)**, 2-(2-ethoxy-2-oxoethyl)-1-methylisoquinolin-2-ium bromide (250 mg, 0.806 mmol), Cs_2CO_3 (263 mg, 0.806 mmol) and diethyl 2-(ethoxymethylene)malonate (0.163 mL, 0.806 mmol) were reacted affording **2f** (70 mg, 28%) as yellow crystals. R_f = 0.64 (SiO_2, AcOEt/hexane, 3 : 1); m.p. 261.2 °C. ^{1}H NMR (600 MHz, $CDCl_3$) δ 8.79 (d, J = 0.8 Hz, 1H), 8.11–8.08 (m, 1H), 8.01 (d, J = 7.1 Hz, 1H), 7.74–7.69 (m, 1H), 7.65–7.58 (m, 2H), 7.11 (d, J = 7.2 Hz, 1H), 6.84 (s, 1H), 4.41 (q, J = 7.1 Hz, 2H), 1.41 (t, J = 7.1 Hz, 3H). ^{13}C NMR (151 MHz, $CDCl_3$) δ 165.0, 158.8, 152.9, 138.6, 134.0, 129.6, 129.2, 128.7, 127.6, 124.3, 121.0, 113.2, 112.5, 103.3, 88.8, 61.4, 14.4 ppm. HRMS (ESI): m/z calcd for $C_{18}H_{13}NO_4Na$, 330.0742 $[M + Na]^+$; found, 330.0746.

Ethyl 2-oxo-10-(pyridin-2-yl)-2*H*-pyrano[2,3-*b*]indolizine-3-carboxylate (2g). According to the general procedure **(condition A)**, 1-(pyridin-2-yl)indolizin-2(3*H*)-one (250 mg, 1.19 mmol), Cs_2CO_3 (387 mg, 1.19 mmol) and diethyl 2-(ethoxymethylene) malonate (0.240 mL, 1.19 mmol) were reacted affording **2g** (177 mg, 44%) as yellow/orange crystals. R_f = 0.37 (SiO_2, AcOEt/hexane, 2 : 1); m.p. 252.6 °C. ^{1}H NMR (500 MHz, $CDCl_3$) δ 9.02 (d, J = 9.1 Hz, 1H), 8.83 (s, 1H), 8.67–8.64 (m, 1H), 8.33 (d, J = 6.8 Hz, 1H), 8.23 (d, J = 8.1 Hz, 1H), 7.78 (td, J = 7.8, 1.9 Hz, 1H), 7.41 (ddd, J = 9.1, 6.9, 1.2 Hz, 1H), 7.16 (ddd, J = 7.5, 4.8, 1.1 Hz, 1H), 7.03 (td, J = 6.9, 1.3 Hz, 1H), 4.42 (q, J = 7.1 Hz, 2H), 1.43 (t, J = 7.1 Hz, 3H). ^{13}C NMR (126 MHz, $CDCl_3$) δ 164.8, 158.4, 151.4, 150.4, 148.9, 139.5, 136.7, 133.4, 127.9, 124.3, 122.6, 122.1, 120.9, 114.3, 111.1, 101.7, 101.2, 61.3, 14.5. HRMS (ESI): m/z calcd for $C_{19}H_{15}N_2O_4$, 335.1032 $[M + H]^+$; found, 335.1031.

Diethyl 2-oxo-2*H*-pyrano[2,3-*b*]indolizine-3,10-dicarboxylate (2h). According to the general procedure **(condition A)**, ethyl 2-oxo-2,3-dihydroindolizine-1-carboxylate generated *in situ* (404 mg, 2.00 mmol), Cs_2CO_3 (652 mg, 2.00 mmol) and diethyl 2 (ethoxymethylene)malonate (0.404 mL, 2.00 mmol) were reacted affording **2h** (35 mg, 5%) as yellow crystals. R_f = 0.43 (SiO_2, AcOEt/hexane, 3 : 1); m.p. 227.9 °C. ^{1}H NMR (500 MHz, $CDCl_3$) δ 8.82 (s, 1H), 8.43 (d, J = 8.8 Hz, 1H), 8.37 (d, J = 6.8 Hz, 1H), 7.50 (t, J = 8.8 Hz, 1H), 7.13 (t, J = 6.8 Hz, 1H), 4.42 (q, J = 24.5 Hz, 2H), 4.40 (q, J = 24.5 Hz, 2H), 1.43 (t, J = 21.3, Hz, 3H), 1.40 (t, J = 21.3, Hz, 3H). ^{13}C NMR (126 MHz, $CDCl_3$) δ 164.5, 162.4, 157.6, 152.3, 140.8, 134.0, 129.1, 124.6, 120.4, 115.1, 110.8, 104.2, 93.8, 61.5, 60.5, 14.5, 14.4 ppm. HRMS (ESI): m/z calcd for $C_{17}H_{15}NO_6Na$, 352.0797 $[M + Na]^+$; found, 352.0798.

General procedure for the synthesis of 2-oxo-2*H*-pyrano[2,3-*b*]indolizine-3-carboxylates (condition B)

In a 20 mL Schlenk flask, pyridinium salt (6 mmol, 1 equiv.), potassium carbonate (6 mmol, 1 equiv.) and diethyl 2-(ethoxymethylene)malonate (6 mmol, 1 equiv.) were added and dissolved in 10 mL of DMF. The reaction mixture changed color and was stirred for 24 hours at room temperature. After completion, the mixture was extracted with DCM, and the combined organic layers were dried over Na_2SO_4 and concentrated under reduced pressure. The crude product was purified by column chromatography (silica, AcOEt/hexane 1 : 1).

Diethyl 2-((3-(ethoxycarbonyl)-6-methyl-2-oxo-2*H*-pyrano[2,3-*b*]indolizin-10-yl)methylene)malonate (2i). According to the general procedure **(condition B)**, 1-(2-ethoxy-2-oxoethyl)-2,6-dimethylpyridin-1-ium bromide (450 mg, 2.3 mmol), potassium carbonate (320 mg, 2.3 mmol) and diethyl 2-(ethoxymethylene) malonate (0.467 mL, 2.3 mmol) were reacted affording **2i** (100 mg, 15%) as yellow/orange crystals. R_f = 0.45 (SiO_2, AcOEt/hexane, 3 : 1); m.p. 210.5 °C. ^{1}H NMR (600 MHz, $CDCl_3$) δ 8.92 (s, 1H), 7.77 (s, 1H), 7.65 (d, J = 8.6 Hz, 1H), 7.36 (dd, J = 8.9, 7.1 Hz, 1H), 6.85 (d, J = 7.1 Hz, 1H), 4.53 (q, J = 7.1 Hz, 2H), 4.35 (q, J = 7.1 Hz, 2H), 4.25 (q, J = 7.2 Hz, 2H), 2.86 (s, 3H), 1.34 (t, J = 7.2 Hz, 3H), 1.32 (t, J = 7.2 Hz, 3H), 1.28 (t, J = 7.2 Hz, 3H). ^{13}C NMR (126 MHz, $CDCl_3$) δ 166.7, 165.1, 165.1, 156.5, 151.5, 141.6, 138.9, 138.1, 128.9, 128.7, 124.7, 116.4, 115.1, 113.3, 102.9, 96.9, 62.4, 61.6, 61.5, 22.1, 14.4, 14.2, 14.0 ppm. HRMS (APCI): m/z calcd for $C_{23}H_{22}NO_8$, 442.1345 $[M - H]^-$; found, 440.1350.

General procedure for direct arylation

A Schlenk flask flushed with argon, was charged with ethyl 6-methyl-2-oxo-2*H*-pyrano[2,3-*b*]indolizine-3-carboxylate (0.55 mmol, 1 equiv.), aryl bromide (0.66 mmol, 1.2 equiv.), potassium acetate (1.11 mmol, 2 equiv.), NMP (3 mL) and $PdCl_2(PPh_3)_2$ (0.027 mmol, 0.05 equiv.). The solution was

stirred at 100 °C for 10 min. Afterwards, water (1.11 mmol, 2 equiv.) was added, and the heating was continued at the same temperature overnight. Then, the mixture was cooled to room temperature and extracted with DCM. The combined organic layers were dried over Na_2SO_4 and concentrated under reduced pressure. The crude product was purified by column chromatography (silica, AcOEt/hexane 1 : 1).

Ethyl 10-(4-cyanophenyl)-6-methyl-2-oxo-2*H*-pyrano[2,3-*b*]indolizine-3-carboxylate (3aa). According to the general procedure for direct arylation, ethyl 6-methyl-2-oxo-2*H*-pyrano[2,3-*b*]indolizine-3-carboxylate (0.55 mmol, 1 equiv.), 4-bromobenzonitrile (0.66 mmol, 1.2 equiv.), potassium acetate (1.11 mmol, 2 equiv.), NMP (3 mL), $PdCl_2(PPh_3)_2$ (0.027 mmol, 0.05 equiv.), and water (1.11 mmol, 2 equiv.) were made to react affording **3aa** (120 mg, 60%) as greenish yellow crystals. R_f = 0.45 (SiO_2, AcOEt/hexane, 3 : 1); m.p. 306.1 °C. ^{1}H NMR (600 MHz, $CDCl_3$) δ 9.06 (s, 1H), 7.84–7.81 (m, 2H), 7.80–7.77 (m, 3H), 7.38 (dd, J = 8.9, 7.0 Hz, 1H), 6.89 (d, J = 7.0 Hz, 1H), 4.42 (q, J = 7.1 Hz, 2H), 2.96 (s, 3H), 1.42 (t, J = 7.1 Hz, 3H). ^{13}C NMR (151 MHz, $CDCl_3$) δ 165.3, 157.4, 150.5, 139.4, 138.9, 138.3, 135.1, 132.7, 129.0, 128.0, 118.9, 115.6, 115.4, 112.5, 110.4, 102.3, 101.4, 61.5, 22.3, 14.4 ppm. HRMS (APCI): m/z calcd for $C_{22}H_{15}N_2O_4$, 371.1032 $[M - H]^-$; found, 371.1036.

Ethyl 6-methyl-10-(4-nitrophenyl)-2-oxo-2*H*-pyrano[2,3-*b*]indolizine-3-carboxylate (3ab). According to the general procedure for direct arylation, ethyl 6-methyl-2-oxo-2*H*-pyrano[2,3-*b*]indolizine-3-carboxylate (0.55 mmol, 1 equiv.), 1-bromo-4-nitrobenzene (0.66 mmol, 1.2 equiv.), potassium acetate (1.11 mmol, 2 equiv.), NMP (3 mL), $PdCl_2(PPh_3)_2$ (0.027 mmol, 0.05 equiv.), and water (1.11 mmol, 2 equiv.) were made to react affording **3ab** (25 mg, 50%) as orange crystals. R_f = 0.45 (SiO_2, AcOEt/hexane, 3 : 1); m.p. 284.3 °C. ^{1}H NMR (500 MHz, $CDCl_3$) δ 9.07 (s, 1H), 8.36 (d, J = 8.8 Hz, 2H), 7.89 (d, J = 8.8 Hz, 2H), 7.83 (d, J = 8.9 Hz, 1H), 7.40 (dd, J = 9.0, 7.0 Hz, 1H), 6.91 (d, J = 7.1 Hz, 1H), 4.43 (q, J = 7.1 Hz, 2H), 2.97 (s, 3H), 1.42 (t, J = 7.1 Hz, 3H). ^{13}C NMR (126 MHz, $CDCl_3$) δ 165.3, 157.3, 150.7, 146.3, 139.4, 139.0, 138.3, 137.2, 129.0, 128.2, 124.3, 115.8, 115.5, 112.5, 102.5, 101.1, 61.5, 22.3, 14.4 ppm. HRMS (APCI): m/z calcd for $C_{21}H_{15}N_2O_6$, 391.0930 $[M - H]^-$; found, 391.0932.

Ethyl 10-(4-(*tert*-butyl)phenyl)-6-methyl-2-oxo-2*H*-pyrano[2,3-*b*]indolizine-3-carboxylate (3ac). According to the general procedure for direct arylation, ethyl 6-methyl-2-oxo-2*H*-pyrano[2,3-*b*]indolizine-3-carboxylate (0.20 mmol, 1 equiv.), 1-bromo-4-(*tert*-butyl)benzene (0.26 mmol, 1.2 equiv.), potassium acetate (0.40 mmol, 2 equiv.), NMP (3 mL), $PdCl_2(PPh_3)_2$ (0.010 mmol, 0.05 equiv.), and water (0.40 mmol, 2 equiv.) were made to react affording **3ac** (14 mg, 17%) as orange/brown crystals. R_f = 0.56 (SiO_2, AcOEt/hexane, 2 : 1); m.p. 241.6 °C. ^{1}H NMR (600 MHz, CD_2Cl_2) δ 8.93 (s, 1H), 7.71 (d, J = 8.7 Hz, 1H), 7.57–7.51 (m, 2H), 7.51–7.46 (m, 2H), 7.24 (dd, J = 8.9, 6.9 Hz, 1H), 6.76 (d, J = 7.0 Hz, 1H), 4.27 (q, J = 7.1 Hz, 2H), 2.84 (s, 3H), 1.32–1.29 (m, 12H). ^{13}C NMR (126 MHz, $CDCl_3$) δ 165.7, 158.1, 150.3, 140.1, 138.5, 137.9, 128.9, 128.5, 127.0, 126.8, 125.9, 116.1, 114.9, 112.5, 103.3, 101.1, 61.2, 34.7, 31.3, 22.2, 14.5 ppm. HRMS (APCI): m/z calcd for $C_{25}H_{26}NO_4$, 404.1862 $[M + H]^+$; found, 404.1861.

Procedure for the synthesis of styryl dye

Ethyl 10-formyl-6-methyl-2-oxo-2*H*-pyrano[2,3-*b*]indolizine-3-carboxylate (4a). In a round bottom flask, $POCl_3$ (0.280 mL, 3 mmol) was added to dry DMF (0.310 mL, 4 mmol), at 0 °C. The ice bath was removed and the solution was stirred for 30 min. A solution of ethyl 6-methyl-2-oxo-2*H*-pyrano[2,3-*b*]indolizine-3-carboxylate (0.250 g, 0.92 mmol) in dry DCE (5 mL) was added and the mixture was stirred at 85 °C for 16 hours. After cooling to room temperature, an aqueous solution of saturated sodium acetate (3 mL) was added and heated again for 1 hour at 100 °C, then the reaction mixture was cooled to room temperature and the water-organic layer was extracted with DCM. The combined organic layers were dried over Na_2SO_4 and concentrated under reduced pressure. The crude product was purified by column chromatography (silica, AcOEt/hexane 1 : 1) affording **4a** (230 mg, 83%) as yellow crystals. R_f = 0.40 (SiO_2, AcOEt/hexane, 3 : 1); m.p. 241.4 °C. ^{1}H NMR (500 MHz, $CDCl_3$) δ 10.29 (s, 1H), 9.03 (s, 1H), 8.54 (d, J = 8.8 Hz, 1H), 7.60 (dd, J = 8.8, 7.2 Hz, 1H), 7.05 (d, J = 7.2 Hz, 1H), 4.43 (q, J = 7.1 Hz, 2H), 2.99 (s, 3H), 1.43 (t, J = 7.1 Hz, 3H). ^{13}C NMR (126 MHz, $CDCl_3$) δ 181.8, 164.8, 156.6, 155.8, 140.6, 139.1, 139.0, 131.5, 118.5, 118.0, 112.2, 103.7, 102.3, 61.7, 22.1, 14.4. ppm. HRMS (APCI): m/z calcd for $C_{16}H_{12}NO_5$, 298.0714 $[M - H]^-$; found, 298.0715.

4-Methylpyridinium iodide (5). Synthesis was conducted according to literature.[64] ^{1}H NMR (500 MHz, DMSO-d_6) δ 8.81 (d, J = 6.4 Hz, 2H), 7.94 (d, J = 6.2 Hz, 2H), 4.26 (s, 3H), 2.58 (s, 3H).

(*E*)-4-(2-(3-(Methoxycarbonyl)-6-methyl-2-oxo-2*H*-pyrano[2,3-*b*]indolizin-10-yl)vinyl)-1-methylpyridin-1-ium iodide (6a). In a round bottom flask, 4-methylpyridinium iodide (18 mg, 0.17 mmol), ethyl 10-formyl-6-methyl-2-oxo-2*H*-pyrano[2,3-*b*]indolizine-3-carboxylate (51 mg, 0.17 mmol) and piperidine (0.017 mL) were dissolved in MeOH (4 mL) and refluxed overnight. After cooling down to room temperature, a precipitate is formed, filtered and washed with MeOH to afford ethyl 10-formyl-6-methyl-2-oxo-2*H*-pyrano[2,3-*b*]indolizine-3-carboxylate as red crystals **6a** (25 mg, 37%). M.p. 250.7 °C. ^{1}H NMR (500 MHz, DMSO-d_6) δ 8.94 (s, 1H), 8.78 (d, J = 6.3 Hz, 2H), 8.34–8.19 (m, 4H), 7.68 (t, J = 7.9 Hz, 1H), 7.31 (d, J = 16.0 Hz, 1H), 7.20 (d, J = 7.1 Hz, 1H), 4.23 (s, 3H), 3.81 (s, 3H), 2.95 (s, 3H). ^{13}C NMR (126 MHz, DMSO-d_6) δ 164.9, 156.7, 153.4, 151.7, 145.0, 141.4, 141.2, 139.5, 130.5, 129.0, 123.0, 121.2, 117.4, 115.6, 113.8, 101.1, 99.2, 52.5, 47.0, 21.5 ppm. HRMS (ESI): m/z calcd for $C_{22}H_{19}N_2O_4$, 375.1345.1501 $[M^+]$; found, 375.1348.

Photophysical measurements

HPLC grade solvents were purchased from Sigma-Aldrich and used as obtained. For optical studies, solutions of molecules at low concentrations were used to avoid dimerization or reabsorption effects. All absorption and fluorescence spectra were taken at room temperature (21 °C). A Shimadzu UV/VIS-NIR

spectrophotometer, model UV-3600i Plus, was used for absorption spectra measurement. Fluorescence spectra were recorded with an FS5 spectrofluorometer from Edinburgh Instruments. Fluorescence quantum yields (Φ_{fl}) of molecules in solvents at 21 °C were determined using Coumarin 153 in EtOH (Φ_{fl} = 0.38) and Rhodamine 6 g in EtOH (Φ_{fl} = 0.95) as references. Solutions of low absorbance (A < 0.1) were used to avoid reabsorption or concentration quenching. Refractive index correction for solvents have been performed in the calculations of quantum yields. Molar absorption coefficient, ε, was calculated from the absorbance, A, of a solution of the given molar concentration, c, in a cuvette of length, l, according to Lambert Beer formula:

$$A = c\,\varepsilon\,l$$

Fluorescence kinetics studies were performed using the time correlated single photon counting technique. A modelocked Coherent Mira-HP picosecond laser pumped by a Verdi 18 laser was used for excitation. The fundamental pulses of the Mira laser were up-converted to 387.5 nm. The temporal width of the excitation pulses was ~280 fs and the instrument response function (IRF) about 40 ps. Fluorescence was dispersed with a 0.25 m Jarrell-Ash monochromator and detected with a HMP-100-07 hybrid detector coupled to an SPC-150 PC module, (Becker&Hickl GmbH). Fluorescence decays were analyzed with deconvolution software using a nonlinear least squares procedure with the Marquardt algorithm. A standard χ^2 test and Durbin–Watson (DW) parameter along with residual and autocorrelation function plots were used to assess the quality of a fit. The estimated accuracy for the determination of decay time was below 10 ps.

Computational details

The calculations were performed using the Gaussian 16 program.[65] The solvent effect was introduced in PCM procedure. The SOC elements were also calculated using the Orca program.[66]

Biological studies

The rat embryonic cardiomyoblast-derived H9c2 cells were loaded with the fluorophore at the final concentration of 500 nM in DMEM medium supplemented with 10% foetal bovine serum, 2 mM glutamine, 100 U ml^{-1} penicillin, and 100 μg ml^{-1} streptomycin, and incubated at 37 °C in a humidified atmosphere containing 5% CO_2 for 15 to 60 minutes. After that, the incubation medium was replaced with FluoroBrite™ DMEM. The measurements were performed with the use of an Olympus IX83 confocal microscope with the silicone objective 60× UPLSAPO 60XS. Registered data were transferred to the ImageJ and analysed for presentation.

Author contributions

Conceptualization: D. T. G. and J. S. A. B.; investigation: J. S. A. B., A. W., I. D.; supervision: D. T. G., A. S.; visualization: J. S. A. B., A. W., I. D.; writing – original draft: J. S. A. B., A. W., I. D.; writing – review and editing: D. T. G., J. S. A. B.

All the authors discussed the results and commented on the manuscript.

Data availability

The data supporting this article have been included as part of the ESI.†

Conflicts of interest

There are no conflicts to declare.

Acknowledgements

This work was supported by the Polish National Science Center, Poland (grants OPUS 2020/37/B/ST4/00017 and HARMONIA 2018/30/M/ST5/00460). This project has received funding from the European Union's Horizon 2020 research and innovation programme under the Marie Skłodowka-Curie grant agreement no 101007804. The work was financially supported by the Foundation for Polish Science (TEAM POIR.04.04.00-00-3CF4/16-00). Calculations were performed at the Interdisciplinary Center for Mathematical and Computational Modeling (ICM) University of Warsaw under computational allocation G95-1734. We thank Joseph Milton for amending the manuscript.

References

1 K. Sun, S. Jin, S. Fang, R. Ma, X. Zhang, M. Gao, W. Zhang, T. Lu and D. Du, N-Heterocyclic carbene-catalyzed formal [3 + 3] annulation of alkynoic acid esters with indolin-3-ones: access to functionalized pyrano[3,2-b]indol-2-ones, *Org. Chem. Front.*, 2019, **6**, 2291–2295.

2 X.-Y. Meng, M.-Y. Sun, F.-J. Zhao, Y.-J. Dang, B. Jiang and S.-J. Tu, Domino Reaction of 2,2-Dihydroxyindene-1,3-dione with Aromatic Amines: Efficient Synthesis of Isochromeno[4,3-b]indol-5(11H)-one Derivatives, *Synthesis*, 2014, 3207–3212.

3 N. S. Masterova, S. Yu. Ryabova, L. M. Alekseeva, M. I. Evstratova, S. S. Kiselev and V. G. Granik, Novel pyrano[3,2-b]indole derivatives: synthesis and some properties, *Russ. Chem. Bull.*, 2010, **59**, 637–641.

4 N. Monakhova, J. Korduláková, A. Vocat, A. Egorova, A. Lepioshkin, E. G. Salina, J. Nosek, E. Repková, J. Zemanová, H. Jurdáková, R. Górová, J. Roh, G. Degiacomi, J. C. Sammartino, M. R. Pasca, S. T. Cole, K. Mikušová and V. Makarov, Design and Synthesis of Pyrano[3,2-b]indolones Showing Antimycobacterial Activity, *ACS Infect. Dis.*, 2021, **7**, 88–100.

5 A. P. Gaywood and H. McNab, Methylene Meldrum's Acid Derivatives of Indoxyl and Their Cyclization Reactions under Flash Vacuum Pyrolysis Conditions, *Synthesis*, 2010, 1361–1364.
6 P. C. Unangst and R. E. Brown, Indole esters as heterocyclic synthons. II. Preparation of 1,3-oxazino[5,6-b]indoles and 3-substituted-pyrano[3,2-b]indoles, *J. Heterocycl. Chem.*, 1984, **21**, 283–288.
7 H. K. Kadam and S. G. Tilve, Unique synthesis of isochromenoindolone via reductive-oxidative cyclisation approach, *Indian J. Chem., Sect. B: Org. Chem. Incl. Med. Chem.*, 2019, **58**, 104–108.
8 X. Zhang, W. Hou, D. Zhang-Negrerie, K. Zhao and Y. Du, Hypervalent Iodine-Mediated Intramolecular trans-Aminocarboxylation and Oxoaminocarboxylation of Alkynes: Divergent Cascade Annulations of Isocoumarins under Metal-Free Conditions, *Org. Lett.*, 2015, **17**, 5252–5255.
9 S. Pathak, D. Das, A. Kundu, S. Maity, N. Guchhait and A. Pramanik, Synthesis of 4-hydroxyindole fused isocoumarin derivatives and their fluorescence "Turn-off" sensing of Cu(II) and Fe(III) ions, *RSC Adv.*, 2015, **5**, 17308–17318.
10 J. L. Bullington and J. H. Dodd, Synthesis of tetrahydroindeno[1,2-b]indol-10-ones and their rearrangement to [2]benzopyrano[4,3-b]indol-5-ones, *J. Org. Chem.*, 1993, **58**, 4833–4836.
11 A. Sugimoto, K. Sakamoto, Y. Fujino, Y. Takashima and M. Ishikawa, Synthesis and Inhibitory Effect on Platelet Aggregation of 2-Phenyl-1 (2H)-phthalazinone Derivatives, *Chem. Pharm. Bull.*, 1985, **33**, 2809–2820.
12 A. J. Frew, G. R. Proctor and J. V. Silverton, Reactions of the sodium salts of some heterocyclic β-ketoesters with dimethyl acetylenedicarboxylate, *J. Chem. Soc., Perkin Trans. 1*, 1980, 1251–1256.
13 A. Arcadi, S. Cacchi, F. Marinelli and P. Pace, 5-Alkyl-5-[2-(o-iodophenylcarbamoyl)vinyl] Derivatives of Meldrum's Acid as Substrates for the Intramolecular Heck Reaction: Application to the Synthesis of Carbazoles, *Synlett*, 1993, 743–744.
14 N. L. Nam and I. I. Grandberg, Condensation of oxindole with acetoacetic ester and acetylacetone, *Chem. Heterocycl. Compd.*, 2006, **42**, 1010–1011.
15 W.-Z. Zhang, M.-W. Yang and X.-B. Lu, Carboxylative cyclization of substituted propenyl ketones using CO2: transition-metal-free synthesis of α-pyrones, *Green Chem.*, 2016, **18**, 4181–4184.
16 G. H. Ko, C. Maeng, H. Jeong, S. H. Han, G. U. Han, K. Lee, H. C. Noh and P. H. Lee, Rhodium(III)-Catalyzed Sequential C–H Activation and Cyclization from N-Methoxyarylamides and 3-Diazooxindoles for the Synthesis of Isochromenoindolones, *Chem. – Asian J.*, 2021, **16**, 3179–3187.
17 S. Park, J. Lee, K. J. Shin, E. Oh and J. H. Seo, Consecutive One-Pot versus Domino Multicomponent Approaches to 3-(Diarylmethylene)oxindoles, *Molecules*, 2017, **22**, 503.
18 Q. Chen, Y. Teng and F. Xu, Lanthanide Silylamide-Catalyzed Synthesis of Pyrano[2,3-b]indol-2-ones, *Org. Lett.*, 2021, **23**, 4785–4790.
19 A. S. Kumar and R. Nagarajan, Cyclization Routes for the Synthesis of Functionalized Pyrano[2,3-b]indolones, Pyrazolo[3,4-b]indoles, and Furo[2,3-b]indoles, *Synthesis*, 2013, 1235–1246.
20 M. Abdel-Megid, A versatile molecule for the synthesis of some new polynuclear bioactive heterocyclic systems, *Int. J. Chem.*, 2006, **16**, 149–157.
21 R. Frutos-Pedreño and J.-A. García-López, 2-Arylacetamides as Versatile Precursors for 3-Aminoisocoumarin and Homophthalimide Derivatives: Palladium-Catalyzed Cascade Double Carbonylation Reactions, *Adv. Synth. Catal.*, 2016, **358**, 2692–2700.
22 X. Peng, Y. Huang, W. Wang, S. Li, G. Hao, S. Ren and Y. R. Chi, N-Heterocyclic Carbene-Catalyzed Remote Enantioselective C–C Bond Formation via 1,6-Addition with Formyl Enynes, *ACS Catal.*, 2024, **14**, 2127–2133.
23 A. Kakehi, S. Ito, K. Nakanishi, K. Watanabe and M. Kitagawa, Preparation of New Nitrogen-bridged Heterocycles. A Facile Synthetic Method of Pyrano[2,3-b]indolizinone Derivatives, *Bull. Chem. Soc. Jpn.*, 1980, **53**, 1115–1120.
24 A. Kakehi, S. Ito, K. Watanabe, M. Kitagawa, S. Takeuchi and T. Hashimoto, Preparation of new nitrogen-bridged heterocycles. Synthesis and some reactions of 2,3-dihydroindolizin-2-one derivatives, *J. Org. Chem.*, 1980, **45**, 5100–5104.
25 A. Kakehi, S. Ito, S. Murakami and H. Sano, Preparation of New Nitrogen-bridged Heterocydes. 8. Syntheses of Some Fused Indolizine Derivatives via the Acid-catalyzed Cyclizations of Functionalized 1- and 3-Vinylindolizines, *Bull. Chem. Soc. Jpn.*, 1984, **57**, 548–552.
26 A. Kakehi, S. Ito and K. Matsubara, Preparation of New Nitrogen-Bridged Heterocycles. 39. One-Pot Synthesis of 2H-Pyrano[3,2-a]indolizin-2-one Derivatives, *Bull. Chem. Soc. Jpn.*, 1995, **68**, 2409–2415.
27 G. Jones, W. R. Jackson and A. M. Halpern, Medium effects on fluorescence quantum yields and lifetimes for coumarin laser dyes, *Chem. Phys. Lett.*, 1980, **72**, 391–395.
28 J. A. Van Gompel and G. B. Schuster, Photophysical behavior of ester-substituted aminocoumarins: a new twist, *J. Phys. Chem.*, 1989, **93**, 1292–1295.
29 B. B. Raju and S. M. B. Costa, Photophysical properties of 7-diethylaminocoumarin dyes in dioxane–water mixtures: hydrogen bonding, dielectric enrichment and polarity effects, *Phys. Chem. Chem. Phys.*, 1999, **1**, 3539–3547.
30 M. Sulpizi, P. Carloni, J. Hutter and U. Rothlisberger, A hybrid TDDFT/MM investigation of the optical properties of aminocoumarins in water and acetonitrile solution, *Phys. Chem. Chem. Phys.*, 2003, **5**, 4798–4805.
31 K. Azuma, S. Suzuki, S. Uchiyama, T. Kajiro, T. Santa and K. Imai, A study of the relationship between the chemical structures and the fluorescence quantum yields of coumarins, quinoxalinones and benzoxazinones for the devel-

opment of sensitive fluorescent derivatization reagents, *Photochem. Photobiol. Sci.*, 2003, **2**, 443–449.
32 M. El-Kemary and W. Rettig, Multiple emission in coumarins with heterocyclic substituents, *Phys. Chem. Chem. Phys.*, 2003, **5**, 5221–5228.
33 X. Liu, Z. Xu and J. M. Cole, Molecular Design of UV–vis Absorption and Emission Properties in Organic Fluorophores: Toward Larger Bathochromic Shifts, Enhanced Molar Extinction Coefficients, and Greater Stokes Shifts, *J. Phys. Chem. C*, 2013, **117**, 16584–16595.
34 M. Cavazzini, S. Quici, S. Orlandi, C. Sissa, F. Terenziani and A. Painelli, Intimately bound coumarin and bis(alkylaminostyryl)benzene fragments: synthesis and energy transfer, *Tetrahedron*, 2013, **69**, 2827–2833.
35 D. Kim, S. Singha, T. Wang, E. Seo, J. H. Lee, S.-J. Lee, K. H. Kim and K. H. Ahn, In vivo two-photon fluorescent imaging of fluoride with a desilylation-based reactive probe, *Chem. Commun.*, 2012, **48**, 10243–10245.
36 I. Kim, D. Kim, S. Sambasivan and K. H. Ahn, Synthesis of π-Extended Coumarins and Evaluation of Their Precursors as Reactive Fluorescent Probes for Mercury Ions, *Asian J. Org. Chem.*, 2012, **1**, 60–64.
37 D. Kim, Q. P. Xuan, H. Moon, Y. W. Jun and K. H. Ahn, Synthesis of Benzocoumarins and Characterization of Their Photophysical Properties, *Asian J. Org. Chem.*, 2014, **3**, 1089–1096.
38 Y. W. Jun, H. R. Kim, Y. J. Reo, M. Dai and K. H. Ahn, Addressing the autofluorescence issue in deep tissue imaging by two-photon microscopy: the significance of far-red emitting dyes, *Chem. Sci.*, 2017, **8**, 7696–7704.
39 Y. J. Reo, Y. W. Jun, S. W. Cho, J. Jeon, H. Roh, S. Singha, M. Dai, S. Sarkar, H. R. Kim, S. Kim, Y. Jin, Y. L. Jung, Y. J. Yang, C. Ban, J. Joo and K. H. Ahn, A systematic study on the discrepancy of fluorescence properties between in solutions and in cells: super-bright, environment-insensitive benzocoumarin dyes, *Chem. Commun.*, 2020, **56**, 10556–10559.
40 Y. Jung, N. K. Park, S. Kang, Y. Huh, J. Jung, J. K. Hur and D. Kim, Latent turn-on fluorescent probe for the detection of toxic malononitrile in water and its practical applications, *Anal. Chim. Acta*, 2020, **1095**, 154–161.
41 A. Mukhopadhyay, T. Hossen, I. Ghosh, A. L. Koner, W. M. Nau, K. Sahu and J. N. Moorthy, Helicity-Dependent Regiodifferentiation in the Excited-State Quenching and Chiroptical Properties of Inward/Outward Helical Coumarins, *Chem. – Eur. J.*, 2017, **23**, 14797–14805.
42 A. Mukhopadhyay, V. K. Maka and J. N. Moorthy, Remarkable influence of 'phane effect' on the excited-state properties of cofacially oriented coumarins, *Phys. Chem. Chem. Phys.*, 2017, **19**, 4758–4767.
43 A. Kakehi, S. Ito, H. Suga, S. Takano and K. Hirata, Preparation of New Nitrogen-Bridged Heterocycles. 45. Smooth Hydrolysis of 6-Membered Heterocyclic 2-Imines with Partial Aromaticity, *Chem. Pharm. Bull.*, 1998, **46**, 1632–1634.
44 C. Galli, "CESIUM ION EFFECT" AND MACROCYCLIZATION. A CRITICAL REVIEW, *Org. Prep. Proced. Int.*, 1992, **24**, 285–307.
45 S. S. Bhalodiya, M. P. Parmar, D. B. Upadhyay, C. D. Patel, D. P. Vala, D. Rajani and H. M. Patel, Cs2CO3-promoted one-pot synthesis of novel tetrahydrobenzofuran-4(2*H*)-ones: *In vitro* antimicrobial, antimalarial activity and *in silico* docking study, *Results Chem.*, 2024, **7**, 101304.
46 P. A. Khardina, E. M. Buev, V. S. Moshkin and V. Y. Sosnovskikh, Novel synthesis of 2,3-dihydrobenzofuran-3-amines from salicylic aldehydes: Trimethylsilyl as traceless activating group, *Tetrahedron Lett.*, 2024, **139**, 154992.
47 P. Li, Y. Ji, W. Chen, X. Zhang and L. Wang, The facile synthesis of 2-bromoindoles via Cs2CO3-promoted intramolecular cyclization of 2-(gem-dibromovinyl)anilines under transition-metal-free conditions, *RSC Adv.*, 2012, **3**, 73–78.
48 J. Ezquerra and J. Alvarez-Builla, 2-Methylpyridinium salts as 1,4-dinucleophiles. II. Westphal condensation with substituted pyridinium substrates, *J. Heterocycl. Chem.*, 1986, **23**, 1151–1157.
49 Z. Chen, S. Zhang, X. Qi, S. Liu, Q. Zhang and Y. Deng, Fluorescent quinolizinium ionic liquids (salts) with unexpectedly high quantum yields up to >99%, *J. Mater. Chem.*, 2011, **21**, 8979–8982.
50 T. S. Chinta Rao, S. Saha, G. B. Raolji, B. Patro, P. Risbood, M. J. Difilippantonio, J. E. Tomaszewski and S. V. Malhotra, Microwave assisted Westphal condensation and its application to synthesis of sempervirine and related compounds, *Tetrahedron Lett.*, 2013, **54**, 487–490.
51 J. V. Greenhill, H. Loghmani-Khouzani and D. J. Maitland, Tautomerism in ketomethylquinolines. Part 2. Further results on 2-ketomethylquinolines, *J. Chem. Soc., Perkin Trans. 1*, 1991, 2831–2840.
52 A. Kakehi, S. Ito and T. Yotsuya, Preparation of New Nitrogen-Bridged Heterocycles. XIII.: Syntheses of Some Tricyclic and Tetracyclic Indolizine Derivatives with Antiallergic Activity, *Chem. Pharm. Bull.*, 1986, **34**, 2435–2442.
53 S. Wu, Q. Cao, X. Wang, K. Cheng and Z. Cheng, Design, synthesis and biological evaluation of mitochondria targeting theranostic agents, *Chem. Commun.*, 2014, **50**, 8919–8922.
54 A. S. Brown, L.-M. Bernal, T. L. Micotto, E. L. Smith and J. N. Wilson, Fluorescent neuroactive probes based on stilbazolium dyes, *Org. Biomol. Chem.*, 2011, **9**, 2142–2148.
55 Y. Liu, B. Wang, J.-T. Hou, P. Xie, W. Li and S. Wang, Molecular engineering and bioimaging applications of C2-alkenyl indole dyes with tunable emission wavelengths covering visible to NIR light, *Bioorg. Chem.*, 2023, **141**, 106905.
56 12 Principles of Green Chemistry, **https://www.acs.org/greenchemistry/principles/12-principles-of-green-chemistry.html**, (accessed 31 July 2024).
57 G. Kobayashi, Y. Matsuda, R. Natsuki, Y. Tominaga, T. Okamura and A. Itamura, Studies on Indole Derivatives. XVII. The Synthesis of Indoxyl Derivatives. (3) The

Reactions of 3-Hydroxy-2-(1-methylthiovinyl)-indole Derivatives with Amines, *Yakugaku Zasshi*, 1973, **93**, 964–970.

58 R. R. Valiev, V. N. Cherepanov, G. V. Baryshnikov and D. Sundholm, First-principles method for calculating the rate constants of internal-conversion and intersystem-crossing transitions, *Phys. Chem. Chem. Phys.*, 2018, **20**, 6121–6133.

59 A. Manian, R. A. Shaw, I. Lyskov, W. Wong and S. P. Russo, Modeling radiative and non-radiative pathways at both the Franck–Condon and Herzberg–Teller approximation level, *J. Chem. Phys.*, 2021, **155**, 054108.

60 A. Kawski, On the Estimation of Excited-State Dipole Moments from Solvatochromic Shifts of Absorption and Fluorescence Spectra, *Z. Naturforsch., A: Phys. Sci.*, 2002, **57**, 255–262.

61 Ł. Kielesiński, I. Deperasińska, O. Morawski, K. V. Vygranenko, E. T. Ouellette and D. T. Gryko, Polarized, V-Shaped, and Conjoined Biscoumarins: From Lack of Dipole Moment Alignment to High Brightness, *J. Org. Chem.*, 2022, **87**, 5961–5975.

62 Z. R. Grabowski, K. Rotkiewicz and W. Rettig, Structural Changes Accompanying Intramolecular Electron Transfer: Focus on Twisted Intramolecular Charge-Transfer States and Structures, *Chem. Rev.*, 2003, **103**, 3899–4032.

63 G. Dyker and O. Muth, Synthesis of Methylene- and Methine-Bridged Oligopyridines, *Eur. J. Org. Chem.*, 2004, 4319–4322.

64 K. Senthil, S. Kalainathan and A. R. Kumar, Effect of additives on the large-size growth of 4-N,N-dimethylamino-4-N-methyl stilbazolium naphthalene-2-sulfonate (DSNS) single crystal: an efficient stilbazolium derivative NLO crystal with potential terahertz wave properties, *CrystEngComm*, 2014, **16**, 9847–9856.

65 M. J. Frisch, G. W. Trucks, H. B. Schlegel, G. E. Scuseria, M. A. Robb, J. R. Cheeseman, G. Scalmani, V. Barone, G. A. Petersson, H. Nakatsuji, X. Li, M. Caricato, A. V. Marenich, J. Bloino, B. G. Janesko, R. Gomperts, B. Mennucci, H. P. Hratchian, J. V. Ortiz, A. F. Izmaylov, J. L. Sonnenberg, D. Williams-Young, F. Ding, F. Lipparini, F. Egidi, J. Goings, B. Peng, A. Petrone, T. Henderson, D. Ranasinghe, V. G. Zakrzewski, J. Gao, N. Rega, G. Zheng, W. Liang, M. Hada, M. Ehara, K. Toyota, R. Fukuda, J. Hasegawa, M. Ishida, T. Nakajima, Y. Honda, O. Kitao, H. Nakai, T. Vreven, K. Throssell, J. A. Montgomery, J. E. Peralta Jr., F. Ogliaro, M. J. Bearpark, J. J. Heyd, E. N. Brothers, K. N. Kudin, V. N. Staroverov, T. A. Keith, R. Kobayashi, J. Normand, K. Raghavachari, A. P. Rendell, J. C. Burant, S. S. Iyengar, J. Tomasi, M. Cossi, J. M. Millam, M. Klene, C. Adamo, R. Cammi, J. W. Ochterski, R. L. Martin, K. Morokuma, O. Farkas, J. B. Foresman and D. J. Fox, *Gaussian 16 (Revision A.03)*, Gaussian Inc., Wallingford CT, 2016.

66 F. Neese, Software update: the ORCA program system, version 4.0, *Wiley Interdiscip. Rev.: Comput. Mol. Sci.*, 2018, **8**, e1327.

ORGANIC CHEMISTRY FRONTIERS

REVIEW

View Article Online
View Journal | View Issue

Cite this: *Org. Chem. Front.*, 2025, **12**, 2860

Advances in the synthesis of indolizines and their π-expanded analogues: update 2016–2024

Jaqueline S. A. Badaro, Bartosz Godlewski and Daniel T. Gryko *

Received 6th November 2024,
Accepted 31st January 2025

DOI: 10.1039/d4qo02082k

rsc.li/frontiers-organic

Indolizine (pyrrolo[1,2-*a*]pyridine) is an isomer of indole. The diversity of synthetic approaches leading to the indolizine skeleton is unrivalled, compared to many other heterocycles of this size. Increasing availability of densely functionalized pyrrole derivatives makes it possible to expand the scope of indolizine synthesis from these substrates. In this article, we describe progress in the development of new strategies that lead to indolizine and its π-expanded analogs during the period 2016–2024. Developments of the past decade combined the optimization of known strategies with the discovery of entirely new approaches. First, we discuss the synthetic pathways leading to the indolizine core from pyridine, followed by describing methods starting from pyrrole derivatives. Finally, we focus on π-expanded indolizines, also describing their optoelectronic properties. Although certain synthetic limitations exist, the newly developed methodologies provide impetus for numerous explorations that use indolizines. We anticipate that our review will help motivate further advances in indolizine synthesis.

10th anniversary statement

In 2019, I published a key paper in *Organic Chemistry Frontiers* (*Org. Chem. Front.*, 2019, **6**, 2939–2948). It revealed new conditions for a multicomponent reaction leading to 1,4-dihydropyrrolo[3,2-*b*]pyrroles, which significantly expanded the substrate scope (both amines and aldehydes) and improved the yields of the heterocyclic products. Eventually, this paper opened new horizons for these exceptionally electron-rich functional dyes. I wish *Organic Chemistry Frontiers* a successful and prosperous second decade of existence!

1. Introduction

Indolizines entered the chemical world in 1890.[1] This isomer of indole has long been overshadowed by indole itself, which took prime position due to its overwhelming presence in the structures of both alkaloids and synthetic, biologically active compounds. Classical methods furnishing the indolizine skeleton, such as the Chichibabin reaction,[2] are well established in the literature. The simplicity of the indolizine core and the presence of a bridging nitrogen atom continued to attract attention from chemists, who developed a plethora of synthesis strategies, which started from either pyridine derivatives or substituted pyrroles. The subject was reviewed in the past[3–8] and quite recently specialized review articles appeared as well,[9–13] followed by major review.[14] Originally interest in the indolizine scaffold was more related to its dehydrogenative derivatives, which are present in some alkaloids.[15] Over time, the picture has changed and in recent decades interest shifted towards optoelectronic-type applications.[16,17] Indolizines' intrinsically strong emission of violet–blue light was intensively exploited by Park's group (Seoul-Fluor dyes);[18,19] this sparked broader research interest that eventually provided impetus for further development. This shift of interest seamlessly translated into the emergence of π-expanded indolizines as a distinct research direction. It turned out that structural modifications enabled a bathochromic shift of the emission to the deep red region and beyond. Here, we present a comprehensive picture of progress in the synthesis of indolizines that has occurred from 2016 to now (Scheme 1).

2. Methods based on pyridine derivatives

The synthesis of indolizines from pyridine derivatives is the most widely recognized approach found in the literature. Pyridine derivatives are readily available, commercially accessible building blocks that are typically bench-stable, air-stable solids. These characteristics make them highly convenient substrates for the construction of indolizine frameworks.

Institute of Organic Chemistry of the Polish Academy of Sciences, 01-224 Warsaw, Poland. E-mail: dtgryko@icho.edu.pl

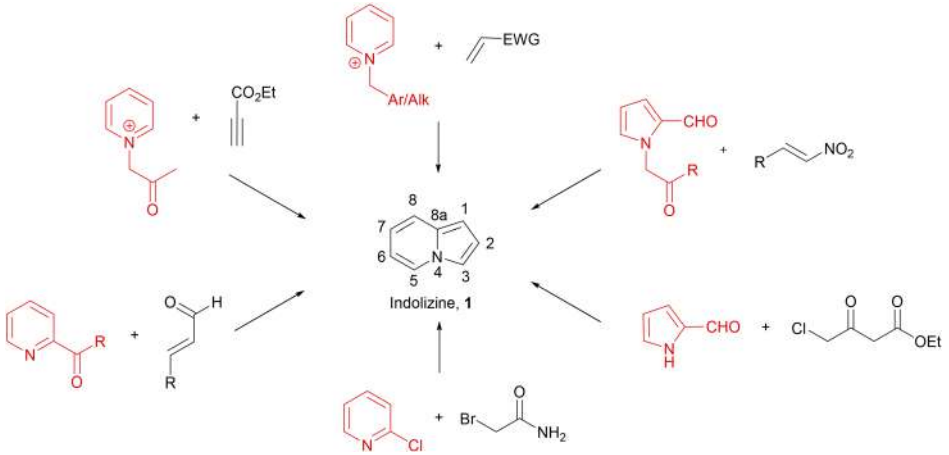

Scheme 1 Overview of synthetic methodologies leading to the indolizine core.

2.1 From pyridinium ylides

One of the most widely used methods in indolizine synthesis is the [3 + 2] annulation of pyridinium ylides with alkynes[20–28] or alkenes. This type of reactivity usually gives rise to indolizines bearing electron withdrawing groups in the C1 and/or C3 positions, as both substrates are commonly activated by such groups (*e.g.* ester or cyano group). Also, using 3-substituted pyridine derivatives can give rise to two regioisomers as annulation can occur on either side of the nitrogen atom.

2.1.1 Ylides generated from pyridinium salts. Pyridinium salts are extremely versatile substrates in indolizine synthesis. Their ease of preparation and the broad availability of simple unsaturated derivatives make this approach particularly convenient. The pyridinium salt can be preformed or formed *in situ*, and then deprotonated with a base to yield pyridinium ylides, which are capable of reacting in [3 + 2] cycloaddition reactions or generally undergo [3 + 2] annulations following various mechanisms.

It must be pointed out that using an alkene substrate for this type of transformation usually implies the need to use an oxidant to give rise to fully aromatic indolizine. In such cases more complex reaction conditions are used.

An archetypical example of this reactivity was recently presented by Moise *et al.* (Scheme 2).[29] A pyridinium salt formed by the reaction of a pyridine derivative and chloroacetone easily undergoes (upon deprotonation with an organic amine) 1,3-cycloaddition with ethyl propiolate to give rise to C1,C3-di-EWG disubstituted indolizines **2**. Similarly, disubstituted alkynes can also efficiently participate in [3 + 2] cycloaddition. He *et al.* synthesized a series of trifluoromethyl substituted indolizines using the same approach.[30] Karamshahi *et al.* also utilized disubstituted alkynes and expanded the reactivity scope to pyrazine derivatives.[31]

Jaqueline S. A. Badaro

Jaqueline S. Araujo Badarò was born in Brazil in 1995 and moved to Turin, Italy, in 2001, where she grew up. She obtained her M.Sc. from the University of Turin in 2020 under the guidance of Professors Cristina Prandi and Loretta Lazzarato. Then she relocated to Warsaw, Poland, to pursue a Ph.D. at the Institute of Organic Chemistry, Polish Academy of Sciences, where she works under the supervision of Prof. Daniel T. Gryko on the synthesis and physicochemical characterization of indolizine derivatives. While completing her Ph.D., Jaqueline decided to transition her career and recently began working as a Project Manager for EU-funded scientific projects.

Bartosz Godlewski

Bartosz Godlewski was born in Warsaw, Poland, in 2000. He graduated summa cum laude *from Warsaw University of Technology (Faculty of Chemistry) in 2024. His B.Eng. and Master of Engineering theses (under the supervision of Dr Maciej Malinowski) were based on the synthesis of novel sugar–porphyrin conjugates and advanced Pd-catalyzed coupling methodology. Then, he joined Professor Daniel Gryko's research group, where he is pursuing his Ph.D. Currently, his research interests are focused on the synthesis of new luminescent organic radicals, with an emphasis on triarylmethane scaffolds.*

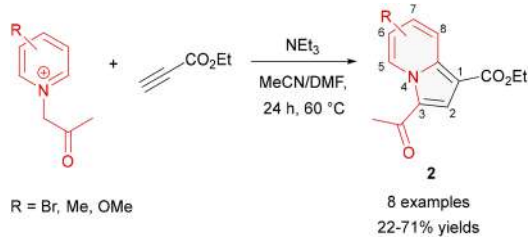

Scheme 2

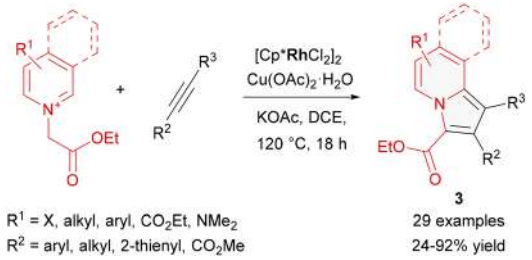

Scheme 3

Scheme 4

Similar conditions have been used by many research groups to yield various indolizine derivatives,[32–40] including ones substituted with charged pyridyl moieties[41] or complex biomolecules such as sugars[42] – conceptually all these reactions use the same strategy.

An example of metal-catalyzed C–H activation applied in indolizine synthesis was presented by Shen *et al.*[43] The authors utilized rhodium(III) catalysis to obtain a wide scope of indolizines **3** substituted with aryl rings (Scheme 3). To date rhodium catalysis has been mostly used in partially reduced indolizine core synthesis, usually starting from unsaturated pyrrole derivatives.[44–48] The methodology was also expanded to alkyl and heteroaryl derivatives as well as to different pyridines. It is worth noting that, contrary to standard approaches, the alkyne does not bear any activating groups. The mechanism proceeds through rhodium(III) C–H insertion, eight-membered ring formation, ring contraction with regeneration of the ester functionality and reductive elimination to give rise to the indolizine skeleton.

It is known that alkenes are also active substrates in the synthesis of indolizines.[49–54] Liu *et al.* reported the reaction between pyridinium salts and various electron-deficient alkenes where TEMPO was used as an organic oxidant (Scheme 4).[55] After a slight reoptimization (lithium hydroxide was used as a base instead of cesium carbonate), this method could also lead to indolizines **4** bearing a wide range of alkyl chains at position C3. This discovery opened a convenient way to access this type of indolizine starting with primary halogenated alkanes. Additionally, disubstituted alkenes such as dimethyl maleate and chromone were well tolerated.

Other recently reported variants of this strategy include metal-catalyzed reactions,[56–58] hydroperoxide-induced oxidation,[59] denitrative synthesis using nitroalkenes,[60] and the denitrative approach combined with the presence of another leaving group (chlorine,[61] sulfanyl[62]).

Tabolin and co-workers used fluoronitro derivatives in indolizine synthesis, which enabled the authors to obtain unique aryl-substituted 1-fluoroindolizines **5** (Scheme 5).[63] A simple copper(II) catalyst was employed; this method tolerated various substituents in either of aryl rings present, as well as the use of quinoline instead of pyridine. The mechanism involves a Michael-type addition of the ylide to the nitroalkene, followed by the formation of a five-membered ring – formally a stepwise [3 + 2] cycloaddition. Copper oxidizes the intermediate product and, finally, formal HNO_2 elimination (which is preferred over HF elimination) occurs yielding indolizine. This novel protocol greatly expands the utility of fluoronitroalkenes, as such substrates are widely used building blocks in the synthesis of various heterocyclic products such as pyrroles,[64] pyrazoles,[65] triazoles[66] and pyrazolo[1,5-*a*]pyridines.[63]

A complementary way to fluoroindolizines has also been developed. 2-Fluoroindolizines can be obtained in the reaction between pyridinium salts and α-CF_3 ketones.[67] These ketones can be perceived as formal equivalents of fluoroacyl alkynes, as it was with nitrofluoroalkenes, which represent formal fluoroalkyne reactivity. A conceptually similar transition-metal-free

Daniel T. Gryko

Daniel T. Gryko obtained his PhD from the Institute of Organic Chemistry of the Polish Academy of Sciences in 1997, under the supervision of Prof. J. Jurczak. After a post-doctoral stay with Prof. J. Lindsey at North Carolina State University (1998–2000), he started his independent career in Poland. He became Full Professor in 2008. The same year, he received the Society of Porphyrins and Phthalocyanines Young Investigator Award and in 2017 the Foundation for Polish Science Award. His current research interests are focused on the synthesis of various functional dyes, as well as on two-photon absorption, solvatofluorochromism, excited-state intramolecular proton transfer and fluorescent probes.

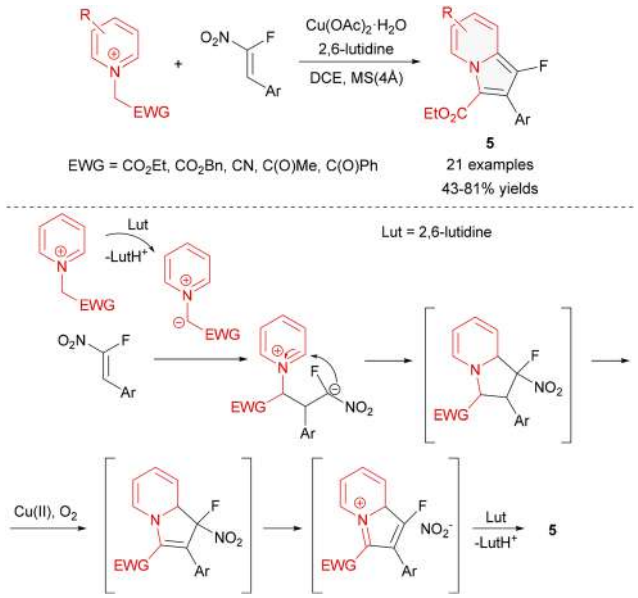

Scheme 5

approach was used to obtain 2-sulfanylindolizines, starting from β,β-disulfanyl-α,β-unsaturated ketones.[68]

Similar reactivity could also be accessed using metal-free conditions (Scheme 6).[69] *gem*-Difluoroalkenes readily underwent [3 + 2] annulation under standard basic conditions. The reaction also proceeded through a difluoro intermediate, which upon fluorine atom elimination and oxidation gave desired indolizines **6**. This methodology was exemplified by using a diverse set of difluorostyrenes, including those where the aryl ring was functionalized with complex biomolecules such as terpenoids, amino acids, and steroids. Although 2-fluoroindolizine synthesis using *gem*-difluoroalkenes was already known, this protocol greatly improved the applicability of such an approach – previously, an unsaturated partner needed to be preactivated by tosylate[70] or yet another halogen group.[71]

Ma *et al.* discovered that β,β-difluoroperoxides were also active substrates in the reaction with pyridinium ylides.[72] These unusual substrates are transformed *in situ* into β-fluoroenone *via* Kornblum–DeLaMare rearrangement and subsequent HF elimination. This fluoro derivative undergoes a standard cycloaddition, HF elimination and oxidation reaction sequence to yield functionalized indolizines.

Scheme 6

Recently, it was proved that nitro and fluoro functionalities were not the only ones that could serve as a formal leaving group in indolizine synthesis. It was found that this role could also be fulfilled by carboxylic acid derivatives, usually generated *in situ* by ring-opening of maleic anhydride induced by nucleophilic attack. One such approach, through a decarboxylative four-component reaction, was proposed by Xu *et al.*[73] This strategy gave rise to C1 amide-substituted indolizines in excellent yields. A drawback of this strategy was the need to use an external oxygen source to facilitate the oxidation process. Unintuitively, the use of sterically hindered pyridinium salts (formed *in situ*) gave the best yields.

A similar strategy was recently presented by Zhang *et al.* who also utilized maleic anhydride in the synthesis of unique C1 and C2 unsubstituted indolizines **7**.[74] A key mechanistic step was the decarboxylation of carboxyl diradical **7a**, generated by TEMPO (Scheme 7). Conditions were compatible with halogen-functionalized α-haloketones, as well as quinoline and isoquinoline substrates. Usually, the group that serves as an activating agent in the alkene substrate is retained in the final product (*e.g.* indolizines **2**, **4**, **5**), while in this approach both carboxylic groups are removed before final aromatization. While this strategy was already recognized in the literature, maleic anhydride was yet to be transformed into the **7a**-type intermediate by other means than metal-based catalytic systems.[75,76] This finding offers an improved and greener method based on using an organic oxidant to activate this simple alkene towards reacting with pyridinium ylides.

Similar indolizines can be obtained by using (*E*)-2-methoxyethene-1-sulfonyl fluoride as an acetylene surrogate. This dis-

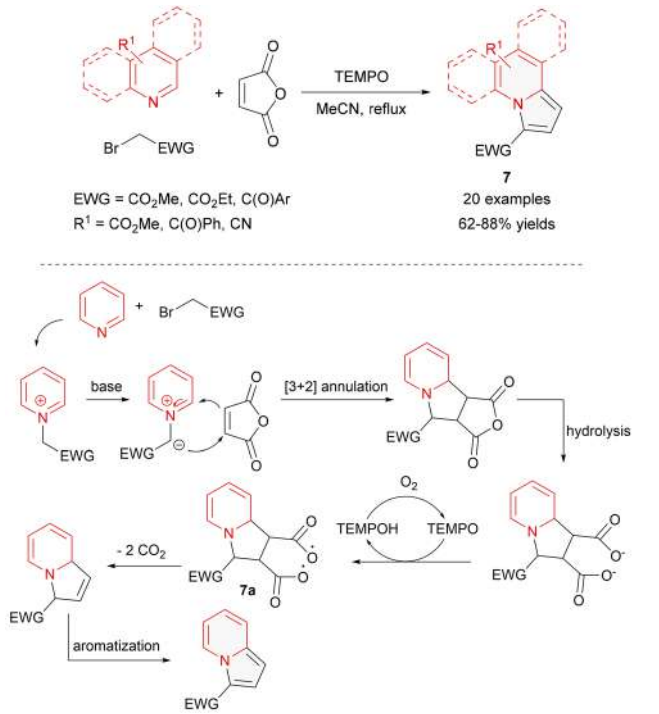

Scheme 7

covery was reported by Ma *et al.*;[77] however, the methodology presented in Scheme 7 is probably preferred due to the wide availability of maleic anhydride compared to Ma's substrate.

A completely novel, unorthodox concept was presented by Zheng *et al.*, who used propargyl sulfonium compounds as partners in [3 + 2] annulation (Scheme 8).[78] Unexpectedly, the reaction did not proceed with participation of the triple bond, but instead sulfonium salts isomerized to allene, which only then reacted with isoquinolinium ylide *via* stepwise [3 + 2] annulation forming **8A/B**. It is worth noting the exceptionally benign conditions – cyclization occurs at room temperature, in the presence of an organic base (compared with methodologies utilizing much harsher conditions, such as those leading to indolizines **4** or **10**), making this approach of particular interest in the late-stage synthesis of the indolizine moiety. In the same year it was proved that 2-bromoallylsulfones were also suitable reagents for generating allenes.[79] Such derivatives similarly furnished C2-methyl indolizine derivatives; however, the degree of chemoselectivity was lower – in some cases the authors observed partial C1-desulfonation.

Cyclic alkenes can also be suitable substrates for indolizine synthesis. This strategy was exemplified by Dong and Huang, who utilized chromones as unsaturated partners (Scheme 9).[80] After stepwise [3 + 2] annulation, the six-membered ring containing an oxygen atom is cleaved open to generate a double bond in the tetrahydroindolizine skeleton. The final oxidative aromatization step leads to 1-(2-hydroxybenzoyl)indolizines **9** in good yields. A similar approach is presented by the synthesis of indolizines **48**, where a chromone derivative is reacted with an appropriate pyrrole derivative. Nitroindoles also exhibit a similar type of reactivity. Babu *et al.* used *N*-tosyl-3-nitroindoles to obtain 1-(2-aminophenyl)indolizines.[81] The reaction proceeded through the standard 1,3-dipolar cycloaddition step, elimination of NO_2, and aromatization with concomitant ring opening, where an amine is formally a leaving group. Such amino derivatives became the basis of further C–H amination reactions, yielding interesting indolizines fused through the C2 position. Later, the same group discovered that utilizing 3-nitrobenzothiophene gave rise to unusual indolizine dyads possessing a disulfide bridge instead of the expected sulfanyl derivative.[82]

A mechanistically unusual reaction was reported by Shu *et al.*[83] A key step was the $K_2S_2O_8$-mediated transformation of DMSO into a thionium ion. Next, it gets attacked by the ylide, and methanethiol is eliminated furnishing an *exo*-methylenic intermediate. This intermediate participates in [3 + 2] cycloaddition, which results in tetrahydroindolizine. Upon oxidation of **10a** and expulsion of pyridine, the reaction converges to the indolizine **10** skeleton with the C2 carbon originating from DMSO, also used as a solvent. The conditions were compatible with various ketoaryl moieties, leading to the final products in good to excellent yields (Scheme 10). While very broad and diverse in terms of scope on the aryl part of the pyridinium salt, this methodology suffers from one limitation – C1 and C3 acyl moieties remain in the same group.

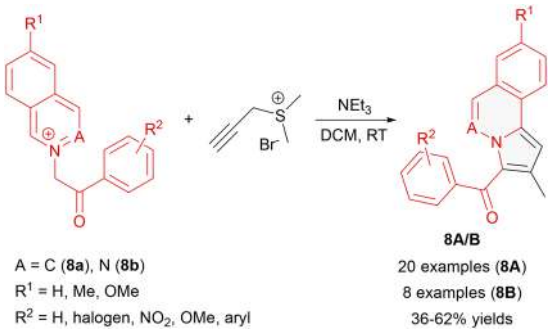

Scheme 8

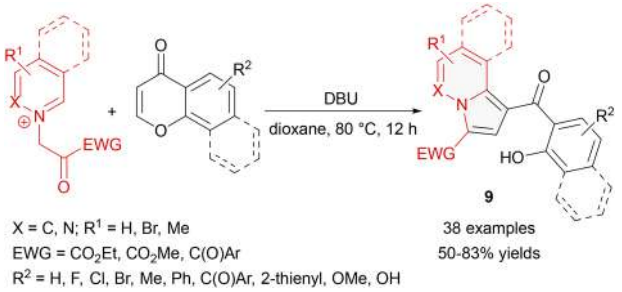

Scheme 9

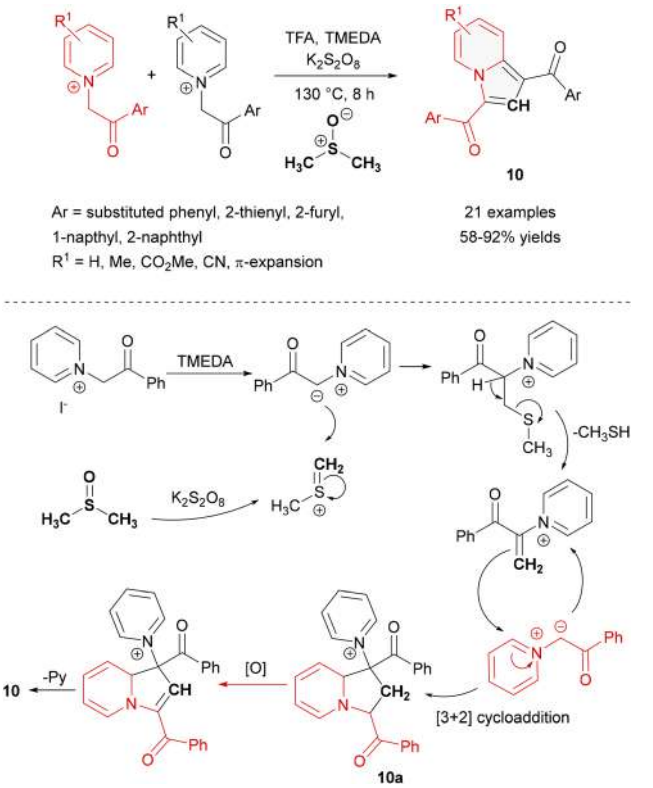

Scheme 10

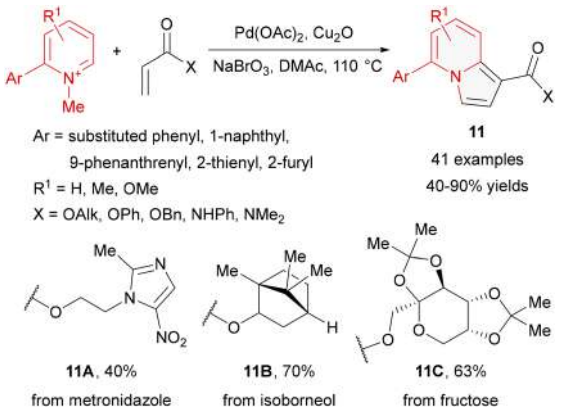

Scheme 11

A particularly elegant approach towards indolizines **11** with free C2 and C3 positions was demonstrated by Gou's group.[84] The authors utilized an *N*-methyl pyridinium salt – a rare substrate in indolizine synthesis, with one of the α-positions in the heterocyclic ring being blocked (Scheme 11). After much optimization, the elaborated Pd/Cu catalytic system proved to be extremely effective, thus overcoming the low reactivity of the weakly acidic C_{sp^3}–H reaction centre. The ester and amide scope was notably broad, allowing the authors to obtain various indolizines functionalized with biomolecules such as sugars, terpenoids and APIs. This method is one of the scarce examples of indolizine synthesis from pyridine starting materials, which can give rise to C3-free indolizine, thanks to the lack of functional groups attached to the carbon atom in the *N*-methyl group.

The C2-carbon atom can also originate from difluorocarbene. Hou *et al.* presented a methodology for C1,C3-disubstituted indolizines, where the carbon atom was introduced by CF_2 reacting with pyridinium ylide (Scheme 12).[85] A series of additions and eliminations led to indolizines **12A**, in which the C1-ester substituent originated from a different ylide molecule. Interestingly, when 2-picolinium salts were used, the reaction proceeded through an intramolecular cyclization step, which resulted in the formation of **12B**. This

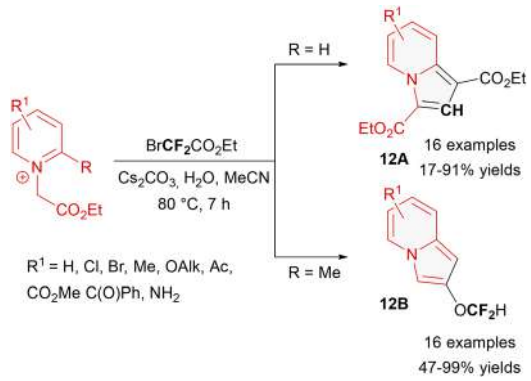

Scheme 12

approach somewhat solves the limitation of the previously presented indolizine **10** synthesis – it is possible to introduce two distinct ethoxycarbonyl groups, serving as a formal acyl group precursor, as well as a handle for further functionalization and C1/C3 group differentiation.

In addition to standard base-mediated and metal-catalyzed approaches, many other conditions were developed for indolizine synthesis from pyridinium ylides and/or salts. The treatment of *in situ*-generated pyridinium salts and alkynes with whole *Yarrowia lipolytica* cells was shown to lead to indolizines in rather good yields.[86] Furthermore, cells originating from horseradish root (*Armoracia rusticana*) are able to catalyze bis-indolizine formation.[87] Unfortunately, the scope of such transformations remains somewhat limited and developments towards greater functional group tolerance could encourage their wider use in organic synthesis. Recently, Schneider and co-workers published a series of articles describing ultrasound-induced indolizine synthesis. This approach can efficiently produce indolizines and is compatible with various functional groups.[88–90] This approach is not only applicable to the standard pyridinium ylide/unsubstituted alkyne protocol, but also to the synthesis of unique chalcogen-derivatized (in the C2 position) indolizines, including selenium and tellurium derivatives. Interestingly, haloalkanes can also mediate indolizine synthesis – this phenomenon has been called "halogen-bond catalysis".[91] Also, many indolizines could be easily obtained under microwave irradiation – this type of reactivity was recently covered in a review by Ghosh and Biswas.[10]

Although the first cases of [3 + 2]cycloaddition leading to the formation of the indolizine core were published a long time ago,[3–5] this strategy continues to be attractive and it has undergone further development. The variant with alkynes as substrates has the advantage that an external oxidant is not necessary whereas the availability of alkenes points to the key advantage of the second version. It seems that the option with alkenes decorated with leaving groups such as fluorine or NO_2 is the 'best of both worlds' combining easily accessible substrates with the lack of a requirement for oxidation.

2.1.2 Ylides generated by different methods. It must be noted that there are several routes to pyridinium ylides other than the reaction of pyridine with suitable halo derivatives and subsequent deprotonation with a suitable base. One particularly important approach is the Ortoleva–King reaction of active methyl or methylene derivatives in the presence of molecular iodine (Scheme 13). Highly functionalized indolizines **13** were obtained by a novel strategy reported by Yavari *et al.*[92] The authors obtained ketenimines *via* a cascade of the Nef isocyanide reaction and the Perkow reaction. Such substrates were reacted with previously prepared quinolinium ylides; the key step was the application of Ortoleva–King reactivity to activate the α-picolinic position. Even though highly reactive ketimine **13a** is utilized in the synthesis, the protocol is compatible with heterocyclic derivatives possessing a pyridine-type nitrogen atom (needed for the C(sp^3)–H activation step), which is scarcely explored in the literature. This approach was

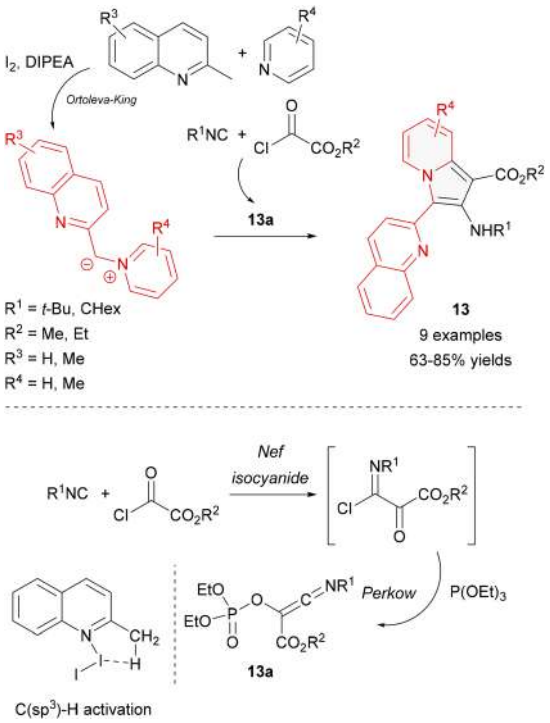

Scheme 13

recently further developed by the same group[93,94] and now is widely recognized in the literature.[95–97]

Another approach to activate acetophenone substrates in the synthesis of indolizines was very recently presented by Zhang *et al.* The authors developed a CuBr-based solvent-free catalytic system, which in the presence of $(NH_4)_2S_2O_8$ yielded bromoacetophenones.[98] Such substrates readily formed ylides and participated in the cyclization with electron-deficient alkenes, including nitrostilbenes, which gave rise to C1-unsubstituted indolizines *via* a denitrative pathway. In addition, an even simpler CuBr-based catalytic system is known, where air plays the role of the sole oxidant.[99]

Peng's group accessed pyridinium ylide reactivity by employing rhodium-catalyzed activation of donor–acceptor diazo compounds (Scheme 14).[100] After classic [3 + 2] annulation, the resulting intermediate undergoes metal-assisted 1,3-ester migration, yielding the final partially reduced indolizines **14**. This reactivity could also be tuned to furnish 1,4-oxazepine derivatives *via* [5 + 2] cycloaddition.

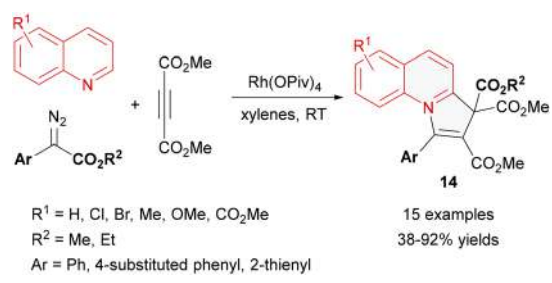

Scheme 14

Diazoacetates were also an efficient ylide precursor under Cu-catalysis conditions.[101] It was proved that natural products such as hemoglobin could be used as the catalyst in such an approach,[102] as well as simple synthetic porphyrins such as TPP iron complexes.[103]

Sharma and coworkers proved that pyridinium ylides could be efficiently obtained by applying electro-oxidative C(sp^3)–H bond functionalization and efficiently transformed into indolizines[104] – this can be perceived as electrochemical Ortoleva–King-type reactivity.

It is obvious from this short description that methodologies relying on ylides generated by different methods than the deprotonation of *N*-alkylpyridinuium salts are yet to come to fruition and at the moment they are not comparable in terms of generality and scope of substituents for what they can offer to indolizine chemistry.

2.2 From *N*-free pyridine derivatives

N-Free pyridines can also participate in indolizine synthesis and yield target heterocycles without the formation of standard pyridinium salts as presented above. Such methods are particularly convenient, as they alleviate the need for any pre-functionalization of the pyridine nitrogen atom before indolizine synthesis.

As a continuation of previous work,[105,106] Tiwari and Rawat developed catalyst-free regiodivergent [2 + 2 + 1] cycloaddition (Scheme 15).[107] Diesters of acetylenedicarboxylic acid underwent nucleophilic addition of pyridine to the triple bond. This adduct then dimerizes and cyclizes in a 5-*exo*-*trig* fashion. Loss of ylide, followed by intramolecular cyclization and aromatization, leads to two molecules of desired indolizine **15A**. The regioselectivity of this reaction was directly influenced by the presence of a functional group on the nitrogen atom. Furthermore, two similar articles were published that described the synthesis of analogous triester derivatives,[108] as well as indolizines that possessed two ester moieties alongside

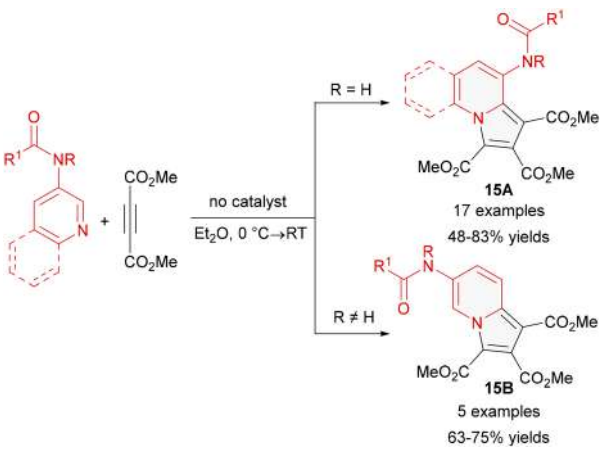

Scheme 15

the nitro group.[109] These approaches remain a very convenient way to construct densely substituted (on pyrrole ring) indolizines, which possess diverse functionalities on the pyridine side of the heterocycle, including amino and halogen groups. Acetophenones were also shown to be suitable substrates for the synthesis of 1,2,3-trisubstituted indolizines from pyridine. Sun *et al.* presented a $CuBr_2$-based catalytic system that smoothly afforded 1,2,3-tri(acyl)indolizines in good yields.[110]

A novel metal-free radical reaction between enaminones and pyridines bearing an EWG at position C4 was recently described.[111] B_2pin_2 plays a crucial role in the reaction mechanism, generating radical species **16a** (Scheme 16). A sequence of migration, cyclization, radical removal, and aromatization gives rise to the final product **16**. This method tolerated various functional groups without loss of efficiency. Noteworthy is the high modularity of such an approach – enaminones are easily synthesized by aldol-type condensation of aryl ketones with DMF–DMA, whereas commercial libraries of substituted pyridines are extremely broad. Recently, advanced DFT calculations were performed by Zhang *et al.*, who showed that such a reaction might proceed through a different route than the Minisci-type addition outlined in Scheme 16.[112] Somewhat similar approaches taking advantage of enaminone reactivity will be mentioned later in the text (sections 2.4 and 2.7).

An easily tunable and concise approach towards indolizines was recently presented by Arndtsen's group (Scheme 17).[113] 2-Bromopyridine can enter a palladium-catalytic cycle, giving a carbonylated intermediate, which then reacts with preformed imine. The product of this transformation undergoes cyclization to the high-energy 1,3-dipolar intermediate **17a**, which is a suitable partner for cycloaddition with an alkyne, yielding indolizines **17**. Interestingly, the carbonyl group originating from the CO molecule is not conserved in the final structure – it is just a means to build up high-energy intermediate **17a**.

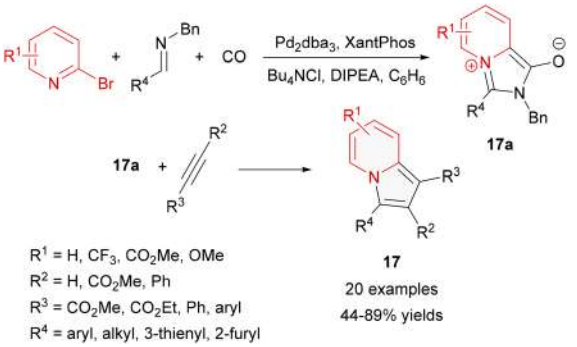

Scheme 17

2-Sulfanylpyridines were also readily transformed into indolizines **18**, by a base-catalyzed reaction with nitroallylic acetates (Scheme 18). The mercapto group fulfilled the role of a handle deciding the regioselectivity of this approach.[114] The mechanism proceeds through the S_N2 reaction with extrusion of the acetate ion, Michael addition and unusual thiirane formation, which is rearranged to give the final product. Previously, it was shown that such MBH-acetates could also be reacted in the same manner with α-acidic picoline derivatives.[115] While interesting, this approach is somewhat restricted by the complexity of the starting material – indolizines substituted with an EWG in position C1 are easily obtained from appropriate ylides and alkenes (*e.g.* indolizine **2**).

A seemingly analogous finding to indolizine **14** synthesis was published by Xu's group (Scheme 19).[116] However, in this case the diazo compound is not a precursor to the pyridinium ylide (as it was for **14**), but instead transforms into a metal carbenoid, which then undergoes carbene/alkyne metathesis. Pyridine attacks the carbenoid species and after cyclization and decarboxylative aromatization, the formal [2 + 2 + 1] annulation product arises. This approach provides access to polycyclic indolizines **19**. It was also suggested that this reaction could proceed through a pyridinium ylide, but it seemed that

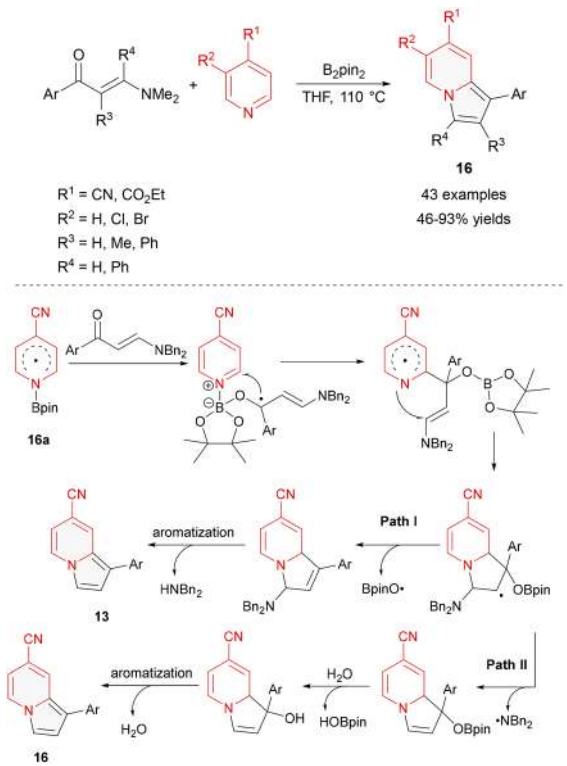

Scheme 16

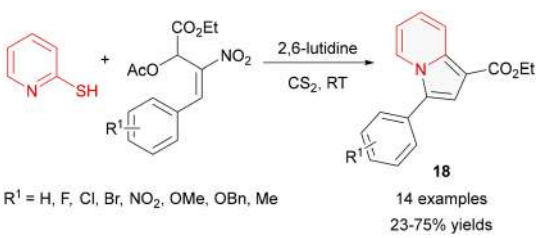

Scheme 18

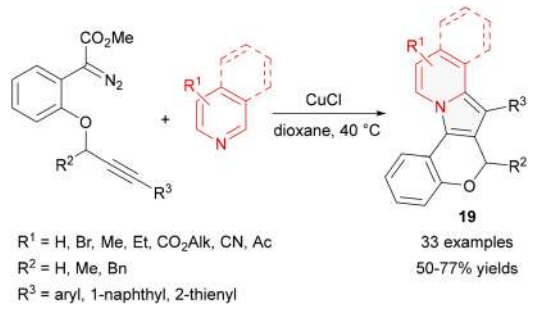

Scheme 19

both pathways contributed somewhat to the formation of the final product.

Recently, Nechaev and co-workers presented a synthetic strategy toward indolizin-1-ols with charged electron acceptors (pyridinium, imidazolium).[117,118] Such compounds are not air-stable and spontaneously dimerize through the C3 position upon exposure to ambient conditions; however, they can be transformed *in situ* into various derivatives, including C3-substituted and π-expanded indolizines (*vide infra*).

One such example described by Nechaev's group was to utilize indolizin-1-ols to synthesize sulfanyl derivatives, as well as tropone-substituted indolizines (Scheme 20).[119] The reactive intermediate, formed in the reaction between *N*-free pyridine and *gem*-difluorocyclopropenes, was immediately trapped by various thiols and electrophilic tropones and underwent oxidative coupling to yield complex C3-substituted indolizines **20**. Through this approach one can smoothly access the inherent nucleophilicity of the C3-position of the indolizine-1-ol core, providing a novel way to functionalize this heterocyclic scaffold.

The same group continued research in the emerging field of using *gem*-diflurocyclopropenes (and their surrogates) in the synthesis of indolizin-1-ols and recently obtained novel unsubstituted 3-mercapto analogues of **20A** by treatment of **20a** with molecular sulfur (**20D**).[120] It is found that such products exist as mesomeric betaines and exhibit extremely attractive photophysical properties.

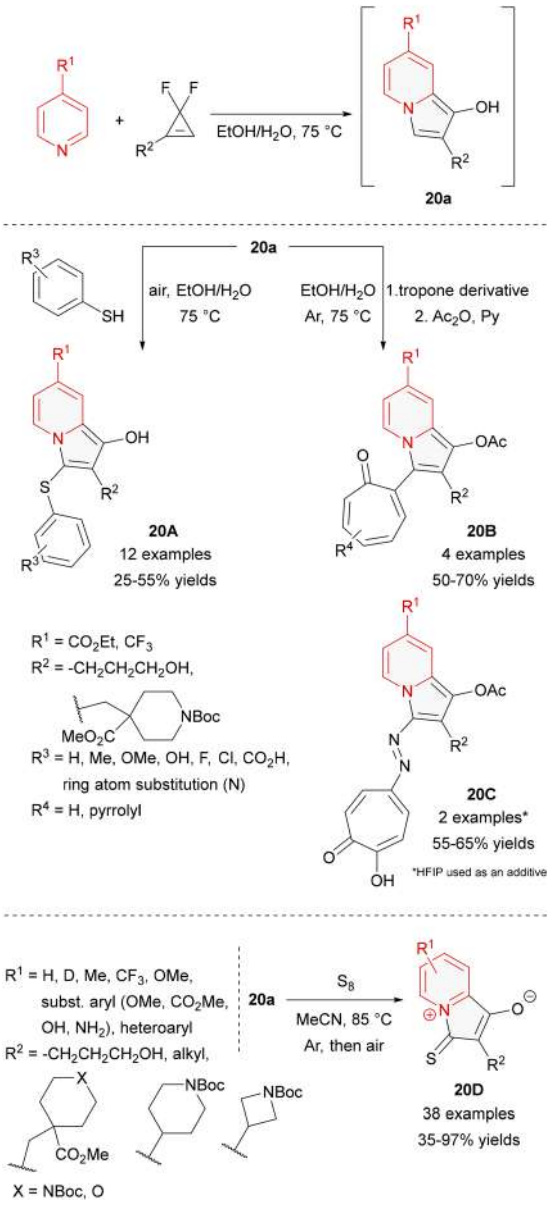

Scheme 20

2.3 From 2-carbonylpyridines

2-Formylpyridines are a convenient precursor to 1-aminoindolizines. Initially discovered by Liu and Yan,[121] the multicomponent reaction utilizing 2-formylpyridines, amines and alkynes was studied by many research groups under Cu-catalysis conditions,[122] using a recyclable Cu/ionic liquid system[123] and Cu-based MOFs.[124] It was later shown that Ag[125] and the Cu/Ce mixed system[126] could also efficiently catalyze this type of reaction. 1-Aminoindolizines proved to be good starting materials in the synthesis of pyridyl enaminones, which could later be transformed into pyridyl-substituted pyrroles.[127]

2-Acylpyridines can also be competent substrates in indolizine synthesis. Zhao *et al.* published a mild methodology for the preparation of 2-formyl and 2-acylated indolizines. 2-Ketopyridines combined with enones under acidic conditions to furnish indolizines in moderate yield. The mechanism of such a transformation is notably straightforward: the protonated enone undergoes conjugate addition with a pyridine-type nitrogen atom, cyclization occurs and after loss of a water molecule and a proton, indolizine is formed.[128]

In 2023 Zhang, Ackermann and co-workers,[129] following on from this earlier discovery,[128] presented an elegant way to obtain highly functionalized indolizine-2-carboaldehydes **21** – valuable synthetic targets used as versatile precursors for distinct indolizine derivatives (Scheme 21). 2-Acylpyridines and α,β-unsaturated aldehydes undergo mild one-pot [3 + 2] annulation under aminocatalytic conditions. The authors opted to use aminosugars derived from biomass, such as glucosamine.

Furthermore, chitosan was also shown to be an effective catalyst for such a transformation under aqueous conditions,

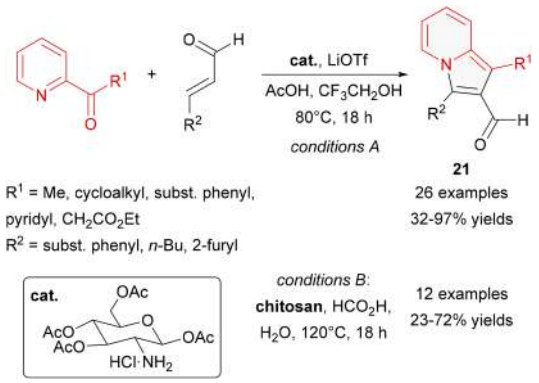

Scheme 21

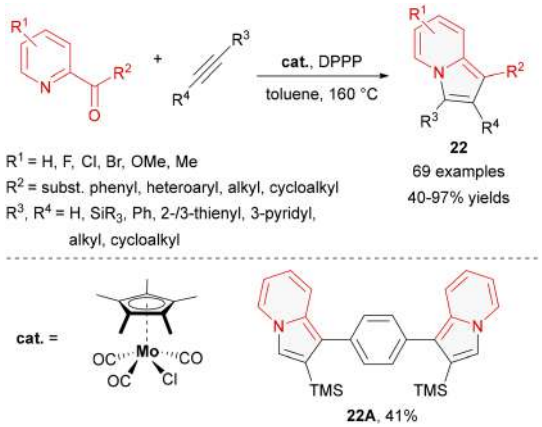

Scheme 22

enabling simple regeneration of the stereoauxilliary. The method tolerated various functional groups, yielding a broad range of 2-formylindolizines in good yields.

Recently, Zhuo's group presented a particularly interesting approach towards various heterocyclic skeletons containing nitrogen, oxygen and sulfur atoms including indolizines **22**.[130] 2-Acylpyridines were employed in a Mo-complex-catalyzed reaction with disubstituted alkynes (Scheme 22). The authors presented a broad scope for their methodology, including complex molecules of biological and medicinal relevance. Zhuo's method remains one of the most versatile ways to construct densely substituted indolizine cores, possessing trialkylsilyl groups, as well as heteroaryl moieties attached at various positions. It should be noted that the described synthesis of the molybdenum catalyst is straightforward and can be realized at the gram-scale in one synthetic step, from commercially available precursors. Combined with exceptional functional group tolerance and applicability to the synthesis of other heterocycles, this approach is particularly noteworthy.

2.4 From α-acidic picoline derivatives

In a complementary way to the pyridinium ylide [3 + 2] annulation approach, CH-acids derived from α-picoline derivatives can also participate in reactions with alkynes or alkenes. In contrast to the method mentioned previously, the mechanisms of these reactions are usually much more complex and often take advantage of the inherent acidity of the α-picolinic position. Still, such substrates are usually available commercially or synthetically, therefore presenting an alternative way to obtain indolizine heterocycles.

One such example was presented by Chen *et al.*, who opted to use 2-pyridylacetate and ynals to obtain 3-acylated indolizines (Scheme 23).[131] The reaction proceeded through Knoevenagel-type condensation and O_2-mediated nucleophilic 5-*exo-dig* ring closure to furnish the desired indolizines **23** in good yields. The radical mechanism was disproved by a control experiment with TEMPO. One can compare such an approach to most classic ylide/alkyne reactions to yield indolizines (*e.g.* indolizine **2**) – both methods are complementary to each other, giving access to indolizines substituted with EWGs at position C3.

Similarly, Wang's group utilized 2-bromoenals, which could be perceived as formal equivalents of ynals; however, in this approach, the mechanism proceeds through a slightly different route.[132]

Interestingly, Chen's group proved that when elemental sulfur (S_8) was present in the reaction mixture, it was possible to obtain indolizinethiones **24** of the same general architecture (Scheme 24).[133] It is also known that the same type of reactivity can be accessed by introducing molecular iodine to the reaction mixture. This approach led Chen's group to expand the scope of picolines, yielding indolizines derived from cyano-, amido- and keto-derivatives of picoline.[134] Mixed iodine–copper catalysis in indolizine synthesis was further explored by He *et al.*, who expanded the scope of this reactivity.[135] Various

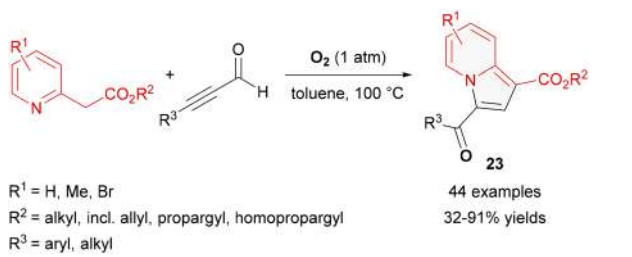

Scheme 23

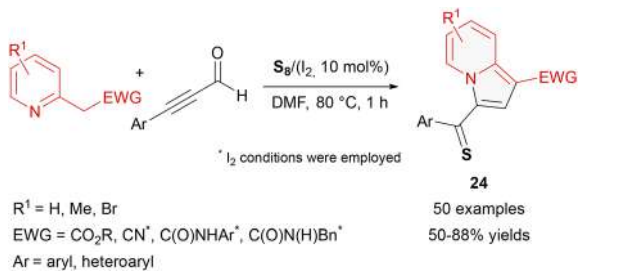

Scheme 24

mono- and di-substituted alkynes were tolerated, even though the conditions seemed more harsh. Furthermore, Yang *et al.* presented using pivalic acid as a catalyst combined with a suitable chalcogen derivative to yield products of interrupted cyclization by nucleophilic attack on the carbon atom directly linked to the C3 position of the indolizine, yielding various alkoxy and thioalkoxy derivatives.[136]

A modification of this approach was presented by Li *et al.*, who utilized a three-component reaction in the synthesis of aminoalkyl indolizines. The Knoevenagel adduct formed *in situ* in the presence of an amine and Zn-catalyst produced the desired 3-(aminoalkyl) derivative in good yields.[137]

In 2006 Bienaymé and co-workers published a new multicomponent reaction transforming 2-cyanomethylpyridine, aldehydes and isonitriles into 3-alkylaminoinolizines.[138] Hulme revealed that the replacement of isonitrile with CH_3COCN led directly to 3-aminoindolizines.[139] Atar's group also took advantage of the availability of 2-vinylpyridines, using them in [4 + 1]-cycloaddition with isonitriles to obtain 3-amino-substituted indolizines **25**.[140] The envisioned multicomponent reaction took place in an ionic liquid and was compatible with various aldehydes (Scheme 25). Indolizine synthesis in ionic liquids was recently explored by different groups, utilizing various known synthetic strategies.[59,123] On the amine side, the scope was somehow limited by the availability of isonitriles – one can compare this finding to the synthesis of indolizines **38**.

An interesting discovery was reported by Chen's group by employing Pd-catalysis with pyridine-based Knoevenagel-type adducts. The authors presented a method to obtain indolizines bearing the same aryl groups in the C2 and C3 positions (Scheme 26).[141] A tentative mechanism was proposed, starting with Pd insertion into the C(sp^2)–H bond. This intermediate then undergoes Heck-type coupling, yielding **26b**. Intermediate **26b** is then intercepted by molecular oxygen, delivering unusual species **26c**. Extrusion of the **26a** fragment leads to the indolizine skeleton, which upon loss of a proton gives rise to desired product **26**. It is worth noting that the presented method is highly tolerant of various functional groups. Most notably, carbon–halogen bonds are preserved under Pd-catalyzed conditions, providing a valuable handle for further functionalization.

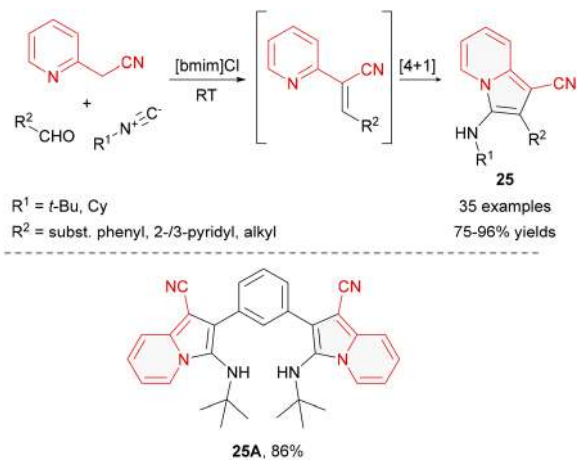

Scheme 25

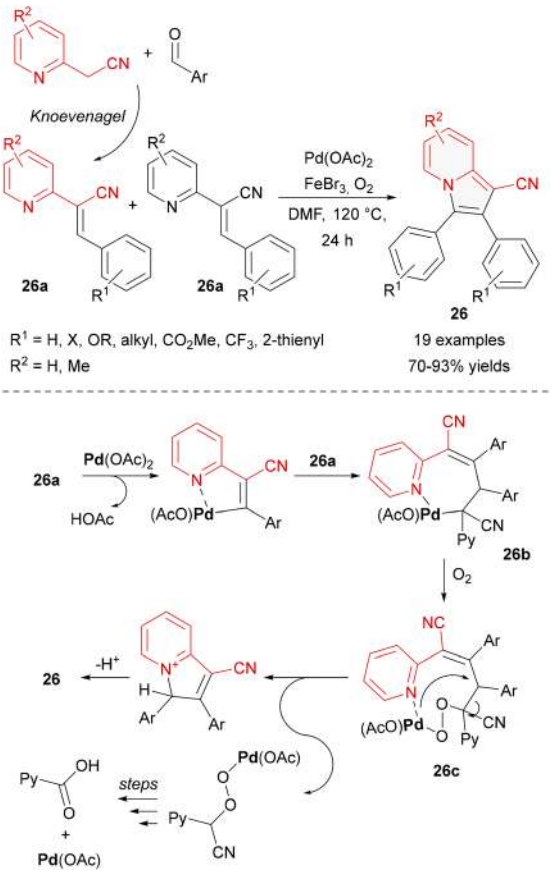

Scheme 26

Joshi and Kim also opted to use Knoevenagel-type condensation as the first step to form the C1–C2 bond of the indolizine skeleton (Scheme 27).[142] They then applied an original strategy to produce the desired heterocycle. The Knoevenagel adduct was cyclopropanated in the Corey–Chaykovsky reaction, and after brief optimization, DDQ was found to be a suitable promoter of the rearrangement to the desired indolizine **27**. A radical mechanism was proposed. This method tolerated various functional groups; the authors also showed DDQ-mediated dimerization pathways, through the C2, C5 and, notably, C7 positions of indolizine – such reactivity is rarely explored.

Similar Knoevenagel adducts are shown to be competent substrates in a highly divergent annulation protocol developed by Kim's group.[143] The reaction of such substrates with methyl nitroacetate can be tuned to furnish not only indolizines substituted with various aroyl groups, but also isoxazoles and 2-acylquinolizin-4-ones. Crucial parameters responsible for deciding the reactivity mode were found to be the choice of base (or lack of) and solvent.

Alkenes prove to be compatible with various methodologies for indolizine synthesis from α-acidic picoline derivatives. A

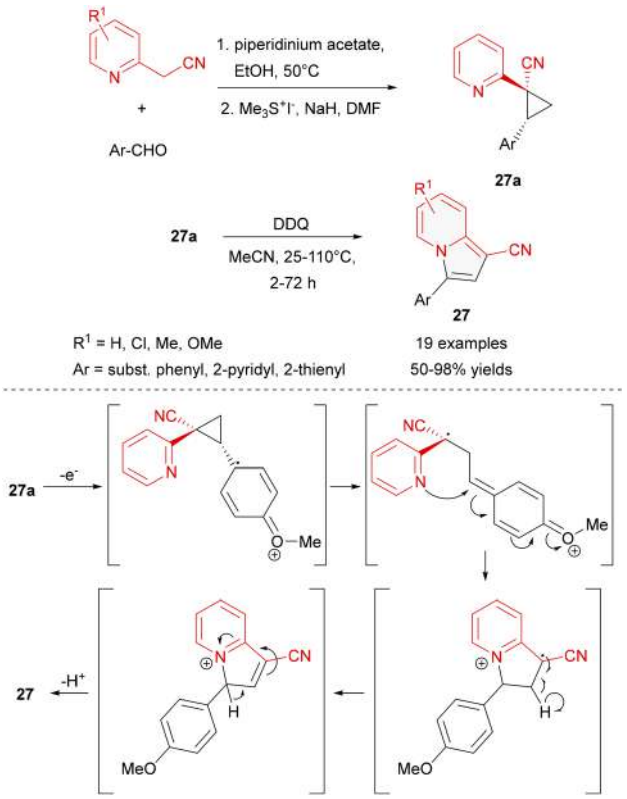

Scheme 27

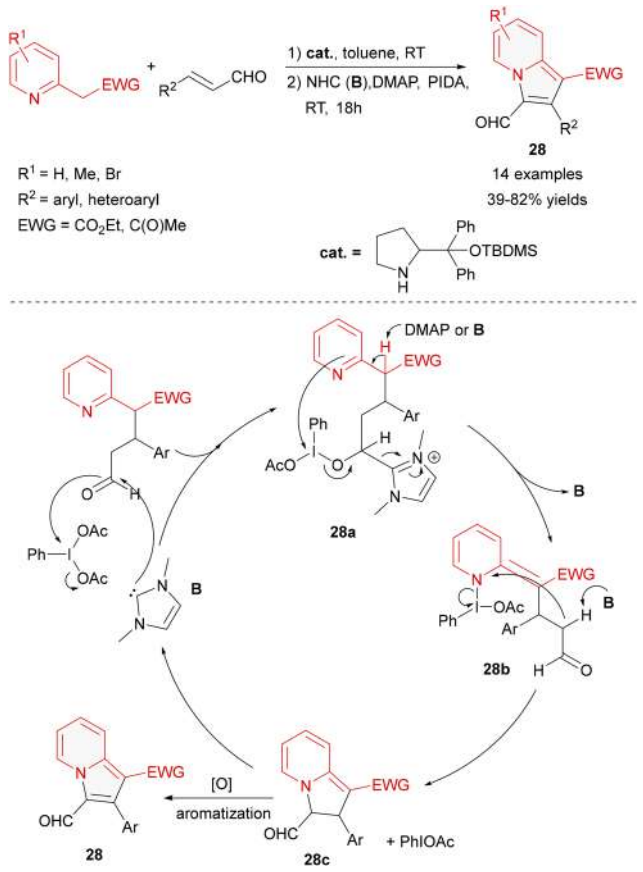

Scheme 28

group developed a regiodivergent protocol for the synthesis of indolizine substituted with EWGs at the C2 and C3 positions, utilizing I_2 mediation and acrylates.[144] Interestingly, the choice of base was a crucial parameter that determined the predominant regioisomer. Lu *et al.* opted to use *gem*-difluoroalkenes as efficient precursors to C2-free indolizines, expanding the utility of such fluoro derivatives in a complementary way to indolizine **6** synthesis.[145] Enaminals can also be used as efficient electrophilic partners, yielding indolizines of the same architecture – this mode of reactivity was recently presented by Li *et al.*[146]

Su *et al.* presented a use for sulfoxonium ylides in indolizine synthesis by the NIS-mediated radical pathway.[147] The sulfur atom was retained in the final structure, giving rise to C3-alkylthiolated indolizines. This mode of reactivity is somewhat unusual; in this case the reactive site is on the sulfur atom and DMSO is not extruded during the reaction.

A novel catalytic relay consisting of amine-induced Michael addition and NHC-promoted cyclization was reported by Wang's group (Scheme 28).[148] α,β-Unsaturated aldehydes were used alongside picolines bearing EWGs. After Michael adduct liberation, the N-heterocyclic carbene and PIDA participate in the formation of intermediate **28a**, blocking the Breslow intermediate. Pyridine then attacks the iodine atom, leading to species **28b**, which cyclizes to yield **28c**. The final aromatization delivers the desired indolizine. Notable is the possibility of using azaarenes to furnish more complex heterocycles, as well as non-standard electron-withdrawing groups such as the pyridyl moiety.

Similarly, Chen *et al.* utilized α-bromonitroalkenes as Michael acceptors.[149] Subsequent S_N2 substitution and aromatization with loss of HNO_2 yielded the desired indolizine. This approach should be compared with the synthesis of indolizines **5**, where Michael addition occurs from the nucleophilic atom of the ylide and the halogen substituent is preserved during heterocycle synthesis. Variance in the choice of pyridine starting material (acidic 2-picoline/pyridinium ylide) can greatly expand the utility of α-halonitroalkenes making them exceptionally versatile substrates in indolizine synthesis.

In the last years, Yang's group published their work on a simple Pd-catalyzed method for indolizine synthesis from activated picoline derivatives and propargyl carbonates (Scheme 29).[150] The Pd catalyst undergoes oxidative addition across the triple bond of propargyl carbonate, generating the (σ-allenyl)palladium(II) species with the release of CO_2. Upon nucleophilic attack of the pyridinium anion on the Pd species, intermediate **29a** is formed, which then isomerizes *via* proton transfer to form **29**. The catalytic cycle is closed by expulsion of indolizine and Pd(0) regeneration. Similar work was presented by the same group – the scope was also expanded to C2-alkylated indolizines using a slightly different catalytic system.[151] This approach enables the synthesis of 3-benzylated

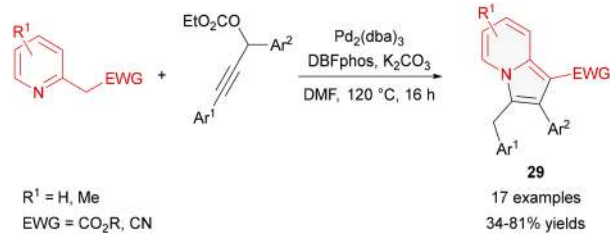

Scheme 29

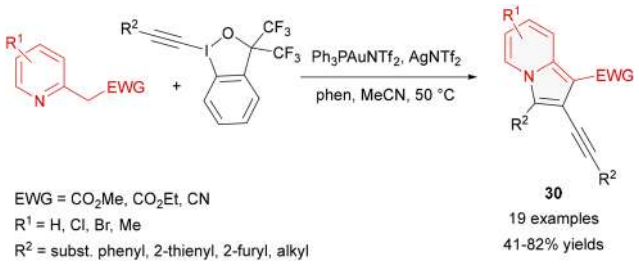

Scheme 30

indolizines, which cannot be obtained directly using a standard pyridinium ylide/alkyne approach, as they do not have an EWG-bearing carbon attached to the nitrogen atom. To date, the only other published methodology towards such indolizines relied on the use of chlorocarbenes and 2-vinylpyridines.[152]

Another original catalytic approach was recently presented by Han *et al.*[153] The authors utilized the dual Ag/Au catalyst to obtain indolizines **30**, which had an unusual architecture, carrying two aryl groups, one directly attached to C3 and one joined to the indolizine core through the C2-alkynyl linker (Scheme 30). This approach could be perceived as complementary to Sonogashira functionalization of bromoindolizines, as bromination does not occur at the C2 position. The mechanism proceeds through a complex sequence of organometallic transformations, with C–H alkynylation of the α-position and iminoaurative cyclization as the key steps. The scope of this approach could also be expanded to the synthesis of azaindolizines.

2.5 From 2-alkylpyridines *via* carbocyclization

Pyridines that possess an unsaturated bond in the 2-alkyl chain can participate in various carbocyclizations to yield indolizines. Usually, multiple bonds are separated from the pyridine ring by at least one sp^3 center or *exo*-sp^2 centre (making this approach different from fully conjugated Knoevenagel adducts presented before).

A notable group of substrates is 2-(hydroxyallyl)-pyridines. One particularly interesting approach was presented by Zeoly *et al.*[154] A one-pot sequential MBH reaction and BIA-catalyzed cyclization furnished tricyclic indolizines **31** (Scheme 31). Other groups have recently presented different systems,

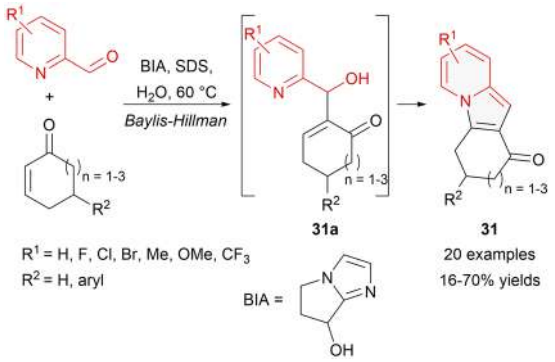

Scheme 31

usually needing isolation of the intermediate allylic alcohol.[155–157] Also, such allylic alcohols can be easily cyclized to target indolizines under simple acidic conditions – this approach was recently elaborated by Lv *et al.*[158]

Similarly, 2-propargylpyridines, which have a hydroxyl function in the α-position can be used in indolizine synthesis. The Pd-catalyzed synthesis of C2-aroylated indolizine was published by Li *et al.*[159] The catalytic cycle was triggered by the oxidative addition of aroyl chloride. This intermediate induces 5-*endo-dig* cyclization, giving rise to the indolizine skeleton. Later, it was proved that similar conditions could be used to obtain complex indolizine-containing bisheterocycles.[160] Also, Cu catalysts can be employed to perform modular indolizine synthesis with optional simultaneous Cadiot–Chodkiewicz-type 2-alkynylation[161] or 2-selanylation.[162]

Structurally similar, 2-(2-enynyl)-pyridines were also used as precursors to the indolizine scaffold. Especially prevalent are 5-*endo-dig* Ag(I)-catalyzed approaches. Selander's group developed conditions towards polycyclic indolizine **32A/B** synthesis using enamines (Scheme 32).[163] Interestingly enough, the structure of the product was decided by the way in which the

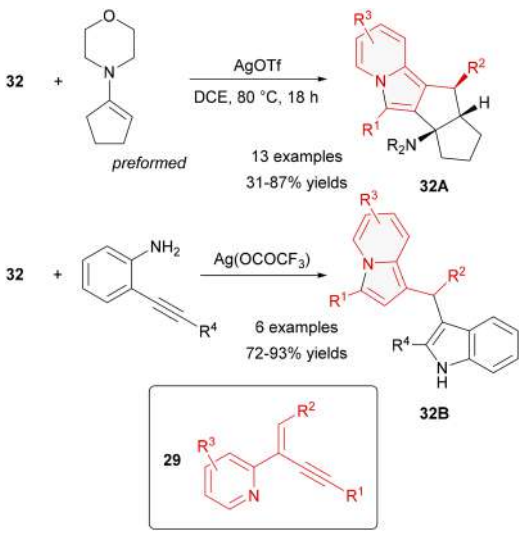

Scheme 32

enamine was formed – *in situ* or prepared beforehand. Anand's group opted to use *o*-alkynylanilines *en route* to complex triarylmethanes **32B** possessing an indolizine moiety,[164] while Lodhi *et al.* presented a novel C(sp^3)-activation method to obtain indolizine-substituted *N*-sulfonyl ketimines.[165] Li *et al.* recently used propargyl amines to yield highly unusual 1-(2*H*-pyrrol-3-yl)indolizines.[166]

2-Propargyloxypyridines can also be used in indolizine synthesis. Rossler *et al.* presented an Au(I)-catalyzed method for the synthesis of 1-aroylated indolizines **33**,[167] proceeding through a crucial allenamide **33a** (Scheme 33). Later, the scope of this methodology was expanded to acetoacetates and malonates.[168]

2-Homopropargylpyridines are valuable substrates in indolizine synthesis as well, especially those possessing a carbonyl function attached to the α-position. Xiao presented a simple base-catalyzed method for obtaining C1,C3-substituted indolizines from such compounds.[169] Concurrently, he proved that iodine could also be a competent catalyst in the aminooxygenative approach, giving rise to C3-acylated indolizines and imidazo[1,2-*a*]pyridines.[170] Recently, Gabriele's group developed a catalytic system to access 2-(indolizin-3-yl)acetamides from 2-homopropargylpyridines *via* a carbonylative pathway.[171] Jørgensen's group presented an indium-based catalytic system that enabled cyclization of 2-homopropargylpyridines using an exceptionally low catalytic loading.[172]

Furthermore, 2-propargylpyridines having only carbon (or silicon) functionalities in the sp^3-hybridized picolinic position (as opposed to indolizine **31** or **32** synthesis) can be cyclized under electrocatalytic conditions. Yang *et al.* presented a mild system for such a transformation (Scheme 34).[173] This approach yielded C1,C3-di-EWG-substituted indolizines **34A**, providing yet another possibility to access the classic substitution pattern in the indolizine core, as exemplified by indolizine **2**. Using terminal alkynes enabled the synthesis of 3-formylindolizes (and their aza-analogues), in a complementary way to Ackermann's synthesis of 2-formylindolizines **21**.

The reactive triple bond can be located further from the pyridine ring. Zhao *et al.* showed that 2-(pyridin-2-yl)-acetic acid propargyl esters could be cyclized under silver catalysis conditions, producing tricyclic indolizines **35** (Scheme 35).[174]

Schulzke's group obtained a series of highly unusual heterocycles – pentathiepines containing an indolizine moiety (**36**).[175] The authors chose 2-alkynylpyridines, which upon treatment with a molybdenum derived catalyst and molecular sulfur yielded a new class of indolizine derivatives (Scheme 36). Aza-analogues of such compounds possess attractive biological properties and have been prepared analogously.[176] Recently, the same group provided some insights into mechanistic aspects of such a transformation, discussing in depth the role of ethoxy substituents at the end of the unsaturated system.[177]

Rao *et al.* utilized a complex spiro-cyclopropyl propargyl pyridine derivative to obtain a new class of oxazepine-fused indolizines **37** under gold catalysis conditions (Scheme 37).[178] The

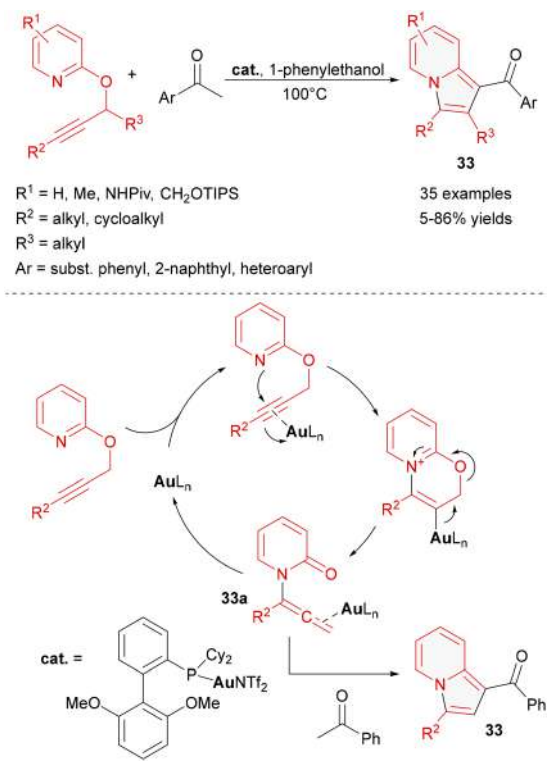

Scheme 33

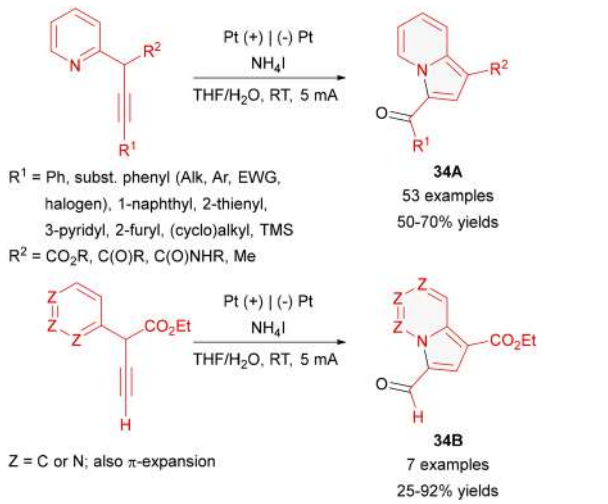

Scheme 34

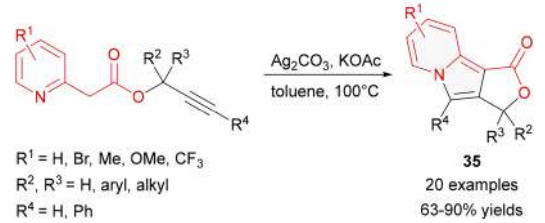

Scheme 35

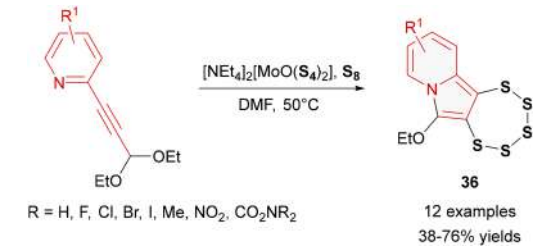

Scheme 36

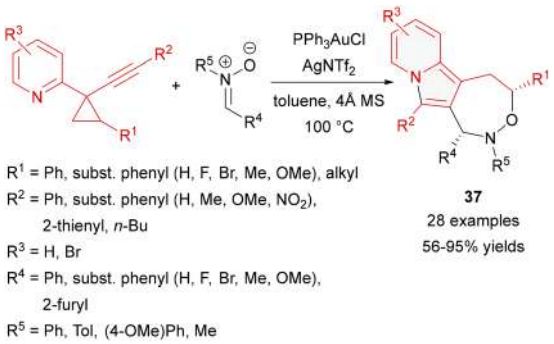

Scheme 37

partially cyclized heterocycle is intercepted by a nitrone and after nucleophilic attack of the gold metal–organic species on the nitrone electrophilic centre the target indolizine is formed. This methodology is an elaboration of a previously known approach, where the authors utilized simpler nucleophiles such as amines, malonates or indoles to trap the reactive cyclopropyl intermediate.[179]

In some cases, the pyridine nitrogen atom can be used as a nucleophilic handle to set off the cascade reaction with an appropriate substrate, which will then cyclize by reacting with an unsaturated bond in the 2-alkyl chain. One such approach was described by Hoye's group.[180] The authors utilized 2-alkynylpyridines and electrophilic allenes to obtain indolizines *via* a cascade of the Baylis–Hilman-type reaction, nucleophilic carbene formation and spontaneous transformation to the indolizine. The same group expanded this strategy to alkynes bearing electron-withdrawing groups to obtain 1-(1-acetoxy-2,2-methylvinyl)indolizines *via* a free carbene intermediate, which after acetoxy group migration yielded the target substituted heterocycle.[181] This novel strategy was also used to obtain other fused azaheterocycles using various 2-alkynyl "iminoheterocycles" such as pyridazine or benzoxazole. Later, Hoye's group showed that the crucial carbene intermediate could be intramolecularly trapped by a double bond located further from the reaction centre.[182] Using such an approach it was possible to obtain cyclopropanated products of intramolecular cyclization, possessing heteroatoms (oxygen, silicon, nitrogen) in the ring connected to the C1 position of indolizine. This highly tolerant protocol was later applied to obtain different fused systems, furthermore the authors presented methods for the post-synthetic functionalization of the target molecule, yielding indolizines with an original architecture and high level of complexity.

Needless to say, from a practical point of view, methods that use simple commercially available compounds as substrates have an intrinsic advantage over all competing methodologies. In this regard, indolizine core syntheses that start from pyridines bearing a simple substituent at position 2 are highly appreciated, especially if a second, typically aliphatic, building block is available as well. Other key factors include the number of commercially available derivatives, the ease of synthesis of non-commercial derivatives and the compatibility of a given reaction with various functional groups. Undoubtedly, one more factor to consider is the 'survival' of highly reactive functional groups under the reaction conditions. The combination of all these arguments points to the following: 1) balancing the limited availability of 2-acylpyridines with easy access to 2-formylindolizines, which were previously almost unknown, the method introduced by Zhao and optimized by Zhang and Ackermann is a 'game-changer';[128,129] 2) for these reasons, a methodology for transforming α,β-unsaturated aldehydes into 3-formylindolizines will also be very useful;[148] and 3) a method giving access to 1,2,3-tri-substituted indolizines from bromopyridines (hundreds of them are commercially available) is worthy of attention.[113]

2.6 From pyridotriazoles

From seminal works by Gevorgyan,[183–185] pyridotriazoles are recognized as niche, but powerful, starting materials in the synthesis of indolizines. These compounds possess interesting 1,3-dipole-like reactivity and can be perceived as formal equivalents of α-diazopyridines (as they exist as a mixture of tautomers).

Wang *et al.* used [3 + 2] annulation of pyridotriazoles to yield indolizines **38**.[186] The reaction mechanism proceeds through the formation of a copper carbenoid species, which then is intercepted by an enamine. The resulting intermediate immediately collapses to an aminocyclopropyl derivative, which rearranges to a five-membered ring. The final aromatization gives rise to the desired indolizine (Scheme 38). Noteworthy to point out is the exceptionally broad scope that tolerates a multitude of chemically different functional groups. Structurally, indolizines **38** close an existing gap in the literature – as stated before, the C3-position of indolizine is usually substituted with an electron-withdrawing group, most often used as a means to activate the pyridine substrate (as in the case of the ylide/alkyne approach *e.g.* **2**). Here, the authors present a way to obtain indolizines substituted at position C3 with highly electron donating groups. Structurally similar EDG-substituted indolizines were presented before (**25**); however, in this case, the scope of amines was much broader. This fact alone can justify using more complex starting materials such as pyridotriazole.

Recently, Hou *et al.* proved that using an elaborate trimetallic rhodium-based catalytic system could enable pyridotriazoles to be reactive towards enamides to yield C2-unsubsti-

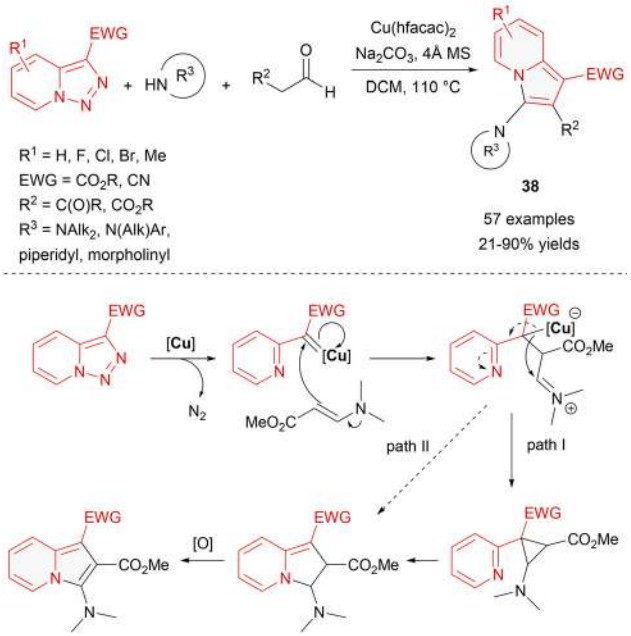

Scheme 38

tuted indolizines.[187] The architecture of the obtained product resembled indolizines **4** and **27** – both obtained under metal-free conditions, which raised the question of the applicability of the authors' approach. It must be noted, however, that such a Rh-catalyzed approach was tuned to yield not only indolizines, but also quinolizones, diversifying the possible pool of products and thus explaining the use of such a complex methodology.

Lee's group developed a Rh–Pd–Mn sequential trimetallic catalytic system to couple pyridotriazoles with 1,3-dienes.[188] The reaction proceeded through [2 + 1]-cyclopropanation, Pd-catalyzed ring expansion and Mn-mediated oxidation to target indolizines possessing vinyl substituents at the C3 position. Adam *et al.* showed that it was possible to obtain indolizines from pyridotriazole and ethyl propiolate using a simple Cu catalyst, although the conditions utilized by the authors were somewhat forceful.[189]

Furthermore, it is known that pyridotriazoles can be formed *in situ* directly from the corresponding 2-formylpyridine derivatives by using tosylhydrazine. Then, they can undergo reactions with alkynes promoted by a Co complex with TPP.[190] This protocol greatly expanded the utility of prior work on the topic by Gevorgyan and tied together the whole branch of synthetic methods by introducing modularity in terms of starting material choice.

2.7 Miscellaneous methods

A similar pattern of substitution to that of indolizines **38** can also be accessed in other ways. Anand's group utilized enamines and unusual 2-pyridinyl-substituted *p*-quinone methides. Instead of the copper carbenoid (as it was for **38**), the enamine attacked the electrophilic centre of the pyridine substrate, which after cyclization and oxidation yielded the desired heterocycle.[191] Unfortunately, the mechanistically crucial *p*-quinone component is retained in the final structure and cannot be easily removed to access reactivity at the C1 position.

On the other hand, the enaminyl component can also be located on the pyridine substrate. Zhang *et al.* presented a method to obtain indolizines bearing sulfanyl or selanyl substituents at the C1 position.[192] The authors opted to use pyridyl enaminones, which upon Tf_2O-induced activation reacted smoothly with thiols to yield the desired heterocycles. Mechanistically this approach falls under both previously discussed categories – pyridine bearing a 2-carbonyl group and an unsaturated bond further along the chain attached to position C2 of the substrate.

In the past years, several groups explored the reactivity of 1,4-zwitterionic thiolates in the synthesis of indolizine. Such uncommon starting materials were utilized in a few different approaches, mostly in reactions with diazo compounds. Most standard protocols consist of Cu-catalyzed thiazine derivative formation and subsequent rearrangement to the indolizine skeleton.[193,194] It is also possible to conduct such syntheses under microwave irradiation conditions.[195] Alternatively, Cheng *et al.* showed that *in situ*-formed sulfenes (from alkanesulfonyl chlorides) were also competent partners in such indolizine synthesis.[196] This approach could be further tuned to obtain complex sulfur-based heterocycles. Cheng *et al.* discovered that it was possible to use even simple alkynes under basic conditions in reactions with 1,4-thiolates.[197] Still, the pathway through which this transformation proceeds is not clear. Further simplification of this methodology was described by the same group – it is possible to utilize α-functionalized bromoalkanes such as bromoacetophenones or bromoacetates.[190] By using these substrates, it is possible to obtain the crucial thiazine intermediate, similar to previously mentioned approaches, which rearranges to the target indolizine, most probably with the formation of a thiirane intermediate *en route* to the desired heterocycle. Another non-classical methodology relying on [(5 + 1) − 1] cyclization of nitroepoxides to pyridinium 1,4-zwitterionic thiolates was developed by Al-Harrasi and co-workers.[198]

Despite its potential and high modularity, the use of 1,4-zwitterionic thiolates is yet to attract wider attention in indolizine synthesis.

The combination of the Ortoleva–King-type approach (towards pyridinium salt synthesis) and the reactivity of α-acidic picoline derivatives was applied by Zhao *et al.*[199] C2-alkylated indolizines **39** with sulfur functionality in the C3 position were constructed from 2-pyridylacetates, aliphatic methyl ketones and *p*-toluenesulfonyl hydrazide (Scheme 39). These products are highly desired because they are crucial scaffolds that possess attractive biological properties. Two alternative routes were proposed, both involving intermediate **39b**, *via* Ortoleva–King-type methyl ketone α-iodination and cyclization. A minor pathway through Kornblum oxidation was also proposed. This approach can be directly compared to

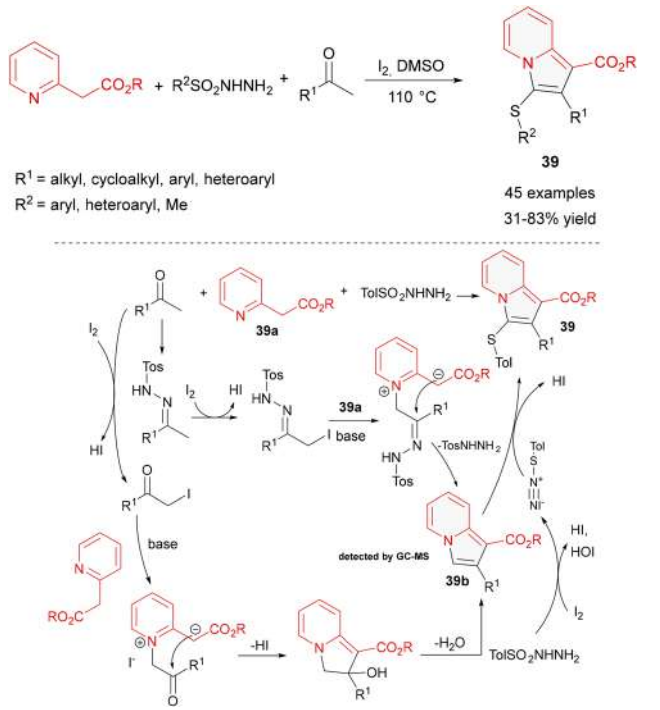

Scheme 39

Nechaev's synthesis of indolizine thioether derivatives **20A**, where the conditions utilized are much more benign, at the cost of starting materials' level of complexity.

A similar approach, I_2-catalyzed Ortoleva–King reactivity, was presented by Wu *et al.*[200] The authors presented a concise way of obtaining C3-pyridyl indolizines from acetophenones and 2-(pyridin-2-yl)acetates. Contrary to indolizine **39** formation, this reaction did not proceed through pyridinium salt formation from iodoacetophenone. The iodo derivative was transformed into phenylglyoxal and the cascade of Knoevenagel condensation, conjugate addition and I_2-mediated cyclization–oxidation led to the desired indolizine.

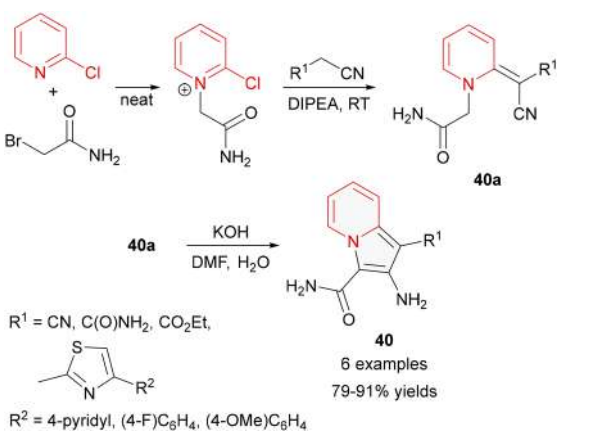

Scheme 40

A particularly simple and effective way of obtaining 2-aminoindolizines **40** was recently published by Kashner *et al.*[201] The authors used 2-chloropyridine to obtain the corresponding pyridinium salt, which underwent nucleophilic aromatic substitution with active acetonitrile derivatives and base-induced ring closure with the formation of the target heterocycle possessing a free amino group at position C2 (Scheme 40). C1-amino derivatives of indolizine are usually synthesized from 2-formylpyridine (section 2.3), thus this method provides a complementary way to access these valuable building blocks.

3. Methods based on pyrrole derivatives

Among the various strategies developed for constructing indolizine frameworks, methods based on pyrrole derivatives have gained particular importance and have become increasingly relevant in recent years compared to traditional pyridine-based approaches. Although conceptually complementary to the latter, pyrrole-based methods face significant challenges due to the higher cost, lower availability, and reduced stability of the pyrrole building blocks. Despite these limitations, the unique reactivity and potential of pyrrole derivatives provide promising opportunities for indolizine synthesis, making them a valuable resource for further exploration.

3.1 From N–H free pyrroles

In 2017, Zhang *et al.* described a base-catalyzed cascade mechanism for the synthesis of 7-cyanoindolizine derivatives, important building blocks in the further synthesis of biologically active compounds.[202] Compound **41** can be obtained by a one-pot tandem reaction of 4,5-disubstituted pyrrole-2-carbaldehydes and 4-bromobut-2-enenitrile in the presence of K_2CO_3 in dry DMF at 70 °C for 6–10 h. The proposed mechanism is *N*-alkylation followed by deprotonation and cyclization, which generates a precursor that, after the removal of water, gives the desired product (Scheme 41).

Similarly, Duan *et al.* proposed a method to obtain the first 6-hydroxy indolizines **42** through a cascade reaction of pyrrole-2-carbaldehyde and 4-halogenated acetoacetic ester in the presence of K_2CO_3 in CH_3CN (Scheme 42).[203]

Both methodologies employ simple base-mediated cascade reactions in aprotic solvents, resulting in polysubstituted indo-

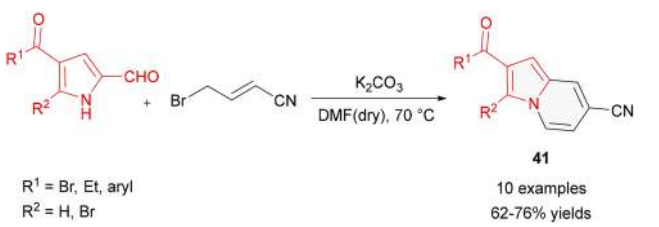

Scheme 41

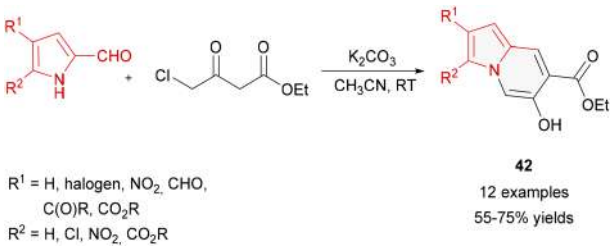

Scheme 42

lizines with various functional groups such as NO_2, Br, and esters. These derivatives offer significant potential for various applications, including the development of fluorescent probes.[204,205]

3.2 From *N*-substituted pyrroles

3.2.1 Base-promoted cyclization and aromatization. Efficient methods were developed for obtaining indolizines with useful substituents such as formyl, cyano, and nitro in position C7, allowing further molecular manipulation.

Zhong and coworkers, in 2017, designed and synthesized 7-nitroindolizines **43** from 1-acetylaryl-2-formylpyrroles and 2-nitrovinylbenzene in the presence of K_2CO_3 (Scheme 43).[206]

A few years later, Gong *et al.* developed a related approach to synthesize 7-formylindolizines **44**. This was achieved *via* an oxidative [4 + 2] annulation between 1-acetylaryl-2-formylpyrroles and enals in the presence of DBU (1,8-diazabicyclo[5.4.0]undec-7-ene) as a base and LiCl as a weak Lewis acid. LiCl is responsible for activating the enal and stabilizing the enolate intermediate during the reaction (Scheme 44).[207] A similar methodology was also proposed by Zhang.[208]

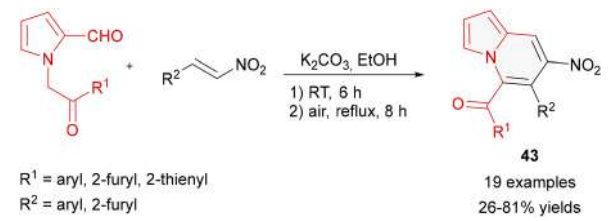

Scheme 43

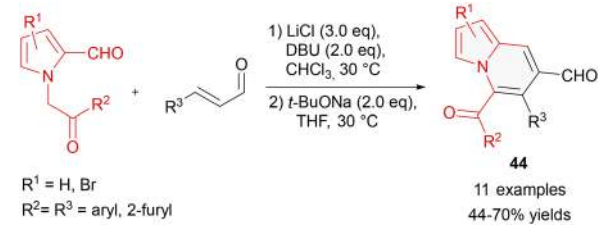

Scheme 44

A complementary approach was proposed by Dorai and Chandrashekharappa to obtain indolizines **45** with a hydroxy group at position C6 and an ester or aldehyde group at position C7, similarly to **42**; both are key groups for post functionalization (Scheme 45). This method operates in the presence of piperidine and under solvent-free conditions.[209]

An alternative strategy proposed by Escalante *et al.* involved the reaction of 2-formyl-*N*-propargylpyrrole, activated methylene compounds, and DBU as a base to produce indolizines **46** with NO_2, CN or CO_2Et at the 7-position, depending on the nucleophile used (Scheme 46).[210] Investigations into the mechanism of this reaction revealed the formation of a 6-*exo-dig* product instead of a more classic Knoevenagel condensation product.

Another approach towards 7-substituted indolizines was described by Kim and his group in 2021 (Scheme 47).[211] They reacted β-ketonitrile and 1-acetylaryl 2-formylpyrroles under basic conditions to afford 5-acylindolizine-7-carbonitrile **47** in good yields and in a stereoselective fashion, *via* a domino Knoevenagel condensation–intramolecular aldol process.

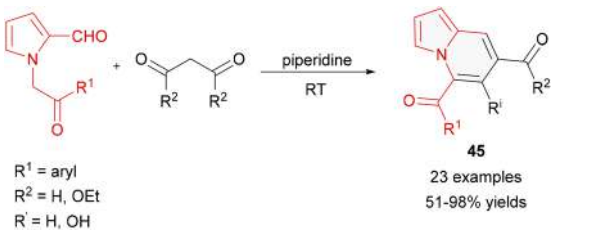

Scheme 45

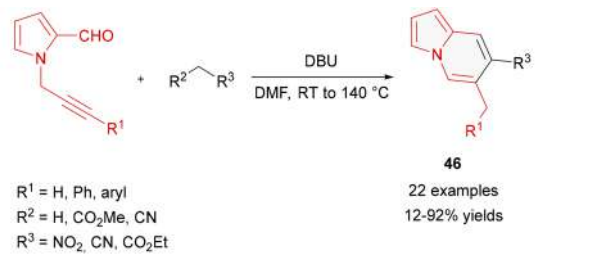

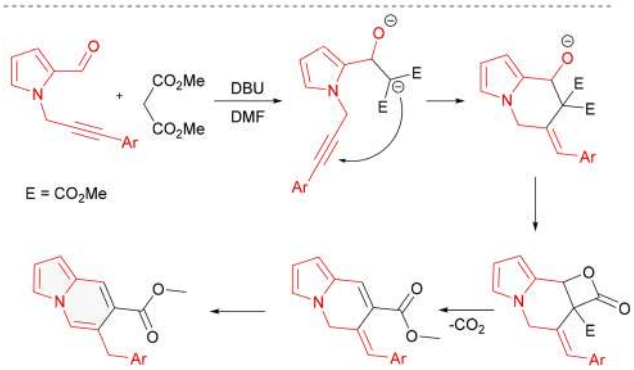

Scheme 46

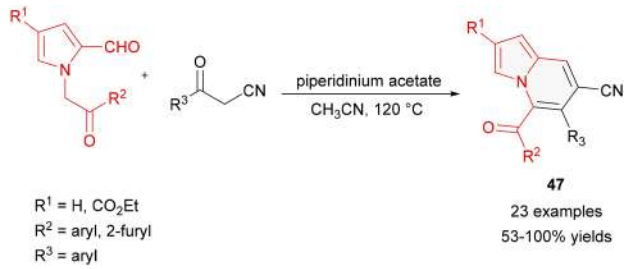

Scheme 47

Each of the presented approaches relies on base-promoted cascade reactions involving 2-formylpyrrole derivatives and electrophilic alkenes or alkynes and is concluded by an oxidative aromatization step to yield the final indolizine product. The key differences are in the different substituents that can be included and the absence of solvent for the Dorai method, which makes it more sustainable than traditional methods.

A few years later, Kim *et al.* presented a base-promoted Michael-aldol double elimination cascade procedure that allowed access to indolizines **48**. This synthesis occurred between a chromone acting as a two-carbon unit for [4 + 2] annulation and a 2-formyl *N*-substituted pyrrole as a four-carbon source (Scheme 48).[212] Using the same methodology, the authors further developed a series of poly-functionalized indolizines and evaluated their anticancer activity.[213]

A viable and complementary method for the synthesis of polysubstituted indolizines, on the pyridine side, such as **49** and **50** employs 1-acetylaryl-2-formylpyrroles *via* Michael cyclization with an electron-deficient acetylene in a water/acetonitrile mixture (Schemes 49 and 50). Wang *et al.* exploited this

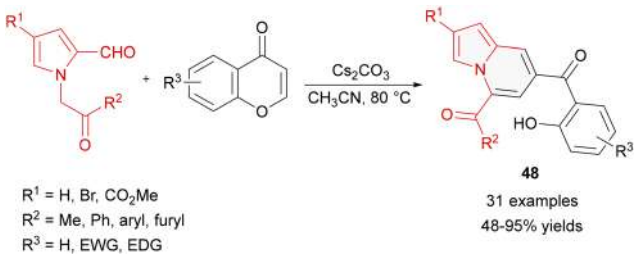

Scheme 48

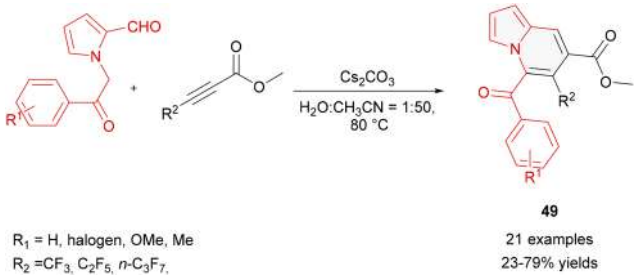

Scheme 49

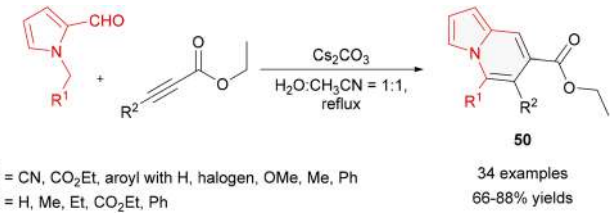

Scheme 50

methodology for the synthesis of perfluoroalkylated indolizines **49**, a valuable functionality in pharmaceutical chemistry.[214] Similarly, Lakshmikanth *et al.* used the same method and proved a broader scope, successfully expanding it to ethyl 2-(2 formyl-1*H*-pyrrol-1-yl) acetate and 2-(2 formyl-1*H*-pyrrol-1-yl) acetonitrile, providing indolizines **50** with diverse functionalities in the 5-position.[215]

As part of ongoing efforts to develop more efficient methodologies for the synthesis of multi-substituted indolizines, Peng *et al.* recently proposed a base promoted oxidative [4 + 2] annulation of pyrrole-2-carbaldehyde derivatives with *o*-HPPAs (*o*-hydroxyphenyl propargylamines).[216] The reaction proceeds *via* 1,6-addition followed by intramolecular cyclization and produced 5,6,7-trisubstituted indolizines **51** in good to excellent yields using DBN as a base (Scheme 51). Compared to previous methods, this provides the same aromatic ketone at C7 as **48** while introducing an additional aromatic system at C6, which is the position that differentiates all the methodologies proposed here.

To date, the discussion has focused on the base-promoted synthesis of substituted indolizines, and in most cases, EWGs and EDGs on pyrroles and electrophilic partners do not affect the reactivity, resulting in a wide scope of products.

Before moving on to more complex methodologies, we present one final example. In 2022, Zhang's group reported the synthesis of rare indolizines **52** that featured a thioether group at C7. This was achieved through [4 + 2] annulation of *N*-substituted pyrrole-2-carboxaldehydes with prop-2-ynylsulfonium salts (Scheme 52).[217] It is worth noting that the propargyl sulfonium salt used in this reaction can be readily prepared by reacting propargyl bromide with dimethylsulfide.

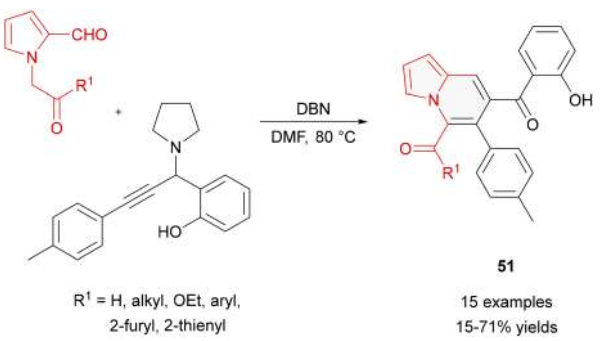

Scheme 51

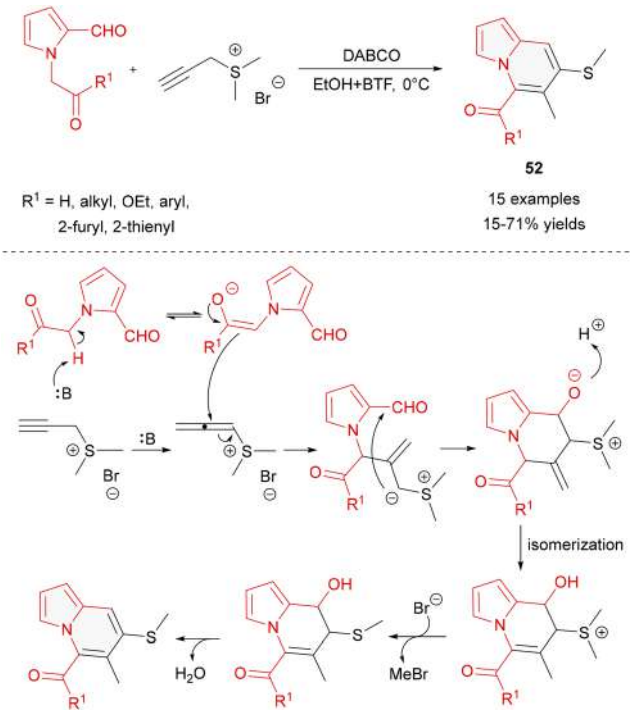

Scheme 52

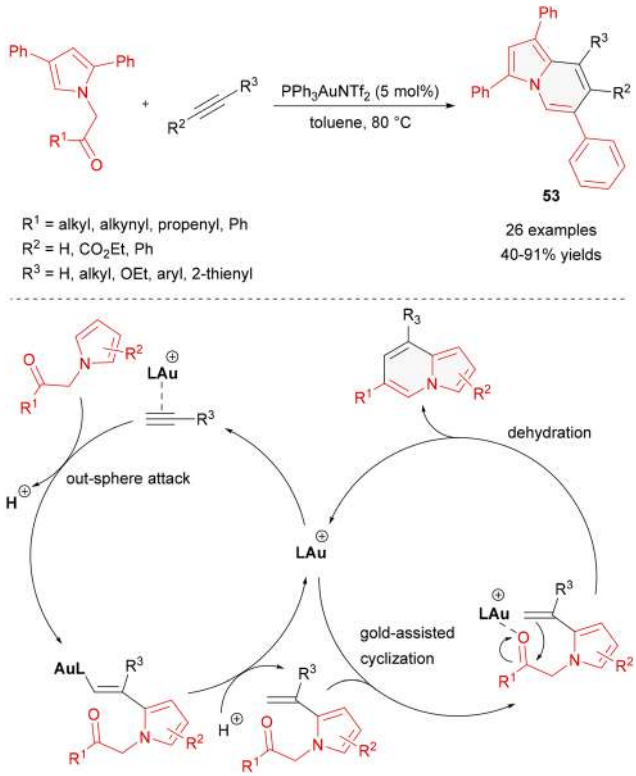

Scheme 53

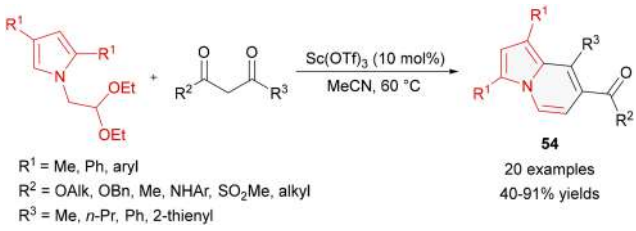

Scheme 54

3.2.2 Transition-metal-catalyzed cyclization and aromatization. An effective and widely adopted alternative to traditional base-promoted methods is the use of transition-metal-catalyzed reactions, which have demonstrated high efficiency in the synthesis of indolizines from both pyridines and *N*-substituted pyrroles.

Notably, Liu's group in 2016 and Gu's group in 2019 developed examples using this type of methodology (Scheme 53). In Liu's work, α-(*N*-pyrrolyl)ketones were reacted with alkynes in a gold-catalyzed intermolecular hydroarylation–cycloaromatization cascade to form indolizines **53**.[218] This type of reactivity is inherently challenging due to the high reactivity of unsubstituted pyrroles, a problem addressed by the authors with the use of a sterically hindered reagent to stabilize the reaction.

The second example involves a [4 + 2] annulation reaction reported by Gu and coworkers in 2019.[219] In this method, 1-(2,2-diethoxyethyl)-2,4-diphenyl-pyrrole was reacted with methyl acetoacetate in the presence of scandium triflate as a catalyst.

This reaction not only provided indolizine products **54** but also demonstrated the versatility of the method by allowing the use of other enolizable ketones or aldehydes, such as acetylacetone, β-ketoamides, and methylsulfonylacetone (Scheme 54). This broader scope allowed the synthesis of additional heterocycles, including indoles, naphthalenes, carbazoles, and pyrido[1,2-*a*]indoles. Such examples illustrate the effectiveness of transition metal catalysis in overcoming the limitations associated with traditional methods and expanding the range of indolizine derivatives that can be synthesized.

3.2.3 Miscellaneous methods. Intramolecular or intermolecular annulations of *N*-substituted pyrroles are also a valid approach towards substituted indolizines.

Kuzu *et al.* developed the synthesis of polysubstituted indolizine derivatives by intermolecular, base-catalyzed, *N*-allene–pyrrole dimerization of the corresponding *N*-pyrrole–alkyne derivatives (Scheme 55).[220] The reaction proceeds through a radical path in which allene dimerization occurs followed by cyclization and two H-shifts and yielded 8-pyrrolo-substituted indolizine **55** in low to excellent efficiency.

Shao *et al.* performed annulations of *N*-substituted pyrrole-2-carbaldehydes and pyrrole-2-carbonitriles that resulted in two different products, despite similar potential nucleophilic and electrophilic sites.[221] Aldol cyclization was the key intermediate in the synthesis of **56A**, while derivatives **56B** (not the focus of this review) were obtained by Mumm rearrangement (Scheme 56). The results demonstrated that substrates with electron-donating groups on the benzene ring yielded products in lower yield than those with electron-withdrawing groups. On the other hand, electron-rich five-membered rings at R^2 such as furanyl and thiophe-

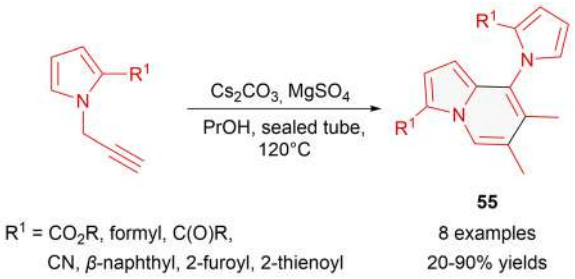

Scheme 55

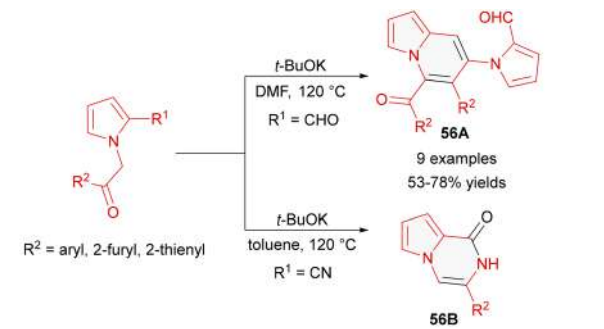

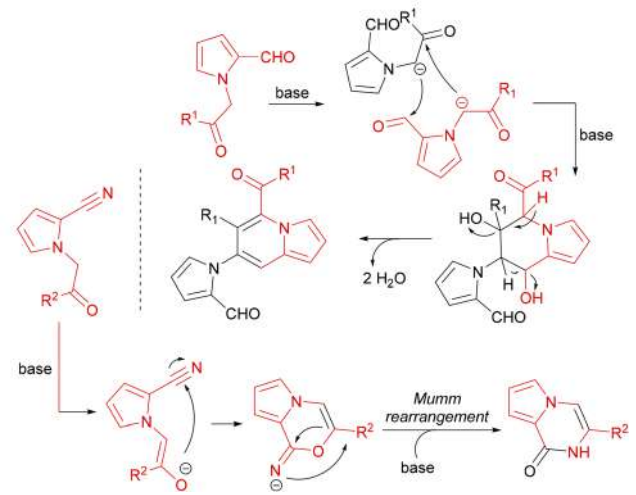

Scheme 56

nyl gave the most efficient transformations. When comparing the two approaches, Kuzu's method demonstrates greater flexibility and a broader functionalization scope, particularly in tolerating different substituents at the C2 position of the pyrrole ring. Additionally, it facilitates the introduction of a pyrrole substituent at C8. On the other hand, Shao's method is more restricted, as it is limited to pyrroles with a formyl group at C2 and leads to C7 pyrrole substituted indolizines. However, Shao's approach provides a greater variety of substituents at the other two positions of the pyridine ring (C5 and C6) where Kuzu's products typically display methyl groups and hydrogen; this limits the diversity of functional groups in the final indolizine products.

Miranda-Sánchez *et al.* presented the synthesis of indolizines and pyrrolo[1,2-*a*]pyrazines from alkyl (*E*)-3-(1*H*-pyrrol-2-yl)acrylates (Scheme 57).[222] In the first case, the reagent was treated with a Lewis acid to obtain **57A**, while in the latter, **57B** (not the main topic of this review) was obtained by cyclization of enaminones in the presence of ammonium acetate as a N source and Li_2CO_3 as a base. Both structures were evaluated by the authors for their antifungal activity, demonstrating a stronger effect compared to reference drugs. This further highlights the potential of these indolizine derivatives as important bioactive molecules.

The final example of indolizines derived from pyrrole derivatives was developed by Liu's group, featuring a gold-catalyzed intramolecular hydroarylation–aromatization of pyrrole–ynes (Scheme 58).[223] Such a method enables the efficient synthesis of indolizines **58**, in good to excellent yields. It also demonstrates compatibility with various functional groups on the aryl ring. The mechanism involves the classic activation of the propargylic alcohol *via* coordination of the gold catalyst, followed by regioselective intramolecular hydroarylation of the alkyne by the pyrrole moiety to form a vinylgold intermediate. The final steps are protodeauration and water elimination. Compared with the previous intramolecular and intermolecular methods, Liu *et al.* were able to obtain indolizines with different substituents on the pyrrole side as well as a free C7 position.

Although the method developed by the Derksen group formally employed pyrazole as a substrate, we chose to include it here because pyrazole acted as a surrogate for pyrrole. In their

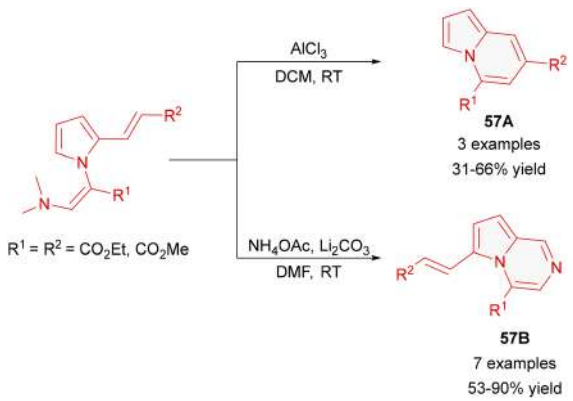

Scheme 57

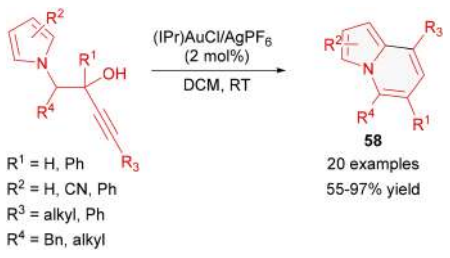

Scheme 58

work, the authors introduced a mild, transition metal-free method for synthesizing indolizines **59** from pyrazolium ylides and two equivalents of electron-deficient alkynes *via* an *N*-deletion mechanism (Scheme 59). Additionally, they proposed the reaction of pyrazolium ylides with isocyanates to yield 1,2-dihydropyrimidines (not discussed here) through a rearrangement process. Both methods offer efficient access to valuable heteroarenes under mild conditions, avoiding the use of transition metals, high temperatures, or strong bases, highlighting the versatility of pyrazolium ylides and their relevance in heterocyclic synthesis.

The fundamental advantage of the intense development of indolizine synthesis from pyrrole derivatives is straightforward access to an indolizine core lacking substituents at positions 1, 2 and 3. The latter compounds are essentially inaccessible when one starts from pyridine chiefly because the second aliphatic reagent to be reactive has to possess various functional groups, which are subsequently present in the structure of the final product.

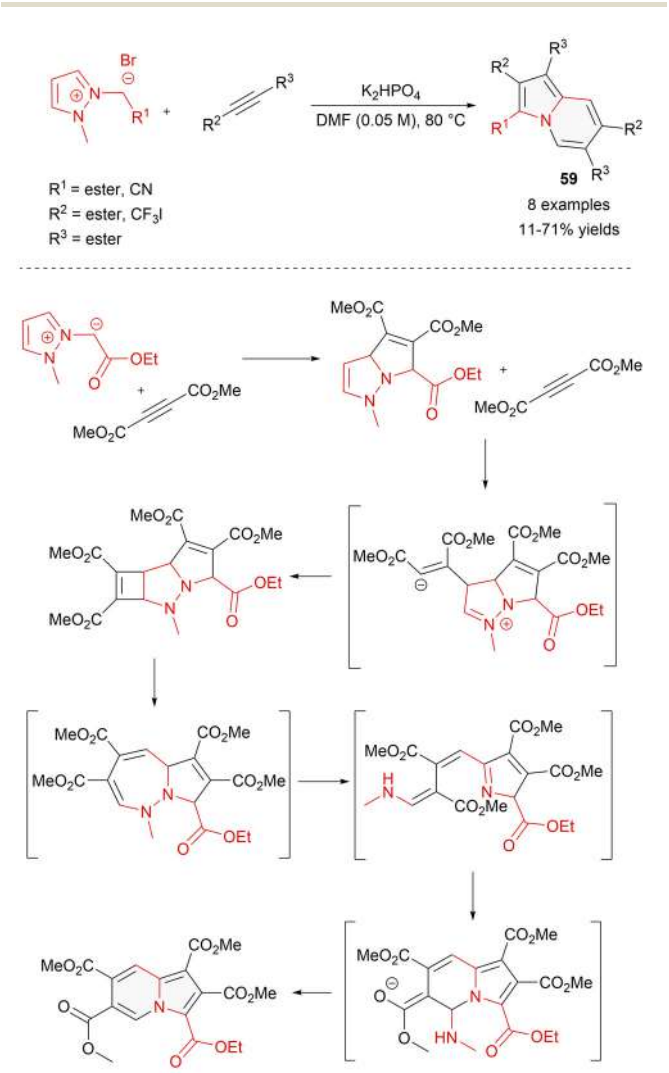

Scheme 59

4. Methods leading to π-expanded indolizines

The ability to synthesize π-expanded indolizines has a significant impact on the development of new photoluminescent materials. This class of molecules exhibits promising optical properties, making them suitable for applications in bioimaging as well as optoelectronic devices such as OLEDs, solar cells, and field-effect transistors.[224] It is important to emphasize that many already presented methods can give access to pyrrolo[1,2-*a*]quinolines[74,100,107] and pyrrolo[2,1-*a*]isoquinolines[43,69,74,78,80,116] starting not from pyridine but from quinoline or isoquinoline respectively. In the next section, we focus on methodologies leading to less known π-expanded indolizines, which require more specific synthetic methods.

4.1 Benzoindolizines

4.1.1 Transition-metal-catalyzed cyclization. Transition-metal-catalyzed cycloaddition has also proved to be effective for the synthesis of expanded indolizines such as benzo[2,1-*a*] indolizines and pyrido[1,2-*a*]indoles. Zeng *et al.* developed a cobalt-catalyzed [4 + 1] cycloaddition of 2-arylpyridines with aldehydes *via* sp^2-C–H activation, yielding 3-acyl benzo[2,1-*a*] indolizines **60** in very high yields.[225] Notably, this reactivity was not restricted to 2-arylpyridines; 2-alkenylpyridines were also compatible. A variety of aldehydes, such as acetaldehyde and oxo-alkyl-acetaldehydes, successfully provided the desired products, although others, including benzaldehyde and acetaldehyde, proved incompatible. In this transformation, the cobalt catalyst plays a dual role: as a transition metal catalyst and as a Lewis acid, as outlined in the proposed mechanism (Scheme 60). The mechanism involves the activation of [CpCo(CO)I_2] by $AgSbF_6$ and $Cu(OAc)_2$, forming a Co(III) species that coordinates with the nitrogen of pyridine, followed by α-ketoaldehyde insertion, protonation, and nucleophilic attack by the pyridine nitrogen to produce the final product.

In 2022 Bora *et al.* developed a rhodium-catalyzed *ortho*-selective carbene insertion strategy to activate the non-acidic sp^2-C–H bond of β-carboline and isoquinoline scaffolds using diazo compounds of diethyl malonate, dimethyl dimedone, and oxindole as coupling partners.[226] With this methodology, they were able to obtain intermediate **61a** with the release of environmentally benign N_2 gas as the sole by-product (Scheme 61). Subsequently, they successfully developed a CN bond annulation of the C–C functionalized product with a catalytic amount of TCCA affording π-expanded indolizines **61**. The reactivity of the diazo compound under the Rh-catalyzed mechanism can also be compared to that displayed for the synthesis of indolizine **14**, with the difference being the site of attack. For **14**, attack is at N of the quinoline, while here it is at the phenyl ring attached to the pyridine.

While the primary difference between the two approaches presented here lies in the type of metal catalyst used and the specific reactions involved, both contribute to the growing

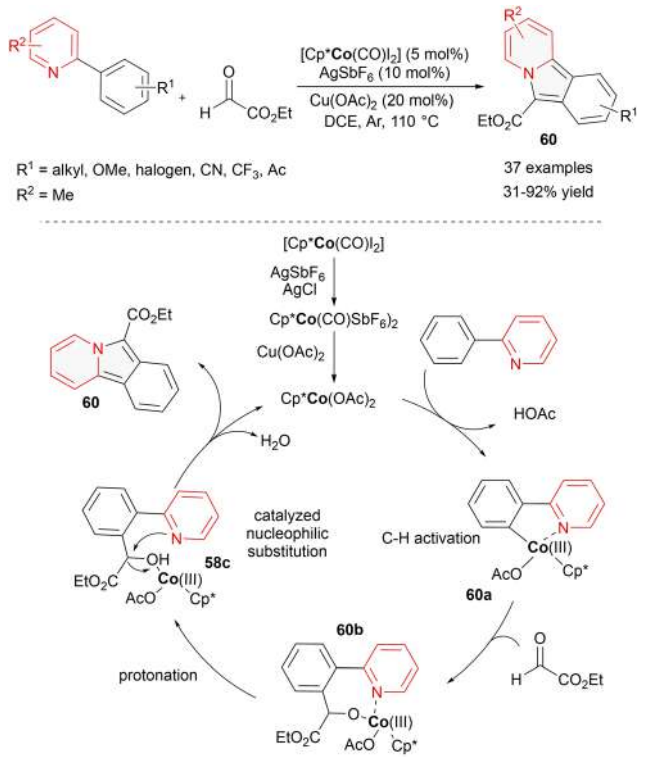

Scheme 60

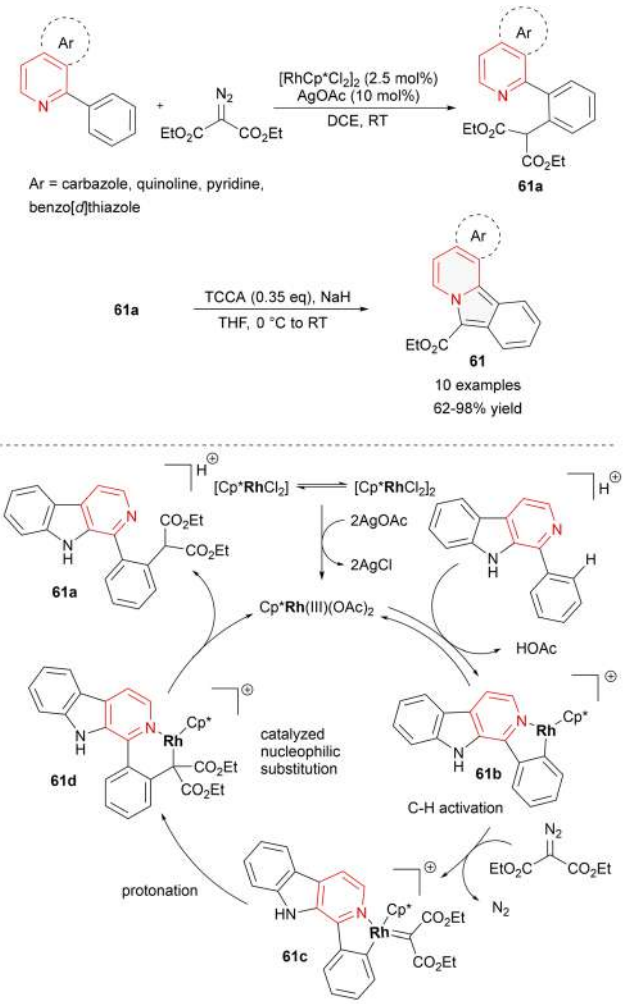

Scheme 61

toolkit of metal-catalyzed strategies for expanding the indolizine family with different functional groups.

Ring-restructuring reactions have emerged as efficient and alternative strategies for the construction of fused polycyclic indolizines.

Van der Eycken and colleagues developed a highly regioselective [3 + 2] cycloreversion reaction between oxazolidine and methyl acrylate, using $Pd(PPh_3)_4$ as a catalyst, achieving the desired indolizine **62** in 72% yield.[227] The proposed mechanism involves a sequence of steps: 6-*exo*-dig cyclization, proton transfer, [3 + 2] cycloaddition, cycloreversion, and final aromatization, as outlined in the catalytic cycle (Scheme 62).

To address the limited availability of 2-arylpyrroles and provide an alternative to more conventional 2-aryl-indole substrates, Luo *et al.* explored the use of 2-arylpyrrolidines as starting materials for the synthesis of pyrrolo[2,1-*a*]isoquinolines. They successfully reported the synthesis of **63** from 5-phenylpyrrolidine-2,3,4-tricarboxylate and diphenylacetylene under aerobic oxidation conditions (Scheme 63).[228] While both methodologies lead to pyrrolo[2,1-*a*]isoquinolines, the latter results in esters as substituents on the pyrrole side, while the former introduces ester, aryl, and alkyl groups. Additionally, **63** features aryl groups at position R^6 and a broader range of substituents at R^1, highlighting their functional diversity compared to the more limited substitution observed in Van der Eycken's product.

Lastly, Shurupova *et al.* developed a new, efficient two-step method for synthesizing substituted pyrido[1,2-*a*]indoles **64** starting from readily accessible pyrylium salts and 2-bromoanilines (Scheme 64).[229] The process involves the transformation of pyrylium salts into pyridinium salts **64a**, followed by intramolecular Pd-catalyzed cyclization to produce the desired N-fused heterocycles. This procedure is thought to follow the intramolecular Heck cyclization reaction pathway and allows for the synthesis of expanded indolizines with alkyl groups at R^3.

4.1.2 Cyclizations lacking transition-metal catalysts. In addition to transition-metal-catalyzed methods, non-metal alternatives also prove to be effective at synthesizing π-expanded indolizines.

In 2016, Outlaw *et al.* proposed another method for the synthesis of benzoindolizines, in particular, they obtained 6-amino-8-cyanobenzo[1,2-*b*]indolizines **65** through a mechanism involving a Wittig reaction followed by N–H deprotonation.[230] This sequence directs the reactivity toward the desired cyclization, favoring the formation of indolizine over carbazole. The synthesis was compatible with various electron-donating groups and electron-withdrawing groups at the 4-position of the indole, while no products were obtained with substituents at the C7 position (Scheme 65). The resulting compounds

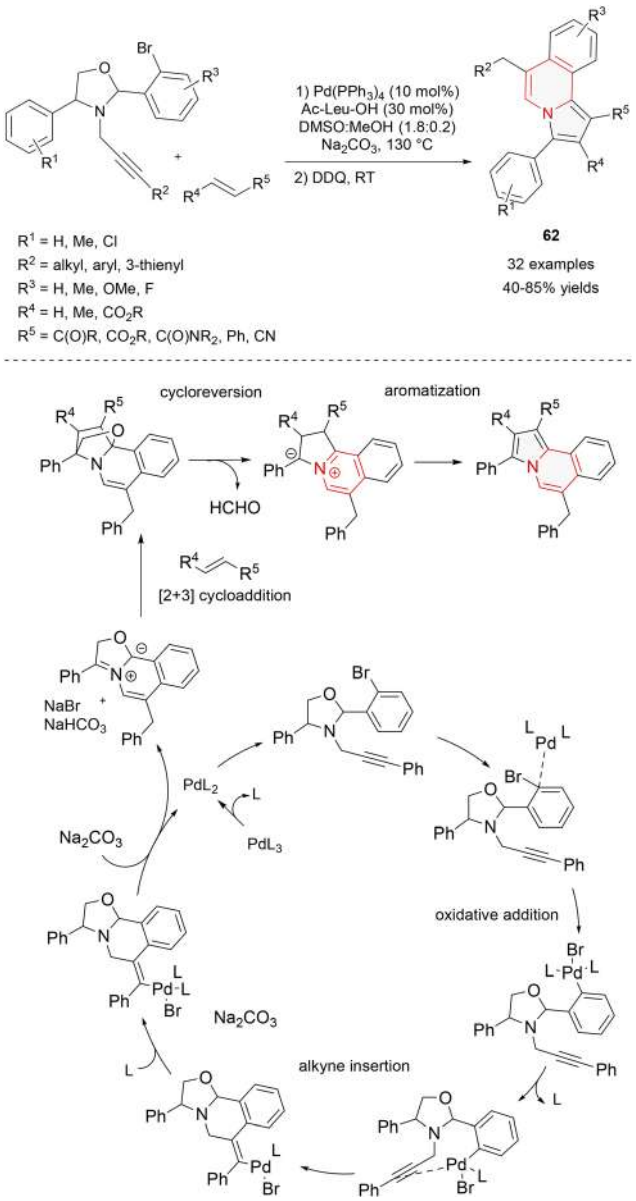

Scheme 62

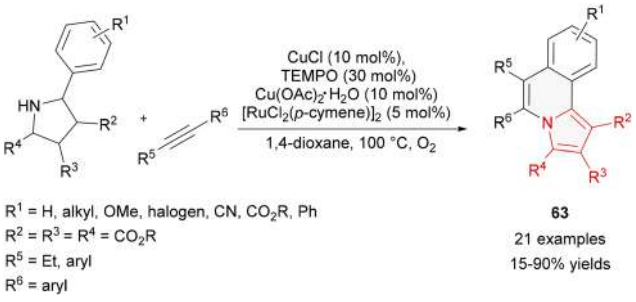

Scheme 63

exhibit pH-dependent optical properties, characterized by a blueshift in fluorescence emission upon protonation. Protonation of the C atom leads to breakdown of the aromaticity and a hypsochromic shift in emission. The absorption spectrum (λ_{abs}) displays three peaks at 270, 340, and 440 nm, while the emission (λ_{em}) ranges between 490 and 520 nm, with average fluorescence quantum yields (Φ_{fl}) of 10%. Upon the addition of trifluoroacetic acid (TFA), a new equilibrium is established, resulting in the emergence of a peak at 440 nm, indicating a shift in emission and an increased quantum yield (20%) for the newly formed non-aromatic structure.

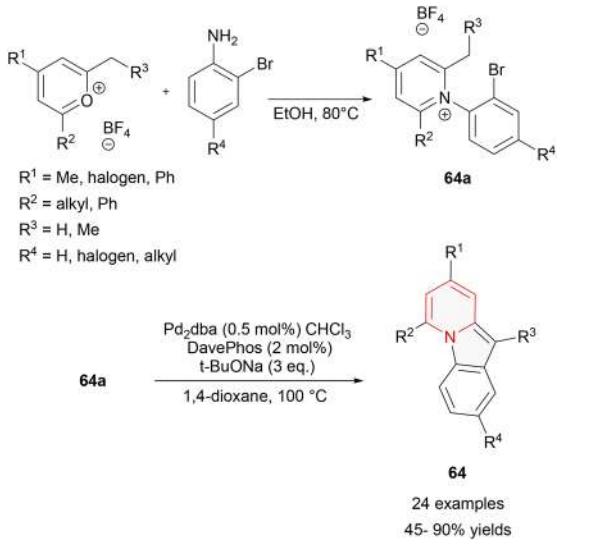

Scheme 64

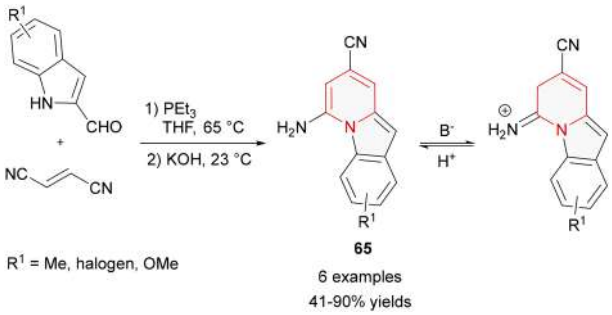

Scheme 65

In order to achieve typically difficult to obtain benzo[*a*]indolizines, two different approaches were proposed recently. The first, developed by Badaro *et al.* in 2022, revisits Kröenke's earlier methodology[231] and involves the reaction of pyridinium or quinolinium salts with chloronitroarenes under basic conditions (Scheme 66). This process proceeds *via C*-arylation, followed by 1,5-electrocyclization, leading to the formation of the target benzo[*a*]indolizines (**66A** and **66B**).[232] Despite the fluorescence quenching effect typically associated with the NO_2 group, the products exhibit a fluorescence quantum yield (Φ_{fl}) of up to 60%, with emission ranging from yellow to red and absorption (λ_{abs}) between 400 and 500 nm.

The second one, published by Khan *et al.* in 2024, exploits the inherent high reactivity of *in situ* generated benzynes

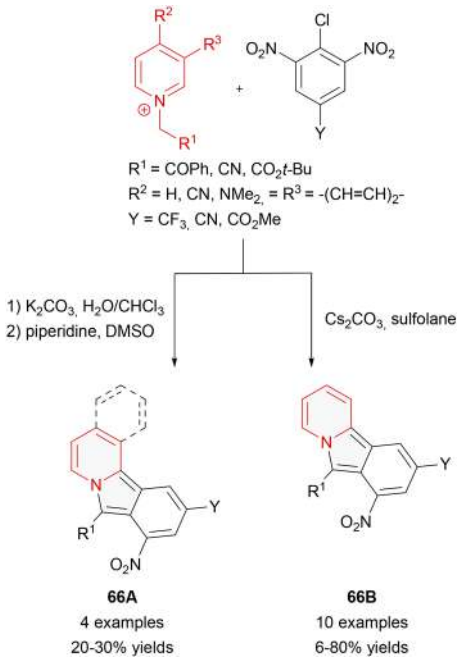

Scheme 66

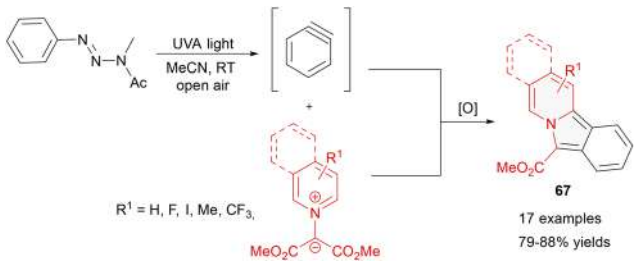

Scheme 67

under UVA (365 nm) irradiation at room temperature in acetonitrile. The reaction proceeds through a [3 + 2] cycloaddition between benzyne and pyridinium ylides, resulting in isoindolo[2,1-*a*]pyridines **67** in high yields (Scheme 67).[233] The key advantages of this methodology over the ones previously developed include the absence of additional reagents, its operation under ambient conditions, and the use of atmospheric oxygen, which collectively enhance its sustainability. A notable drawback, however, is the requirement for suitable benzyne precursors, which must be synthesized in advance, limiting the scope of substituents on the final product.

4.2 'Pyridine'- and 'azepine'-expanded indolizines

In 2023, Zeng *et al.* developed a method for synthesizing 1,2,3-trisubstituted indolizine-2-carbaldehydes **21** using recyclable biomass-derived chitosan as a stereoauxiliary aminocatalyst.[129] Among the synthesized indolizines, 3-(4-bromophenyl)-1-(pyridin-4-yl)indolizine-2-carbaldehyde exhibited potential for further transformations, including reduction, arylation, condensation, and [5 + 1] annulation reactions (Scheme 68). The

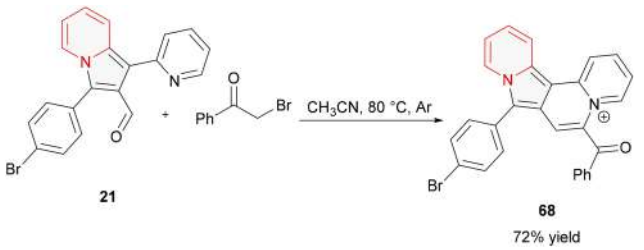

Scheme 68

last reaction resulted in the formation of 6-benzoyl-8-(4-bromophenyl)indolizino[1,2-*a*]quinolizin-5-ium salt **68**, representing an unusual π-extension of the indolizine framework.

Miao *et al.* developed a copper-promoted annulation of α,β-unsaturated *O*-acyl ketoximes with isoquinolinium *N*-ylides with the objective of obtaining benzo[7,8]indolizino[1,2-*c*]quinolines **69**, containing the expanded indolizine core present in many natural products and showing important biological activities.[234] Despite the well-known lability of *N*-substituted imines, the authors were able to obtain N–H-substituted indolizines by breaking of the N–O bond; these were sufficiently stable to undergo reaction under oxidative and heating conditions without evolving to the expected dimerization, instead, giving the final benzo[7,8]indolizino[1,2-*c*]quinolines in good to excellent yields (Scheme 69). In this process, isoquinolinium salt and *O*-acetyl 3-(2-bromophenyl)-1-(*p*-tolyl)prop-2-en-1-oxime were used as reagents, with $Cu(OAc)_2$ acting as both the catalyst and oxidant. 2-Picolinic acid served as a ligand, K_2CO_3 as a base and pyridine *N*-oxide (PNO) as a co-oxidant. The reaction was carried out in toluene at 80 °C.

As an alternative, Sokolova *et al.* proposed a pseudo-three-component reaction of *N*-(cyanomethyl)pyridinium and vinamidinium perchlorates or other 1,3-dielectrophiles such as enaminones to form 3- or 2-substituted pyrido[2,3-*b*]indolizine-10-carbonitriles **70** (Scheme 70).[235] Products obtained with this new method show visibly strong green light fluorescence with Φ_{fl} of 0.4–0.8. Photophysical studies showed that the absorption band with partial vibrational resolution was in the region of 350–470 nm, while the emission band fell between 460 and 490 nm.

In addition to the previous method, Yi *et al.* proposed an alternative approach for synthesizing pyrido[3,2-*b*]indolizines,

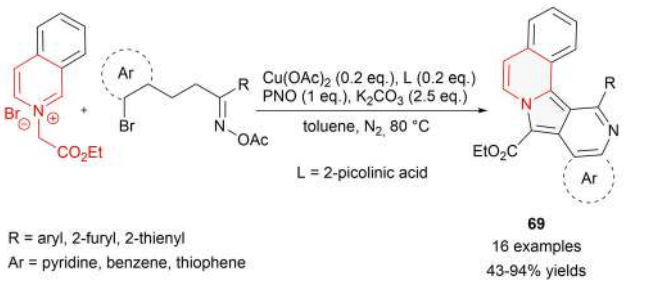

Scheme 69

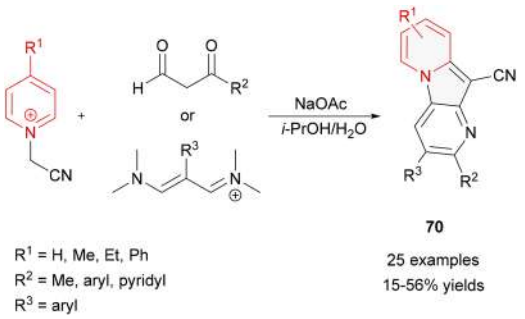

Scheme 70

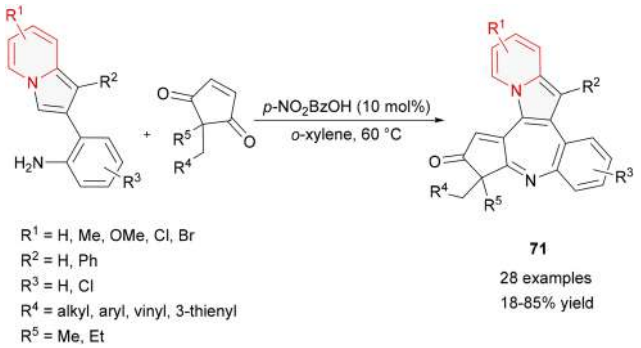

Scheme 71

driven by the goal of developing a fluorescent scaffold for fluorogenic bioimaging.[224] The synthesis involves a five-step sequence, beginning with Sonogashira coupling using a suitable terminal alkyne, followed by base-promoted 5-*endo-dig* cyclization, aldol condensation/cyclization, and concluding with oxidative aromatization. Although this method is more time-intensive and complex, it enables access to a different isomer, expanding the structural diversity of pyridoindolizines.

Song and coworkers were able to synthesize polycyclic indolizine-fused azepines **71** under mild conditions with a Brønsted acid as a catalyst (Scheme 71).[236] The development of unusual nitrogen-containing heterocyclic azepines (nitrogen-containing 7-membered ring) in planar π-systems was an ambitious goal and never achieved previously. The mechanism involves the Friedel–Crafts addition of *ortho*-indolizinyl anilines and cyclopentene-1,3-diones, oxygen, and a final Schiff-base condensation that can be described as a formal [5 + 2] cycloaddition. Compounds exhibited broad absorption bands with λ_{max} at 306 or 308 nm and Φ_{fl} in the 10–20% range.

4.3 Indolizine-imides

Although formally the presence of an imide functionality fused to the indolizine core at positions 1 and 2 or 2 and 3 does not provide π-expansion of the chromophore, the strong relationship between aromatic imides and the chemistry of fluorescent functional dyes prompted us to include these compounds in this section. Pyrrolo-indolizine-diones are an important class of heterocyclic compounds with significant relevance in medicinal chemistry and drug design. Their unique bicyclic structure, which combines imides and indolizine rings, provides a versatile scaffold for the development of biologically active molecules.

Recently, a few different methods were proposed based on pyridines and maleimides that gave rise to different representatives of this class. The direct construction of pyrrolo[3,4-*a*]indolizine-1,3(2*H*)-diones **72** from pyridines, acetophenones and maleimides under transition-metal-free catalytic conditions (Scheme 72) presented by Ablajan and coworkers is one of those.[237] Reactivity follows the expected path: acetophenone is converted into α-iodoacetophenone, which reacts with pyridine to form the pyridinium ylide. Release of HI in the presence of a base affords azomethine ylide. An intermediate is formed from azomethine ylide and *N*-phenylmaleimide through a 1,3-dipolar cycloaddition reaction, and finally the desired product is obtained after oxidation.

An alternative method to obtain the 1*H*-pyrrolo[3,4-*b*]indolizine-1,3-dione **73**, an isomer of the previous indolizine, was developed by Yan's group and involved 2-(pyridine-2-yl)acetate derivatives with maleimides through a transition-metal-catalyzed oxidative annulation reaction.[238] The mechanism proceeded *via* [3 + 2] annulation, achieved by heating a mixture of the two substrates in the presence of Ag_2CO_3 as an oxidant and $Cu(OAc)\cdot H_2O$ as a catalyst in chlorobenzene. The following steps were a sequential single-electron transfer (SET) reaction, Michael addition, imine–enamine tautomerization, another SET, intramolecular cyclization, and finally dehydrogenative aromatization (Scheme 73).

In a similar study, Chupakhin *et al.* developed an alternative transition-metal-catalyzed method to synthesize maleimide-expanded indolizines **74** through the denitrogenative decomposition of (*E*)-3-(2-pyridylmethylene)-4-diazopyrrolidine-2,5-diones, using Rh(II) acetate as a catalyst (Scheme 74).[239] The reaction generates a Rh(II) carbene species, which then undergoes ring closure, facilitated by the reactive nitrogen present in pyridine. This same mechanism was described by Peng for the synthesis of indolizines **14**.

While all three methods involve maleimides and pyridines, they differ in their catalytic requirements, reaction pathways, and product structures. The last two approaches enable the formation of pyrrolo[3,4-*b*]indolizine-1,3-diones with (Yan) or without (Chupakhin) EWGs at C1. However, the latter approach

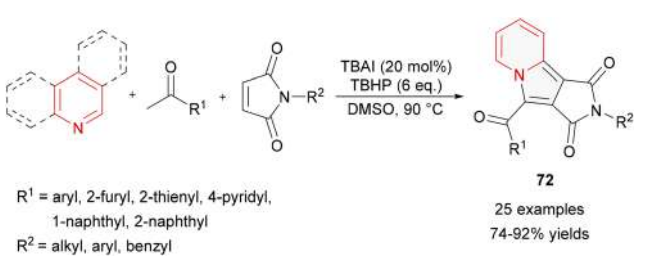

Scheme 72

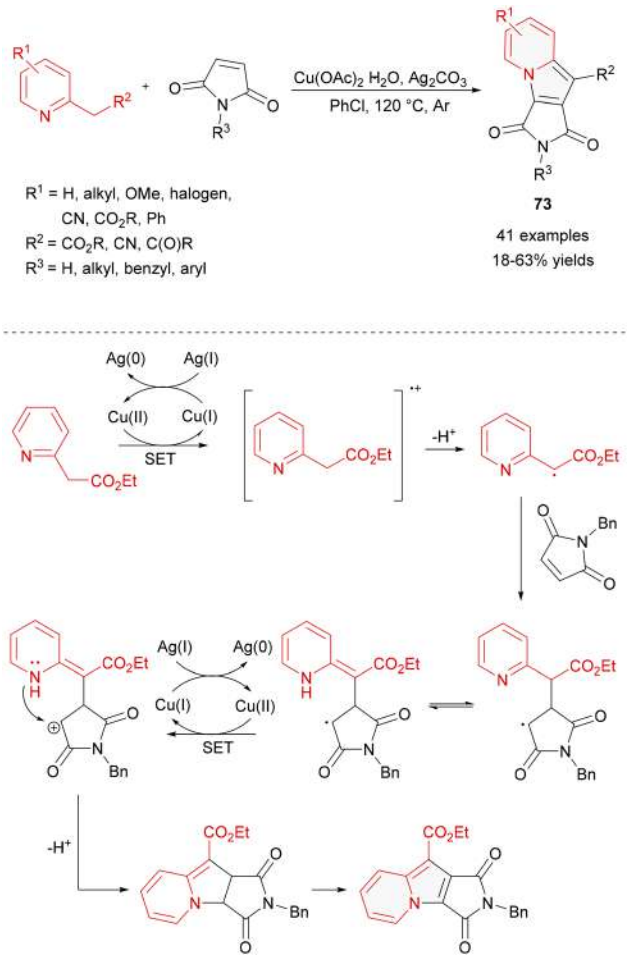

Scheme 73

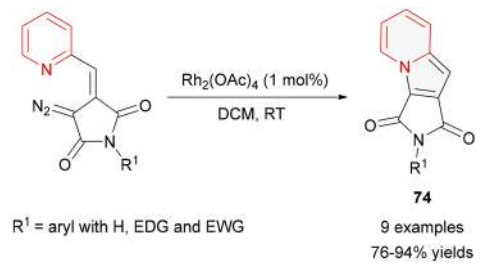

Scheme 74

is less convenient in terms of substrate availability since it must be prepared in two steps.

4.4 'Chromone'- and 'pyrano-expanded indolizines

Another interesting expansion of indolizines is *via* annulation with chromone, as credited to Zhu and co-workers. They pioneered the synthesis of chromone-fused pyrrolo[2,1-*a*]isoquinolines and indolizino[8,7-*b*]indoles **75** using ethyl-3-(2-acetylphenoxy)acrylate as a reagent, alongside pyridine, tetrahydroisoquinoline, or noreleagnine in a one-pot protocol

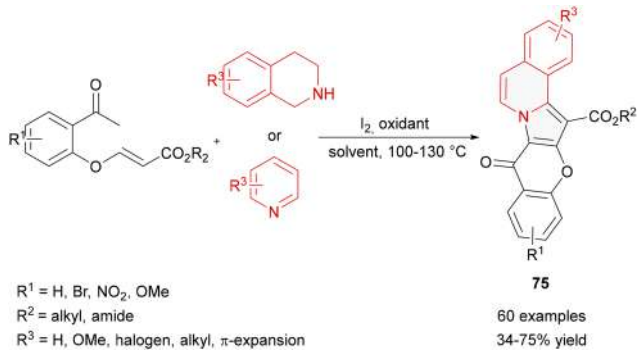

Scheme 75

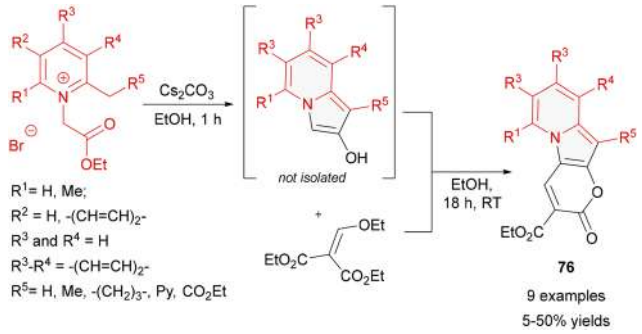

Scheme 76

(Scheme 75).[240,241] The reaction mechanism involves several key steps: α-iodination in the presence of I_2, followed by oxidation in DMSO or TBPB; nucleophilic addition with enol tautomerization in the presence of TFA; an intramolecular 1,3-dipolar cycloaddition; and a final oxidation step to generate the desired product (a comparable mechanism was described for **39** and **72** exploiting Ortoleva–King reactivity).

In pursuit of strongly luminescent dyes, Badaro *et al.* recently revisited the synthesis of pyrano[2,3-*b*]indolizin-2-ones from picolinium salts and diethyl 2-(ethoxymethylene)malonate developed by Kakehi in the last century.[242] This reaction proceeds under basic conditions through a Dieckmann condensation and a Friedel–Crafts reaction with final intramolecular transesterification (Scheme 76).[243] Their recent approach improved the yield and accelerated the process compared to the first method proposed, as well as amplified the scope by providing various pyrano-indolizine derivatives **76** in good yields through a one-pot procedure. Furthermore, the authors performed functionalization reactions on the obtained structure of **76** and synthesized a styryl derivative for cell staining. Spectroscopic investigations showed that the obtained dyes possessed absorption and emission spectra in the blue–green region and fluorescence quantum yields up to 92%.

4.5 Naphthoquinone expanded indolizines

Another common type of expansion of the indolizine core is condensation to the 1,4-naphthoquinone moiety. Indeed

various reactions combining quinones, pyridines and β-ketoesters were described in the 1950s.[244–246]

Das *et al.* performed a skeletal transformation of naphthoquinone-fused furans and pyridine derivatives to naphthoquinone-fused indolizines **77** in the presence of a catalytic amount of anhydrous $FeCl_3$ and hexafluoroisopropanol (HFIP) as the solvent (Scheme 77).[247] In the same article, the authors described the synthesis of the precursor naphthoquinone-fused furan, which was obtained through a Rh(II)-catalyzed synthesis from β-ketosulfoxonium ylides and 1,4-naphthoquinone.

In 2022 Nagarkar and Dapurkar developed isomeric naphthoquinone-based indolizines **78** on a gram scale with the use of a 4′,5′-dinitroanacardic acid copper(II) complex (2 : 1) as a homogeneous catalyst (Scheme 78).[248] The outcome of this work proved the superiority of a sustainable copper catalyst over a conventional copper salt at room temperature due to its structural advantages and the ability to provide excellent regioselectivity. The proposed mechanism predicts the action of the catalyst in three of the four reaction steps. First, it is

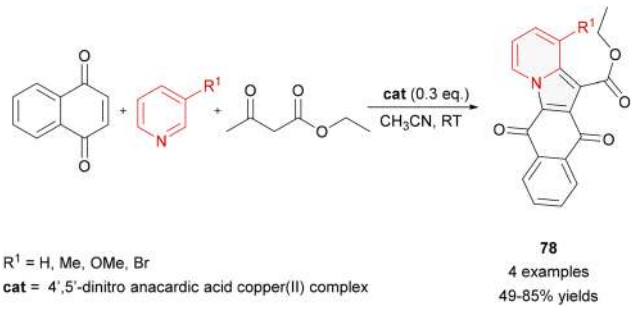

Scheme 78

responsible for the reaction between naphthoquinone and pyridine to obtain an intermediate, which undergoes a second catalyzed reaction with ethyl acetoacetate. At this point, ring formation occurs, leading to the last step of oxidative aromatization, which is also catalyzed by the Cu(II) complex.

Kim and co-workers described two methodologies for the synthesis of quinone–indolizine hybrids **79A** and **79B** starting from pyrrole-derived substrates and showing promising anticancer activity (Scheme 79). The first reaction proceeds through a domino Michael addition–intramolecular aldol reaction–dehydration and final aromatization, all under basic conditions.[249] The second reaction, instead, is a Cu(II)-catalyzed domino [4 + 2] annulation process consisting of intermolecular Michael addition, Thorpe–Ziegler type cyclization, and final oxidation.[250] The differences in these methods lie in the mechanisms as well as in the pyrrole derivatives used. In the first case, a more classic 2-formyl *N*-substituted pyrrole was used, while the latter was based on *N*-substituted pyrrole-2-carbonitriles.

In 2023 Maiti *et al.* presented a diversity-oriented synthesis of annulated indolizines through a multicomponent reaction

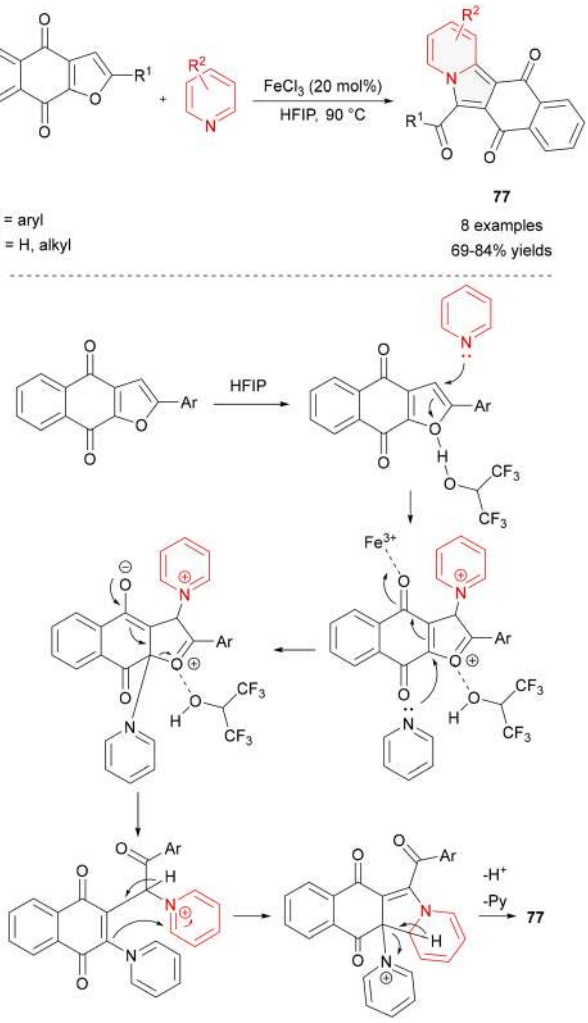

Scheme 77

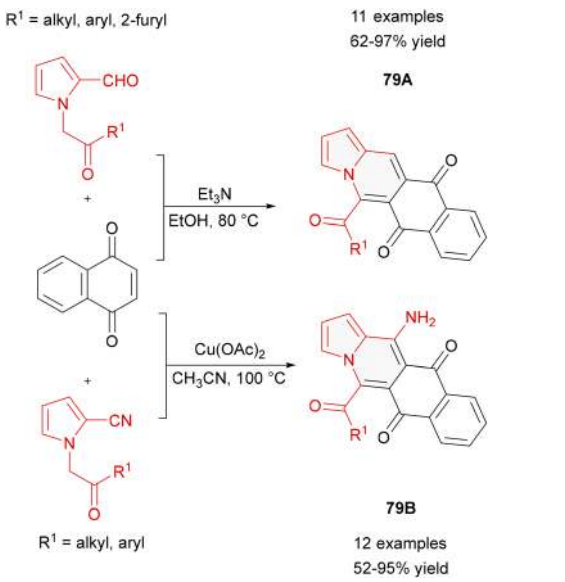

Scheme 79

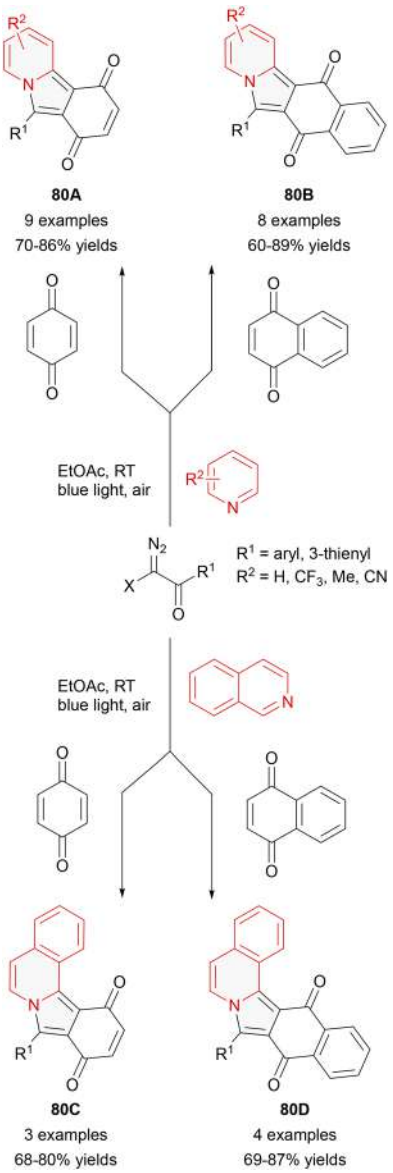

Scheme 80

catalyzed by blue LED irradiation (Scheme 80).[251] The developed method involves reacting pyridine or isoquinoline, aryl diazoacetates, and either 1,4-benzoquinone or 1,4-naphthoquinone in a stoichiometric ratio of 2 : 1.2 : 1. The reaction is carried out in ethyl acetate as the solvent and is conducted under blue LED irradiation at room temperature.

The derivatives corresponding to isoindolo[2,1-*a*]pyridine **80A**, isoindolo[2,1-*a*]isoquinoline **80B**, isoquinolino[2,1-*a*]isoindole-7,12-dione **80C**, or pyrido[2,1-*a*]isoindole-7,12-dione **80D** were obtained in moderate to good yields. Among these, the pentacyclic annulated indolizine **80D** (DASS-fluor) demonstrated intriguing photophysical properties and was evaluated as a fluorescent probe by the authors. It exhibited solvatochromic emission, with λ_{em} shifting from 507 nm to 559 nm in solvents of increasing polarity, and a fluorescence quantum yield (Φ_{fl}) of 0.05 in water. DASS-fluor successfully detected and differentiated the formation of lysosomal and non-lysosomal lipid droplets under both normal and stimulated cellular conditions, making it a promising fluorescent marker for hepatosteatosis.

Recently, Gaweł and co-workers developed a method for the synthesis of indolizinequinones **81**[252] from methylquinones, I_2 and pyridine derivatives in DMSO as an improvement of Delcanale's protocol.[244,253] Moreover, the obtained indolizinequinone could be further functionalized to yield substituted indoloindolizines **82** in one pot.

In the first step, acetylene derivatives are added to the carbonyl groups of quinone **81** through a butyllithium-mediated reaction. The resulting intermediate **81a** undergoes reductive elimination with the introduction of $SnCl_2$ in 10% aqueous HCl solution (Scheme 81). The photophysical properties of the obtained products were also described and covered the visible range around 434 nm for absorption and 621 nm for emission. The largest bathochromic shift was observed for the expanded system having six fused aromatic rings (λ_{abs} = 594 nm and λ_{em} = 621 nm with Φ_{fl} of 17%).

The methodologies presented differ in their catalytic approaches and in the specific isomers of naphthoquinone-fused indolizines they yield. Das and Maiti's methods produce naphthoquinone-fused indolizines on the pyrrole side, specifically dihydrobenzo[*f*]pyrido[2,1-*a*]isoindole frameworks. While Das employs $FeCl_3$ in HFIP, Maiti's approach stands out for its sustainability, using blue LED irradiation under mild conditions. In contrast, Nagarkar and Gaweł's approach yields dihydrobenzo[*f*]pyrido[1,2-*a*]indole isomers, with Nagarkar's Cu(II) complex offering enhanced regioselectivity and Gaweł's iodine-based method enabling π-expanded pyridine functionalization. Kim's work uniquely delivers naphthoquinone-fused indolizines on the pyridine side. Together, these approaches provide access to the full range of naphthoquinone-fused indolizine isomers, varying in both the fusion position and substituents.

4.6 Miscellaneous

In addition to the previous classes of expanded indolizines presented, herein we describe some more unusual cores.

Zou *et al.* developed a chemoselective coupling strategy that utilized a two-atom unit derived from *N*-substituted pyrrole-2-carbaldehydes and a four-atom unit from *N*-substituted pyrrole-2-carbonitriles, yielding the pyrrolo[1′,2′:1,6]pyrazino[2,3-*g*]indolizine dye **83** (Scheme 82).[254] This compound exhibited remarkable aggregation-induced emission (AIE) properties, with the pyrrolo[1′,2′:1,6]pyrazino[2,3-*g*]indolizine moiety functioning as the stator and the two phenyl rings serving as rotors. This configuration aligns seamlessly with the well-established mechanism underlying AIE. All the λ_{em} bands of the dyes are located around 550 nm, while Φ_{fl} varies and depends on the substituents on the rotor part of the system. The product having CF_3 and NMe_2 as *para*-substituents on the aryl rings showed a signal at the longest wavelength, which could be ascribed to the formation of a donor–π–acceptor structure between the strong electron-withdrawing trifluoro-

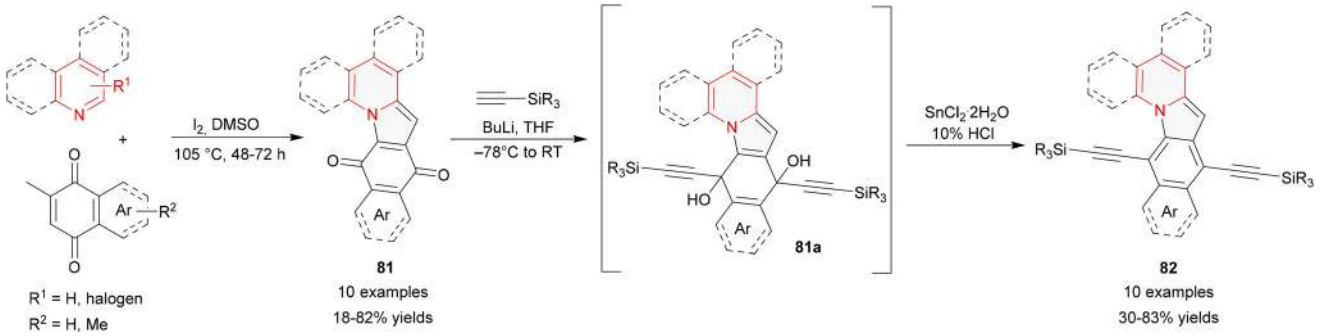

Scheme 81

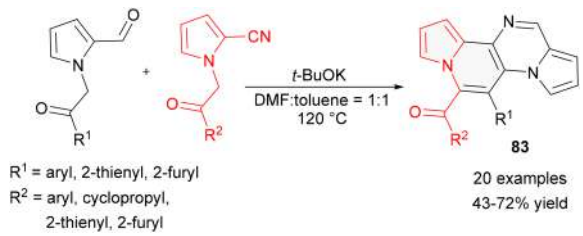

Scheme 82

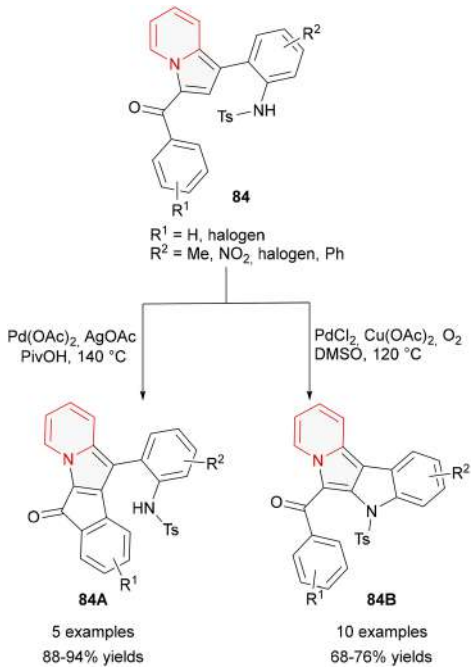

Scheme 83

methyl group and the electron-donating dimethylamino group.

Babu *et al.* developed a 1,3-dipolar cycloaddition of pyridinium ylides with electron-deficient aromatic systems such as 3-nitroindoles, for the synthesis of indolizines **84**.[255] Contrary to the natural nucleophilic characteristic of indoles, the presence of electron-withdrawing groups at positions 2 or 3 reverts the nucleophilic characteristic of this class, thus making the system a good electrophile prone to dipolar cycloaddition reactions and allowing for the synthesis of annulated heterocycles (Scheme 83). From this perspective, two possible ring-closing pathways from compound **84** were evaluated, leading to the formation of 6*H*-indeno[1,2-*b*]indolizin-6-one **84A** and indolizino[2,1-*b*]indoles **84B** *via* two different Pd-catalyzed mechanisms. The first pathway proceeds through C–H amination, while the second involves dual C–H activation.

Langer *et al.*, in 2023, developed a straightforward method for the synthesis of quite rare thienoindolizine structures *via* nucleophilic substitution followed by intramolecular cyclization (Scheme 84).[256] 3-Bromo-2-(2,2-difluorovinyl)thiophene and 5-fluoro-1*H*-indole were used as substrates to obtain **85a** under basic conditions (K_3PO_4) by double substitution of the F atoms. The intermediate was then used by the authors to achieve the final thieno[3,2-*g*]-, thieno[3,4-*g*]- and thieno[2,3-*g*]indolizine moieties **85**, depending on the thiophene isomer used, through a Pd-catalyzed intramolecular cyclization. The synthesized compounds exhibit strong absorption between 250 and 320 nm. The emission maxima are located between 421 nm and 487 nm, and Φ_{fl} is around 20%.

Kim and coworkers proposed the synthesis of the indolizine intermediate **86a** from pyridine-2-acetonitrile, 2-bromo-benzaldehyde, and TMSCN *via* a one-pot three-component reaction. The obtained indolizine was then used to yield 5-aryl-5*H*-indolizino[3,2-*b*]indole **86** *via* a Cu-catalyzed Ullmann-type double C–N coupling reaction (Scheme 85).[257] Mechanistic studies proved that the intramolecular C–N coupling was much faster than the intermolecular one allowing for the alkylation and sulfonylation of N instead of arylation.

Zhang *et al.* reported the synthesis of a novel fused hexacyclic indolizine derivative **87** through a one-pot reaction.[258] This process involves the thermal generation of high-energy benzynes *via* hexadehydro-Diels–Alder (HDDA) cycloisomerization from tetraynes, followed by a stepwise [3 + 2] cycloaddition with commercially available (trimethylsilyl)ethynylpyridine, resulting in the unique expanded indolizine in over 80% yield (Scheme 86).

Starting from a methodology similar to that presented for the synthesis of pseudo-betaine **20D**, Nechaev *et al.* developed

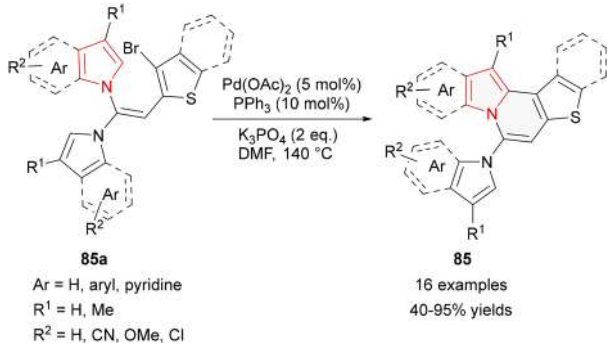

Scheme 84

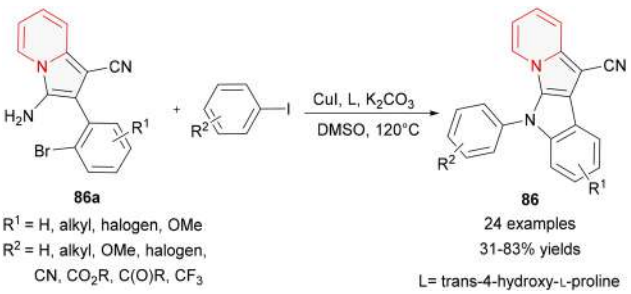

Scheme 85

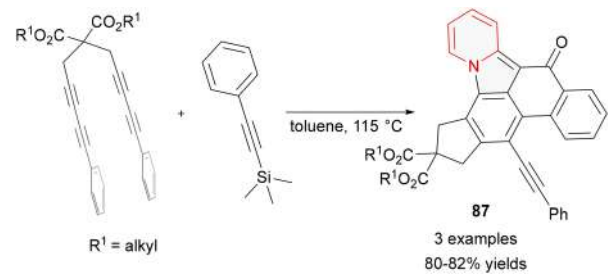

Scheme 86

an efficient route to an unusual tetracyclic compound, 4-oxo-4,6-dihydrocyclopenta[4,5]pyrimido[2,1,6-*cd*]indolizine (**88**).[259] The process began with the formation of (*E*)-3-arylimino-3*H*-indolizin-4-ium-1-olates, achieved through the reaction of 3-difluorocyclopropenes, pyridines, and anilines under oxidative conditions using sodium iodate ($NaIO_3$). This step was followed by the cycloaddition reaction of **88a** with dimethylaminofulvene, leading to the final expanded indolizine framework (Scheme 87). Other less attractive methodologies leading to functionalized pyrrolo[2,1-*a*]isoquinolines follow the cascade [3 + 2]/[4 + 2] cycloaddition of complex enaminones with vinylene carbonate.[260]

4.7 Vertically expanded indolizines

Other interesting classes of π-expanded indolizines include pyrrolo[2,1,5-*cd*]indolizines, also known as cyclo[2,2,3]-azines,

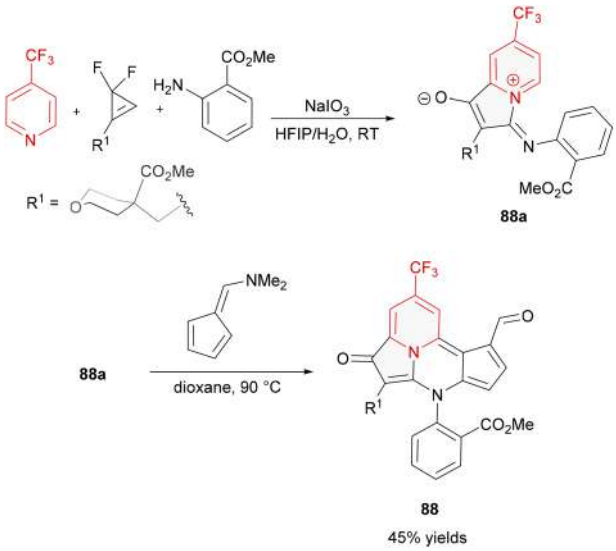

Scheme 87

and imidazo[1,2-*a*]pyridines, commonly referred to as azacyclazines. These compounds are valuable building blocks for drug development, as well as for fluorescent probes and luminescent materials.

In 2015 Ji and co-workers developed a method for the synthesis of pyrrolo[2,1,5-*cd*]indolizines **89** from 1- and/or 2-substituted indolizine and electron-rich alkynes through the Pd $(OAc)_2$-catalyzed dehydrogenative Heck annelation reaction (Scheme 88).[261] In addition to the main reagents, an acid such as 2,6-difluorobenzoic acid was needed to improve the reaction selectivity between dimerization and Heck annelation. A wide range of functional groups were tolerated in both the indolizine and diarylacetylene, and the products were obtained in moderate to excellent yields.

Much more recently Huang *et al.* published a mechanochemically driven dehydrogenative coupling strategy, utilizing piezoelectric materials ($BaTiO_3$) to facilitate the synthesis of pyrrolo[2,1,5-*cd*]indolizines **90** *via* an intermolecular [3 + 2] cycloaddition between allenes and indolizines (Scheme 89).[262] This approach offers several key advantages compared to the classic ones, including the elimination of organic solvents, simple experimental procedures, scalability, and high conversion efficiency.

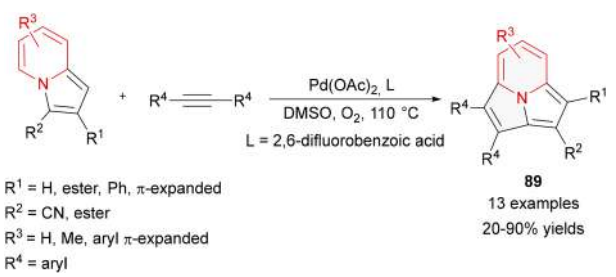

Scheme 88

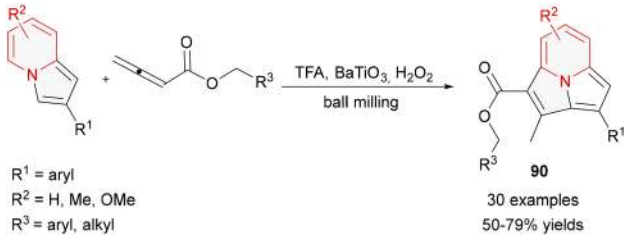

Scheme 89

While Ji's Pd-catalyzed approach provides broader substrate compatibility and proven efficacy, Huang's mechanochemical method excels in sustainability and operational simplicity, representing a promising step toward greener synthetic methodologies.

When considering azacyclazines, Ghosh *et al.* developed a palladium-catalyzed direct arylation of 2-alkyl-imidazo[1,2-*a*]pyridine with alkynes for the synthesis of 2-alkyl-imidazo[5,1,2-*cd*]indolizines **91** through an oxidative coupling (Scheme 90).[263] Synthesized imidazo[5,1,2-*cd*]indolizines exhibit λ_{abs} peaks in the range of 388–396 nm, while λ_{em} is in the range of 518–532 nm with one broad emission peak and Φ_{fl} around 15%. The exception to this trend is the compound with OMe substituents on the aryl ring of the alkyne, which shows an additional peak at 427 nm and the highest Φ_{fl} (0.44).

Following this trend, in 2023 Meena *et al.* reported a Pd(OAc)$_2$-catalyzed C–H functionalization of 2-arylimidazo[1,2-*a*]pyridines with cinnamaldehyde to obtain 1,7-diarylimidazo[5,1,2-*cd*]-indolizine-6-carbaldehyde **92**.[264] These reaction conditions allowed annulated products to be produced in good yields, with a wide substrate scope, and showed excellent functional group tolerance (Scheme 91).

Additional ring expansion on the azacyclazine core can be achieved by the annulation of imidazo[1,2-*a*]pyridines with substituted benzenes as the benzyne precursor.

To synthesize expanded benzo[*a*]imidazo[5,1,2-*cd*]indolizines **93**, Adimurthy *et al.* developed the reaction of imidazo

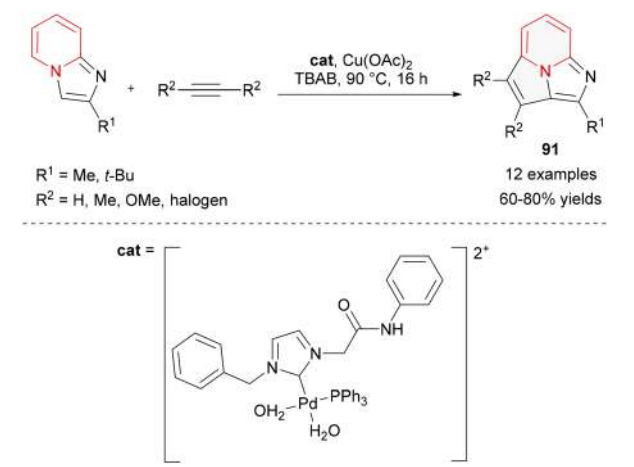

Scheme 90

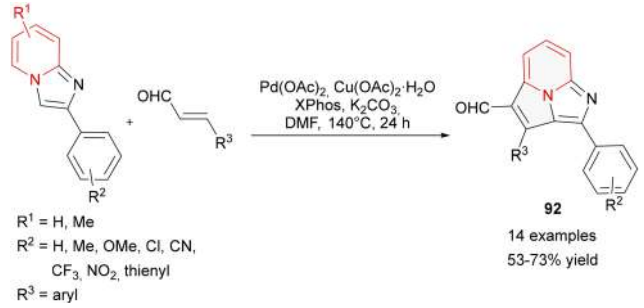

Scheme 91

[1,2-*a*]pyridines and 2-(trimethylsilyl) phenyltrifluoromethanesulfonate (Scheme 92) under basic conditions (K_2CO_3).[265] Both electron-rich and electron-deficient groups at different positions on the phenyl rings and on the pyridyl ring were tolerated. λ_{em} for the obtained products is in the visible region in the range of 420–600 nm with Φ_{fl} of 0.33–0.68.

Toward a more environmentally friendly approach, Raval and coworkers proposed a microwave-irradiated, ligand-free mechanism (Scheme 93) to access 1-phenylbenzo[*a*]imidazo[5,1,2-*cd*]indolizine derivatives **94** using imidazo[1,2-*a*]pyridine, 1,2-diiodobenzene, and K_2CO_3.[266] This allowed for minimized side reactions compared to classic methodologies, shorter reaction times, and increased yields. λ_{abs} peaks of the products are located between 415 and 428 nm and λ_{em} is in the range of 406–520 nm.

In conclusion, Raval's methodology offers a significant improvement over the transition-metal-catalyzed approaches reported by Ghosh and Meena, as it avoids the use of ligands and operates under microwave irradiation, resulting in

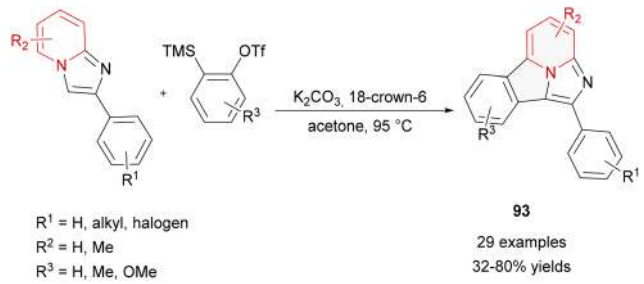

Scheme 92

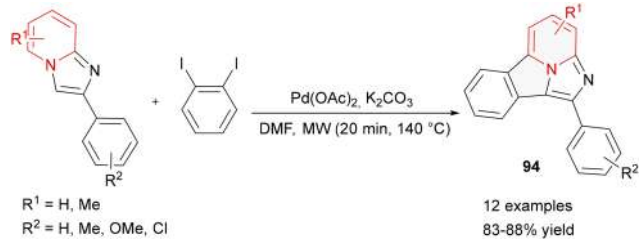

Scheme 93

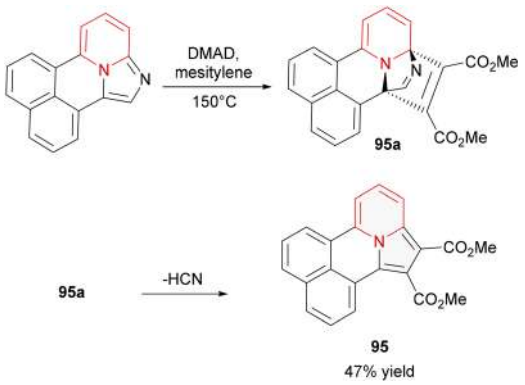

Scheme 94

expanded indolizines with reduced side reactions, shorter reaction times, and higher yields. However, Adimurthy's approach stands out as the most sustainable, using simple base-mediated conditions without any transition metals or specialized equipment, while still producing benzo-expanded indolizines with reasonable yields.

From imidazo[1,2-*a*]pyridines, in 2015 Firmansyah *et al.* proposed the synthesis of completely new 'naphthalene' expanded imidazo[1,5-*a*]pyridine and imidazo[1,2-*a*]pyridines, which led to the formation of the first dimethyl benzo[*de*]indolizino[3,4,5-*ab*]isoquinoline-1,2-dicarboxylate **95** in 47% yield.[267] The reaction mechanism is thought to proceed through a Diels–Alder reaction at the imidazole moiety of **95a** followed by a retro-Diels–Alder reaction with the elimination of HCN (Scheme 94).

An another approach was described by Li and co-workers.[268] 3,4-Di-vinylindolizine undergoes a 12π-electrocyclization offering a route to obtain azepinoindolizine.

A completely new approach and a new indolizine-based molecular architecture were revealed by Liu and co-workers. The authors discovered that pyrazino[2,3-*b*:5,6-*b*′]diindolizine could be easily prepared in four steps from 1,4-diacetyl-2,5-diketopiperazine and pyridine. This heretofore unknown pentacyclic heterocycle has an exceptionally high-lying HOMO (−4.65 eV).[269]

5. Indolizine-fused fluorophores

To conclude this review, we include a few recent and relevant examples of indolizines fused to other fluorophores, such as coumarins and BODIPYs, as well as extended indolizine systems that generate NIR and SWIR emissive fluorophores. These include indolizine-cyanines, Si-Ros indolizines, Phospha-Ros indolizines, and fluorenium indolizine dyes.

Rusanov *et al.* worked on the development of a new methodology for the synthesis of pentacyclic lamellarin analogues.[270] The indolizine intermediate **96** was obtained by a [3 + 2] cycloaddition reaction between available pyridinium ylides, α-nitrostilbenes and benzoyl peroxide as an oxidant. The following steps consisted of *O*-demethylation of the *ortho*-methoxy group followed by a final lactonization to obtain the coumarin-fused indolizine product **97** (Scheme 95).

Song and co-workers presented a rhodium-catalyzed C–H functionalization–annulation of pyrrole-substituted BODIPYs with alkynes, in which the pyrrole acted as a directing group toward the generation of [*b*]-aryl fused BODIPYs **98A** and **98B**.[271] Taking advantage of this methodology, asymmetric diindolizine-fused BODIPY could also be synthesized by performing the reaction firstly with an electron-rich alkyne and lastly with an electron-deficient one (Scheme 96).

BODIPYs fused with two indolizine units exhibit a broad absorption spectrum, ranging from 600 to 800 nm, which compared to the precursor, show a remarkable redshift. The fluorescence emission spectra are also consistent with the expected bathochromic shift, and it is around 900 nm, and the quantum yield is low, as expected when the NIR emission is reached. The catalytic cycle begins with the coordination of BODIPY with $CpRh(III)X_2$, forming intermediate **98a**. This intermediate then undergoes cyclorhodation, generating the classic five-membered rhodacyclic species **98b**. Next, the insertion of the alkyne into the N–Rh or C–Rh bond of **98b** results in the formation of a seven-membered rhodacycle, either **98c** or **98d**, respectively. Finally, the reductive elimination of **98c** or **98d** produces the product **98A/B**. The active $CpRh(III)X_2$ species is regenerated with the help of CuX_2. Delcamp and colleagues focused their research mainly on the development of infrared-emissive indolizines. Expanding on earlier work on indolizine-squaraine dyes and rhodindolizine dyes,[272,273] in 2019, they reported the synthesis of C1, C3, and C5 cyanine-indolizines **99A–C** from phenyl indolizine precursors and methine bridges in the presence of perchloric acid (Scheme 97).[274] UV–vis–NIR absorption measurements in DCM, MeCN, DMSO, and a 1 : 1 MeCN : H_2O mixture revealed that increasing the length of the methine bridges caused a redshift in absorption. Among the six newly synthesized dyes, the C5 derivative demonstrated the

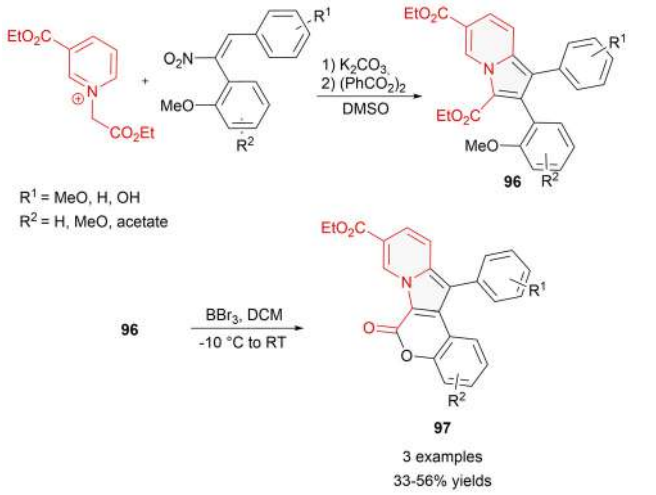

Scheme 95

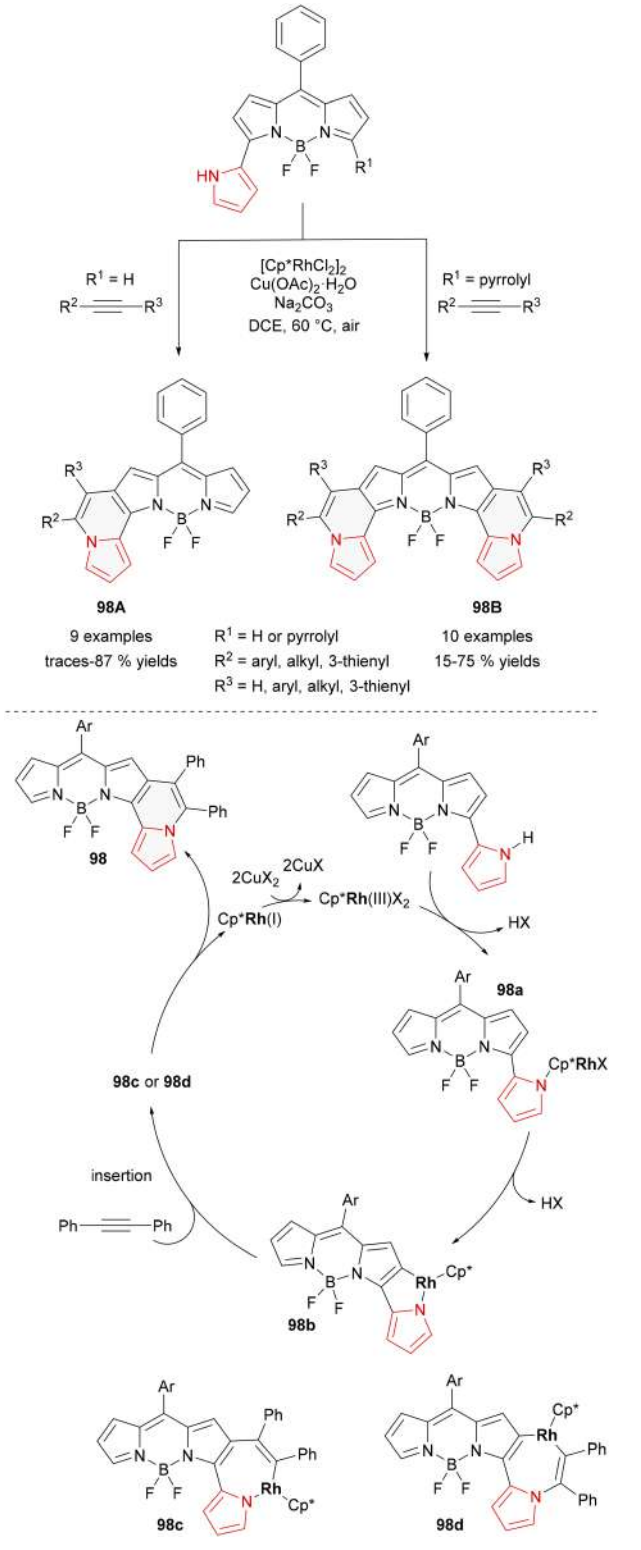

Scheme 96

highest quantum yields for a dye emitting near 900 nm, ranging from 1 to 3%, depending on the solvent.

In 2024 they managed to reach the SWIR region, bathochromically shifting the absorption and emission of existing xanthene–indolizine dyes through the substitution of O with Si and the addition of a dimethylaminoaryl substituent to the indolizine core.[275] Three different SiRos **100A–C** were obtained *via* a deoxygenation reaction followed by a silylation cyclization reaction and subsequent oxidation to yield the silicon-substituted xanthene core. A palladium-catalyzed C–H activation reaction is then used to install the respective indolizine **100a**, **b** and **c** donors. A Grignard reaction followed by an acidic work-up yields the final SiRos fluorophores as perchlorate salts (Scheme 98). These dyes obtained have λ_{em} max peaks of 1300 nm, 1557 nm and 1700 nm in DCM, along with fluorescence quantum yields of 0.0056%, 0.0025% and 0.0011%, respectively.

The same group also proposed the substitution of oxygen with P═O to achieve Phospha-RosIndolizine (**101**), which exhibited a bathochromically shifted emission at 1450 nm, compared to SiRos1300 (Scheme 99).[276] The synthetic pathway followed the same steps as those for the previously mentioned fluorophore, with the exception of the second step, where $PhPCl_2$ was used as the phosphorus source, and TBAB as the oxidating agent.

With the ambition to push the photophysical properties of dyes even deeper to the infrared region, Delcamp's group was able to exploit the antiaromatic characteristic of the central five-membered ring of the fluorenium dyes first presented by Grzybowski and co-workers[277] to obtain FluIndz **102** (Scheme 100).[278] Thanks to these new structures, which are a combination of a fluorenium dye and different substituted indolizines, emission at 2000–2500 nm was possible. In conclusion, Delcamp and colleagues have made substantial strides in advancing infrared-emissive indolizines, with each successive modification pushing the emission wavelengths further into the infrared region. This has resulted in a deeper understanding of the photophysical properties of indolizine-based dyes but also provided an ambitious drive to expand their applicability to a broader range of infrared applications, providing a unique contrast with earlier works, which were more limited to the visible or near-infrared region.

The unsubstituted indolizine absorbs ultraviolet radiation and emits violet–blue light.[279,280] Adding electron-donating groups (auxochromes) obviously shift both absorption and emission bathochromically.

Fusion of the indolizine with benzene rings gradually shifts the absorption bathochromically, although the strength of the effect depends heavily on the pattern of fusion. In the case of benzo[1,2-*b*]indolizine **65** the effect is rather small and becomes stronger in the case of benzo[*a*]indolizines (**66B**, Table 1). The fluorescence quantum yields of π-expanded indolizines vary but they tend to be large, often exceeding 40%. This is particularly visible in the case of pyrido[2,3-*b*]indolizines **70** (Table 1). The hybrid dyes possessing a coumarin-type structure and indolizine scaffold (pyranoindolizines **76**) have a strong greenish–yellow emission. Strong polarization induced by the presence of electron-withdrawing C═O groups at positions 1 and 2 (dyes **90D**) causes a very strong bathochromic shift of both absorption and emission (to 620 nm). A moderate bathochromic shift can also be observed in the case of thie-

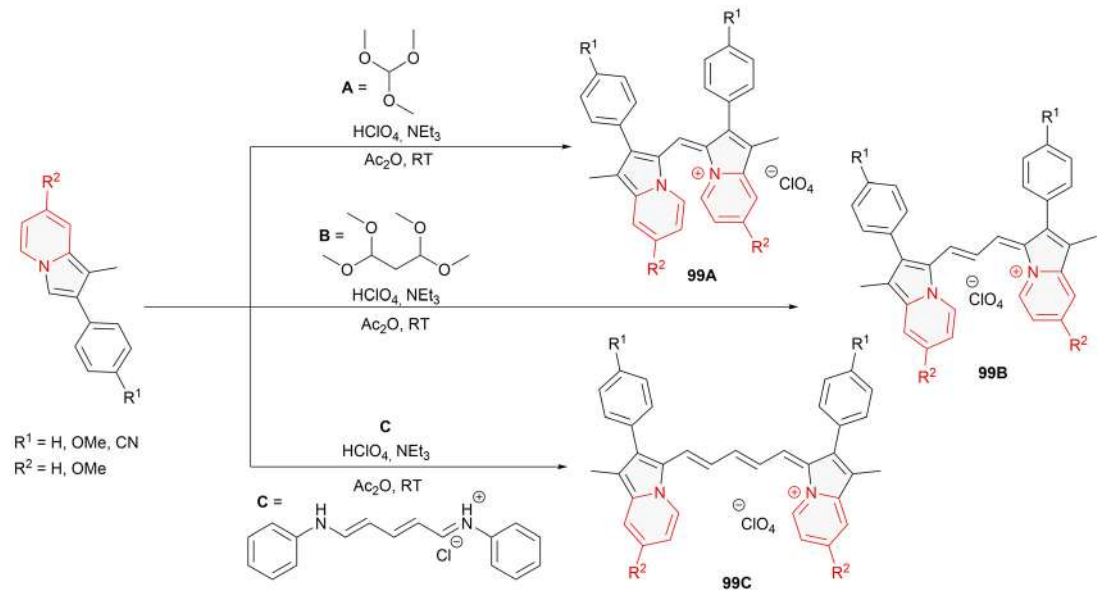

Scheme 97

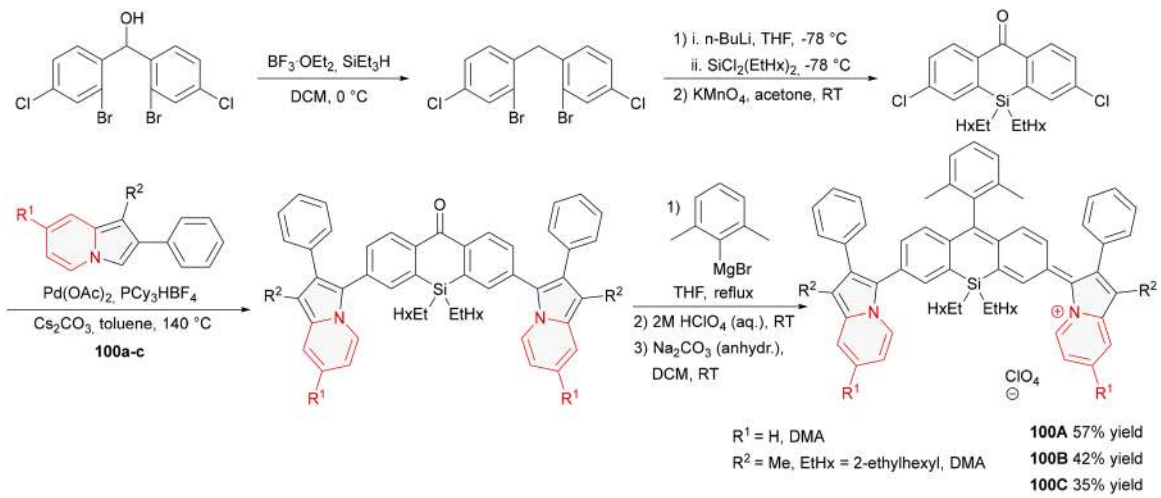

Scheme 98

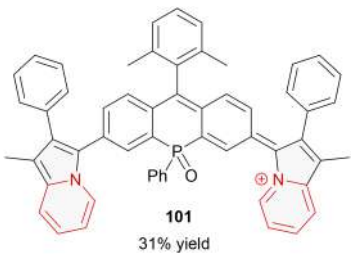

Scheme 99

noindolizines and azacyclazines (**84** and **91**, Table 1). Naturally blue emission of indolizine can be transformed into red emission with significant π-expansion of the chromophore (see dyes **82**). Delcamp's groundbreaking work has proved that by using indolizine as an electron-rich moiety, which replaces the classical dialkylamino group in cyanine and rhodamine dyes, it is possible to move the emission to NIR and by combining this approach with replacing oxygen with silicon, emission can even move to the NIR-2 region of the electromagnetic spectrum (**99A/C**, **100A/C**, **101** and **102**, Table 1). A small fluorescence quantum yield was still large enough to enable fluorescence imaging.

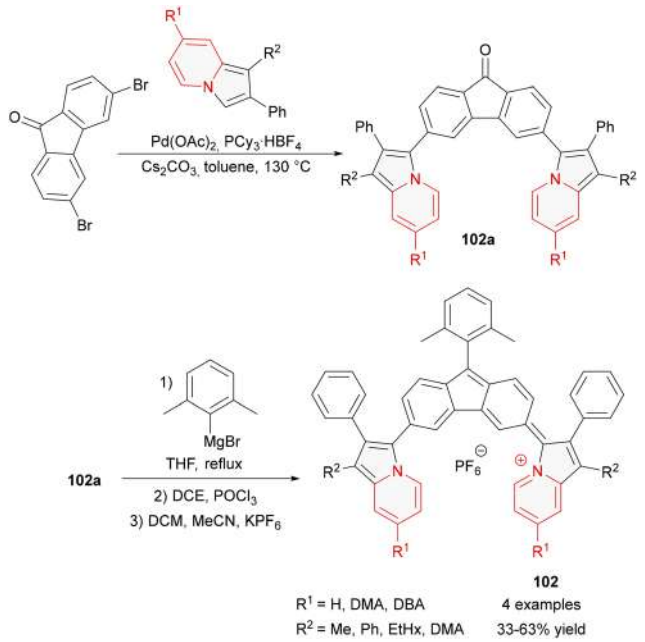

Scheme 100

6. Summary and outlook

In spite of the long history of indolizines, which translates to the existence of many classical synthetic methodologies, in the last decade numerous new strategies have been developed. Collectively, the new synthesis strategies highlight the compatibility of indolizines with changing targets in modern organic chemistry.[281–283] One pivotal factor is the availability of starting materials possessing a diverse range of substituents. Limited availability typically causes minuscule usage unless a very unique pattern of substituents can be obtained.

The difference in availability and stability was always a big advantage of pyridines over pyrroles as favored starting materials in indolizine synthesis. In this respect, the most notable recent trend is the strong development of methods starting from pyrrole derivatives. They have two key advantages. First of all, many methods starting from pyrrole derivatives rely on straightforward acid–base catalysis rather than on transition metals. Secondly, they offer access to unique substitution patterns on the indolizine core.

Indolizine synthesis often relies on the presence of various reactive functional groups in the substrate structures. These groups undergo transformations into one of the core atoms. In this regard it is noteworthy to point out that developments of the last decade enabled, for the first time, indolizine cores to be built that possessed key functional groups such as NH_2, NR_2, OH and CHO without the need for post-functionalization (Table 2).

Among many interesting developments of the last decade, the unveiling of the following methods deserves particular attention: (1) Gou's method, transforming *N*-methyl pyridinium salts into indolizines **39** with an elaborated Pd/Cu catalytic system;[84] (2) Duan's method, furnishing 6-hydroxyindolizines **42** from pyrrole-2-carbaldehyde and 4-halogenated acetoacetic ester;[203] (3) Gu's approach, in which scandium triflate catalyzes the transformation of 1-(2,2-diethoxyethyl)pyrroles and methyl acetoacetate into heavily substituted indolizines **54**;[219] (4) the synthesis of 2-formylindolizines **21** from 2-acetylpyridines and cinnamaldehydes;[129] and (5) the simple preparation of pyrrolo[2,1,5-*cd*]indolizines **89** from indolizines and alkynes.[261] Indolizine and its simple derivatives emit violet–blue light. In view of the global search for new materials possessing desirable optoelectronic properties, it is therefore not surprising that major developments in the last years have focused on methods leading to π-expanded indolizines. Moreover, due to its intrinsic electron-rich character, an indolizine core seems to be an ideal candidate for an electron-donating moiety in cross-conjugated chromophores. Interestingly, π-expanded derivatives are still mostly prepared from pyridine and quinolines. From humble beginnings, developments in the field of π-expanded indolizines have culminated in the work of Delcamp and co-workers, who demonstrated the trans-

Table 1 Photophysical data for representative π-expanded indolizines

Dye	λ_{abs} max range [nm]	Molar absorption coefficient range ε_{max} [M^{-1} cm^{-1}]	λ_{em} max range [nm]	Fluorescence quantum yield range Φ_{fl} [%]
65[230]	270, 340, 440	—	490–520 ≈ 10	
66A/B[232]	370–550	5000–14 000	490–830 < 1–58	
70[235]	350–470	—	460–490	40–80
71[236]	420–440	—	500–550	10–25
76[243]	430–510	16 000–30 000	450–650 < 1–92	
80D[251]	430–480	2100–23 000	500–620	5–80
84[256]	250–320	25 000–64 000	421–487	5–25
91[263]	388–356	—	518–532 ≈ 15	
93[265]	390–400	—	420–600	33–38
94[266]	415–428	—	406–520	—
82[252]	430–600	—	500–620	3–75
98A/B[271]	600–800	44 000–180 000	900 < 1–9	
99A/C[274]	640–830	11 000–210 000	690–900 < 1–3	
100A/C[275]	1100–1440	35 000–122 000	1300–1700	0.0011–0.0033
101[276]	1294	61 000	1450	Not calculated
102[278]	1400–2000	20 000–46 000	2000–2500	Not calculated

Table 2 Synthetic accessibility of indolizines possessing key functional groups

Functional group	Position	Ref.
CHO	2	128 and 129
CHO	3	148
CHO	5	207 and 209
NH_2	2	201
NH_2	3	139
NHR	3	138, 140 and 186
NR_2	1	121–126
OH	2	242 and 243
OH	6	203 and 209

formation of indolizines into cyanine-type dyes with spectacular emissions in the near infra-red part of the electromagnetic spectrum.[274–278] Notwithstanding this progress, there are still numerous synthetic limitations that have to be overcome in the near future. The main envisioned areas for synthetic exploration are as follows: (1) densely substituted indolizines and π-expanded indolizines; (2) the transformation of indolizines into polar, water-soluble probes for fluorescence imaging; (3) and finally the development of a straightforward method for the preparation of unsubstituted indolizine. Although indolizines have been known for over 130 years, there are still numerous possible structures that have never been assembled or investigated. We hope that in addition to organizing knowledge on this topic, this review will serve as a catalyst to spark further studies.

Author contributions

Writing – original draft: J.S.A.B., B.G., D.T.G.; writing – review & editing: J.S.A.B., B.G., D.T.G.

Data availability

There are no data supporting this article since this is a review article.

Conflicts of interest

There are no conflicts to declare.

Acknowledgements

This work was financially supported by the Foundation for Polish Science (TEAM POIR.04.04.00-00-3CF4/16-00).

References

1 A. Angeli, *Gazz. Chim. Ital.*, 1890, **26**, 753–761.
2 A. E. Tschitschibabin, Tautomerie in der Pyridin–Reihe, *Berichte Dtsch. Chem. Ges. B Ser.*, 1927, **60**, 1607–1617.
3 E. T. Borrows and D. O. Holland, The chemistry of the pyrrocolines and the octahydropyrrocolines, *Chem. Rev.*, 1948, **42**, 611–643.
4 *Heterocyclic Compounds*, ed. H. R. Ing and R. C. Elderfield, WILEY, 1952, vol. 3.
5 T. Uchida and K. Matsumoto, Methods for the Construction of the Indolizine Nucleus, *Synthesis*, 1976, 209–236.
6 H. L. Blewitt, *Special Topics in Heterocyclic Chemistry*, Wiley, 2009, vol. 30.
7 F. J. Swinbourne, J. H. Hunt and G. Klinkert, in *Advances in Heterocyclic Chemistry*, Elsevier, 1979, vol. 23, pp. 103–170.
8 B. Sadowski, J. Klajn and D. T. Gryko, Recent advances in the synthesis of indolizines and their π-expanded analogues, *Org. Biomol. Chem.*, 2016, **14**, 7804–7828.
9 J. Hui, Y. Ma, J. Zhao and H. Cao, Recent advances in the synthesis of indolizine and its derivatives by radical cyclization/cross-coupling, *Org. Biomol. Chem.*, 2021, **19**, 10245–10258.
10 S. Ghosh and K. Biswas, Microwave-assisted synthesis of indolizine derivatives: Recent developments: A review (2003-present), *Synth. Commun.*, 2024, **54**, 505–525.
11 A. A. Nevskaya, A. D. Zinoveva, E. V. Van der Eycken and L. G. Voskressensky, Synthetic Strategies for the Construction of Indolizines and Indolizine-fused Compounds: Thienoindolizines and Indolizinoindoles, *Asian J. Org. Chem.*, 2023, **12**, e202300359.
12 Priyanka, P. Rani, Kiran and J. Sindhu, Indolizine: A Promising Framework for Developing a Diverse Array of C–H Functionalized Hybrids, *ChemistrySelect*, 2023, **8**, e202203531.
13 X. Liu, H. Fu, Q. Hu and H. Cao, Recent Advances on the Construction of Functionalized Indolizine and Imidazo [1,2-*a*]pyridine Derivatives, *Chem. Rec.*, 2024, **24**, e202400135.
14 J. Huang, C. Li, X. Li, G. Li, Z. Yang, Y. Yu, Y. Xie, H. Huang, F. Yu and Z. He, Recent Advances in the Development of Indolizine Scaffolds: Synthetic Methodology and Mechanistic Insights, *Chin. J. Chem.*, 2025, **43**, 315–348.
15 J. P. Michael, Indolizidine and quinolizidine alkaloids, *Nat. Prod. Rep.*, 2008, **25**, 139–165.
16 Y. R. Song, C. W. Lim and T. W. Kim, Synthesis and photophysical properties of 1,2-diphenylindolizine derivatives: fluorescent blue-emitting materials for organic light-emitting device, *Luminescence*, 2016, **31**, 364–371.
17 Y. Ge, A. Liu, J. Dong, G. Duan, X. Cao and F. Li, A simple pH fluorescent probe based on new fluorophore indolizine for imaging of living cells, *Sens. Actuators, B*, 2017, **247**, 46–52.
18 E. Kim, M. Koh, J. Ryu and S. B. Park, Combinatorial Discovery of Full-Color-Tunable Emissive Fluorescent Probes Using a Single Core Skeleton, 1,2-Dihydropyrrolo

[3,4-*b*]indolizin-3-one, *J. Am. Chem. Soc.*, 2008, **130**, 12206–12207.

19 H. Son, D. Kim, S. Kim, W. Gi Byun and S. Bum Park, Unveiling the Structure-Fluorogenic Property Relationship of Seoul-Fluor-Derived Bioorthogonal Tetrazine Probes, *Angew. Chem., Int. Ed.*, 2024, **62**, e202421982.

20 G. Kaupp, D. Hunkler and I. Zimmermann, Fragmentierende Ringverengungen des 1:2-Addukts aus Pyridin und Acetylendicarbonsäure-dimethylester, *Chem. Ber.*, 1982, **115**, 2467–2477.

21 J. Agejas, A. M. Cuadro, M. Pastor, J. J. Vaquera, J. L. García-Navío and J. Alvarez-Builla, *N*-(Pyridylmethyl) azinium Salts: Precursors of Pyridyl-stabilised Azinium *N*-Ylides, *Tetrahedron*, 1995, **51**, 12425–12438.

22 J. Štetinová, M. Dandárová, J. Kováč, D. Mesárošová and J. Leško, 1,3-Dipolar cycloadditions of ylide of 5-nitro-2-furfurylpyridinium bromide in indolizine synthesis, *Collect. Czech. Chem. Commun.*, 1982, **47**, 1738–1745.

23 Y. Miki, Y. Hiroishi, H. Hachiken and S. Takemura, Acid-catalyzed reactions of 1- and 3-(α-hydroxybenzyl)indolizines, *J. Heterocycl. Chem.*, 1991, **28**, 45–48.

24 T. Shimo, M. Ohe, K. Somekawa and O. Tsuge, Preparation of 3-(2H-pyran-2-on-6-yl)indolizines and the diels-alder reactions with some olefinic and acetylenic dienophiles, *J. Heterocycl. Chem.*, 1991, **28**, 1831–1833.

25 O. Tsuge, S. Kanemasa, S. Kuraoka and S. Takenaka, *N*-(trimethylsilylmethyl) pyridinium trifluoromethanesulfonates as facile precursors for nonstabilized pyridinium methylides, *Chem. Lett.*, 1984, **13**, 279–280.

26 Y. Miki, H. Kinoshita, T. Yoshimaru, S. Takemura and M. Ikeda, A Novel Synthesis of Pyrrolo[2,1,5-*de*]quinolizinones (Cycl[3.3.2]azinones), *Heterocycles*, 1987, **26**, 199.

27 N. S. Prostakov, A. V. Varlamov, N. Saksena, A. A. Savina, G. Datta Rai and L. V. Maslova, γ-Trimethylsilyl(triphenylsilyl) pyridines in syntheses of silicon-containing pyridinium ylids and indolizines, *Chem. Heterocycl. Compd.*, 1980, **16**, 748–751.

28 A. Tanaka and T. Usui, Studies on Furan Derivatives. VII. Reactions of α-(2-Furyl)-β-(5-nitro-2-furyl) ethynyl, *Chem. Pharm. Bull.*, 1979, **27**, 3078–3085.

29 I.-M. Moise, E. Bîcu, A. Farce, J. Dubois and A. Ghinet, Indolizine-phenothiazine hybrids as the first dual inhibitors of tubulin polymerization and farnesyltransferase with synergistic antitumor activity, *Bioorg. Chem.*, 2020, **103**, 104184.

30 D. He, Y. Xu, J. Han, H. Deng, M. Shao, J. Chen, H. Zhang and W. Cao, Facile one-pot tandem synthesis of perfluoroalkylated indolizines under metal-free mild conditions, *Tetrahedron*, 2017, **73**, 938–944.

31 Z. Karamshahi and R. Ghorbani-Vaghei, Facile synthesis of indolizines using layered double hydroxides@poly(p-phenylenediamine) as a catalyst with a green tool (neat technology), *Appl. Organomet. Chem.*, 2020, **34**, 1–12.

32 S. Chandrashekharappa, K. N. Venugopala, C. Tratrat, F. M. Mahomoodally, B. E. Aldhubiab, M. Haroun, R. Venugopala, M. K. Mohan, R. S. Kulkarni, M. V. Attimarad, S. Harsha and B. Odhav, Efficient synthesis and characterization of novel indolizines: exploration of in vitro COX-2 inhibitory activity and molecular modelling studies, *New J. Chem.*, 2018, **42**, 4893–4901.

33 M. Choyal, L. K. Agarwal and N. Gupta, Regioselective Synthesis of Functionalized Indolizines under Mild Conditions, *Org. Prep. Proced. Int.*, 2023, **55**, 358–371.

34 E. Georgescu, F. Georgescu, A. Nicolescu, F. Dumitrascu, C. Draghici, M. M. Popa, A. T. Marinoiu and C. Deleanu, Indolizines and azaindolizines substituted with a phenylureidobenzoyl moiety by 1,3-dipolar cycloadditon of their corresponding n-ylides with acetylenes, *Rev. Roum. Chim.*, 2018, **63**, 535–543.

35 G. Mahanthesha, T. Suresh and Y. D. Bodke, Synthesis and characterization of (3-Chlorophenyl)(1-(5-phenyl-1,3,4-oxadiazol-2-yl)indolizin-3-yl)methanone derivatives as anticancer and antimicrobial agents, *Chem. Data Collect.*, 2021, **33**, 100691.

36 M. C. Sardaru, A. M. Craciun, C. M. Al Matarneh, I. A. Sandu, R. M. Amarandi, L. Popovici, C. I. Ciobanu, D. Peptanariu, M. Pinteala, I. I. Mangalagiu and R. Danac, Cytotoxic substituted indolizines as new colchicine site tubulin polymerisation inhibitors, *J. Enzyme Inhib. Med. Chem.*, 2020, **35**, 1581–1595.

37 K. N. Venugopala, S. Chandrashekharappa, C. Tratrat, P. K. Deb, R. D. Nagdeve, S. K. Nayak, M. A. Morsy, P. Borah, F. M. Mahomoodally, R. P. Mailavaram, M. Attimarad, B. E. Aldhubiab, N. Sreeharsha, A. B. Nair, O. I. Alwassil, M. Haroun, V. Mohanlall, P. Shinu, R. Venugopala, M. Kandeel, B. P. Nandeshwarappa and Y. F. Ibrahim, Crystallography, Molecular Modeling, and COX-2 Inhibition Studies on Indolizine Derivatives, *Molecules*, 2021, **26**, 3550.

38 K. N. Venugopala, S. Chandrashekharappa, P. K. Deb, N. A. Al-Shar'i, M. Pillay, P. Tiwari, D. Chopra, P. Borah, R. Tamhaev, L. Mourey, C. Lherbet, B. E. Aldhubiab, C. Tratrat, M. Attimarad, A. B. Nair, N. Sreeharsha, R. P. Mailavaram, R. Venugopala, V. Mohanlall and M. A. Morsy, Identification of potent indolizine derivatives against *Mycobacterial tuberculosis*: *In vitro* anti-TB properties, *in silico* target validation, molecular docking and dynamics studies, *Int. J. Biol. Macromol.*, 2024, **274**, 133285.

39 R. D. Nagdeve, J. S. Thakur, S. Chandrashekharappa, K. M. Bairagi, P. K. Deb, K. N. Venugopala, P. K. Mondal, M. Polentarutti, O. I. Alwassil, V. Mohanlall and S. K. Nayak, Crystal structure, hydrogen bonding interactions, Hirshfeld surfaces, energy frameworks, and DFT calculation of Diethyl 3-(4-substitutedbenzoyl)indolizine-1,2-dicarboxylates, *J. Mol. Struct.*, 2024, **1308**, 138080.

40 S. U. Shende, P. Tiwari, S. Kidwai, R. Singh and S. Chandrashekharappa, Synthesis and structural elucidation of novel quaternary pyridinium salt and indolizine derivatives as an anti-tubercular agent: *In Silico* and *In Vitro* screening, *J. Mol. Struct.*, 2025, **1321**, 139851.

41 I. Baussanne, O. Firstova, A. B. Dediu, C. Larosa, B. Furdui, I. O. Ghinea, A. Thomas, S. Chierici, R. Dinica and M. Demeunynck, Interest of novel *N*-alkylpyridinium-indolizine hybrids in the field of Alzheimer's disease: Synthesis, characterization and evaluation of antioxidant activity, cholinesterase inhibition, and amyloid fibrillation interference, *Bioorg. Chem.*, 2021, **116**, 105390.

42 M. Kong, X. Zhou, Q. Chen, F. Zhang and Y. Zhao, Efficient synthesis of novel indolizine C-nucleoside analogues via coupling of sugar alkynes, pyridines and α-bromo carbonyl compounds in one pot, *Carbohydr. Res.*, 2021, **505**, 108337.

43 B. Shen, B. Li and B. Wang, Rh(III)-Catalyzed Oxidative Annulation Leading to Substituted Indolizines by Cleavage of C(sp^2)-H/C(sp^3)-H Bonds, *Org. Lett.*, 2016, **18**, 2816–2819.

44 R. Settambolo, A. Caiazzo and R. Lazzaroni, An original approach to 5,6-dihydroindolizines from 1-allylpyrroles by a tandem hydroformylation/cyclization/dehydration sequence, *Tetrahedron Lett.*, 2001, **42**, 4045–4048.

45 R. Settambolo, S. Savi, A. Caiazzo and R. Lazzaroni, A shortcut hydroformylation route to 7-formyl-5,6-dihydroindolizine from 1-allyl-2-formylpyrrole, *J. Organomet. Chem.*, 2001, **619**, 241–244.

46 R. Lazzaroni, R. Settambolo, S. Rocchiccioli and G. Guazzelli, From chiral and prochiral *N*-allylpyrroles to stereodefined pyrrole fused architectures: A particular application of the rhodium-catalyzed hydroformylation, *J. Organomet. Chem.*, 2007, **692**, 1812–1816.

47 G. Guazzelli and R. Settambolo, 4-Indolylbutanals from rhodium-catalyzed hydroformylation of allylindoles as precursors of benzofused indolizines, *Tetrahedron Lett.*, 2007, **48**, 6034–6038.

48 R. Settambolo, Crucial Role of β-Elimination in Determining Regio- and Chemoselectivity of the Rhodium-Catalyzed Hydroformylation of *N*-Allylpyrroles: A New Approach to 5,6-Dihydroindolizines, *Synthesis*, 2010, 2915–2921.

49 B. Wang, X. Zhang, J. Li, X. Jiang, Y. Hu and H. Hu, Preparation of indolizine-3-carboxamides and indolizine-3-carbonitriles by 1,3-dipolar cycloaddition of *N*-(cyanomethyl)pyridinium ylides to alkenes in the presence of tetrakispyridinecobalt(II) dichromate or manganese(IV) oxide, *J. Chem. Soc., Perkin Trans. 1*, 1999, 1571–1576.

50 X. Zhang, W. Cao, X. Wei and H. Hu, A Convenient Synthesis Of 1-Acyl Indolizines by 1,3-Dipolar Cycloaddition Reactions of Pyridinium Ylides and α,β-Unsaturated Aldehydes or Ketones in the Presence of Tetrakis-Pyridine Cobalt Dichromate, *Synth. Commun.*, 1997, **27**, 1395–1403.

51 Y. Tominaga, Y. Ichihara, T. Mori, C. Kamio and A. Hosomi, Polarized ethylene. V. Synthesis of 1-substituted indolizine, pyrazolo[1,5-*a*]pyridine, and their related compounds using methoxyethylene derivatives, *J. Heterocycl. Chem.*, 1990, **27**, 263–268.

52 P. B. Terent'ev, S. M. Vinogradova and A. N. Kost, Reaction of 2- and 4-vinylpyridines with phenacylpyridinium ylids, *Chem. Heterocycl. Compd.*, 1980, **16**, 506–511.

53 X. Wei, Y. Hu, T. Li and H. Hu, A facile one-step synthesis of aromatic indolizines by 1,3-dipolar cycloaddition of pyridinium and related heteroaromatic ylides with alkenes in the presence of TPCD [$Copy_4(HCrO_4)_2$], *J. Chem. Soc., Perkin Trans. 1*, 1993, 2487–2489.

54 C. Wang, H. Hu, J. Xu and W. Kan, One-pot synthesis of indolizine via 1,3-dipolar cycloaddition using a sub-equivalent amount of $K_2Cr_2O_7$ as an efficient oxidant under base free conditions, *RSC Adv.*, 2015, **5**, 41255–41258.

55 Y. Liu, H. Hu, J. Zhou, W. Wang, Y. He and C. Wang, Application of primary halogenated hydrocarbons for the synthesis of 3-aryl and 3-alkyl indolizines, *Org. Biomol. Chem.*, 2017, **15**, 5016–5024.

56 C. Li, X. Tang, X. He, S. Xue, J. Xu and Y. Li, Copper-catalyzed formation of indolizine derivatives via one-pot reactions of chalcones, benzyl bromides and pyridines, *Tetrahedron*, 2020, **76**, 131347.

57 H. Kim, M. Shin and E. Kim, Fluorescent Fluoride Sensor Based on Indolizine Core Skeleton for Bioimaging, *Bull. Korean Chem. Soc.*, 2021, **42**, 95–98.

58 B. Zhou, H. Xv, K. Zhang, X. Han, S. Liu, J. He, J. Sun, Y. Li and Y. Liu, An efficient approach to indolizine-3-carboxylates *via* Cu(I)-promoted decarboxylative cycloaddition of alkenoic acids, *Tetrahedron*, 2025, **171**, 134423.

59 X. Zhang, G. P. Lu, Z. B. Xu and C. Cai, Facile Synthesis of Indolizines via 1,3-Dipolar Cycloadditions in [Omim]Br: The Promotion of the Reaction through Noncovalent Interactions, *ACS Sustainable Chem. Eng.*, 2017, **5**, 9279–9285.

60 D. A. Rusanov, S. Mutasim Alfadul, E. Y. Portnyagina, E. A. Silyanova, N. A. Kuznetsov, K. E. Podpovetny, A. V. Samet, V. V. Semenov and M. V. Babak, Toward "E–Ring–Free" Lamellarin Analogues: Synthesis and Preliminary Biological Evaluation, *ChemBioChem*, 2023, **24**, 1–8.

61 A. V. Aksenov, N. A. Arutiunov, N. K. Kirilov, D. A. Aksenov, I. Y. Grishin, N. A. Aksenov, H. Wang, L. Du, T. Betancourt, S. C. Pelly, A. Kornienko and M. Rubin, -Annulation of pyridinium ylides with 1-chloro-2-nitrostyrenes unveils a tubulin polymerization inhibitor, *Org. Biomol. Chem.*, 2021, **19**, 7234–7245.

62 Y. Chen, Y. Liu, H. Yang, Z. Li and X. Xu, Catalyst-free oxidative [3 + 2]-annulation of (2-nitroethene-1,1-diyl)bis (methylsulfane) and pyridinium ylides: Efficient synthesis of (methylsulfanyl)indolizines heterocycles, *J. Heterocycl. Chem.*, 2023, **60**, 1894–1902.

63 V. A. Motornov, A. A. Tabolin, Y. V. Nelyubina, V. G. Nenajdenko and S. L. Ioffe, Copper-mediated oxidative [3 + 2]-annulation of nitroalkenes and pyridinium ylides: general access to functionalized indolizines and efficient synthesis of 1-fluoroindolizines, *Org. Biomol. Chem.*, 2019, **17**, 1442–1454.

64 V. A. Motornov, A. A. Tabolin, Y. V. Nelyubina, V. G. Nenajdenko and S. L. Ioffe, Copper-catalyzed [3 + 2]-cycloaddition of α-halonitroalkenes with azomethine ylides: facile synthesis of multisubstituted pyrrolidines and pyrroles, *Org. Biomol. Chem.*, 2021, **19**, 3413–3427.

65 N. Zhang, H. Ma, C. W. Cheung, F.-G. Zhang, M. Jasiński, J.-A. Ma and J. Nie, Regioselective [3 + 2] cycloaddition of di/trifluoromethylated hydrazonoyl chlorides with fluorinated nitroalkenes: a facile access to 3-di/trifluoroalkyl-5-fluoropyrazoles, *Org. Biomol. Chem.*, 2023, **21**, 5040–5045.

66 S. Jana, S. Adhikari, M. R. Cox and S. Roy, Regioselective synthesis of 4-fluoro-1,5-disubstituted-1,2,3-triazoles from synthetic surrogates of α-fluoroalkynes, *Chem. Commun.*, 2020, **56**, 1871–1874.

67 S. Shu, L. Wang, L. Lv and Z. Li, Copper-Catalyzed [3 + 2] Annulation of Pyridinium Ylides with α-CF_3 Ketones: Synthesis of Functionalized 2-Fluoroindolizines, *Asian J. Org. Chem.*, 2023, **12**, 10–13.

68 V. Ramesh, N. S. Devi, M. Velusamy and S. Shanmugam, Catalyst free Synthesis of Highly Functionalized Indolizines from In Situ Generated Pyridinium Ylides via One-Pot Multicomponent Reaction, *ChemistrySelect*, 2019, **4**, 3717–3721.

69 J.-Q. Zhang, D. Hu, J. Song and H. Ren, [3 + 2]-Annulation of gem-Difluoroalkenes and Pyridinium Ylides: Access to Functionalized 2-Fluoroindolizines, *J. Org. Chem.*, 2021, **86**, 4646–4660.

70 X. Fang, Y.-M. Wu, J. Deng and S.-W. Wang, Synthesis of monofluorinated indolizines and their derivatives by the 1,3-dipolar reaction of *N*-ylides with fluorinated vinyl tosylates, *Tetrahedron*, 2004, **60**, 5487–5493.

71 K. Wu and Q.-Y. Chen, Synthesis of Fluorinated Indolizines and 4*H*-Pyrrolo[1,2-*a*]benzimidazoles via 1,3-Dipolar Cycloaddition of Fluoroalkenes to *N*-Ylides, *Synthesis*, 2002, 0035–0040.

72 Y. Ma, H. Zhang, X. Du, S. Fang, K. Yin, G. Du, Z. Tian and Z. Zhou, β,β-Difluoro Peroxides as Fluorinated C2-Building Blocks for the Construction of Functionalized Indolizines, *Molecules*, 2024, **29**, 5927.

73 J. Xu, H. Hu, Y. Liu, X. Wang, Y. Kan and C. Wang, Four–Component Reaction for the Synthesis of Indolizines by Copper–Catalyzed Aerobic Oxidative Dehydrogenative Aromatization, *Eur. J. Org. Chem.*, 2017, 257–261.

74 Y. Zhang, W. Wang, J. Sun and Y. Liu, TEMPO-catalyzed decarboxylation reactions for the synthesis of 1,2-unsubstituted indolizines, *J. Heterocycl. Chem.*, 2020, **57**, 210–217.

75 Y. Liu, Y. Zhang, Y.-M. Shen, H.-W. Hu and J.-H. Xu, Regioselective synthesis of 3-acylindolizines and benzo-analogues via 1,3-dipolar cycloadditions of *N*-ylides with maleic anhydride, *Org. Biomol. Chem.*, 2010, **8**, 2449–2456.

76 F. Wang, Y. Shen, H. Hu, X. Wang, H. Wu and Y. Liu, Copper(II)-Catalyzed Indolizines Formation Followed by Dehydrogenative Functionalization Cascade to Synthesize 1-Bromoindolizines, *J. Org. Chem.*, 2014, **79**, 9556–9566.

77 J. Ma, W. Lin and H.-L. Qin, (*E*,)-2-Methoxyethene-1-sulfonyl fluoride as a precursor of acetylene for synthesis of C1/C2 non-functionalized pyrrolo[2,1-*a*]isoquinoline derivatives, *New J. Chem.*, 2023, **47**, 16332–16336.

78 J. Zheng, X. He, H. Xu, H. Liu and W. Yang, A formal [3 + 2] annulation reaction of propargyl sulfonium compounds and: N -ylides: Access to pyrrolo[2,1- *a*] quinolines, pyrrolo [2,1- *a*] phthalazines and indolizines, *Org. Biomol. Chem.*, 2020, **18**, 8867–8875.

79 C. Jadala, V. Ganga Reddy, N. Hari Krishna, N. Shankaraiah and A. Kamal, Base-mediated 1,3-dipolar cycloaddition of pyridinium bromides with bromoallyl sulfones: a facile access to indolizine scaffolds, *Org. Biomol. Chem.*, 2020, **18**, 8694–8701.

80 K. K. Dong and Q. Huang, Metal-free synthesis of novel indolizines from chromones and pyridinium salts via 1,3-dipolar cycloaddition, ring-opening and aromatization, *Tetrahedron Lett.*, 2019, **60**, 1871–1874.

81 S. A. Babu, A. A. M. Mohan, N. Paul, J. Mathew and J. John, Tandem Reactions of Electrophilic Indoles toward Indolizines and Their Subsequent Transformations through Pd(II)-Mediated C–H Functionalization to Access Polyring-Fused *N*-Heterocycles, *ACS Omega*, 2024, **9**, 16196–16206.

82 S. A. Babu, R. A. R., N. P. R., V. K. Omanakuttan, R. P., S. Varughese and J. John, Unprecedented access to functionalized pyrrolo[2,1-*a*]isoquinolines from the domino reaction of isoquinolinium ylides and electrophilic benzannulated heterocycles, *Org. Biomol. Chem.*, 2021, **19**, 1807–1817.

83 W.-M. Shu, J.-X. He, X.-F. Zhang, S. Wang and A.-X. Wu, TFA-Mediated DMSO-Participant Sequential Oxidation/1,3-Dipolar Cycloaddition Cascade of Pyridinium Ylides for the Assembly of Indolizines, *J. Org. Chem.*, 2019, **84**, 2962–2968.

84 Q. Gou, Q. Zhu, M. Deng, W. Li, X. Ran, J. Xie, H. Huang, X. Tan and M. Zhu, The regioselective annulation of *N*-methylpyridinium ylides with alkenes enabled by palladium catalysis: access to 3-unsubstituted indolizine derivatives, *Org. Chem. Front.*, 2022, **9**, 4719–4725.

85 X. Hou, S. Zhou, Y. Li, M. Guo, W. Zhao, X. Tang and G. Wang, Synthesis of Indolizines from Pyridinium Salts and Ethyl Bromodifluoroacetate, *Org. Lett.*, 2020, **22**, 9313–9318.

86 A. V. Botezatu, G. Horincar, I. O. Ghinea, B. Furdui, G. E. Bahrim, V. Barbu, F. Balanescu, L. Favier and R. M. Dinica, Whole-cells of Yarrowia lipolytica applied in "one pot" indolizine biosynthesis, *Catalysts*, 2020, **10**, 1–16.

87 A. V. D. Botezatu, G. E. Bahrim, C. V. Ungureanu, A. C. Busuioc, B. Furdui and R. M. Dinica, Green "one-pot" fluorescent bis-indolizine synthesis with whole-cell plant biocatalysis, *Green Process. Synth.*, 2023, **12**, 20230046.

88 M. M. Vieira, B. T. Dalberto, F. L. Coelho and P. H. Schneider, Ultrasound-promoted regioselective syn-

thesis of chalcogeno-indolizines by a stepwise 1,3-dipolar cycloaddition, *Ultrason. Sonochem.*, 2020, **68**, 105228.

89 M. M. Vieira, B. T. Dalberto, N. B. Padilha, H. C. S. Junior, F. S. Rodembusch and P. H. Schneider, Experimental and theoretical insights on the photophysical properties of ester-substituted indolizines, *J. Mol. Struct.*, 2024, **1295**, 136726.

90 M. M. Vieira, B. T. Dalberto, N. B. Padilha, H. C. S. Junior, F. S. Rodembusch and P. H. Schneider, Fast and efficient one-pot ultrasound-mediated synthesis of solid state (full color tunable) fluorescent indolizine derivatives, *Dyes Pigm.*, 2023, **216**, 111332.

91 D. Qiu, H. Ni and Y. Su, Halogen Bond-Catalyzed Oxidative Annulation of *N*-Alkyl Pyridinium Salts and Alkenes with Air as a Sole Oxidant: Metal-free Synthesis of Indolizines, *ChemistrySelect*, 2023, **8**, 1–5.

92 I. Yavari, M. Naeimabadi, R. Hosseinpour and M. Halvagar, A One-Pot Synthesis of Highly Functionalized Indolizines by 1,3-Dipolar Cycloaddition of Azomethine Ylides and Phosphorylated Hydroxyketenimines, *Synlett*, 2016, 2601–2605.

93 I. Yavari, K. Ghafouri, M. Naeimabadi and M. R. Halvagar, A Synthesis of Functionalized 2-Indolizin-3-yl-1,3-benzothiazoles from 1-(1,3-Benzothiazol-2-ylmethyl)pyridinium Iodide and -Acetylenic Esters, *Synlett*, 2017, 243–245.

94 I. Yavari and M. Naeimabadi, Synthesis of 3-(quinolin-2-yl)indolizines through iodine-mediated sp^3C–H functionalization of azaarenes, *Synth. Commun.*, 2018, **48**, 632–637.

95 Y. Fang, L. He, W. Pan and Y. Yang, Iodine-mediated one-pot synthesis of C-3 acylated indolizines from pyridines, aryl methyl ketones and acrylate derivatives, *Tetrahedron*, 2019, **75**, 3767–3771.

96 I. Yavari, J. Sheykhahmadi, M. Naeimabadi and M. R. Halvagar, Iodine-mediated sp^3 C-H functionalization of methyl ketones: a one-pot synthesis of functionalized indolizines via the 1,3-dipolar cycloaddition reaction between pyridinium ylides and ynones, *Mol. Divers.*, 2017, **21**, 1–8.

97 Q. Zhang, K. Ablajan, B. Wang, H. Ma and Z. Guo, One–Pot Synthesis of Indolizines Using TBHP as the Methylene Source Under Metal–Free Condition, *Eur. J. Org. Chem.*, 2020, 262–266.

98 X. Zhang, J. Zhang, Z. Liu, W. Bi, J. Shen and G. Li, Efficient Solvent-Free Synthesis of Indolizines Using CuBr Catalyst from Pyridine, Acetophenone, and Electron-Deficient Alkenes, *Molecules*, 2024, **29**, 2061.

99 X. Zhang, P. Wang, J. Han, X. Guo and B. Chen, CuBr-Catalyzed Synthesis of Indolizines from Pyridine, Acetophenone and Chalcone under Solvent-Free Conditions, *ChemistrySelect*, 2018, **3**, 3014–3017.

100 M. He, N. Chen, J. Wang and S. Peng, Rhodium-Catalyzed Regiodivergent [3 + 2] and [5 + 2] Cycloadditions of Quinolinium Ylides with Alkynes, *Org. Lett.*, 2019, **21**, 5167–5171.

101 H. R. Chen, Z. Y. Hu, H. L. Qin and H. Tang, A novel three-component reaction for constructing indolizine-containing aliphatic sulfonyl fluorides, *Org. Chem. Front.*, 2021, **8**, 1185–1189.

102 F. Li, X. Tang, Y. Xu, C. Wang, L. Zhang, J. Zhang, J. Liu, Z. Li and L. Wang, Hemoglobin-Catalyzed Synthesis of Indolizines Under Mild Conditions, *Eur. J. Org. Chem.*, 2019, 7720–7724.

103 T. Douglas, A. Pordea and J. Dowden, Iron-Catalyzed Indolizine Synthesis from Pyridines, Diazo Compounds, and Alkynes, *Org. Lett.*, 2017, **19**, 6396–6399.

104 B. K. Malviya, A. K. Jassal, M. Karnatak, V. P. Verma and S. Sharma, Electro-Oxidative sp^3C-H Bond Functionalization and Annulation Cascade: Synthesis of Novel Heterocyclic Substituted Indolizines, *J. Org. Chem.*, 2022, **87**, 2898–2911.

105 R. Sarkar, T. Chaudhuri, A. Karmakar and C. Mukhopadhyay, Synthesis and photophysics of selective functionalized π-conjugated, blue light emitting, highly fluorescent C7-imidazo indolizine derivatives, *Org. Biomol. Chem.*, 2015, **13**, 11674–11686.

106 J. Sun, H. Hu, F. Wang, H. Wu and Y. Liu, Copper(II)-catalyzed cleavage of carbon–carbon triple bond to synthesize 1,2,3-triesterindolizines, *RSC Adv.*, 2014, **4**, 36498–36501.

107 S. Tiwari and D. S. Rawat, Regiodivergent Synthesis of Densely Functionalized Indolizines via (2 + 2 + 1) Cycloaddition, *J. Org. Chem.*, 2023, **88**, 6805–6815.

108 M. Piltan and S. Kalantari, One–Pot Synthesis of Regioselective Polysubstituted Indolizines via Three–Component Reactions of Dialkyl Acetylendicarboxylates, Dialkylchloro Malonates, and Pyridines, *J. Heterocycl. Chem.*, 2017, **54**, 743–748.

109 M. Piltan and S. Kalantari, Synthesis of New Polysubstituted Indolizines from Pyridine, Bromonitromethane, and Dialkyl Acetylenedicarboxylates, *J. Heterocycl. Chem.*, 2017, **54**, 301–304.

110 J. Sun, J. Han, Y. Zhang and Y. Liu, $CuBr_2$-Promoted Multicomponent Aerobic Reaction for the Synthesis of 1,2,3-Triaroylindolizines, *J. Heterocycl. Chem.*, 2019, **56**, 2253–2261.

111 X. Li, Z. Chen, W. Chen, X. Xie, H. Zhou, Y. Liao, F. Yu and J. Huang, B_2pin_2-Mediated Cascade Cyclization/Aromatization Reaction: Facial Access to Functionalized Indolizines, *Org. Lett.*, 2022, **24**, 7372–7377.

112 X. Zhang, X. Cao, L. Wei, Z. Wang, Y. Wei, L. Xu and G. Huang, A pyridine-boryl radical mediated cascade reaction towards the synthesis of indolizines: a computational mechanistic analysis, *Org. Chem. Front.*, 2024, **11**, 4168–4175.

113 S. A. Roy, J. Zgheib, C. Zhou and B. A. Arndtsen, Palladium catalyzed synthesis of indolizines via the carbonylative coupling of bromopyridines, imines and alkynes, *Chem. Sci.*, 2021, **12**, 2251–2256.

114 S. Roy, An unusual route to synthesize indolizines through a domino SN_2/michael addition reaction between 2-mercaptopyridine and nitroallylic acetates, *Eur. J. Org. Chem.*, 2019, 765–769.

115 H. Zhu, N. Shao, T. Chen and H. Zou, Functionalized heterocyclic scaffolds derived from Morita–Baylis–Hillman Acetates, *Chem. Commun.*, 2013, **49**, 7738–7740.

116 S. Dong, J. Huang, H. Sha, L. Qiu, W. Hu and X. Xu, Copper-catalyzed formal [1 + 2 + 2]-annulation of alkyne-tethered diazoacetates and pyridines: Access to polycyclic indolizines, *Org. Biomol. Chem.*, 2020, **18**, 1926–1932.

117 I. V. Nechaev, G. V. Cherkaev, P. N. Solyev and N. V. Boev, Synthesis and Aerobic Dehydrogenation of Indolizin-1-ol Derivatives, *J. Org. Chem.*, 2021, **86**, 4220–4235.

118 I. V. Nechaev and G. V. Cherkaev, Indolizin-1-ols with Charged Electron Acceptors: A Direct Way to 3*H*-Indolizinium-1-olates with Donor Functions, *J. Org. Chem.*, 2022, **87**, 14137–14154.

119 I. V. Nechaev and G. V. Cherkaev, Radical and Ionic Reactions of Indolizin-1-ols: Synthesis of 3-Arylsulfanyl-, 3-(Tropon-2-yl)- and 3-(Tropolon-5-ylazo)-1-hydroxyindolizines from 3,3-Difluorocyclopropenes, *J. Org. Chem.*, 2021, **86**, 7687–7700.

120 I. V. Nechaev and G. V. Cherkaev, 3-Thioxo-3H-indolizinium-1-olates and related pseudo-cross-conjugated heterocyclic mesomeric betaines: synthesis and spectral features, *J. Org. Chem.*, 2024, **89**, 11215–11232.

121 B. Yan and Y. Liu, Gold-Catalyzed Multicomponent Synthesis of Aminoindolizines from Aldehydes, Amines, and Alkynes under Solvent-Free Conditions or in Water, *Org. Lett.*, 2007, **9**, 4323–4326.

122 T. Antón-Cánovas, S. Achelle, M. Paz Fernández-Liencres, A. Navarro, F. Alonso and J. Rodríguez-López, Acidochromism of amino-substituted indolizine chromophores: Towards white light emission, *J. Mol. Liq.*, 2023, **380**, 121758.

123 M. Mohammod, V. Guguloth, C. S. Vasam and N. S. Thirukovela, Clean and efficient synthesis of 3-aminoindolizines in one-pot using recyclable CuCN/[bmim]PF_6 system, *Synth. Commun.*, 2022, **52**, 1254–1267.

124 G. H. Dang, H. Q. Lam, A. T. Nguyen, D. T. Le, T. Truong and N. T. S. Phan, Synthesis of indolizines through aldehyde-amine-alkyne couplings using metal-organic framework Cu-MOF-74 as an efficient heterogeneous catalyst, *J. Catal.*, 2016, **337**, 167–176.

125 V. Guguloth, R. Balaboina, S. Paidakula, N. S. Thirukovela and R. Vadde, AgI-promoted one-pot synthesis of aminoindolizines via sequential Mannich-Grignard addition and intramolecular cyclization in water, *J. Heterocycl. Chem.*, 2021, **58**, 900–904.

126 H. Wang, D. Shi, Y. Meng, M. Hai, Y. Shu, B. Liu and Z. Duan, Synthesis of Propargylamine and Indolazine Derivatives via Three-Component Reaction Catalyzed by CuO_x/CeO_2 Materials, *ChemistrySelect*, 2023, **8**, e202300472.

127 M. J. González-Soria and F. Alonso, Substrate-Controlled Divergent Synthesis of Enaminones and Pyrroles from Indolizines and Nitroso Compounds, *Adv. Synth. Catal.*, 2019, **361**, 5005–5017.

128 Y. C. Yuan, T. Z. Liu and B. X. Zhao, Metal-Free Catalyzed Synthesis of Fluorescent Indolizine Derivatives, *J. Org. Chem.*, 2021, **86**, 12737–12744.

129 K. Zeng, R. Mei, S. Dechert, L. Ackermann and K. Zhang, A recyclable stereoauxiliary aminocatalyzed strategy for one-pot synthesis of indolizine-2-carbaldehydes, *Commun. Chem.*, 2023, **6**, 40.

130 J.-L. Wang, G.-Y. Wu, J.-N. Luo, J.-L. Liu and C.-X. Zhuo, Catalytic Intermolecular Deoxygenative Coupling of Carbonyl Compounds with Alkynes by a Cp*Mo(II)-Catalyst, *J. Am. Chem. Soc.*, 2024, **146**, 5605–5613.

131 Z. Chen, P. Liang, X. Ma, H. Luo, G. Xu, T. Liu, X. Wen, J. Zheng and H. Ye, Catalyst-Free Annulation of 2-Pyridylacetates and Ynals with Molecular Oxygen: An Access to 3-Acylated Indolizines, *J. Org. Chem.*, 2019, **84**, 1630–1639.

132 Y. Liu, Y. Yu, Y. Fu, Y. Liu, L. Shi, H. Li and W. Wang, Transition-metal-free synthesis of indolizines via [3 + 2]-annulation from α-bromoenals and 2-substituted azaarenes, *Org. Chem. Front.*, 2017, **4**, 2119–2123.

133 Z. Chen, P. Liang, F. Xu, Z. Deng, L. Long, G. Luo and M. Ye, Metal-Free Aminothiation of Alkynes: Three-Component Tandem Annulation toward Indolizine Thiones from 2-Alkylpyridines, Ynals, and Elemental Sulfur, *J. Org. Chem.*, 2019, **84**, 12639–12647.

134 J. Zheng, L. Chen, X. Liu, W. Xu, Y. Wang, Q. He, H. Liu, M. Ye, G. Luo and Z. Chen, I_2-Catalyzed Intermolecular Cyclization to Synthesis of 3-Acylated Indolizines, *ChemistrySelect*, 2020, **5**, 13198–13201.

135 L. He, Y. Yang, X. Liu, G. Liang, C. Li, D. Wang and W. Pan, Iodine-Mediated Oxidative Cyclization of 2-(Pyridin-2-yl)acetate Derivatives with Alkynes: Condition-Controlled Selective Synthesis of Multisubstituted Indolizines, *Synthesis*, 2020, 459–470.

136 D. Yang, Y. Yu, Y. Wu, H. Feng, X. Li and H. Cao, One-Pot Regiospecific Synthesis of Indolizines: A Solvent-Free, Metal-Free, Three-Component Reaction of 2-(Pyridin-2-yl) acetates, Ynals, and Alcohols or Thiols, *Org. Lett.*, 2018, **20**, 2477–2480.

137 J. Li, D. Yang, H. Wang, B. Zhu and H. Cao, Zn-Catalyzed [3 + 2]-Annulation Strategy: Straightforward Access to Aminoalkyl Indolizines, *Eur. J. Org. Chem.*, 2019, 6611–6617.

138 K. Bedjeguelal, H. Bienaymé, A. Dumoulin, S. Poigny, P. Schmitt and E. Tam, Discovery of protein–protein binding disruptors using multi-component condensations small molecules, *Bioorg. Med. Chem. Lett.*, 2006, **16**, 3998–4001.

139 G. Martinez-Ariza, B. T. Mehari, L. A. G. Pinho, C. Foley, K. Day, J. C. Jewett and C. Hulme, Synthesis of fluorescent heterocycles via a Knoevenagel/[4 + 1]-cycloaddition cascade using acetyl cyanide, *Org. Biomol. Chem.*, 2017, **15**, 6076–6079.

140 A. H. Jadhav, A. B. Atar and J. Kang, A [bmim]Cl-promoted domino protocol using an isocyanide-based [4 + 1]-cycloaddition reaction for the synthesis of diversely functiona-

lized 3-Alkylamino-2-Alkyl/aryl/hetero-Aryl indolizine-1-carbonitriles under solvent-free conditions, *New J. Chem.*, 2020, **44**, 3241–3248.

141 C. Lu, M. Ye, M. Li, Z. Zhang, Y. He, L. Long and Z. Chen, Transition-metal-switchable divergent synthesis of nitrile-containing pyrazolo[1,5-*a*]pyridines and indolizines, *Chin. Chem. Lett.*, 2021, **32**, 3967–3971.

142 D. R. Joshi and I. Kim, Regioselective Synthesis of 1-Cyano-3-arylindolizines: Construction of Pyrroles via DDQ–Mediated Ring Closure of Cyclopropyl Pyridines, *Adv. Synth. Catal.*, 2022, **364**, 3016–3022.

143 S. Lee, W. Kim and I. Kim, Divergent Annulation Modes of (*Z*,)-4-Aryl-4-oxo-2-(pyridin-2-yl)but-2-enenitrile and Methyl Nitroacetate: Selective Access to 2-Acyl-4H-quinolizin-4-one, Isoxazole, and 2-Acylindolizine, *ACS Omega*, 2024, **9**, 38126–38141.

144 Y. Fang, F. Li, Y. Yang, X. Liu and W. Pan, Iodine Mediated Base-Controlled Regio-Selective Annulation of 2-(Pyridin-2-yl)acetate Derivatives with Acrylic Esters for the Synthesis of Indolizines, *Adv. Synth. Catal.*, 2020, **362**, 1333–1344.

145 C. J. Lu, X. Yu, Y. T. Chen, Q. B. Song and H. Wang, Indolizine synthesis: Via copper-catalyzed cyclization of gem -difluoroalkenes and 2-(pyridin-2-yl)acetate derivatives, *Org. Chem. Front.*, 2020, **7**, 2313–2318.

146 Y.-D. Li, W.-M. Zhang, K.-H. Zhao, C.-H. Zhang and S.-J. Yan, I_2–catalyzed cascade annulation of 2-(pyridin–2–yl)acetate derivatives with N,N–dimethylenamine ketones: Site-selective synthesis of functionalized indolizines, *Tetrahedron*, 2024, **159**, 134015.

147 K. Su, X. Guo, L. Zhu, Y. Liu, Y. Lu and B. Chen, Indolizine synthesis: Via radical cyclization and demethylation of sulfoxonium ylides and 2-(pyridin-2-yl)acetate derivatives, *Org. Chem. Front.*, 2021, **8**, 4177–4182.

148 H. Li, X. Li, Y. Yu, J. Li, Y. Liu, H. Li and W. Wang, Synthesis of Indolizines via Reaction of 2-Substitued Azaarenes with Enals by an Amine-NHC Relay Catalysis, *Org. Lett.*, 2017, **19**, 2010–2013.

149 K. Chen, R. Zhou, G. Zhu, L. Tang, L. Huang and Q. He, Metal-Free Synthesis of Functionalized Indolizines via a Cascade Michael/SN_2/Aromatization Reaction of 2-Alkylazaarene Derivatives with Bromonitroolefins, *ACS Omega*, 2024, **9**, 49980–49985.

150 Y. Yang, T. Wu and Y. Fang, Palladium-Catalyzed Regioselective Coupling of Secondary Propargyl Carbonates and Ethyl 2-(pyridin-2-yl)acetate Derivatives: Facile Access to C-3 Benzylated Indolizines, *Synlett*, 2018, 1909–1913.

151 T. Wu, M. Chen and Y. Yang, Synthesis of Indolizines via Palladium Catalyzed Annulation of Propargyl Carbonates and 2-(Pyridin-2-yl)acetonitrile Derivatives, *J. Org. Chem.*, 2017, **82**, 11304–11309.

152 R. Bonneau, Y. N. Romashin, M. T. H. Liu and S. E. MacPherson, Synthesis of 3-substituted indolizines from the reaction of chlorocarbenes with 2-vinylpyridine, *J. Chem. Soc., Chem. Commun.*, 1994, 509–510.

153 C. Han, Y. Liu, X. Tian, F. Rominger and A. S. K. Hashmi, Dual Gold/Silver Catalysis: Indolizines from 2-Substituted Pyridine Derivatives via a Tandem C(sp^3)–H Alkynylation/Iminoauration, *Org. Lett.*, 2021, **23**, 9480–9484.

154 L. A. Zeoly, L. V. Acconcia, M. T. Rodrigues, H. Santos, R. A. Cormanich, J. C. Paniagua, A. Moyano and F. Coelho, One-pot organocatalyzed synthesis of tricyclic indolizines, *Org. Biomol. Chem.*, 2023, **21**, 3567–3581.

155 R. A. Cormanich, L. A. Zeoly, H. Santos, N. S. Camilo, M. Bühl and F. Coelho, Origin of the Diastereoselectivity of the Heterogeneous Hydrogenation of a Substituted Indolizine, *J. Org. Chem.*, 2020, **85**, 11541–11548.

156 K. C. Sekgota, M. Isaacs, H. C. Hoppe, R. Seldon, D. F. Warner, S. D. Khanye and P. T. Kaye, Propylphosphonic acid anhydride–mediated amidation of Morita–Baylis–Hillman–derived indolizine-2-carboxylic acids, *J. Chem. Res.*, 2021, **45**, 674–678.

157 Y. Xue, X. He, T. Yang, Y. Wang, Z. Liu, G. Zhang, Y. Wang, K. Wang, L. Zhang and L. Zhang, Discovery of fused heterocyclic carboxamide derivatives as novel α7-nAChR agonists: Synthesis, preliminary SAR and biological evaluation, *Eur. J. Med. Chem.*, 2019, **182**, 111618.

158 X. Lv, P. Gao, X. Zhao and Z. Jiang, Metal-Free Construction of Multisubstituted Indolizines via Intramolecular Amination of Allylic Alcohols, *J. Org. Chem.*, 2023, **88**, 9459–9468.

159 Y. Li, W. Xiong, Z. Zhang and T. Xu, Synthesis of indolizine derivatives triggered by the oxidative addition of aroyl chloride to Pd(0) complex, *J. Org. Chem.*, 2020, **85**, 6392–6399.

160 X. Xiao, P. Han, H. Zhou and J. Liu, Palladium-Catalyzed Difunctionalization of Alkenes by Relay Coupling with Propargylic Pyridines: Synthesis of Indolizine and Indolizinone-Containing Bisheterocycles, *J. Org. Chem.*, 2021, **86**, 18179–18191.

161 K. H. Oh, S. M. Kim, S. Y. Park and J. K. Park, Base-Controlled Cu-Catalyzed Tandem Cyclization/Alkynylation for the Synthesis of Indolizines, *Org. Lett.*, 2016, **18**, 2204–2207.

162 T. A. C. Goulart, D. F. Back and G. Zeni, Copper–Catalyzed Carbon–Nitrogen/Carbon–Selenium Bonds Formation: Synthesis of 2-(Organochalcogenyl)–indolizines, *Adv. Synth. Catal.*, 2017, **359**, 1901–1911.

163 S. R. Pathipati, A. Van Der Werf and N. Selander, Diastereoselective Synthesis of Polycyclic Indolizines with 2-(2-Enynyl)pyridines and Enamines, *Org. Lett.*, 2018, **20**, 3691–3694.

164 D. K. Paluru, S. Mahesh, F. Ahmad and R. Vijaya Anand, A Cascade Synthesis of Hetero-arylated Triarylmethanes Through a Double 5-endo-dig Cyclization Sequence, *Chem. – Asian J.*, 2019, **14**, 4688–4695.

165 R. Lodhi, A. K. Patel and S. Samanta, AgOTf/Et_3N Cooperative Catalysis Enabled One-Pot Access to α-(Indolizinylethyl)-Substituted *N*-Sulfonyl Ketimines via an Imino-Alkyne Cyclization, *Asian J. Org. Chem.*, 2022, **11**, 1–6.

166 F. Li, Q. Yang, M. Y. Liu, P. X. An, Y. L. Du and Y. B. Wang, Ag(I)-Mediated Annulation of 2-(2-Enynyl)pyridines and Propargyl Amines to Access 1-(2*H*-Pyrrol-3-yl)indolizines, *J. Org. Chem.*, 2024, **89**, 304–312.

167 M. D. Rossler, C. T. Hartgerink, E. E. Zerull, B. L. Boss, A. K. Frndak, M. M. Mason, L. A. Nickerson, E. O. Romero, J. E. Van De Burg, R. J. Staples and C. E. Anderson, Au(I)-Catalyzed Synthesis of Trisubstituted Indolizines from 2-Propargyloxypyridines and Methyl Ketones, *Org. Lett.*, 2019, **21**, 5591–5595.

168 C. E. Anderson, H. I. Bos, D. M. Dreher, C. T. Hartgerink, C. J. Scholtens and R. J. Staples, Synthesis of Ester-Substituted Indolizines from 2-Propargyloxypyridines and 1,3-Dicarbonyls, *J. Org. Chem.*, 2022, **87**, 10241–10249.

169 K. Xiao, C. Zhu, M. Lin, C. Song and J. Chang, Base–Promoted Cycloisomerization for the Synthesis of Indolizines and Related Heterocycles, *ChemistrySelect*, 2018, **3**, 11270–11272.

170 Y. He, W. Yin, J. Wang, J. Huang, X. Pang, C. Gan, F. Yang and C. Huang, I_2-Catalyzed intramolecular dehydrogenative aminooxygenation of alkynes to acylated imidazo[1,2-*a*] pyridines and indolizines, *Org. Chem. Front.*, 2018, **5**, 1772–1776.

171 I. Ziccarelli, R. Amuso, R. Mancuso, A. Maggiore, G. Lamberti, P. Vitale, V. Maiorano, L. Veltri and B. Gabriele, Synthesis and Photochemical Characterization of Indolizine Fluorophores Obtained by a Multicomponent Palladium Iodide–Catalyzed Oxidative Aminocarbonylation Approach, *Eur. J. Org. Chem.*, 2024, e202400013.

172 M. Meazza, L. A. Leth, J. D. Erickson and K. A. Jørgensen, Indium(III)-catalyzed Aza-Conia-Ene Reaction for the Synthesis of Indolizines, *Chem. – Eur. J.*, 2017, **23**, 7905–7909.

173 Q.-L. Yang, R.-C. Ma, Z.-H. Li, W.-W. Li, G.-R. Qu and H.-M. Guo, Electrochemically-initiated intramolecular 1,2-amino oxygenation of alkynes: facile access to formyl- and acyl-substituted indolizines, *Org. Chem. Front.*, 2022, **9**, 4990–4997.

174 H.-Y. Zhao, Y. Wang, X.-L. Cao, Q.-F. Pang, H. Wang and Y. Pan, Synthesis of fused tricyclic indolizines by intramolecular silver-mediated double cyclization of 2-(pyridin-2-yl)acetic acid propargyl esters, *RSC Adv.*, 2017, **7**, 24011–24014.

175 R. Tallarita, L. M. Jacobsen, B. J. Elvers, S. Richter, S. S. M. Bandaru, J. V. Correia and C. Schulzke, Synthesis of Seven Indolizine-Derived Pentathiepines: Strong Electronic Structure Response to Nitro Substitution in Position C-9, *Molecules*, 2023, **29**, 216.

176 L. Wolff, S. S. M. Bandaru, E. Eger, H.-N. Lam, M. Napierkowski, D. Baecker, C. Schulzke and P. J. Bednarski, Comprehensive Evaluation of Biological Effects of Pentathiepins on Various Human Cancer Cell Lines and Insights into Their Mode of Action, *Int. J. Mol. Sci.*, 2021, **22**, 7631.

177 R. Tallarita, L. M. Jacobsen, S. S. M. Bandaru, B. J. Elvers and C. Schulzke, The Role of –OEt Substituents in Molybdenum-Assisted Pentathiepine Formation—Access to Diversely Functionalized Azines, *Molecules*, 2024, **29**, 3806.

178 F. Rao, M. Cheng, Z. Hu, X. Chen, S. Zhao and Z. Chen, Gold-catalyzed intermolecular tandem cyclization/[4 + 3] cycloaddition of 2-(1-alkynyl)-cyclopropyl pyridines with nitrones: an efficient strategy for the synthesis of [1,2]oxazepino[5,4-*a*] indolizines, *Org. Chem. Front.*, 2024, **11**, 3685–3691.

179 R.-R. Liu, S.-C. Ye, C.-J. Lu, B. Xiang, J. Gao and Y.-X. Jia, Au-catalyzed ring-opening reactions of 2-(1-alkynyl-cyclopropyl)pyridines with nucleophiles, *Org. Biomol. Chem.*, 2015, **13**, 4855–4858.

180 R. Wang, Q. Xu and T. R. Hoye, Reactions of Electrophilic Allenoates [and Isocyanates/Isothiocyanates] with a 2-Alkynylpyridine via a Free Carbene Intermediate, *Org. Lett.*, 2024, **26**, 7805–7808.

181 Q. Xu and T. R. Hoye, Free carbenes from complementarily paired alkynes, *Nat. Chem.*, 2024, **16**, 1083–1092.

182 A. L. Guzman, A. N. Mann and T. R. Hoye, Alkynes to (Free) Carbenes to Polycyclic Cyclopropanes, *J. Am. Chem. Soc.*, 2024, **146**, 28642–28647.

183 S. Chuprakov, F. W. Hwang and V. Gevorgyan, Rh-Catalyzed Transannulation of Pyridotriazoles with Alkynes and Nitriles, *Angew. Chem., Int. Ed.*, 2007, **46**, 4757–4759.

184 S. Chuprakov and V. Gevorgyan, Regiodivergent Metal-Catalyzed Rearrangement of 3-Iminocyclopropenes into *N*-Fused Heterocycles, *Org. Lett.*, 2007, **9**, 4463–4466.

185 V. Helan, A. V. Gulevich and V. Gevorgyan, Cu-catalyzed transannulation reaction of pyridotriazoles with terminal alkynes under aerobic conditions: efficient synthesis of indolizines, *Chem. Sci.*, 2015, **6**, 1928–1931.

186 E. Wang, J. Luo, L. Zhang, J. Zhang and Y. Jiang, Copper-Catalyzed Oxidative [3 + 2] Cycloaddition of Enamines and Pyridotriazoles toward Indolizines, *Org. Lett.*, 2024, **26**, 1249–1254.

187 X. Hou, R. Wang, F. Fang, Z. Qu, J. Zhou, T. Yu, D. Wang, H. Liu and Y. Zhou, Rh(III)-Catalyzed C–H Activation/Annulation for the Construction of Quinolizinones and Indolizines, *Org. Lett.*, 2024, **26**, 4451–4456.

188 H. Kim, S. Kim, J. Kim, J.-Y. Son, Y. Baek, K. Um and P. H. Lee, One-Pot Synthesis of Indolizines via Sequential Rhodium-Catalyzed [2 + 1]-Cyclopropanation, Palladium-Catalyzed Ring Expansion, and Oxidation Reactions from Pyridotriazoles and 1,3-Dienes, *Org. Lett.*, 2017, **19**, 5677–5680.

189 R. Adam, S. Alom, B. Abarca and R. Ballesteros, Reactivity of [1,2,3]Triazolo[1,5-*a*]pyridines as 1,3-dipoles, *Tetrahedron*, 2016, **72**, 8436–8441.

190 S. Roy, S. K. Das and B. Chattopadhyay, Cobalt(II)-based Metalloradical Activation of 2-(Diazomethyl)pyridines for Radical Transannulation and Cyclopropanation, *Angew. Chem., Int. Ed.*, 2018, **57**, 2238–2243.

191 F. Ahmad, P. K. Ranga, S. Fatma, A. Kumar and R. Vijaya Anand, Cu(II)-Catalyzed [3 + 2]-Annulation of 2-Pyridinyl-substituted p-Quinone Methides with Enaminones:

Access to Functionalized Indolizine Derivatives, *Adv. Synth. Catal.*, 2023, **365**, 3271–3276.

192 C. Zhang, W. Wang, X. Zhu, L. Chen, H. Luo, M. Guo, D. Liu, F. Liu, H. Zhang, Q. Li and J. Lin, Synthesis of Indolizines via Tf_2O-Mediated Cascade Reaction of Pyridyl-enaminones with Thiophenols/Thioalcohols, *Org. Lett.*, 2023, **25**, 1192–1197.

193 R. Monreal-Corona, À. Díaz-Jiménez, A. Roglans, A. Poater and A. Pla-Quintana, Indolizine Synthesis through Annulation of Pyridinium 1,4-Thiolates and Copper Carbenes: A Predictive Catalysis Approach, *Adv. Synth. Catal.*, 2023, **365**, 760–766.

194 W. Li, H. Wang, Y. Zhang, L. Zhao, P. Guo, H. Cao and X. Liu, Copper-Catalyzed Formal [4 + 1] Annulation toward Diverse Trifunctionalized Indolizines from Pyridinium 1,4-Zwitterionic Thiolates and Diazos, *J. Org. Chem.*, 2023, **88**, 7199–7207.

195 S. Sun, Y. Wei and J. Xu, Microwave-mediated stereocontrolled annulations of diazo(aryl)methyl(diaryl)phosphine oxides with pyridinium 1,4-zwitterionic thiolates, *Chem. Commun.*, 2022, **59**, 239–242.

196 B. Cheng, Y. Li, X. Zhang, S. Duan, H. Li, Y. He, Y. Li, T. Wang and H. Zhai, Two Reaction Modes of Pyridinium 1,4-Zwitterionic Thiolates with Sulfenes: Synthesis of 3*H*-1,2-Dithiole 2,2-Dioxides, 1,9a-Dihydropyrido[2,1-*c*,][1,4] thiazines, and Indolizines, *Org. Lett.*, 2020, **22**, 5817–5821.

197 B. Cheng, X. Zhang, Y. Li, H. Li, Y. He, Y. Li, T. Wang and H. Zhai, Synthesis of indolizines from pyridinium 1,4-zwitterionic thiolates and α-functionalized bromoalkanes via a stepwise [(5 + 1)−1] pathway, *Chem. Commun.*, 2020, **56**, 8396–8399.

198 A. Almaani, A. Takallou, Y. Lotfi Nosood, S. Al-Shidhani, M. Reza Hosseini, M. U. Anwar and A. Al-Harrasi, [(5 + 1)−1] Cyclization of Nitroepoxides to Pyridinium 1,4-Zwitterionic Thiolates for the Synthesis of Indolizine Derivatives, *Adv. Synth. Catal.*, 2025, **367**, e202400961.

199 P. Zhao, Z. C. Yu, L. F. Wang, Y. Zhou, Y. D. Wu, Y. Ma and A. X. Wu, I_2-Promoted in Situ Cyclization-Rethiolation Reaction: Synthesis of 2-Aliphatic- or Aromatic-Substituted Indolizines, *J. Org. Chem.*, 2022, **87**, 15197–15209.

200 X. Wu, P. Zhao, X. Geng, J. Zhang, X. Gong, Y. Wu and A. Wu, Direct Oxidative Cleavage of Multiple Csp^3−H Bonds and a C–C Bond in 2-(Pyridin-2-yl)acetate Derivatives: Formal [3 + 1 + 1] Synthesis of 3-(Pyridin-2-yl) indolizine Skeletons, *Org. Lett.*, 2017, **19**, 3319–3322.

201 O. Y. Kashner, K. O. Bocharov and G. E. Khoroshilov, The synthesis of 2-amino-3-carboxamideindolizines with using pyridinium salt and C-nucleophiles–derivatives acetonitrile, *Results Chem.*, 2024, **12**, 101861.

202 X.-S. Zhang, B. Wang, J. Jia, Y.-Q. Ge and J. Wang, Synthesis of 7-cyanoindolizine derivatives via a tandem reaction, *Heterocycl. Commun.*, 2017, **23**, 71–74.

203 G. Duan, H. Liu, L. Zhang, C. Yuan, Y. Li and Y. Ge, Access to 6-hydroxy indolizines and related imidazo[1,5-*a*] pyridines through the SN_2 substitution/condensation/tautomerization cascade process, *RSC Adv.*, 2021, **11**, 25624–25627.

204 Y. Li, S. Ren, G. Shi, C. Yuan, G. Duan and Y. Ge, Simple and commercially available imidazo[1,2-*a*]pyridine-8-carboxylic acid-based fluorescent pH probe for basic conditions, *J. Lumin.*, 2023, **255**, 119547.

205 R. Cui, Y. Gao, H. Ge, G. Shi, Y. Li, H. Liu, C. Ma, Y. Ge and C. Liu, A turn-on fluorescent probe based on indolizine for the detection of sulfite, *New J. Chem.*, 2022, **46**, 8088–8093.

206 W. Zhong, H. Zhu and H. Zou, "One-pot" cascade approach to 5,6-dihydroindolizines and indolizines from pyrrole-2-carbaldehydes and nitroethylenes, *Tetrahedron*, 2017, **73**, 3181–3187.

207 M. Gong, J. Guo, P. Jiang, Y. Zhang, Z. Fu and W. Huang, Facile Synthesis of Polysubstituted Indolizines via One-Pot Reaction of 1-Acetylaryl 2-Formylpyrroles and Enals, *Chem. – Asian J.*, 2020, **15**, 352–355.

208 Y.-Y. Zhang, L. Li, A.-J. Ma, W.-F. Wang and J.-B. Peng, Base-promoted [4 + 2] annulation of pyrrole-2-carbaldehyde derivatives with β,γ-unsaturated α-ketoesters: syntheses of 5,6-dihydroindolizines, *Org. Biomol. Chem.*, 2022, **20**, 8633–8637.

209 S. T. Dorai and S. Chandrashekharappa, Tandem Knoevenagel-Aldol Cyclization Towards Di and Trisubstituted Pyridines: Use of Malonaldehyde and Diethyl Malonate for the Synthesis of Indolizine, *Eur. J. Org. Chem.*, 2024, e202400906.

210 C. H. Escalante, F. A. Carmona-Hernández, A. Hernández-López, E. I. Martínez-Mora, F. Delgado and J. Tamariz, Cascade synthesis of indolizines and pyrrolo[1,2-*a*]pyrazines from 2-formyl-1-propargylpyrroles, *Org. Biomol. Chem.*, 2022, **20**, 396–409.

211 S. Kim, J. H. Lee, S. H. Yoon and I. Kim, A regioselective [4 + 2] annulation approach to 5-acylindolizine-7-carbonitriles: generation of poly-substituted pyridines, *Org. Biomol. Chem.*, 2021, **19**, 5806–5817.

212 D. R. Joshi and I. Kim, Michael-Aldol Double Elimination Cascade to Make Pyridines: Use of Chromone for the Synthesis of Indolizines, *J. Org. Chem.*, 2021, **86**, 10235–10248.

213 Y. Lee, D. R. Joshi, W. Namkung and I. Kim, Generation of a poly-functionalized indolizine scaffold and its anticancer activity in pancreatic cancer cells, *Bioorg. Chem.*, 2022, **126**, 105877.

214 X. Wang, X. Sun, N. Li, J. Chen, H. Zhang, H. Deng, J.-H. Lin and W. Cao, The synthesis of perfluoroalkylated indolizines *via* tandem cyclization/aromatization, *J. Fluor. Chem.*, 2021, **251**, 109900.

215 K. Lakshmikanth, S. M. Saini, S. T. Dorai and S. Chandrashekharappa, Tandem-Michael-cyclization cascade to make pyridines: Use of electron-deficient acetylenes for the synthesis of indolizines in aqueous media, *Tetrahedron*, 2023, **142**, 133516.

216 Y.-Q. Wang, L.-J. Chen, R.-L. Yang, M. Lang and J.-B. Peng, Oxidative [4 + 2] Annulation of Pyrrole-2-carbaldehyde

Derivatives with o-Hydroxyphenyl Propargylamines: Syntheses of 5,6,7-Trisubstituted Indolizines, *Chem. – Eur. J.*, 2024, **30**, e202402487.

217 L. Fu, J. Wang, X. Chen, T. Shi, Z. Shao, J. Chen, C. Tian, Z. Zhou, H. Zhu and J. Zhang, [4 + 2]-Annulation of prop-2-ynylsulfonium salts and *N*-substituted pyrrole-2-carboxaldehydes: access to indolizines containing a thioether group, *New J. Chem.*, 2022, **46**, 941–944.

218 X. Li, X. Xie and Y. Liu, Gold(I)-Catalyzed Cascade Hydroarylation/Cycloaromatization to Indolizines via Pyridine Ring Construction, *J. Org. Chem.*, 2016, **81**, 3688–3699.

219 W. Huang, S. Chen, J. Yang, A. El-Harairy, X. Wang, M. Li and Y. Gu, Modular Synthesis of Bicyclic and Tricyclic (Aza-) Arenes from Nucleophilic (Aza-)Arenes with Electrophilic Side Arms via [4 + 2] Annulation Reactions, *Adv. Synth. Catal.*, 2019, **361**, 4369–4378.

220 B. Kuzu, S. Gül, M. Tan, N. Menges and M. Balci, Synthesis of Indolizines by Dimerization of *N*-Propargylated Pyrroles via Allene Intermediates, *ChemistrySelect*, 2021, **6**, 2366–2372.

221 N. Shao, J. Li, H. Zhu, S. Zhang and H. Zou, Functionalized *N*-containing heterocyclic scaffolds derived from *N*-substituted pyrroles via inter- and intramolecular annulations, *Tetrahedron*, 2018, **74**, 6088–6094.

222 D. Miranda-Sánchez, C. H. Escalante, D. Andrade-Pavón, O. Gómez-García, E. Barrera, L. Villa-Tanaca, F. Delgado and J. Tamariz, Pyrrole-Based Enaminones as Building Blocks for the Synthesis of Indolizines and Pyrrolo[1,2-*a*]pyrazines Showing Potent Antifungal Activity, *Molecules*, 2023, **28**, 7223.

223 X. Li, J. Zhao, X. Xie and Y. Liu, Synthesis of functionalized indolizines via gold(I)-catalyzed intramolecular hydroarylation/aromatization of pyrrole-ynes, *Org. Biomol. Chem.*, 2017, **15**, 8119–8133.

224 S. Yi, D. Kim, W. Cho, J. H. Lee, J. H. Kwon, J. Kim and S. B. Park, Rational Design of Pyrido[3,2-*b*]indolizine as a Tunable Fluorescent Scaffold for Fluorogenic Bioimaging, *JACS Au*, 2024, **4**, 2896–2906.

225 X. Chen, X. Hu, Y. Deng, H. Jiang and W. Zeng, A [4 + 1] Cyclative Capture Access to Indolizines via Cobalt(III)-Catalyzed Csp^2 –H Bond Functionalization, *Org. Lett.*, 2016, **18**, 4742–4745.

226 D. Bora, S. E. John, M. S. Galla, M. Sathish and N. Shankaraiah, Rh(III)-catalysed site-selective alkylation of β-carbolines/isoquinolines and tandem CH/CN functionalization to construct indolizine-indole frameworks, *Mol. Catal.*, 2022, **533**, 112783.

227 X. Xu, H. Feng, X. Zhang, L. Song, L. Van Meervelt, J. Van der Eycken, J. N. Harvey and E. V. Van der Eycken, Pd-Catalyzed Ring Restructuring of Oxazolidines with Alkenes Leading to Fused Polycyclic Indolizines, *Org. Lett.*, 2022, **24**, 1232–1236.

228 Z. Luo, H. Hu, C. Wang, Z. Yang and Y. Wang, A domino reaction for the synthesis of pyrrolo[2,1-*a*]isoquinolines from 2-aryl-pyrrolidines and alkynes promoted by a four-component catalytic system under aerobic conditions, *RSC Adv.*, 2023, **13**, 35617–35620.

229 O. V. Shurupova, E. S. Tarasova, S. A. Rzhevskiy, L. I. Minaeva, M. A. Topchiy and A. F. Asachenko, Novel convenient 2-step synthesis of pyrido[1,2-*a*]indoles from pyrylium salts and o-bromoanilines, *Org. Biomol. Chem.*, 2024, **22**, 6742–6747.

230 V. K. Outlaw, J. Zhou, A. E. Bragg and C. A. Townsend, Unusual blue-shifted acid-responsive photoluminescence behavior in 6-amino-8-cyanobenzo[1,2-*b*]indolizines, *RSC Adv.*, 2016, **6**, 61249–61253.

231 W. Augstein and F. Kröhnke, Synthesen des Benzo[*a*]- und des Naphtho[2.3-b]indolizin-Ringsystems, *Justus Liebigs Ann. Chem.*, 1966, **697**, 158–170.

232 J. S. A. Badaro, B. Koszarna, M. H. E. Bousquet, E. T. Ouellette, D. Jacquemin and D. T. Gryko, The Kröhnke synthesis of benzo[a]indolizines revisited: towards small, red light emitters, *Org. Chem. Front.*, 2022, **9**, 1861–1874.

233 H. Khan, D. Barman and S. Sen, Light-Induced Generation and Cycloaddition Reactions of Benzyne: Synthesis of Naphthoxindoles E and Annulated Indolizines, *J. Org. Chem.*, 2024, **89**, 6257–6262.

234 C.-B. Miao, X.-Q. Qiang, X. Xu, X.-Q. Song, S.-Q. Zhou, X. Lyu and H.-T. Yang, Synthesis of Stable N–H Imines with a Benzo[7,8]indolizine Core and Benzo[7,8]indolizino[1,2-*c*]quinolines via Copper-Catalyzed Annulation of α,β-Unsaturated O-Acyl Ketoximes with Isoquinolinium *N*-Ylides, *Org. Lett.*, 2022, **24**, 3828–3833.

235 E. A. Sokolova, A. A. Festa, N. E. Golantsov, N. S. Lukonina, I. N. Ioffe, A. V. Varlamov and L. G. Voskressensky, Highly Fluorescent Pyrido[2,3-*b*]indolizine-10-Carbonitriles through Pseudo Three-Component Reactions of *N*-(Cyanomethyl)pyridinium Salts, *Eur. J. Org. Chem.*, 2019, 6770–6775.

236 Q. Ni, L. Zhang, Z. Zhu and X. Song, Formal [5 + 2] cycloaddition of ortho-indolizinyl anilines with cyclopentenediones: access to planar indolizine-fused azepines, *Org. Chem. Front.*, 2023, **10**, 2526–2531.

237 Q. Zhang, B. Wang, H. Ma and K. Ablajan, Transition-metal-free catalyzed [3 + 2] cycloadditions/oxidative aromatization reactions for the synthesis of annulated indolizines, *New J. Chem.*, 2019, **43**, 17000–17003.

238 K.-H. Lv, Q.-S. Zhao, K.-H. Zhao, J.-M. Yang and S.-J. Yan, Cu-Catalyzed Oxidative [3 + 2] Annulation of 2-(Pyridine-2-yl)acetates with Maleimides: Synthesis of 1*H*-Pyrrolo[3,4-*b*]indolizine-1,3-diones, *J. Org. Chem.*, 2022, **87**, 15301–15311.

239 E. Chupakhin, O. Bakulina, D. Dar'in and M. Krasavin, Facile entry into the 1*H*-pyrrolo[3,4-*b*]indolizine-1,3(2*H*)-dione scaffold *via* intramolecular Rh(II) carbene trapping, *Tetrahedron Lett.*, 2021, **85**, 153467.

240 Z.-H. Shang, X.-J. Zhang, Y.-M. Li, R.-X. Wu, H.-R. Zhang, L.-Y. Qin, X. Ni, Y. Yan, A.-X. Wu and Y.-P. Zhu, One-Pot Synthesis of Chromone-Fused Pyrrolo[2,1-*a*]isoquinolines and Indolizino[8,7-*b*]indoles: Iodine-Promoted Oxidative

[2 + 2 + 1] Annulation of O-Acetylphenoxyacrylates with Tetrahydroisoquinolines and Noreleagnines, *J. Org. Chem.*, 2021, **86**, 15733–15742.

241 X.-J. Zhang, Z. Wang, H. Zhang, J.-J. Gao, K.-R. Yang, W.-Y. Fan, R.-X. Wu, M.-L. Feng, W. Zhu and Y.-P. Zhu, Iodine-Mediated Domino Cyclization for One-Pot Synthesis of Indolizine-Fused Chromones via Metal-Free sp^3 C–H Functionalization, *J. Org. Chem.*, 2022, **87**, 835–845.

242 A. Kakehi, S. Ito, K. Watanabe, M. Kitagawa, S. Takeuchi and T. Hashimoto, Preparation of new nitrogen-bridged heterocycles. Synthesis and some reactions of 2,3-dihydroindolizin-2-one derivatives, *J. Org. Chem.*, 1980, **45**, 5100–5104.

243 J. S. A. Badaro, A. Wrzosek, O. Morawski, A. Szewczyk, I. Deperasińska and D. T. Gryko, Strongly fluorescent indolizine-based coumarin analogs, *Org. Chem. Front.*, 2024, **11**, 6627–6641.

244 E. F. Pratt, R. W. Luckenbaugh and R. L. Erickson, Reactions of naphthoquinones with malonic ester and its analogs. II. Reactions with acetoacetic ester and pyridine or quinoline, *J. Org. Chem.*, 1954, **19**, 176–182.

245 E. F. Pratt, R. G. Rice and R. W. Luckenbaugh, Reactions of Naphthoquinones with Malonic Ester and its Analogs. III. 1-Substituted Phthaloyl- and Phthaloylbenzopyrrocolines1, *J. Am. Chem. Soc.*, 1957, **79**, 1212–1217.

246 E. F. Pratt and J. C. Keresztesy, Jr., Syntheses of indolizino- and dihydroindolizinoquinoxalines, *J. Org. Chem.*, 1967, **32**, 49–53.

247 D. Das, A. Das, S. Islam, A. R. Das, A. Banerjee, R. Majumder and D. Bandyopadhyay, Fused Furan Moieties from Enol-like Compounds and β-Keto Sulfoxonium Ylides Involving sp^2 C–H Activation and Concomitant Tandem C–O Annulation, *Org. Lett.*, 2023, **25**, 4493–4497.

248 R. Nagarkar and S. Dapurkar, Dinitro Anacardic Acid Copper(II) Complex—A Bio-based Catalyst for Room Temperature Synthesis of Indolizine, *ChemistrySelect*, 2022, **7**, e202202420.

249 D. R. Joshi, Y. Seo, Y. Heo, S. Park, Y. Lee, W. Namkung and I. Kim, Domino [4 + 2] Annulation Access to Quinone–Indolizine Hybrids: Anticancer *N*-Fused Polycycles, *J. Org. Chem.*, 2020, **85**, 10994–11005.

250 S. Lee, Y. Lee, W. Namkung and I. Kim, Access to 8-Aminoindolizine Fused with Quinone via $Cu(OAc)_2$-Catalyzed Domino [4 + 2] Annulation, *Synthesis*, 2024, 1799–1806.

251 D. Maiti, S. Munan, S. Singh, R. Das, A. Samanta and S. Sen, Light induced diversity-oriented synthesis (DOS) library of annulated indolizine fluorophores for imaging non-lysosomal lipid droplets (LDs), *J. Mater. Chem. B*, 2023, **11**, 2191–2199.

252 A. Pareek, M. Y. Mehboob, M. Cieplak, M. Majdecki, H. Szabat, K. Noworyta, P. Połczyński, M. Morawiak, P. S. Sharma, C. Foroutan-Nejad and P. Gaweł, Indoloindolizines: The Complete Story of a Polycyclic Aromatic Scaffold from Theoretical Design to Organic Field-Effect Transistor Applications, *J. Am. Chem. Soc.*, 2025, DOI: 10.1021/jacs.4c16189.

253 A. Citterio, M. Fochi, A. Marion, A. Mele, R. Sebastiano and M. Delcanale, ChemInform Abstract: Synthesis of Naphtho[2,3-*b*]indolizine-6,11-dione Derivatives by Iodine Oxidation of 2-Alkyl-1,4-naphthoquinones in the Presence of Substituted Pyridines, *Heterocycles*, 1998, **48**, 1993–2002.

254 J. Li, S. Zhang and H. Zou, One-pot chemoselective domino condensation to form a fused pyrrolo–pyrazino–indolizine framework: discovery of novel AIE molecules, *Org. Chem. Front.*, 2020, **7**, 1218–1223.

255 S. A. Babu, A. A. M. Mohan, N. Paul, J. Mathew and J. John, Tandem Reactions of Electrophilic Indoles toward Indolizines and Their Subsequent Transformations through Pd(II)-Mediated C–H Functionalization to Access Polyring-Fused *N*-Heterocycles, *ACS Omega*, 2024, **9**, 16196–16206.

256 E. Ausekle, P. Ehlers, A. Villinger, M. A. Argüello Cordero, S. Lochbrunner and P. Langer, Thienoindolizines and their Benzo-Fused Derivatives: Synthesis and Physical Properties, *Chem. – Eur. J.*, 2023, **29**, e202301038.

257 S. Nam and I. Kim, Cu-Catalyzed Ullmann-Type Double C–N Coupling Approach to 5-Aryl-5*H*-indolizino[3,2-*b*]indoles, *J. Org. Chem.*, 2023, **88**, 745–754.

258 Y. Zhang, Y. Lei, K. Zhang, Q. Hu, M. Chang and Y. Hu, Single-Pot Reaction of Novel Fused Indolizine Derivatives, *Org. Lett.*, 2024, **26**, 8267–8271.

259 I. V. Nechaev, G. V. Cherkaev and A. B. Sheremetev, Unique Pseudo-Cross-Conjugated Mesomeric Betaines via an Iodate-Promoted Reaction of 3,3-Difluorocyclopropenes, Pyridines, and Anilines, *J. Org. Chem.*, 2022, **87**, 652–669.

260 J.-B. Ma, Q.-S. Zhao, Y.-M. Yin, S. Yang, J.-Q. Shao and S.-J. Yan, Cascade [3 + 2]/[4 + 2] Cycloaddition of Enaminones with Vinylene Carbonate for the Synthesis of Functionalized Pyrrolo[2,1-*a*]isoquinoline Derivatives, *Org. Lett.*, 2024, **26**, 9752–9758.

261 H. Hu, G. Li, W. Hu, Y. Liu, X. Wang, Y. Kan and M. Ji, Synthesis of Pyrrolo[2,1,5-*cd*]indolizines through Dehydrogenative Heck Annelation of Indolizines with Diaryl Acetylenes Using Dioxygen as an Oxidant, *Org. Lett.*, 2015, **17**, 1114–1117.

262 M. Huang, L. Deng, T. Lao, Z. Zhang, Z. Su, Y. Yu and H. Cao, Dehydrogenation Coupling and [3 + 2] Cycloaddition of Indolizines with Allenes in the Presence of Piezoelectric Materials under Ball Milling Conditions, *J. Org. Chem.*, 2024, **89**, 9733–9743.

263 S. K. Ghosh, D. Ghosh, R. Maitra, Y.-T. Kuo and H. M. Lee, Palladium-Catalyzed Oxidative Cyclization for the Synthesis of 2-Alkylimidazo[5,1,2-*cd*]indolizines, *Eur. J. Org. Chem.*, 2016, 5722–5731.

264 N. Meena, V. N. Shinde, Sonam, P. N. Swami, K. Rangan and A. Kumar, Catalyst-controlled regiodivergent oxidative

annulation of 2-arylimidazo[1,2-*a*]pyridines with cinnamaldehyde derivatives for construction of fused *N*-heterocyclic frameworks, *J. Org. Chem.*, 2023, **88**, 12902–12913.

265 R. Semwal, A. Joshi, R. Kumar and S. Adimurthy, Annulation of imidazo[1,2-*a*]pyridines under metal-free conditions, *New J. Chem.*, 2020, **44**, 20530–20534.

266 R. V. Prajapati, V. D. Prajapati, V. B. Purohit, J. R. Avalani, R. D. Kamani, N. H. Sapariya, S. C. Karad and D. K. Raval, Microwave-Assisted Palladium-catalyzed double C–H Activation: One-pot Synthesis of Benzo[*a*]imidazo[5,1,2-*cd*]indolizines from 2-Phenylimidazo[1,2-*a*]pyridines and 1,2-Diiodobenzene, *ChemistrySelect*, 2022, **7**, e202201436.

267 D. Firmansyah, M. Banasiewicz and D. T. Gryko, Vertically-expanded imidazo[1,2-*a*]pyridines and imidazo[1,5-*a*]pyridine via dehydrogenative coupling, *Org. Biomol. Chem.*, 2015, **13**, 1367–1374.

268 J. Han, X. Tang, X. Cheng, T. Zeng, Y. Tian, Y. Gong and B. Li, Copper-Catalyzed Nucleophilic Cycloisomerization Cascade Constructing Azepinoindolizine, *Org. Lett.*, 2024, **26**, 8057–8062.

269 C. L. Anderson, T. Zhang, M. Qi, Z. Chen, C. Yang, S. J. Teat, N. S. Settineri, E. A. Dailing, A. Garzón-Ruiz, A. Navarro, Y. Lv and Y. Liu, Exceptional Electron-Rich Heteroaromatic Pentacycle for Ultralow Band Gap Conjugated Polymers and Photothermal Therapy, *J. Am. Chem. Soc.*, 2023, **145**, 5474–5485.

270 D. A. Rusanov, S. Mutasim Alfadul, E. Yu. Portnyagina, E. A. Silyanova, N. A. Kuznetsov, K. E. Podpovetny, A. V. Samet, V. V. Semenov and M. V. Babak, Toward "E-Ring-Free" Lamellarin Analogues: Synthesis and Preliminary Biological Evaluation, *ChemBioChem*, 2023, **24**, e202300161.

271 B. Zhou, M. Guo, Q. Pan, M. Zhou, L. Xu, Y. Rao, K. Wang, B. Yin, J. Zhou and J. Song, Rhodium-catalyzed annulation of pyrrole substituted BODIPYs with alkynes to access π-extended polycyclic heteroaromatic molecules and NIR absorption, *Org. Chem. Front.*, 2021, **8**, 868–875.

272 C. S. L. Rathnamalala, J. N. Gayton, A. L. Dorris, S. A. Autry, W. Meador, N. I. Hammer, J. H. Delcamp and C. N. Scott, Donor–Acceptor–Donor NIR II Emissive Rhodindolizine Dye Synthesized by C–H Bond Functionalization, *J. Org. Chem.*, 2019, **84**, 13186–13193.

273 W. E. Meador, S. A. Autry, R. N. Bessetti, J. N. Gayton, A. S. Flynt, N. I. Hammer and J. H. Delcamp, Water-Soluble NIR Absorbing and Emitting Indolizine Cyanine and Indolizine Squaraine Dyes for Biological Imaging, *J. Org. Chem.*, 2020, **85**, 4089–4095.

274 J. Gayton, S. A. Autry, W. Meador, S. R. Parkin, G. A. Hill Jr., N. I. Hammer and J. H. Delcamp, Indolizine-Cyanine Dyes: Near Infrared Emissive Cyanine Dyes with Increased Stokes Shifts, *J. Org. Chem.*, 2019, **84**, 687–697.

275 W. E. Meador, E. Y. Lin, I. Lim, H. C. Friedman, D. Ndaleh, A. K. Shaik, N. I. Hammer, B. Yang, J. R. Caram, E. M. Sletten and J. H. Delcamp, Silicon-RosIndolizine fluorophores with shortwave infrared absorption and emission profiles enable in vivo fluorescence imaging, *Nat. Chem.*, 2024, **16**, 970–978.

276 M. A. Saucier, N. A. Kruse, B. E. Seidel, N. I. Hammer, G. S. Tschumper and J. H. Delcamp, Phospha-RosIndolizine Dye with Shortwave Infrared (SWIR) Absorption and Emission, *J. Org. Chem.*, 2024, **89**, 9092–9097.

277 M. Grzybowski, O. Morawski, K. Nowak and P. Garbacz, Fluorene analogues of xanthenes – low molecular weight near-infrared dyes, *Chem. Commun.*, 2022, **58**, 5455–5458.

278 W. E. Meador, M. A. Saucier, M. R. Tucker, N. A. Kruse, A. J. Mobley, C. R. Brower, S. R. Parkin, K. M. Clark, N. I. Hammer, G. S. Tschumper and J. H. Delcamp, Extended shortwave infrared absorbing antiaromatic fluorenium-indolizine chromophores, *Chem. Sci.*, 2024, **15**, 12349–12360.

279 V. Boekelheide and W. Feely, Notes - Convenient Synthesis of Pyrrocoline, *J. Org. Chem.*, 1957, **22**, 589–592.

280 A. Ohsawa, T. Kawaguchi and H. Igeta, Flash vacuum pyrolysis of substituted pyridine *N*-oxides and its application to syntheses of heterocyclic compounds, *J. Org. Chem.*, 1982, **47**, 3497–3503.

281 A. F. Kassir, N. Rad, P. Klochowicz and J. M. Granda, Diversity-oriented chiral phosphoric acid catalyzed alkylation of indolizines with aminals, *Org. Chem. Front.*, 2024, **11**, 7186–7198.

282 D. B. Granger, Y. Mei, K. J. Thorley, S. R. Parkin, O. D. Jurchescu and J. E. Anthony, Synthesis and Electrical Properties of Derivatives of 1,4-bis(trialkylsilylethynyl)benzo[2,3-*b*:5,6-*b*′]diindolizines, *Org. Lett.*, 2016, **18**, 6050–6053.

283 X. Liu, W. Jiang, C. Huang, S. Ma, Q. Wang and H. Cao, Electrochemical phosphorothiolation and 1,4-S→C phospho-Fries rearrangement: controlled access to phosphorothiolated and mercapto-phosphono substituted indolizines, *Org. Chem. Front.*, 2023, **10**, 5198–5204.

GDCh Research Article Angewandte International Edition Chemie www.angewandte.org

How to cite: *Angew. Chem. Int. Ed.* **2025**, e202508044
doi.org/10.1002/anie.202508044

Polymethine Dyes

Hybrid of Indolizine and Merocyanine—A New Class of Organelle-Specific Dyes

Jaqueline S. A. Badaro, Beata Koszarna, Maja Perkowska, Kristiana Kandere-Grzybowska, Diana V. Kolygina, Olaf Morawski, Juhee Park, Bartosz Grzybowski, Irena Deperasińska,* and Daniel T Gryko**

Dedicated to Prof. Jonathan Lindsey on his 70th birthday

Abstract: Unlocking the potential of electron-rich 2-hydroxyindolizines led to the discovery of a new class of dyes—indolizine-merocyanines (IndMer) and indolizine-cyanines. Tandem Friedel–Crafts alkylation followed by intramolecular nucleophilic aromatic substitution afforded structurally diverse dyes, as both the nucleophilic and electrophilic partners can be broadly modified. A convergent fragment coupling strategy allowed rapid access to these π-conjugated merocyanines in three steps from pyridines. Uniform distribution of the HOMO and LUMO combined with negligible change of dipole moment upon excitation is responsible for the intense orange or red emission of this new family of reasonably photostable dyes in a broad range of solvents. The new merocyanine dyes have the potential to target a variety of organelles—both uncharged and positively charged indolizine–merocyanines localize a subset of cellular lysosomes, positively charged indolizine–cyanine hybrid accumulates in mitochondria, while coumarin–merocyanine shows context-dependent localization to mitochondria and RNA-rich nucleoli of the living cells.

Introduction

Fluorescein, rhodamine, and rhodol were all discovered in the 19th century, and over the course of 140 years, extensive effort has been devoted to advancing the photophysical properties of these ubiquitous dyes through structural modifications. In particular π-expansion[1–7] and replacement of the xanthene oxygen atom bridge with silicon,[8–11] phosphorus,[12,13] sulfur,[14] or carbon[15–18] in scaffolds of rhodamine,[19–22] fluorescein,[23,24] and rhodol[25] have proven popular and effective (Figure 1).

Other notable modifications encompass altering the size of the middle ring[26,27] and replacing dialkylamino groups as a donor with indolizine,[28,29] allowing further modulation of the photophysical properties.

The key application of xanthene dyes is fluorescence imaging, which has become a powerful tool for molecular biology due to its merits of real-time monitoring capability, non-invasive nature, and high spatiotemporal resolution.[30,31] Compared to classical fluorescence microscopy, fluorescence imaging in the near-infrared window (NIR, 750–1700 nm) allows for both deeper tissue penetration and a higher signal-to-noise ratio for noninvasive in vivo imaging at subcentimeter tissue depths, due to decreased scattering.[32–35] Advancements in this imaging technique have demanded more stringent and challenging properties to be included in dyes, which currently available dyes do not entirely fulfill. Indeed, NIR dyes lack a large fluorescence quantum yield (Φ_{fl}) and photostability.[36,37,7,38] Some of the modern, highly modified xanthene dyes possess emission in NIR often with reasonable quantum yield.[39,40]

In the context of addressing the above challenges, an interesting question emerges about possible modifications of electron-donating moiety especially by an electron-rich aromatic heterocycle. The hypothesis underlying our current work is that by incorporating the entire indolizine[41] moiety

[*] J. S. A. Badaro, Dr. B. Koszarna, M. Perkowska, Prof. B. Grzybowski, Prof. D. T Gryko
Institute of Organic Chemistry of Polish Academy of Sciences, Kasprzaka 44/52, Warsaw 01-224, Poland
E-mail: grzybor72@unist.ac.kr
dtgryko@icho.edu.pl

Dr. K. Kandere-Grzybowska, Dr. D. V. Kolygina, J. Park, Prof. B. Grzybowski
Center for Algorithmic and Robotized Synthesis, Institute for Basic Science (IBS), Ulsan 44919, Republic of Korea

Dr. K. Kandere-Grzybowska
Department of Biomedical Engineering, Ulsan National Institute of Science and Technology (UNIST), 50 UNIST-gil, Ulsan 44919, Republic of Korea

Prof. B. Grzybowski
Department of Chemistry, Ulsan National Institute of Science and Technology (UNIST), 50 UNIST-gil, Ulsan 44919, Republic of Korea

Dr. O. Morawski, Dr. I. Deperasińska
Institute of Physics, Polish Academy of Sciences, Al. Lotników 32/46, Warsaw 02-668, Poland
E-mail: deper@ifpan.edu.pl

Additional supporting information can be found online in the Supporting Information section

into the molecule as an electron donor, while simultaneously fusing it with the rest of the structure, a novel conjugated π-system could be formed, potentially exhibiting remarkable photophysical properties (Figure 1). We aim to address this general idea by constructing a merocyanine,[42,43] in which the electron-rich indolizine scaffold would form one large, planar π-expanded system. Needless to say, accomplishing this task would require establishing a brand-new synthetic methodology. In the process we discovered several structurally unique organelle-specific dyes with excitation in far-red range.

Results and Discussion

Design and Synthesis

To overcome the aforementioned challenges, we propose a molecular design strategy that, compared to previous concepts, offers significant advantages in terms of simplicity and efficiency. Our key idea was to employ the tandem Friedel–Crafts alkylation/nucleophilic aromatic substitution, which we previously discovered for the reaction of 2,3,5,6-tetrafluoro-4-hydroxybenzaldehyde (**1**) with aminophenols.[44] Instead of benzene derivatives, we decided to use 2-hydroxyindolizine as a nucleophilic coupling partner. Highly electron-rich 2-hydroxyindolizines can be obtained in situ using the methodology originally developed by Kakehi's group[45] and optimized by us.[46] Rewardingly, 2-hydroxyindolizine **2**, possessing an additional methyl group in position 3, reacted smoothly with aldehyde **1** under neutral conditions (xylenes, 80 °C, overnight) furnishing compound **3a** in 72% yield (Scheme 1). A straightforward examination of the NMR data confirmed that the product has the expected indolizine-merocyanine (IndMer) structure. Preliminary photophysical studies revealed strong fluorescence with an emission maximum (λ_{em}^{max}) at 577 nm. With a proof of concept thus established, we began to explore this new core and its chemistry. We found that both the π-expansion of the 2-hydroxyindolizine substrate and its 3-substituted derivatives are typically compatible with the new synthetic strategy, giving rise to various IndMer dyes **3b–f** (Scheme 1). Mildly electron-donating alkyl groups and electron-withdrawing groups, such as an ester or pyridine, were well tolerated. On the other hand, when strongly electron-donating groups were present at the pyridine core, the corresponding 2-hydroxyindolizines could not be generated via Dieckmann condensation.

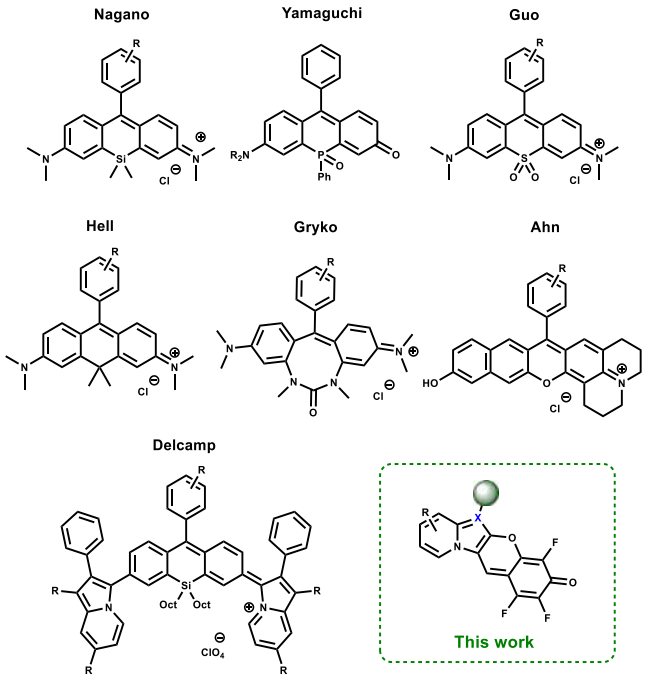

Figure 1. Examples of core-modified rhodamines and rhodols.

The products **3b–f** were obtained in 26%–90% yields and were conveniently harnessed by precipitation owing to their poor solubility in the reaction medium. The only exception was dye **3b,** which was designed specifically to improve solubility and was purified by column chromatography. Having demonstrated that the synthesis of new merocyanines is straightforward and effective, we next turned our attention to an analogue possessing an additional nitrogen atom at position 3, i.e., a derivative of imidazo[1,2-*a*]pyridine.[47,48] To our delight, 2-hydroxyimidazo[1,2-a]pyridine was transformed into the corresponding dye **3Ng** (ImPMer), under the same conditions as described earlier in 62% yield (Scheme 1). Due to the low yield and poor stability of other 2-hydroxyimidazo[1,2-*a*]pyridines, we decided to carry out the reaction in situ, starting with the corresponding 2-aminopyridines. This approach allowed us to obtain two additional ImPMer dyes, **3Nh** and **3Ni**, with overall yields of 24% and 44%, respectively. Finally, IndMer **3e** possessing pyridyl substituent was quaternized to obtain the positively charge salt **3eMe** (Scheme 1, see Supporting Information for details).

Encouraged by these results, we also explored the possibility of using different types of aromatic aldehydes sharing the same features (i.e., halogen atom in vicinal position to CHO and electron-deficient character of the aromatic ring) but possessing different electron-donating groups at position 4. Reaction of indolizine **2b** with 2,3,5,6-tetrafluoro-4-(piperidin-1-yl)benzaldehyde (**1N**)[49] unexpectedly led to product **4** in 10% yield, a dye formed by the reaction of two molecules of indolizine and one molecule of aldehyde, as confirmed by NMR and HRMS (Scheme 2). This structure can be compared with that of a V-shaped bis-xanthene dye.[4] In contrast to other above-described dyes, compound **4** is non-planar and has a slightly twisted geometry because of the steric hindrance between the two indolizine units in close spatial proximity. By contrast, the reaction of coumarin-based aldehyde **1C**[50] led to the formation of cyanine-type dye **5**, in 27% yield, albeit both time and the temperature had to be extended (Scheme 2).

To further demonstrate the robustness and synthetic utility of this protocol, we performed the synthesis of dye **3a** on a 20 mmol scale, which gave 4.6 g of product (76% yield) indicating the synthetic potential of this method for bulk-scale synthesis.

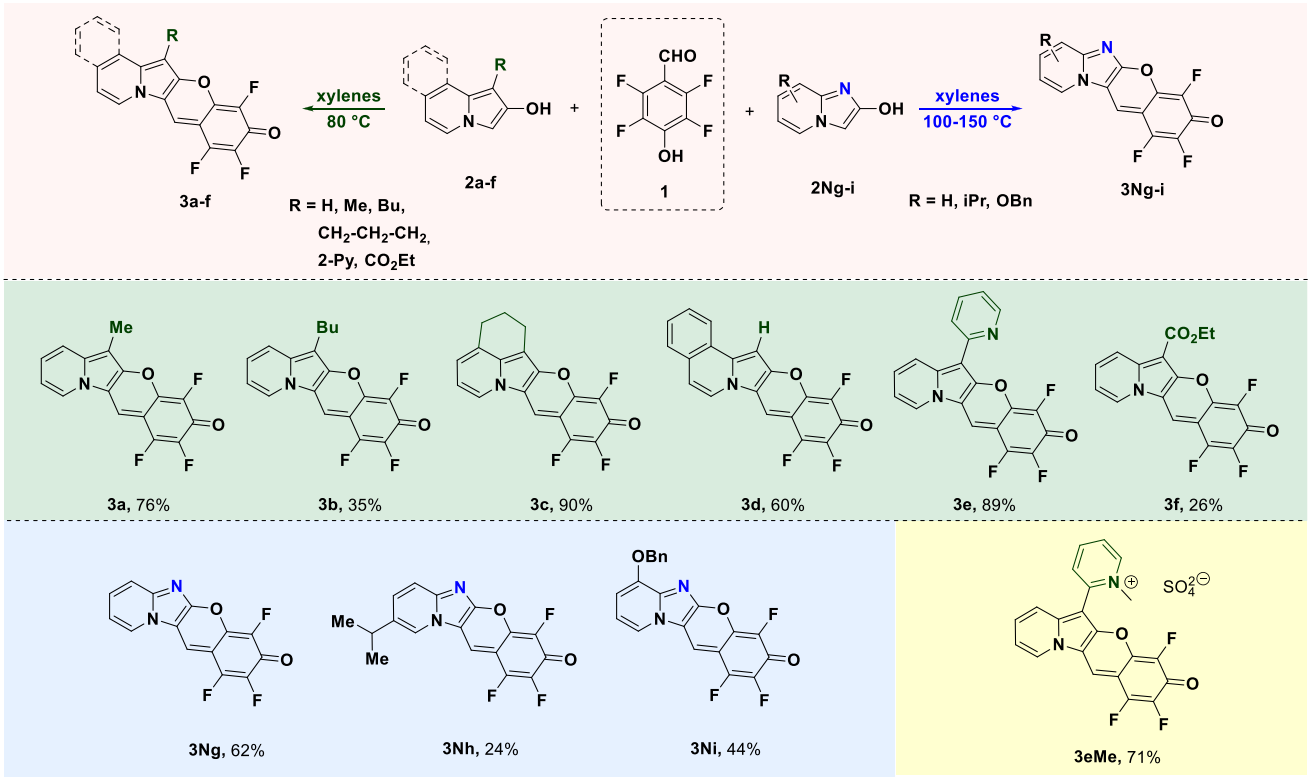

Scheme 1. Straightforward synthesis of the indolizine–merocyanines (IndMer) and imidazo[1,2-*a*]pyridine-merocyanines (ImPMer).

Photophysics

With a diverse series of new polymethine dyes in hand, we performed comprehensive photophysical characterization (Table 1 and Table S1, Figures 2 and 3 and Figure S1). UV–Vis absorption and emission spectra were recorded in DCM, THF, and DMSO for all dyes. The absorption and emission of this new family of dyes exhibited only a slight bathochromic shift ($\lambda_{abs}{}^{max} \approx 570$ nm vs. 550 nm, and $\lambda_{em}{}^{max} \approx 580$ nm vs. 540 nm) when compared to typical rhodols.[25,51] In comparison to the majority of merocyanine dyes, IndMer and ImPMer surprisingly showed no solvatochromism. When comparing the photophysical properties of IndMer dyes with various substituents at position 3 (Figure 2), one can notice that the influence of electron-donating alkyls and the electron-withdrawing ester group is rather negligible. In contrast, insertion of a nitrogen atom at position 3 (ImPMers **3Ng**, **3Nh,** and **3Ni**) causes the significant (≈30 nm) blue-shift for both absorption and emission. It is also important to emphasize that fluorescence quantum yields (Φ_{fl}) are above 50% in most cases, even in DMSO. The Stokes shifts for all these dyes are around 500 cm^{-1}, consistent with the structural rigidity of this class of molecules and the negligible influence of solvent polarity on this π-conjugated system.

Bis-indolizine **4** (Figure 3), structurally comparable to a V-shaped dimeric xanthene dye,[4] displays a bathochromically shifted λ_{em} (585 nm vs. 547 nm) with a small decrease in Φ_{fl} (32 vs. 40%). The properties of indolizine-cyanine **5** (Figure 3)

Table 1: Photophysical properties of synthesized dyes in DCM and DMSO.

		$\lambda_{abs}{}^{max}$ (nm)	ε_{max} ($M^{-1}cm^{-1}$)	$\lambda_{em}{}^{max}$ (nm)	Φ_{fl} (%)
3a	DCM	570	87 000	577	74
3a	DMSO	567	75 000	580	53
3b	DCM	571	97 000	579	77
3b	DMSO	567	70 000	584	62
3c	DCM	570	56 000	578	67
3c	DMSO	567	44 000	583	40
3d	DCM	557	30 000	569	57
3d	DMSO	550	40 000	566	49
3e	DCM	575	14 000	593	67
3e	DMSO	569	42 000	593	56
3f	DCM	554	30 000	567	53
3f	DMSO	545	39 000	562	50
3Ng	DCM	541	10 000	565	36
3Ng	DMSO	530	30 000	558	29
3Nh	DCM	543	37 000	566	42
3Nh	DMSO	531	37 000	557	35
3Ni	DCM	541	29 000	565	42
3Ni	DMSO	533	33 000	558	35
4	DCM	537	41 000	585	32
4	DMSO	531	20 000	600	5
5	DCM	624	31 000	705	2
5	DMSO	616	8000	735	<1
3eMe	DCM	554	33 000	570	43
3eMe	DMSO	554	36 000	570	56

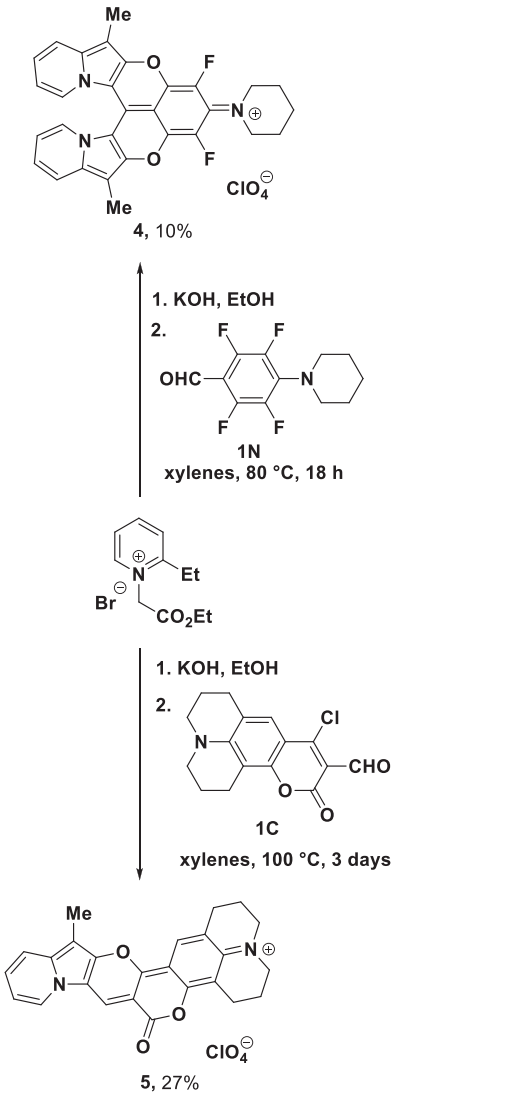

Scheme 2. The synthesis of two indolizine-cyanine hybrids **4** and **5** from aldehydes **1N** and **1C**.

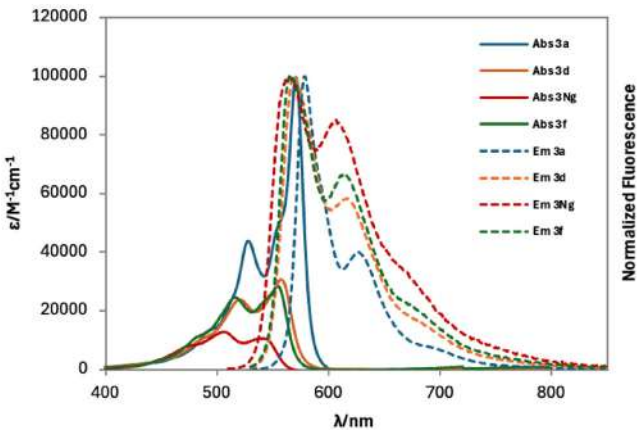

Figure 2. UV–vis absorption spectra (solid lines) and fluorescence spectra (dashed lines) of compounds **3a**, **3d**, **3Ng,** and **3f** measured in DCM.

are strikingly different—$\lambda_{abs}{}^{max}$ is shifted to 624 nm and $\lambda_{em}{}^{max}$ is beyond 700 nm, although fluorescence quantum yield is rather low (2% in DCM). For selected dyes spectra were also recorded in H_2O/DMSO to simulate biological environment (see Table S1). In the case of merocyanines **3Nh** and **4** Φ_{fl} was comparable to results in pure DMSO, whereas for merocyanines **5** and **3eMe** it was markedly larger. Only in the case of merocyanine **3b** emission in H_2O/DMSO was weaker than in other solvents.

The comparison between the strong prompt fluorescence observed for compounds **3a**, **3b**, **3Ng**, and **5**, and the very weak signal (close to noise level) detected in the delayed emission clearly indicates that none of the studied dyes exhibit phosphorescence, even at 5 K (Figure S3).

To assess the photostability of compounds **3eMe**, and **5** in aqueous medium, their solutions were irradiated with a Xe lamp for approximately 2 h, while monitoring the absorption maxima over time (Figure 4 and Figure S4). The photostability of Rhodamine 6G was also evaluated under the same conditions and used as a reference. In general, the new merocyanines showed slightly lower, yet comparable, photostability relative to the reference. All tested compounds exhibited a limited (less than 10%) and quasi-linear decay with minor deviations. Notably, compound **3eMe** demonstrated the highest stability. Photostability was also studied in DCM and DMF, and those cases, Bodipy was used as a reference (Figure S4).

The limited photostability of new merocyanines prompted us to study what are the photodecomposition products. The photodegradation of xanthene dyes was investigated numerous times[52–54] although typically these studies focused either on improving the photostability or on halogenated derivatives.[55] The solution of dye **3b** was irradiated in quartz vessel using a xenon lamp. It turned out that that the number of photodecomposition products exceeded 20 species and purification of the vast majority of them proved impossible because of their small quantities and the tendency to decompose further during column chromatography. Most of them were more polar than dye **3b** and displayed strong blue fluorescence. For one crude decomposition product, both the molecular mass and the number of aromatic signals suggested the dimeric structure. The chemical shift of the aromatic signals, along with the observation of strong blue fluorescence, suggests the presence of an isolated indolizine chromophore. The analysis of ^{1}H NMR spectrum as well as MS proved inconclusive, although several hypothetical structures were suggested (see Supporting Information).

Computational Studies

To understand how differences in the structure relate to the observed photophysics, we performed computational studies for a selection of dyes (**3a**, **3d**, **3Ng**, **5**) via DFT and TDDFT O3LYP and M06/6–31G(d,p) methods.[56–59] The calculation results are collected in Tables S3–S8 and Figures S6–S9. Table S3 provides data on the absorption and fluorescence energies and oscillator strengths characterizing the molecules

optimized in the ground – S_0 and electronically excited – S_1 states, respectively.

The calculations were performed with two functionals. The transition energies and oscillator strengths calculated with the O3LYP functional are slightly smaller than those calculated with M06, but the results obtained with both functionals correlate with each other (Figure S6).

Moreover, calculations with both functionals consistently lead to the conclusion that the studied group of dyes are characterized by a large dipole moment in the ground S_0 state (16–19 D), which changes little in the excited S_1 state (see Table S3). From the point of view of the classical theory of the solvent effect on electronic spectra,[60] this feature means that the solute–solvent interaction energies in both electronic states are comparable, and therefore the polarity of the solvent should not affect the absorption and fluorescence energies, as confirmed in Table 1.

Minimizing solvent impact created conditions for partial extraction of the vibrational structure of absorption and fluorescence spectra, usually blurred by polarity effects.[61] Based on the calculation results for the optimized structures of the molecule in the ground and excited states, the absorption and fluorescence spectra can be simulated (see Supporting Information for details).[57,58] Figure S8 shows a simulation of the absorption spectra of **3a**, **3d**, and **3Ng**. As seen, these simulations quite accurately reflect the positions and relationships between the spectra obtained experimentally (Figure 2). The ability to reproduce the vibronic structure of dyes provides information about the structural changes in the excited molecule. For example, the Franck–Condon factors (base for simulation – Figure S7) are an important element in the expressions for the rate constants of nonradiative processes.[62] Without going into details and to simplify, the higher the ratio of the intensity of the vibronic structure band relative to the first (0,0) band, the higher the FC factor. Thus, the intensity distribution in the **3a**, **3d**, and **3Ng** spectra leads to the expectation of an increase in the rate constant of nonradiative transitions in this ordering. It should be added here that the vibronic structure in the spectra of the studied group of compounds is much less extended than in the spectra of aromatic hydrocarbons, i.e., their geometry changes are much smaller during electronic excitation.

Figure 5 shows the calculated energy diagram of molecule **3a** together with the simulations of absorption and fluorescence spectra. Figure 5 shows the HOMO and LUMO orbitals of molecule **3a**, as the single configuration (HOMO, LUMO) describes the electronic transition between the S_0 and S_1 states. This is a π–π* transition with large oscillator strengths (Table S3). As can be seen, both the HOMO and LUMO are characterized by uniform density distributions over the entire molecule.

The shapes of the HOMO and LUMO orbitals for the other molecules considered here, as well as the shapes of other frontier orbitals, HOMO −1 and LUMO +1, along with data on their energies, are shown in Table S6. It allows us to claim that the shapes of the HOMO and LUMO of parent dye **3a** are preserved with substitutions or π-expansion of the IndMer chromophore; however, the effects of structure

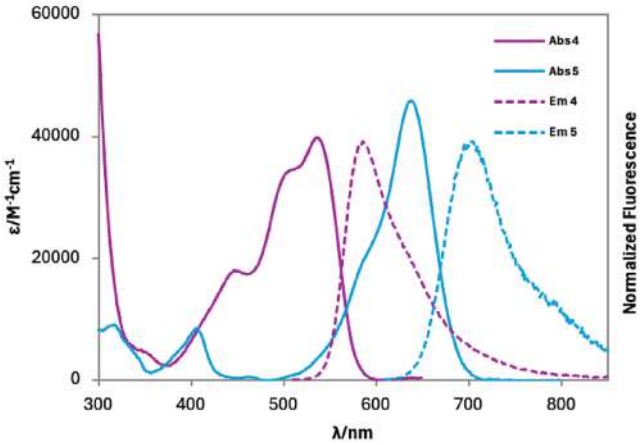

Figure 3. UV–vis absorption spectra (solid lines) and fluorescence spectra (dashed lines) of compounds **4** and **5** measured in DCM.

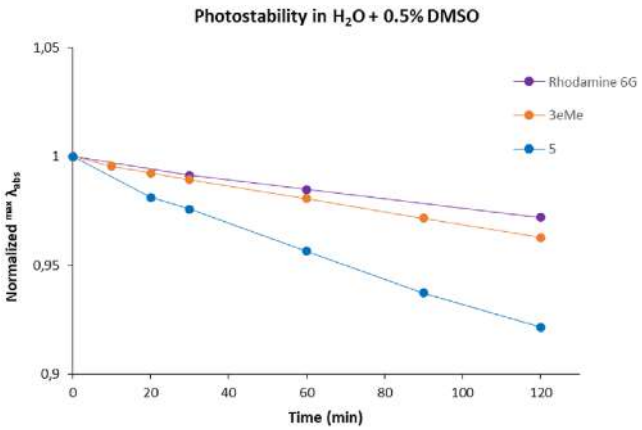

Figure 4. Photostability of dyes **3eMe** and **5** compared to Rhodamine 6G in H_2O + 0,5% DMSO.

modifications are visible in changes of the shapes of HOMO −1 and LUMO +1.

Therefore, more pronounced effects of structure modification may occur in processes involving these orbitals. Such a process is intersystem crossing (ISC) $S_1 \rightarrow T_2$, because the T_2 state is based on the configuration of the HOMO −1 and LUMO. According to the calculation results, the T_2 energy in molecule **3a** is clearly lower than the S_1 energy, but the energy gap decreases with modifications of the molecular structure (Table S5). The spin—orbit coupling elements between S_1 and T_2 are not large, but in conditions close to resonance, the intersystem crossing process can be triggered. The results of O3LYP and M06 calculations are not completely consistent, but based on the O3LYP data, in the cases of **3Ng** and **5**, it is likely that the reason for the experimentally observed decrease in fluorescence efficiency is the $S_1 \rightarrow T_2$ ISC process. In summary, the strong spatial overlap of HOMO and LUMO combined with the lack of change of dipole moment in the excited state are responsible for the strong emission of IndMer and ImPMer dyes in polar solvents. In addition, strong emission is facilitated by good separation and lack of coupling of the S_1 state with other electronic states.

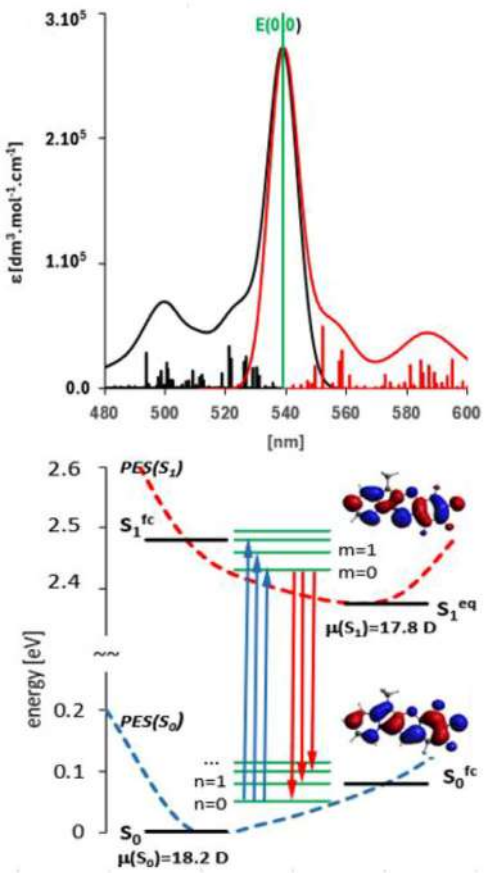

Figure 5. (*bottom*) Diagram of energy, HOMO and LUMO orbitals, and dipole moments for **3a** optimized in S_0 and S_1 electronic states. In the center of the figure, the vibronic states of the molecule in S_0 and S_1 are symbolically shown. Transitions between them, with intensities described by Franck–Condon factors, build absorption and fluorescence spectra—their simulation is shown at *the top* of the figure. The strongest line in both spectra is the E(0,0) line, corresponding to the transition between $n = o$ and $m = 0$, which means that the structure of **3a** undergoes relatively small changes at the transitions between S_0 and S_1. Detailed data on the FC factors and spectra simulation are in the Supporting Information.

Fluorescence Imaging

The aqueous solubility of compounds **4**, **5,** and **3b** was assessed (Table S2), with values ranging from 0.28 mg per 100 mL (**3b**) to 2.31 mg per 100 mL (**5**), corresponding to approximately 10–80 μM. These results confirm the suitability of these compounds for bioimaging experiments.

Confocal microscopy studies in HT1080 fibrosarcoma and MRC5 normal human lung fibroblast cells showed that merocyanine hybrid dyes are cell-permeable and have the potential to target a variety of organelles in live cells. Specifically, both uncharged and positively charged indolizine-merocyanines **3b, 3e, 3Nh,** and **3eMe** localize to cytoplasmic puncta consistent with localization to endosomes and lysosomes (Figures S10–S12; but not significantly to lipid droplets, see Figures S13 and S14), positively charged indolizine-cyanine hybrid **4** accumulates in mitochondria (Figure S15), while related dye **5** shows context-dependent localization to

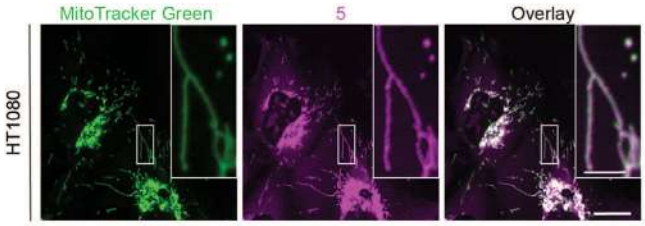

Figure 6. Subcellular localization of dye **5** in living HT1080 fibrosarcoma cells. Cells were loaded with 200 nM dye **5** (magenta), along with the 50 nM MitoTracker Green FM dye (green), and images were recorded using confocal fluorescence microscopy. The fluorescence of MitoTracker Green FM (green) was recorded with excitation at 487 nm and an emission range of 500–550 nm, and the fluorescence of molecule **5** (magenta) was recorded with excitation at 638 nm and an emission range of 663–738 nm. The brightness and contrast for individual color channels were adjusted and advanced denoising filter was applied using NIS Element's software to improve visualization of colocalization. Colocalized pixels appear white in overlays, and colocalization is assessed by Pearson's correlation coefficient (r), see Figures S16–S18 for more details. Scale bars are 10 μm for the main images and 5 μm for the insets.

mitochondria and RNA-rich nucleoli (Figures S16–S18). The latter observation aligns with recent reports of single fluorescent probes exhibiting dual localization in mitochondria and nucleoli through mechanisms such as pH-responsiveness, concentration-dependent redistribution, and energy-sensitive migration, with some dyes further enabling density mapping of subcellular environments.[63–68] This dual localization ability provides a valuable platform for studying mitochondrial damage and monitoring mitochondrial state in live cells under physiological and stress conditions.

Despite maximal $\lambda_{abs} \approx$ 530–575 nm, uncharged dyes **3b**, **3e**, and **3Nh** displayed an unexpected increase in the brightness of green emission in live cells (Figure S10), suggesting that these dyes may be sensitive to their local environment, such as organelle pH, protein–lipid interactions, dye aggregation, or spatial confinement. Although positive charge is often associated with mitochondrial localization, in the case of our dyes this correlation appears more nuanced and is not strictly predictive. As mentioned above, **3eMe** localizes to a subset of lysosomes (Figure S12), while dye **4** exclusively stains the mitochondria. The Pearson's correlation coefficient between dye **4** and MitoTracker Green FM was $r = 0.94$ and 0.92 for HT1080 and MRC5 cells, respectively. Despite the low quantum yield for dye **5** in vitro, we observed unexpected bright fluorescence in live cells, specifically in mitochondria and nucleoli (Figures S17 and S18). On one hand, reproducible but low-intensity mitochondrial labeling was achieved when using low concentrations of molecule **5** in the presence of serum (FluoroBrite DMEM supplemented with 5% FBS, 1 h at 37 °C, 200 nM) (Figure 6 and Figure S16). Mitochondrial localization was confirmed by a high Pearson's correlation coefficient between the fluorescence of dye **5** and the MitoTracker Green FM for HT1080 ($r = 0.89$) and slightly lower values for MRC5 cells ($r = 0.60$). On the other hand, with higher concentrations of dye **5** in serum-free media (FluoroBrite DMEM, 1 h at 37 °C, 1 μM), we observed specific nucleolar staining reminiscent of RNA-selective dyes,

such as SYTO RNASelect (Figures S17 and S18). Both mitochondria and nucleoli are RNA-rich, suggesting that the localization of dye **5** is influenced not solely by its delocalized cationic charge, but also by its planar structure, which may promote selective—and possibly fluorogenic—interactions with RNA, a hypothesis to be explored in future studies. In addition, dye **5** displayed excellent photostability in live cells retaining ≈ 93% of its fluorescence after 5 min of continuous imaging, while dye **3eMe** showed above-average photostability retaining ≈ 50% of its fluorescence in similar experiments (Figures S19 and S20). Importantly, all dyes were used for organelle staining at concentrations that did not noticeably affect cell viability (Figure S21).

Conclusion

It is possible to directly condense 2,3,5,6-tetrafluoro-4-hydroxybenzaldehyde with 2-hydroxyindolizines in a tandem process embracing Friedel–Crafts alkylation and nucleophilic aromatic substitution. Highly electron-rich 2-hydroxyindolizines serve as analogues to 3-dialkylaminophenols enabling the formation of heretofore unknown hybrid dyes—indolizine-merocyanines (IndMer). This strategy can be extended to π-expanded 2-hydroxyindolizines and 2-hydroxyimidazo[1,2-*a*]pyridines. Replacing 2,3,5,6-tetrafluoro-4-hydroxybenzaldehyde with 3-formyl-4-chloro-7-dialkylaminocoumarin enables the synthesis of positively charged indolizine-cyanine. Salient features of our approach include exceptionally simple synthesis, broad structural tolerance, and compatibility with a large scale. Indolizine and imidazo[1,2-*a*]pyridine as donors are game changers in the design of merocyanines: in a simple manner, a diverse range of strongly orange-red-emitting dyes can be prepared. Their fluorescence is mostly resistant to solvent polarity, and they possess reasonable photostability. Replacing the hydroxy group with an amino group at the *para* position of the electrophilic partner diverges the reaction pathway and a helicene-like bis-indolizine is formed, which emit around 600 nm. The simultaneous manipulation of various structural details makes it possible to obtain dyes with large molar absorption coefficients, fluorescence quantum yields > 50% and good photostability. TD-DFT calculations rationalize their strong emission in polar solvents. Positively charged indolizine–cyanine dyes selectively mark mitochondria or RNA-rich nucleoli of the living cells, whereas neutral ones permeate the membranes or enter through endocytosis and localize in a subset of cellular endosomes and lysosomes. We expect that the introduction of this new structural concept within the merocyanine family will open up an innovative avenue for dye chemistry.

Author Contributions

The manuscript was written through contributions of all authors. All authors have given approval to the final version of the manuscript.

Acknowledgements

This project has received funding from the European Union's Horizon 2020 Research and Innovation Program under the Marie Skłodowska-Curie grant agreement no. 101007804 and from European Research Council (ARCHIMEDES, 101097337). Views and opinions expressed are, however, those of the authors only and do not necessarily reflect those of the European Union or the European Research Council Executive Agency. Neither the European Union nor the granting authority can be held responsible for them. The work was financially supported by the Polish National Science Centre, Poland (OPUS 2020/37/B/ST4/00017). The authors thank Joseph Milton for proofreading the manuscript. Calculations were performed at the Interdisciplinary Center for Mathematical and Computational Modeling (ICM) University of Warsaw under computational allocation G98-2100. B.A.G., K.K.G, J.P. and D.V.K. were supported by the Institute for Basic Science (IBS-R020-D1).

Conflict of Interests

The authors declare no conflict of interest.

Data Availability Statement

The data that support the findings of this study are available in the supplementary material of this article.

Keywords: Fluorescence · Indolizine · Merocyanines · Polymethine dyes · Xanthene

[1] A. Katori, E. Azuma, H. Ishimura, K. Kuramochi, K. Tsubaki, *J. Org. Chem.* **2015**, *80*, 4603–4610.
[2] M. Rosenberg, M. Santella, S. A. Bogh, A. V. Muñoz, H. O. B. Andersen, O. Hammerich, I. Bora, K. Lincke, B. W. Laursen, *J. Org. Chem.* **2019**, *84*, 2556–2567.
[3] L. G. Wang, I. Munhenzva, M. Sibrian-Vazquez, J. O. Escobedo, C. H. Kitts, F. R. Fronczek, R. M. Strongin, *J. Org. Chem.* **2019**, *84*, 2585–2595.
[4] A. Yamagami, H. Ishimura, A. Katori, K. Kuramochi, K. Tsubaki, *Org. Biomol. Chem.* **2016**, *14*, 10963–10972.
[5] Y. Yang, M. Lowry, X. Xu, J. O. Escobedo, M. Sibrian-Vazquez, L. Wong, C. M. Schowalter, T. J. Jensen, F. R. Fronczek, I. M. Warner, R. M. Strongin, *Proc. Nat. Acad. Sci.* **2008**, *105*, 8829–8834.
[6] M. Dai, Y. J. Reo, C. W. Song, Y. J. Yang, K. H. Ahn, *Chem. Sci.* **2020**, *11*, 8901–8911.
[7] M. Dai, Y. J. Yang, S. Sarkar, K. H. Ahn, *Chem. Soc. Rev.* **2023**, *52*, 6344–6358.
[8] P. Shieh, V. T. Dien, B. J. Beahm, J. M. Castellano, T. Wyss-Coray, C. R. Bertozzi, *J. Am. Chem. Soc.* **2015**, *137*, 7145–7151.
[9] G. Lukinavičius, L. Reymond, K. Umezawa, O. Sallin, E. D'Este, F. Göttfert, H. Ta, S. W. Hell, Y. Urano, K. Johnsson, *J. Am. Chem. Soc.* **2016**, *138*, 9365–9368.
[10] T. Ikeno, T. Nagano, K. Hanaoka, *Chem. Asian J.* **2017**, *12*, 1435–1446.

[11] Y. Koide, Y. Urano, K. Hanaoka, T. Terai, T. Nagano, *ACS Chem. Biol.* **2011**, *6*, 600–608.
[12] M. Grzybowski, M. Taki, S. Yamaguchi, *Chem. - Eur. J.* **2017**, *23*, 13028–13032.
[13] H. Ogasawara, Y. Tanaka, M. Taki, S. Yamaguchi, *Chem. Sci.* **2021**, *12*, 7902–7907.
[14] J. Liu, Y.-Q. Sun, H. Zhang, H. Shi, Y. Shi, W. Guo, *ACS Appl. Mater. Interfaces* **2016**, *8*, 22953–22962.
[15] A. N. Butkevich, G. Yu Mitronova, S. C. Sidenstein, J. L. Klocke, D. Kamin, D. N. H. Meineke, E. D'Este, P.-T. Kraemer, J. G. Danzl, V. N. Belov, S. W. Hell, *Angew. Chem. Int. Ed.* **2016**, *55*, 3290–3294.
[16] J. B. Grimm, A. J. Sung, W. R. Legant, P. Hulamm, S. M. Matlosz, E. Betzig, L. D. Lavis, *ACS Chem. Biol.* **2013**, *8*, 1303–1310.
[17] M. V. Sednev, C. A. Wurm, V. N. Belov, S. W. Hell, *Bioconjugate Chem.* **2013**, *24*, 690–700.
[18] H. C. Daly, S. S. Matikonda, H. C. Steffens, B. Ruehle, U. Resch-Genger, J. Ivanic, M. J. Schnermann, *Photochem. Photobiol.* **2022**, *98*, 325–333.
[19] S. Takahashi, Y. Kagami, K. Hanaoka, T. Terai, T. Komatsu, T. Ueno, M. Uchiyama, I. Koyama-Honda, N. Mizushima, T. Taguchi, H. Arai, T. Nagano, Y. Urano, *J. Am. Chem. Soc.* **2018**, *140*, 5925–5933.
[20] L. D. Lavis, *Biochemistry* **2017**, *56*, 5165–5170.
[21] Y.-J. Gong, X.-B. Zhang, G.-J. Mao, L. Su, H.-M. Meng, W. Tan, S. Feng, G. Zhang, *Chem. Sci.* **2016**, *7*, 2275–2285.
[22] J. Chan, S. C. Dodani, C. J. Chang, *Nature Chem.* **2012**, *4*, 973–984.
[23] C. Deo, S.-H. Sheu, J. Seo, D. E. Clapham, L. D. Lavis, *J. Am. Chem. Soc.* **2019**, *141*, 13734–13738.
[24] P. Shieh, M. J. Hangauer, C. R. Bertozzi, *J. Am. Chem. Soc.* **2012**, *134*, 17428–17431.
[25] Y. M. Poronik, K. V. Vygranenko, D. Gryko, D. T. Gryko, *Chem. Soc. Rev.* **2019**, *48*, 5242–5265.
[26] Y. M. Poronik, F. Ambicki, S.-M. Tseng, P.-T. Chou, I. Deperasińska, D. T. Gryko, *J. Org. Chem.* **2020**, *85*, 5973–5980.
[27] M. Grzybowski, O. Morawski, K. Nowak, P. Garbacz, *Chem. Commun.* **2022**, *58*, 5455–5458.
[28] W. E. Meador, E. Y. Lin, I. Lim, H. C. Friedman, D. Ndaleh, A. K. Shaik, N. I. Hammer, B. Yang, J. R. Caram, E. M. Sletten, J. H. Delcamp, *Nat. Chem.* **2024**, *16*, 970–978.
[29] M. A. Saucier, N. A. Kruse, B. E. Seidel, N. I. Hammer, G. S. Tschumper, J. H. Delcamp, *J. Org. Chem.* **2024**, *89*, 9092–9097.
[30] G. Jiang, H. Liu, H. Liu, G. Ke, T.-B. Ren, B. Xiong, X.-B. Zhang, L. Yuan, *Angew. Chem. Inter. Edi.* **2024**, *63*, e202315217.
[31] J. B. Grimm, L. D. Lavis, *Nat. Methods* **2022**, *19*, 149–158.
[32] G. Hong, A. L. Antaris, H. Dai, *Nature Biomed. Eng.* **2017**, *1*, 0010.
[33] G. Hong, S. Diao, A. L. Antaris, H. Dai, *Chem. Rev.* **2015**, *115*, 10816–10906.
[34] L. Xu, Q. Zhang, X. Wang, W. Lin, *Coord. Chem. Rev.* **2024**, *519*, 216122.
[35] Y. Gao, Z. Lei, *Anal. Bioanal. Chem.* **2023**, *415*, 3789–3797.
[36] X. Ren, C. Wang, X. Wu, M. Rong, R. Huang, Q. Liang, T. Shen, H. Sun, R. Zhang, Z. Zhang, X. Liu, X. Song, J. W. Foley, *J. Am. Chem. Soc.* **2024**, *146*, 6566–6579.
[37] J. B. Grimm, L. Xie, J. C. Casler, R. Patel, A. N. Tkachuk, N. Falco, H. Choi, J. Lippincott-Schwartz, T. A. Brown, B. S. Glick, Z. Liu, L. D. Lavis, *JACS Au* **2021**, *1*, 690–696.
[38] M. Isselstein, L. Zhang, V. Glembockyte, O. Brix, G. Cosa, P. Tinnefeld, T. Cordes, *J. Phys. Chem. Lett.* **2020**, *11*, 4462–4480.
[39] X.-Y. Ran, Y.-F. Wei, Y.-L. Wu, L.-R. Dai, W.-L. Xia, P.-Z. Zhou, K. Li, *J. Mater. Chem. B* **2025**, *13*, 2952–2977.
[40] P. Lu, S.-M. Dai, H. Zhou, F. Wang, W.-R. Dong, J.-H. Jiang, *Chem. Sci.* **2024**, *15*, 2221–2228.
[41] J. S. A. Badaro, B. Godlewski, D. T. Gryko, *Org. Chem. Front.* **2025**, *12*, 2860–2907.
[42] A. V. Kulinich, A. A. Ishchenko, *Chem. Rec.* **2024**, *24*, e202300262.
[43] A. V. Kulinich, A. A. Ishchenko, *Chem. Rev.* **2024**, *124*, 12086–12144.
[44] B. Bardi, K. V. Vygranenko, B. Koszarna, O. Vakuliuk, Ł. Dobrzycki, D. T. Gryko, F. Terenziani, A. Painelli, *Chem. - Eur. J.* **2023**, *29*, e202300979.
[45] A. Kakehi, S. Ito, K. Nakanishi, K. Watanabe, M. Kitagawa, *Bull. Chem. Soci. Jpn.* **1980**, *53*, 1115–1120.
[46] J. S. A. Badaro, A. Wrzosek, O. Morawski, A. Szewczyk, I. Deperasińska, D. T. Gryko, *Org. Chem. Front.* **2024**, *11*, 6627–6641
[47] F. Reindel, *Berichte der deutschen chemischen Gesellschaft (A and B Series)* **1924**, *57*, 1381–1386.
[48] K. Pandey, V. N. Shinde, K. Rangan, A. Kumar, *Tetrahedron* **2020**, *76*, 131499.
[49] E. Hendrickx, Y. Zhang, K. B. Ferrio, J. A. Herlocker, J. Anderson, N. R. Armstrong, E. A. Mash, A. P. Persoons, N. Peyghambarian, B. Kippelen, *J. Mater. Chem.* **1999**, *9*, 2251–2258.
[50] G. Yin, T. Niu, T. Yu, Y. Gan, X. Sun, P. Yin, H. Chen, Y. Zhang, H. Li, S. Yao, *Angew. Chem. Inter. Ed.* **2019**, *58*, 4557–4561.
[51] T. Peng, D. Yang, *Org. Lett.* **2010**, *12*, 496–499.
[52] R. Zondervan, F. Kulzer, M. A. Kol'chenk, M. Orrit, *J. Phys. Chem. A* **2004**, *108*, 1657–1665.
[53] P. V. Kamat, M. A. Fox, *J. Phys. Chem.* **1984**, *88*, 2297–2302.
[54] M. Martínek, L. Ludvíková, M. Šranková, R. Navrátil, L. Muchová, J. Huzlík, L. Vítek, P. Klán, P. Šebej, *Org. Biomol. Chem.* **2022**, *21*, 93–97.
[55] D. C. Neckers, O. M. Valdes-Aguilera, in *Advances in Photochemistry*, John Wiley & Sons, Ltd, Hoboken, NJ **1993**, pp. 315–394.
[56] M. J. Frisch, G. W. Trucks, H. B. Schlegel, G. E. Scuseria, M. A. Robb, J. R. Cheeseman, G. Scalmani, V. Barone, G. A. Petersson, H. Nakatsuji, X. Li, M. Caricato, A. V. Marenich, J. Bloino, B. G. Janesko, R. Gomperts, B. Mennucci, H. P. Hratchian, J. V. Ortiz, A. F. Izmaylov, J. L. Sonnenberg, D. Williams-Young, F. Ding, F. Lipparini, F. Egidi, J. Goings, B. Peng, A. Petrone, T. Henderson, D. Ranasinghe, et al., Gaussian 16, Rev.B.01, Wallingford, CT, **2016**.
[57] V. Barone, J. Bloino, M. Biczysko, F. Santoro, *J. Chem. Theory Comput.* **2009**, *5*, 540–554.
[58] J. Bloino, M. Biczysko, F. Santoro, V. Barone, *J. Chem. Theory Comput.* **2010**, *6*, 1256–1274.
[59] F. Neese, *WIREs Comput. Mole. Sci.* **2022**, *12*, e1606.
[60] A. Kawski, Z. Naturforsch, *A: Phys. Sci.* **2002**, *57*, 255–262.
[61] J. Cerezo, F. J. A. Ferrer, F. Santoro, *Phys. Chem. Chem. Phys.* **2015**, *17*, 11401–11411.
[62] R. R. Valiev, V. N. Cherepanov, G. V. Baryshnikov, D. Sundholm, *Phys. Chem. Chem. Phys.* **2018**, *20*, 6121–6133.
[63] T. Dutta, S. Das, I. Gupta, A. L. Koner, *Chem. Sci.* **2022**, *13*, 12987–12995.
[64] Y. Wang, Q. Lin, Y. Liu, C. Li, Z. Liu, X. Yu, K.-N. Wang, *Anal. Chem.* **2024**, *96*, 9808–9816.
[65] C. Li, C. Zong, Y. Liu, Z. Liu, K.-N. Wang, X. Yu, *Chin. Chem. Lett.* **2024**, *35*, 108323.
[66] R. Yang, X. He, G. Niu, F. Meng, Q. Lu, Z. Liu, X. Yu, *ACS Sens.* **2021**, *6*, 1552–1559.
[67] S. Yang, Z. Zhang, C. Dai, J. Li, M. Tian, *Chem. Eng. J.* **2023**, *451*, 139032.
[68] E. Ge, B. Dong, Z. Gou, M. Tian, *Anal. Chem.* **2022**, *94*, 960–967.

Manuscript received: April 10, 2025
Revised manuscript received: August 13, 2025
Accepted manuscript online: September 19, 2025
Version of record online: ■■, ■■

Institute of Organic Chemistry
Polish Academy of Sciences

Jaqueline Stella Araujo Badarò
+48 22 343 20 37
jaqueline.badaro@icho.edu.pl

Warsaw 28th September 2025

I declare that my contribution to the following publication consisted of:

1. **Badaro, J. S. A.**; Koszarna, B.; Bousquet, M. H. E.; Ouellette, E. T.; Jacquemin, D.; Gryko, D. T. 'The Kröhnke synthesis of benzo[a]indolizines revisited: towards small, red light emitters', Org. Chem. Front. 2022, 9, 1861-1874. https://doi.org/10.1039/D2QO00097K

2. **Badaro, J. S. A.**; Wrzosek, A; Morawski, O.; Szewczyk, A; Deperasinska, I; Gryko, D. T. 'Strongly fluorescent indolizine-based coumarin analogs' Org. Chem. Front., 2024, 11, 6627-6641. https://doi.org/10.1039/D4QO01216J

3. **Badaro, J. S. A**; Koszarna, B.; Perkowska, M.; Kandere-Grzybowska, K.; Kolygina, D. V.; Morawski, O.; Park, J.; Grzybowski, B.; Deperasinska, I.; Gryko, D. T., 'The Hybrid of Indolizine and Merocyanine - A New Class of Organelle-specific Dyes', Angew. Chem. Int. Ed. 2025, 64, doi.org/10.1002/anie.202508044.

   co-development of research concepts, synthesis, characterization, absorption and fluorescence measurements, photostability measurements, interpretation of results and preparation of the manuscript.

4. **Badaro, J. S. A.**; Godlewski, B.; Gryko, D. T., 'Advances in the synthesis of indolizines and their π-expanded analogues: update 2016-2024', Org. Chem. Front., 2025, 12, 2860-2907. https://doi.org/10.1039/D4QO02082K

Writing and editing of the text of one of the chapters, drwing figures for one of the chapters and revising the final version of the manuscript.

Yours sincerely

Jaqueline Stella Araujo Badaro

Institute of Organic Chemistry
Polish Academy of Sciences

Professor Daniel Gryko
Director

+48 22 343 23 21
daniel.gryko@icho.edu.pl

Warsaw 25th September 2025

I declare that my contribution to the following publications consisted of:

- Badaro, J. S. A.; Koszarna, B.; Bousquet, M. H. E.; Ouellette, E. T.; Jacquemin, D.; **Gryko, D. T.** 'The Kröhnke synthesis of benzo[*a*]indolizines revisited: towards small, red light emitters', *Org. Chem. Front*. **2022**, *9*, 1861-1874. https://doi.org/10.1039/D2QO00097K

  Co-development of research concepts, interpretation of results and preparation of the final version of the manuscript.

- Badaro, J. S. A.; Wrzosek, A; Morawski, O.; Szewczyk, A; Deperasińska, I; **Gryko, D. T.** 'Strongly fluorescent indolizine-based coumarin analogs' *Org. Chem. Front.*, **2024**, *11*, 6627–6641."

  Co-development of research concepts, interpretation of results and preparation of the final version of the manuscript.

- Badaro, J. S. A.; Godlewski, B.; **Gryko, D. T.,** 'Advances in the synthesis of indolizines and their π-expanded analogues: update 2016–2024', *Org. Chem. Front.*, **2025**, *12*, 2860-2907. https://doi.org/10.1039/D4QO02082K".

  Development of the review concept, writing the introduction and summary/outlook as well as editing of the final version of the manuscript.

- Badaro, J. S. A; Koszarna, B.; Perkowska, M.; Kandere-Grzybowska, K.; Kolygina, D. V.; Morawski, O.; Park, J.; Grzybowski, B.; Deperasińska, I.; **Gryko, D. T.**, 'The Hybrid of Indolizine and Merocyanine – A New Class of Organelle-specific Dyes', *Angew. Chem. Int. Ed*. **2025**, *64*, doi.org/10.1002/anie.202508044.

  Co-development of research concepts, interpretation of results and preparation of the final version of the manuscript.

Yours sincerely

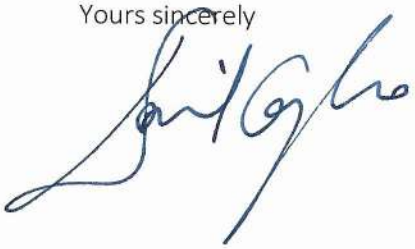

Institute of Organic Chemistry
Polish Academy of Sciences

dr Beata Koszarna

+48 22 343 20 37
beata.koszarna@icho.edu.pl

Warsaw 23rd September 2025

I declare that my contribution to the following publications consisted of:

1. J. S. A. Badaro, B. Koszarna, M. H. E. Bousquet, E. T. Ouellette, D. Jacquemin, D. T. Gryko; ***"The Krohnke synthesis of benzo[a]indolizines revisited: towards small, red light emitters"***; Org. Chem. Front., **2022**, 9, 1861-1874

2. J. S. A. Badaro, B. Koszarna, M. Perkowska, K. Kandere-Grzybowska, D. V. Kolygina, O. Morawski, J. Park, B. Grzybowski, I. Deperasińska, D. T. Gryko; ***"The Hybrid of Indolizine and Merocyanine – A New Class of Organelle-specific Dyes"***; Angewandte Chemie, 2025, In Press

I participated in absorption and fluorescence measurements, supervised laboratory work, and contributed to manuscript drafting.

Beata Koszarna

Yours sincerely

Institute of Organic Chemistry
Polish Academy of Sciences

Maja Perkowska
+48 737 389 032
maja.perkowska@icho.edu.pl
Instytut Chemii Organicznej PAN
Marcina Kasprzaka 44/52
01-224 Warsaw

Warsaw 25rd September 2025

Statement

I declare that my contribution to the following publication consisted of:

Jaqueline S. A. Badaro, Beata Koszarna, Maja Perkowska, Kristiana Kandere-Grzybowska, Diana V. Kolygina, Olaf Morawski, Juhee Park, Bartosz Grzybowski, Irena Deperasińska and Daniel T Gryko, *Angewandte Chemie, 2025, In Press, "The Hybrid of Indolizine and Merocyanine – A New Class of Organelle-specific Dyes".*

I participated in the synthesis, absorption and fluorescence measurements of some reported dyes. I was also involved in measuring the melting temperatures of the dyes and creating the graphical abstract.

Yours sincerely

Maja Perkowska

Instytut Chemii Organicznej
Polskiej Akademii Nauk

Bartosz Godlewski
bartosz.godlewski@icho.edu.pl
Intitute of Organic Chemistry PAS
Kasprzaka 44/52, 01-224 Warsaw, Poland

Warsaw, 23.09.2025

STATEMENT

I hereby declare that my contribution to publication:

"*Advances in the Synthesis of Indolizines and Their π-Expanded Analogues: Update 2016–2024*"; J. S. A. Badaro, B. Godlewski and D. T. Gryko, *Org. Chem. Front.*, 2025, **12**, 2860–2907

is as follows:

writing and editing the text of one of the chapters, drawing figures for one of the chapters and revising the final version of the manuscript.

Bartosz Godlewski

GodlewskiB

INSTYTUT FIZYKI POLSKIEJ AKADEMII NAUK
INSTITUTE OF PHYSICS, POLISH ACADEMY OF SCIENCES
02-668 WARSZAWA, Al. LOTNIKÓW 32/46
fax: (48-22) 843-0926; http://info.ifpan.edu.pl

dr hab. Irena Deperasińska e-mail: deper@ifpan.edu.pl

Warszawa, 23.09.2025

Declaration

I declare that my contribution to the following publications:

1. **Jaqueline S. A. Badaro** et al., The Hybrid of Indolizine and Merocyanine – A New Class of Organelle-specific Dyes, *accepted for publication in Angewandte Chemie International Edition*

2. **Jaqueline S. A. Badaro** et al., Strongly Fluorescent Indolizine-based Coumarin Analogs, *Org. Chem. Front., 2024, 11, 6627*

consisted of performing DFT calculations of the electronic transition energies in compounds **3a**, **3d**, **3Ng**, **5** in the case of the first publication and **2b**, **2a**, **2c**. **2e**. **2f**. **4a**, **3aa**, **3ac**, **3ab** and **6a** in the case of the second publication.

I. Deperasińska

INSTYTUT FIZYKI POLSKIEJ AKADEMII NAUK
INSTITUTE OF PHYSICS, POLISH ACADEMY OF SCIENCES
02-668 WARSZAWA, Al. LOTNIKÓW 32/46
fax: (48-22) 843-0926; http://info.ifpan.edu.pl

dr hab. Olaf Morawski

e-mail: morawo@ifpan.edu.pl

Warszawa, 23.09.2025

Declaration

I declare that my contribution to the following publications:

1. **Jaqueline S. A. Badaro** et al., The Hybrid of Indolizine and Merocyanine – A New Class of Organelle-specific Dyes, *accepted for publication in Angewandte Chemie International Edition*

2. **Jaqueline S. A. Badaro** et al., Strongly Fluorescent Indolizine-based Coumarin Analogs, *Org. Chem. Front., 2024, 11, 6627*

consisted of performing measurements of all fluorescence decay profiles for all compounds in both publications as well as performing for them deconvolution calculations to obtain decay times.

O. Morawski

nencki institute
of experimental biology

Dr. Antoni Wrzosek

A.Wrzosek@nencki.edu.pl

Ref. Contribution Letter

Warsaw, 23/09/2025

To whom it may concern

I hereby declare that my contribution to the publication:

Jaqueline S. A. Badaro, Antoni Wrzosek, Olaf Morawski, Adam Szewczyk, Irena Deperasińska and Daniel T. Gryko. ***Org. Chem. Front.***, 2024,**11**, 6627-6641. **"Strongly Fluorescent Indolizine-based Coumarin Analogs"**

I performed the confocal microscopy measurements for this work. I participated in the proofreading of the section on confocal microscopy studies.

Sincerely,

Antoni Wrzosek

Dr. Antoni Wrzosek

Nencki Institute of Experimental Biology, Polish Academy of Sciences
3 Pasteur St., 02-093 Warsaw, Poland
phone: +48 22 58 92 207, email: dyrekcja@nencki.edu.pl
www.nencki.edu.pl

Prof. Adam Szewczyk

A.Szewczyk@nencki.edu.pl

Ref. Contribution Letter

Warsaw, 23/09/2025

To whom it may concern

I hereby declare that my contribution to the publication:

Jaqueline S. A. Badaro, Antoni Wrzosek, Olaf Morawski, Adam Szewczyk, Irena Deperasińska and Daniel T. Gryko. ***Org. Chem. Front.***, 2024,**11**, 6627-6641. **"Strongly Fluorescent Indolizine-based Coumarin Analogs"**

I participated in the proofreading of the section on confocal microscopy studies.

Sincerely,

Prof. Adam Szewczyk

Nencki Institute of Experimental Biology, Polish Academy of Sciences
3 Pasteur St., 02-093 Warsaw, Poland
phone: +48 22 58 92 207, email: dyrekcja@nencki.edu.pl
www.nencki.edu.pl

Manon Bousquet
mhe.bousquet@gmail.com

Ref. **Contribution Letter**

Nantes, 20/09/2025

To whom it may concern,

I hereby declare that my contribution to the publications below:

1. **Jaqueline S. A. Badaro,** Beata Koszarna, Manon H. E. Bousquet, Erik T. Ouellette, Denis Jacquemin and Daniel T. Gryko. ***Org. Chem. Front.***, 2022,**9**, 1861-1874. **"The Kröhnke synthesis of benzo[*a*]indolizines revisited: towards small, red light emitters"**

I realized the theoretical part of this work and wrote the theoretical section of this manuscript.

With best regards.

Manon Bousquet

CEISAM
www.ceisam.sciences.univ-nantes.fr
UMR CNRS 6230
Faculté des Sciences et Techniques
Université de Nantes
2 Rue de la Houssinière, Nantes,
France

Erik T. Ouellette
+1 (303) 514-9116 | ouelletteerik@berkeley.edu

September 22nd, 2025

To whom it may concern,

I hereby declare that my contribution to the publications listed below is as follows:

1. Badaro, J. S. A.; Koszarna, B.; Bousquet, M. H. E.; **Ouellette, E. T.**; Jacquemin, D.; Gryko, D. T. "The Kröhnke synthesis of benzo[*a*]indolizines revisited: towards small, red light emitters." *Org. Chem. Front.* **2022**, *9*, 1861-1874.

I collected single-crystal x-ray diffraction (SCXRD) measurements, analyzed data, and developed structural solutions of relevant compounds from the manuscript.

Sincerely,

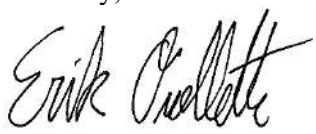

Erik T. Ouellette

Prof. Denis Jacquemin
Denis.Jacquemin@univ-nantes.fr

Ref. **Contribution Letter**

Nantes, 19/09/2025

To whom it may concern,

I hereby declare that my contribution to the publications below:

1. **Jaqueline S. A. Badaro,** Beata Koszarna, Manon H. E. Bousquet, Erik T. Ouellette, Denis Jacquemin and Daniel T. Gryko. ***Org. Chem. Front.***, 2022,**9**, 1861-1874. **"The Kröhnke synthesis of benzo[*a*]indolizines revisited: towards small, red light emitters"**

I supervised the theoretical part of this work and contributed to write the theoretical section of this manuscript. I was involved in the proof checking of the full manuscript.

With best regards.

Prof. Denis Jacquemin

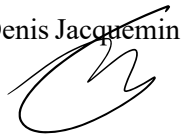

CEISAM
www.ceisam.sciences.univ-nantes.fr
UMR CNRS 6230
Faculté des Sciences et Techniques
Université de Nantes
2 Rue de la Houssinière, Nantes,
France

Ulsan National Institute of Science and Technology
IBS Center for Algorithmic and Robotized Synthesis
AMRB 103, Office 307
50, UNIST-gil, Ulsan 44919, Republic of Korea

STATEMENT

September 22, 2025

I hereby declare that my contributions to the publication listed below is as follows:

Jaqueline S. A. Badaro, Beata Koszarna, Maja Perkowska, Kristiana Kandere-Grzybowska, Diana V. Kolygina, Olaf Morawski, Juhee Park, Bartosz Grzybowski, Irena Deperasińska, and Daniel T Gryko. The Hybrid of Indolizine and Merocyanine – A New Class of Organelle-specific Dyes. *Angew. Chem. Int. Ed.* In Press, 2025.

I designed and performed confocal imaging of the fluorescent compounds in living cells, specifically for Figure S10, Figure S11, Figure S12 ab, Figure S13, Figure S14, Fig S15 (with MRC5 cells), Figure S16 ab, Figure S17 (with MRC5 cells), Figure S18, Figure S19, and Figure S20. I analyzed the corresponding images and produced the figures related to confocal imaging. I contributed to the Materials and Methods part for ESI section 6 Imaging.

Sincerely,

Diana V. Kolygina
Senior Researcher
Center for Algorithmic and Robotized Synthesis, Institute for Basic Science (IBS)

IBS Center for Algorithmic and Robotized Synthesis
AMRB 103, Office 301D
50, UNIST-gil, Ulsan 44919, Republic of Korea

STATEMENT

September 22, 2025

I hereby declare that my contribution to the publication listed below is as follows:

> Jaqueline S. A. Badaro, Beata Koszarna, Maja Perkowska, Kristiana Kandere-Grzybowska, Diana V. Kolygina,] Olaf Morawski, Juhee Park, Bartosz Grzybowski, Irena Deperasińska and Daniel T Gryko, Angewandte Chemie, 2025, In Press, *The Hybrid of Indolizine and Merocyanine – A New Class of Organelle-specific Dyes*

For the S21 data, I performed cytotoxicity assays using multiple cell lines and various compounds, analyzed the IC50 values, and provided a detailed description of the experimental methods.

Sincerely,

Juhee Park

Senior Research Engineering Staff, IBS CARS

Ulsan National Institute of Science and Technology
IBS Center for Algorithmic and Robotized Synthesis
AMRB 103, Office 307
50, UNIST-gil, Ulsan 44919, Republic of Korea

STATEMENT

September 22, 2025

I hereby declare that my contributions to the publication listed below is as follows:

Jaqueline S. A. Badaro, Beata Koszarna, Maja Perkowska, Kristiana Kandere-Grzybowska, Diana V. Kolygina, Olaf Morawski, Juhee Park, Bartosz Grzybowski, Irena Deperasińska, and Daniel T Gryko. The Hybrid of Indolizine and Merocyanine – A New Class of Organelle-specific Dyes. *Angew. Chem. Int. Ed.* In Press, 2025.

I designed experiments and supervised the work related to confocal imaging of the dyes in living cells. Specifically, I performed confocal imaging for Fig 6, Fig S12c,d, Fig S15, Fig S16c,d, Fig S17 (experiments with HT1080 cells), and analyzed the corresponding images. I co-wrote the Materials and Methods section for ESI Section 6 Imaging, and contributed text to the manuscript for section on fluorescent imaging.

Sincerely,

Kristiana Kandere-Grzybowska
Adjunct Professor, UNIST
Senior Research Fellow, IBS CARS

Ulsan National Institute of Science and Technology
IBS Center for Algorithmic and Robotized Synthesis
50, UNIST-gil, Ulsan 44919, Republic of Korea

STATEMENT

September 29, 2025

I hereby declare that my contribution to the publication listed below is as follows:

Jaqueline S. A. Badaro, Beata Koszarna, Maja Perkowska, Kristiana Kandere-Grzybowska, Diana V. Kolygina, Olaf Morawski, Juhee Park, Bartosz Grzybowski, Irena Deperasińska and Daniel T Gryko, Angewandte Chemie, 2025, In Press, *The Hybrid of Indolizine and Merocyanine – A New Class of Organelle-specific Dyes*

I supervised the work performed by the other coauthors from UNIST related to confocal imaging of the dyes and revised the manuscript.

Sincerely,

Bartosz Grzybowksi

Distinguished Professor, Department of Chemistry, UNIST
Director, Center for Algorithmic and Robotized Synthesis (CARS),
Institute for Basic Science